UNIVERSITY OF CALIFORNIA

Santa Barbara

Development of a General S_N2 Approach to 1,2-*cis*-Glycosides and Catalytic Access to Electron-Rich 2-Aminofurans

A dissertation submitted in partial satisfaction of the

requirements for the degree Doctor of Philosophy

in Chemistry

by

Xu Ma

Committee in charge:

Professor Liming Zhang, Chair

Professor Mahdi Abu-Omar

Professor Javier Read de Alaniz

Professor Armen Zakarian

December 2021

The dissertation of Xu Ma is approved.

_____

Mahdi Abu-Omar

_____

Javier Read de Alaniz

_____

Armen Zakarian

_____

Liming Zhang, Committee Chair

December 2021

Development of a General S_N2 Approach to 1,2-*cis*-Glycosides and Catalytic Access to Electron-Rich 2-Aminofurans

by

Xu Ma

ACKNOWLEDGEMENTS

First and foremost, I would like to express my deep appreciation to my Ph.D. advisor, Prof. Liming Zhang. His extreme enthusiasm and devotion to organic chemistry constantly inspire me to work harder and think deeply during my five years' doctoral study. Before I came here, I was a blank page, and only with his guidance, expertise, help, and encouragement, I learn a lot of organic chemistry knowledge. Besides that, he also reminds me of the importance of maintaining a positive attitude toward research and keeping a healthy and regular working schedule which would be invaluable for the rest of my life.

Meanwhile, I would like to thank my Ph.D. committee members, Prof. Armen Zakarian, Prof. Mahdi Abu-Omar, and Prof. Javier Read de Alaniz, for their valuable advice through my graduate study.

I would also like to give my cheers to all my labmates. Besides sharing knowledge and experiences in chemistry, they have become my best friends and made my life more enjoyable. Especially Dr. Zhitong Zheng, Xijun Zhu, and Dr. Yongliang Zhang, without their help, the progress of my projects would be substantially slower. My appreciation also goes to Dr. Hongjun Zhou, Dr. Dmitriy Uchenik, Dr. Rachel Behrens for their technical support in my research. Of course, I would like to express my gratitude to my collaborators, Yue Fu, and Prof. Peng Liu, for doing an excellent DFT calculation. I would also like to thank all my roommates for their kind help and support.

Finally, I would like to express my appreciation to my whole family for their unconditional love and support. I want to thank my parents Jiasheng Ma and Tingfeng Liu. They always encouraged me and helped me pursue higher education, and their life values shaped me into the person I am.

VITA OF XU MA

December 2021

EDUCATION

2016 - 2021 Ph.D. in Organic Chemistry

University of California, Santa Barbara

2011 - 2015 BS in chemistry

Wuhan University, PRC.

PROFESSIONAL EMPLOYMENT

2016 - 2021 Graduate Researcher in Prof. Liming Zhang's group, *UCSB*

2016 - 2018 Graduate Teaching Assistant in Department of Chemistry and Biochemistry, *UCSB*

2013 - 2015 Undergraduate Researcher in Prof. Aiwen Lei's group, *Wuhan University*

PUBLICATIONS

9. **Ma, X.**; † Zhang, Y.; † Zhu, X.; Zhang, L., A Generally Applicable S_N2 Strategy toward 1,2-*cis*-Furanosides. *Manuscript submitted.*

8. **Ma, X.;** † Zheng, Z.; †Fu, Y.; † Zhu, X.; Liu, P.; Zhang, L., A "Traceless" Directing Group Enables Catalytic S_N2 Glycosylation toward 1, 2-*cis*-Glycopyranosides. *J. Am. Chem. Soc.* **2021**, *143*, 11908–11913.

7. Zheng, Z.; † **Ma, X.**; † Cheng, X.; Zhao, K.; Gutman, K.; Li, T.; Zhang, L., Homogeneous Gold-Catalyzed Oxidation Reactions. *Chem. Rev.* **2021**, *121*, 8979–9038.

6. Li, X.; † **Ma, X.**; † Wang, Z.; Liu, P. N.; Zhang, L., Bifunctional Phosphine Ligand Enabled Gold-Catalyzed Alkynamide Cycloisomerization: Access to Electron-Rich 2-Aminofurans and Their Diels–Alder Adducts. *Angew.Chem. Int. Ed.* **2019**, *58*,17180 – 17184.

5. Zheng, Z.; Wang, Y.; **Ma, X.**; Li, Y.; Zhang, L., Non-Diazo C− H Insertion Approach to Cyclobutanones through Oxidative Gold Catalysis. *Angew. Chem. Int. Ed.* **2020**, *59*, 17398 – 17402.

4. Liao, S.; Porta, A.; Cheng, X.; Ma**, X.**; Zanoni, G.; Zhang, L., Bifunctional Ligand Enables Efficient Gold-Catalyzed Hydroalkenylation of Propargylic Alcohol. *Angew. Chem. Int. Ed.* **2018**, *57*,8250 –8254.

3. Dong, X.; Chen, L.; Zheng, Z.; **Ma, X.**; Luo, Z.; Zhang, L., Silver-catalyzed stereoselective formation of glycosides using glycosyl ynenoates as donors. *Chem. Commun.*, **2018**,*54*, 8626-8629.

2. Li, X.; Wang, Z.; **Ma, X.**; Liu, P.-n.; Zhang, L., Designed bifunctional phosphine ligand-enabled gold-catalyzed isomerizations of ynamides and allenamides: Stereoselective and regioselective formation of 1-amido-1, 3-dienes. *Org. Lett.* **2017**, *19*, 5744–5747.

1. Yuan, J.; **Ma, X.**; Yi, H.; Liu, C.; Lei, A., I_2-catalyzed oxidative C (sp^3)–H/S–H coupling: utilizing alkanes and mercaptans as the nucleophiles. *Chem. Commun.*, **2014**,*50*, 14386-14389.

CONFERENCE PRESENTATIONS

"Research in Zhang Group - Catalytic S_N2-Type Glycosylation Enabled by A Traceless Directing Group" Poster at the University of California Chemical Symposium, Virtual meeting, 03/2021.

AWARDS

2019 Robert H. DeWolfe Teaching Fellowship in Organic Chemistry, *UC Santa Barbara*

2014 Outstanding Student Award, *Wuhan University*

2014 Third Prize Scholarship, *Wuhan University*

ABSTRACT

Development of a General S_N2 Approach to 1,2-*cis*-Glycosides and Catalytic Access to Electron-Rich 2-Aminofurans

by

Xu Ma

The advance of glycoscience hinges on efficient access to oligosaccharides and glycans of defined yet diverse configurations and connectivities. Synthesis of 1,2-*cis* glycosidic bonds remains synthetically challenging, and a general synthetic approach to achieving their high stereoselective construction that is applicable to every sugar type has yet to be developed despite over a century of intense research in carbohydrate chemistry. This deficiency hinders the development of automation in carbohydrate synthesis, despite some recent progress. A major part of my dissertation describes a working solution in addressing this long-standing challenge via an S_N2 strategy featuring a directing group on the anomeric leaving group. Such a directing group is employed to promote the acceptor attack at the backend of the anomeric carbon-leaving group bond (hence realizing an S_N2 process) upon gold activation. This unique approach makes the directing group "traceless" in the glycoside products and permits the strategy to be of general applicability as the installation of the directing group and hence the adaptation of the strategy is not limited to any specific sugar types. The strategy is successfully applied to the synthesis of a range of 1,2-*cis*-pyranosides and furanosides with good to excellent stereoselectivities.

In addition, this dissertation describes a gold-catalyzed in situ access to 2-aminofurans. The highly electron-rich nature of this class of furans makes it difficult to prepare by other means but endows them with exceptional synthetic value. With bifunctional phosphine

ligands specifically designed for cooperative gold catalysis, acetylenic amides are efficiently transformed into 2-aminofurans in a single step, which are further converted into functional products in one pot.

TABLE OF CONTENTS

LIST OF SCHEMES, FIGURES, AND TABLES

1. Catalytic Access to Electron-Rich 2-Aminofurans

1.1 General Introduction to Homogeneous Gold(I) Catalysis

Gold often occurs in its pure form in nature, which is a bright, slightly reddish yellow, soft but dense, malleable metal. And it has been used for coinage, jewelry, and many types of arts since ancient times.[1] However, in contrast to its widespread in human society, gold catalysis in organic synthesis has been seldom studied until the dawn of the new millennium.

Scheme 1. Early Reports of Homogenous Gold Catalysis in Organic Synthesis

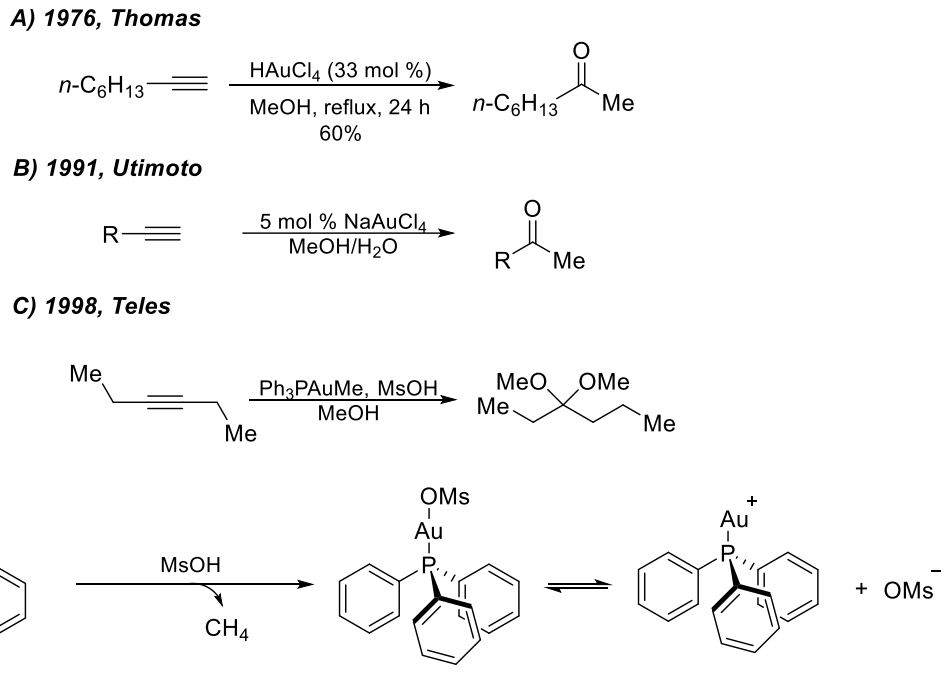

One early report of homogenous gold catalysis was an alkyne hydration reaction reported by the Thomas group in 1976 (**Scheme 1A**).[2] Later, in 1991, the Utimoto group improved this type of reaction by using a catalytic amount of $NaAuCl_4$ (**Scheme 1B**).[3] In 1998, The Teles group generated PPh_3AuOMs in-situ from PPh_3AuMe (**Scheme 1C**) [4] and

applied it to the nucleophilic additions to the alkynes, marking a breakthrough in the development of homogeneous gold catalysis. The Teles' work showed that ligand could be introduced to cationic gold catalysts like other transition metal catalysis. Ever since this pioneering work, there has been a "gold rush" in the last two decades, and many novel gold catalysts applying various ligands have been synthesized (**Figure 1**).

Figure 1. Components of Common Gold(I) Catalysts

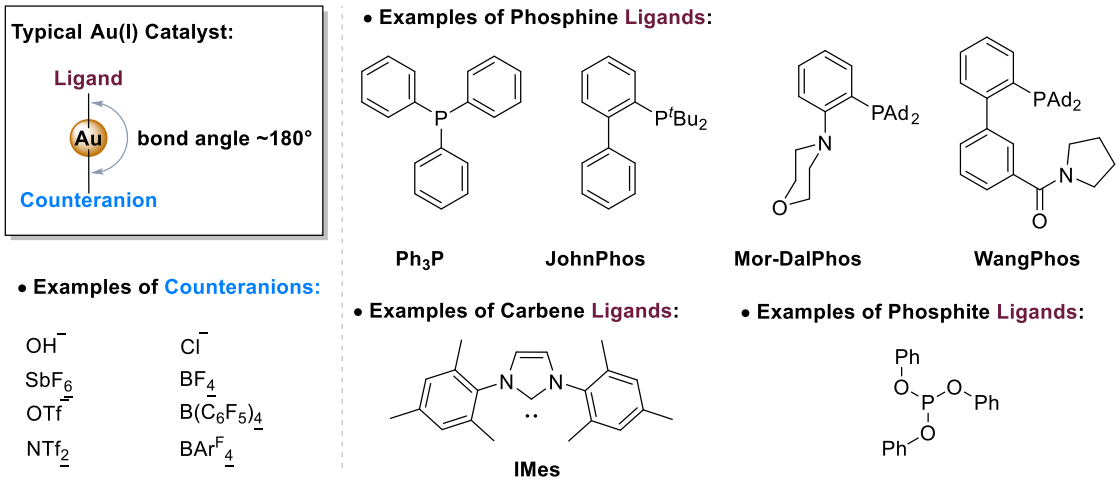

Gold(I) predominantly forms linear bis-coordinated complexes, although more coordination numbers are possible.[5] The advent of various ligands from other transition metal catalysis, especially Pd catalysis, opened fertile ground for their applications in homogenous gold(I) catalysis. Many ligands have been developed or employed, and some representative ones are listed in Figure 1. The gold center's catalytic activities are tunable by introducing ligands with different electronic, steric, and chiral properties. As demonstrated in many cases, ligands play a significant role in achieving desirable control of chemo-, regio-, and stereoselectivities in gold-catalyzed reactions.[6-17]. On the other hand, non-coordinating or weakly coordinating counteranions are required for catalytically active gold

catalysts. Moreover, counteranions have also been shown to affect the activities of gold catalysts as well as the reaction outcome. However, the exact nature of "counteranion effects" is yet to be fully rationalized.[18]

Scheme 2. Anti-nucleophilic Attack to Au(I)-Activated C-C Unsaturated Bond

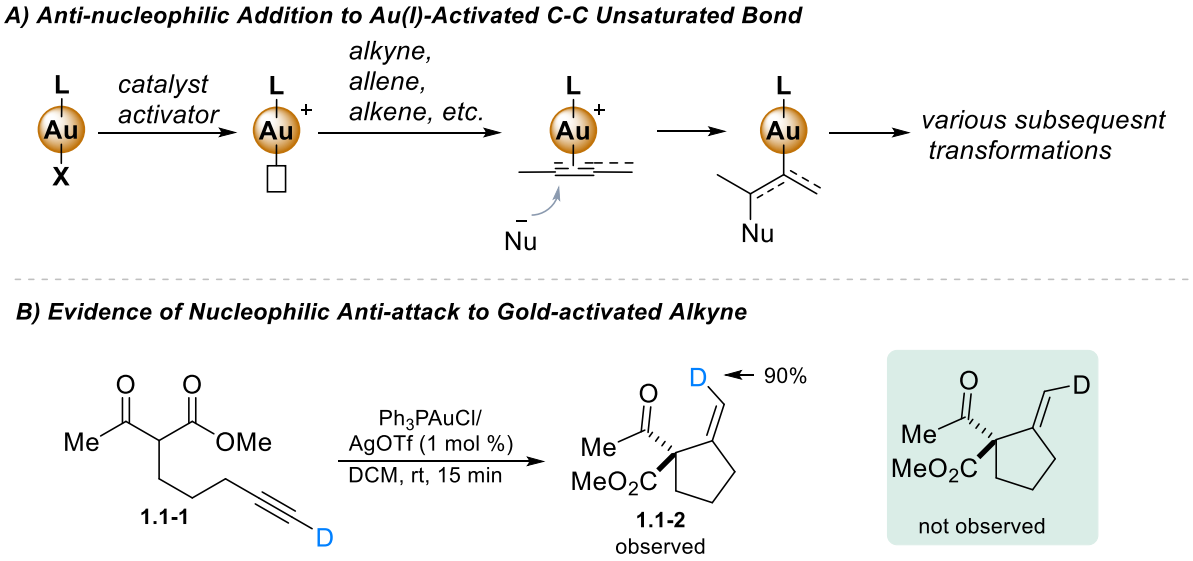

Gold(I) catalysts are soft and carbophilic Lewis acids capable of activating unsaturated bonds like alkynes and allenes and, to a lesser content, alkenes (**Scheme 2A**). After activation, the subsequent gold-π complex is susceptible to attacks by a diverse array of nucleophiles. Such nucleophilic attack strictly follows an *anti*-addition manner, which was initially proved by a study performed by the Toste group in early 2004.[19] As shown in Scheme 2B, with the deuterated α-ketoester **1.1-1** as the substrate, the author observed only one isomer **1.1-2**, indicating a mechanism involving a *trans*- nucleophilic attack by the 1,3-dicarbonyl nucleophile at a gold(I)-activated C-C triple bond.

Relativistic effects provided a theoretical framework for rationalizing the observed reactivity of gold: The contracted 6s orbital and expanded 5d orbitals in gold account for the

attributes of gold(I) catalysts (**Figure 2**).[20] The contracted 6s orbital results in a relatively low-lying lowest unoccupied molecular orbital (LUMO), making the gold(I) catalysts Lewis acidic. This feature would render anti-nucleophilic addition to the activated C-C π-bond. Besides, the contracted 6*s* orbital imposes a strong shielding effect to the more defused 5*d* orbitals and makes the highest unoccupied molecular orbital (HOMO) lie relatively higher. The latter feature would allow gold to engage in back-bonding into the α-carbocation and stabilize the formation of gold carbene or carbenoid.

Figure 2. Relativistic Effects in Gold

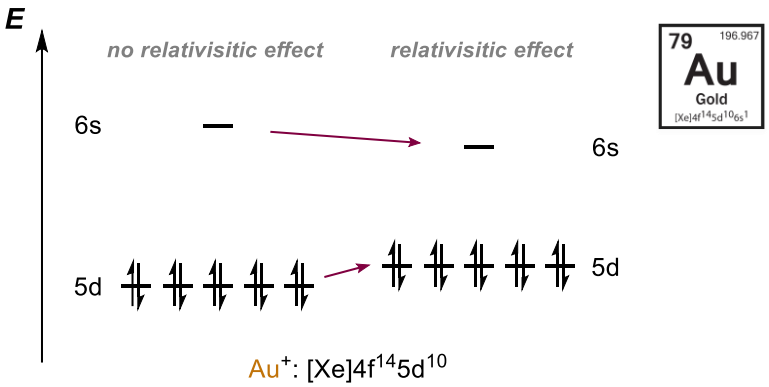

For a gold-catalyzed reaction, after the initial *anti*-attack, the intermediate **1.1-3** can undergo functionalization at its α or β position to furnish different products (**Scheme 3**). When alkyne or allene is employed as the substrate, for the reactions to happen at the α position, due to the nucleophilicity of the alkene double bond and the labile nature of the Au-C(sp^2) bond, the alkenyl gold can further react with an electrophile (E^+) to form bi-functionalized alkenes **1.1-4** or **1.1-6**. Alternatively, the gold centers of **1.1-3A** or **1.1-3D** can push electrons back from their filled d-orbital, meanwhile picking up electrophiles at their β position. The latter process will lead to reactive carbenoid species **1.1-7** or **1.1-9**.

When the substrate is alkene, the Au-C(sp^3) bond (**1.1-3B**) may go through protodeauration to afford the product **1.1-5**, albeit it is a slow process and often accompanied by reversal back to the alkene substrate.[21] Alternatively, if a leaving group is present at the β position, the subsequent elimination can result in olefin **1.1-8**.

Scheme 3. General Reaction Modes of Gold(I) Catalysis

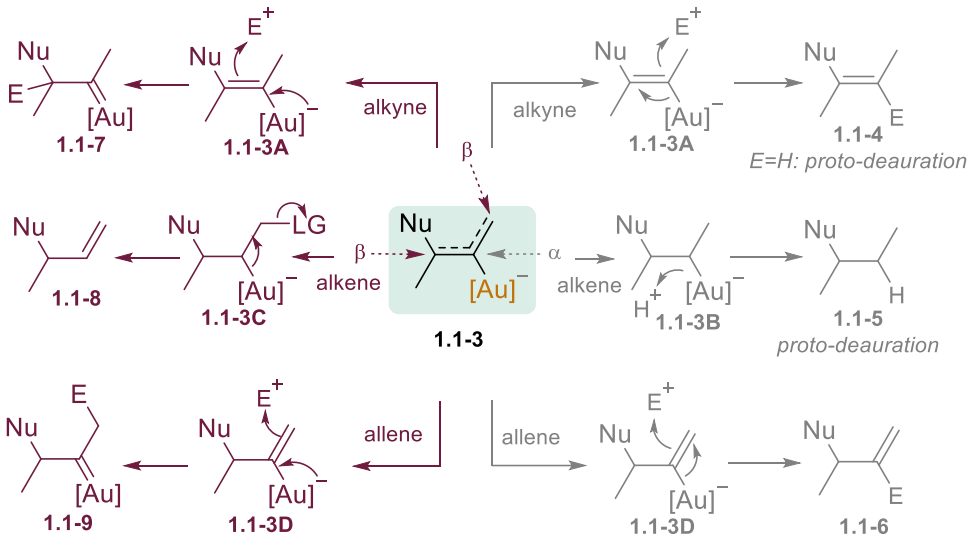

1.2 Bifunctional Ligands Enabled Gold Catalyzed Alkyne Isomerization

The first successful implementation of bifunctional biaryl-2-yl phosphine ligands in gold(I) catalysis was reported by our group in 2014.[22] As shown in **Scheme 4B**, in the form of a general base catalysis, an amide group at the 3'-position of the ligand **L1** directs and promotes nucleophilic attack at the gold -activated alkyne (**Scheme 4B**, proposed transition state), delivering product **1.2-3**. The cooperative activation of both nucleophile and alkyne is unprecedented in homogeneous gold catalysis, considering the spatial challenge of using ligand to reach anti-approaching nucleophile in a linear P-Au-alkyne centroid structure.

With such a ligand, the corresponding gold(I) catalyst becomes highly efficient in catalyzing acid addition to alkynes, with a turnover number up to 34400.

Scheme 4. The First Successful Implementation of Bifunctional Biaryl-2-yl Phosphine Ligand in Gold(I) Catalysis

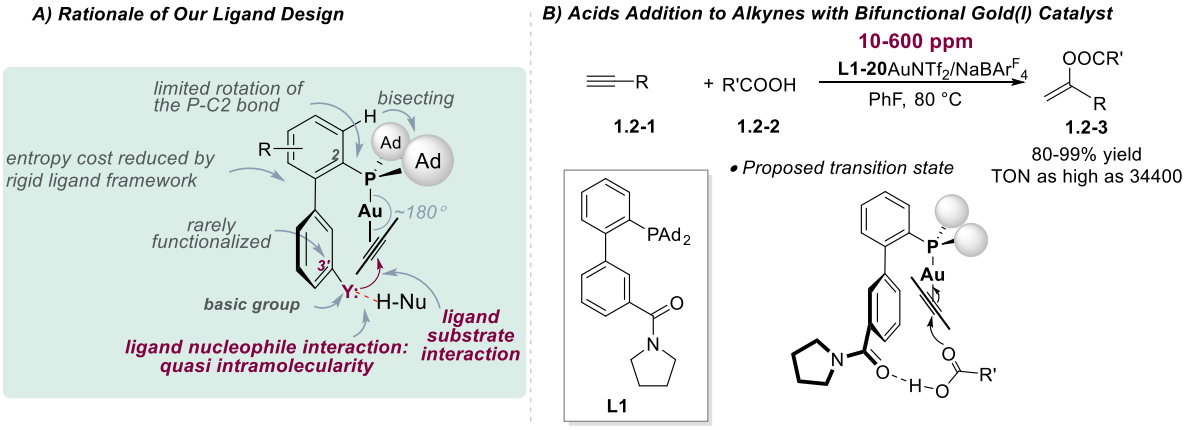

Later in 2014, our group envisioned that by installing an amino group at the bottom half of the pendant benzene ring in the type of biaryl-2-yl phosphine ligand, the amino group might be sufficiently basic to pick up the proton at the propargylic position, the acidity of which should be enhanced by the coordination of the Lewis acidic gold(I) catalyst. In the first successful implementation of this design, alkynes **1.2-4** were isomerized into conjugated dienes **1.2-5** with good to excellent *E*-selectivities under mild conditions by employing the 3,5-dimethyl piperidine-functionalized biphenyl-2-ylphosphine **L2** as the ligand (**Scheme 5A**).[23] In the proposed mechanism, using 1-phenyl-1-hexyne as an example (**Scheme 5B**), L2Au$^+$ would enable the desired propargylic (pK$_a$ >30 in DMSO) deprotonation even with a weak base (ligand aniline, pK$_a$ value in DMSO ~4). The *ipso*-

Scheme 5. The First Implementation of Soft Propargylic Deprotonation in Gold(I) Catalysis

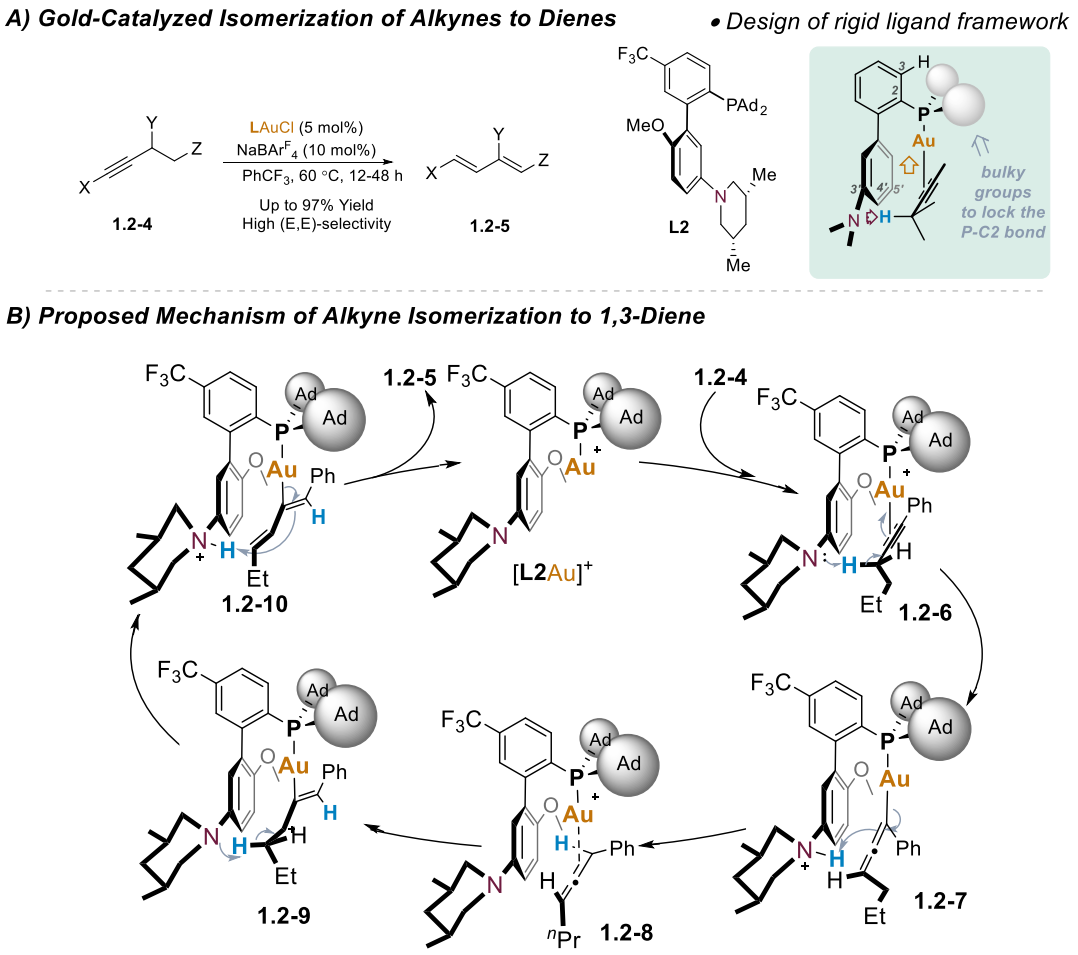

protodeauration of the thus-generated allenylgold intermediate **1.2-7**, and subsequent activation of the allene intermediate by the same Au(I) catalyst would lead to the formation of the gold(I)-substituted allylic cation **1.2-8**. The structure **1.2-9** would place the hydrogen *α*- to the allyl carbocation near the aniline nitrogen, enabling another facilitated proton abstraction. The resulting dienylgold intermediate **1.2-10** again undergoes *ipso*-protodeauration to deliver the diene product **1.2-5** and regenerate the catalyst. Later, in 2016, a DFT study supported the proposed mechanism and further revealed that the soft propargylic deprotonation followed a syn-periplanar process.[24]

In 2017, our group further applied this isomerization strategy to ynamides and allenylamides (**Scheme 6**) to afford dienylamide products.[25] Moreover, the synthesis of 1-amido-1,3-dienes from the gold catalyzed ynamide isomerization could be rendered in tandem with Diels-Alder reaction in one pot, enabling rapid assembly of versatile cyclic structures. The one-pot intermolecular Diels-Alder reaction of **1.2-10** and dienophile N-phenylmaleimide resulted in the cycloadduct **1.2-11** in 78% yield. In the case of terminating the reaction by an intermolecular Diels-Alder reaction, the ynamide **1.2-12** featuring an *α, β*-unsaturated sulfone moiety tethered at the nitrogen atom underwent this tandem process smoothly, affording the hexahydroindole **1.2-13** in 51% yield.

A major issue with the isomerization of aliphatic internal alkynes into dienes is the lack of regiochemical control in the formation of allene intermediates and their further isomerization to the products. To circumvent the regiochemical issues in the allene formation, in early 2017, our group employed the gold (I)-catalyzed [3,3]-rearrangement of propargylic esters to produce the carboxyallenes intermediate **1.2-17** regiospecifically

Scheme 6. Ligand Enabled Ynamides and Allenylamides Isomerizations and One-pot Cascade Reaction

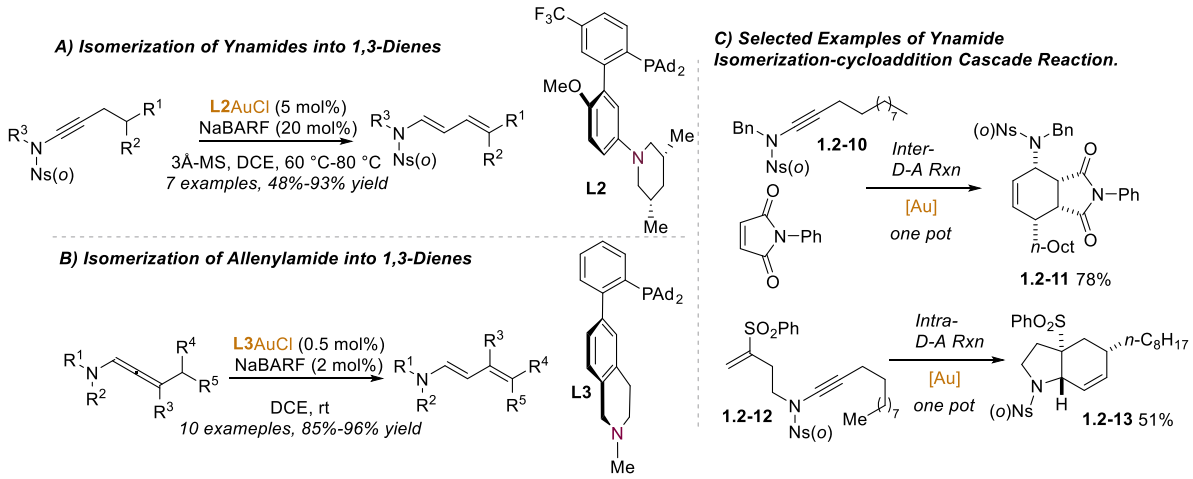

(**Scheme 7A**). [26] By positioning the ligand tertiary amino group at different locations (**Scheme 7B**) and changing the substrate steric, the isomerization of the in situ generated **1.2-17** could be achieved with opposite regioselectivities. As shown in **Scheme 7**, with pivalates substrates and ligand **L4**, which possess a bulky tertiary amine at the C3'–C5' level, the deprotonation occurred at the sterically less hindered Cα position of the vinyl oxocarbenium intermediate **1.2-18**, leading to the selective formation of the dienyl ester **1.2-15**. However, with ligand **L3**, which processed methyl-substituted nitrogen at a spatially lower position, and R replaced by a methyl group, the deprotonation occurred at Cα' of the vinyl oxocarbenium species, as shown in **1.2-18**. This study highlighted the importance of the positions for an amino group in a bifunctional biphenyl-2-ylphosphine ligands.

Scheme 7. Ligand-Controlled Regiodivergent and Stereoselective Isomerizations of Propargylic Esters

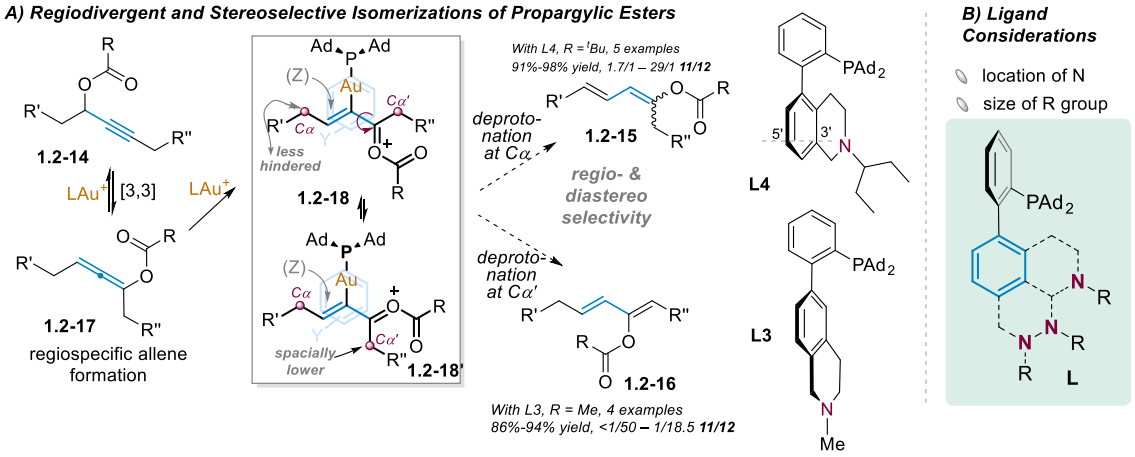

1.3 Synthesis of Electron Rich Furans

Furan is a very important heterocyclic unit[27-29] that widely exists in natural products and biologically important molecules[30, 31] and is often used as building blocks in material science

and organic synthesis.[32] Metal-catalyzed cycloisomerization of acetylenic ketones provides rapid access to 2-substituted and 2,5-disubstituted furans. The general ease of substrate preparation further enhances the synthetic utility of the approach. Previous literature has presented methods using either Pd or Cu catalysis at elevated temperatures (e.g., 100 ˚C) to catalyze the transformation of ynones into furans.[18,19] The proposed mechanism involves an in situ generated allenylic ketone intermediate **1.3-1**, which subsequently undergoes a metal-catalyzed cyclization to furnish the 2,5-disubstituted furan product. However, the reaction scopes are limited to generally alkyl/aryl-substituted furans. To the best of our knowledge, direct conversion of ynoates into valuable electron-rich 2-alkoxylfurans, and the more challenging synthesis of 2-aminofurans from acetylenic amides remained elusive at the time of our work.

Scheme 8. Isomerization of Acetylenic Ketone to Furan

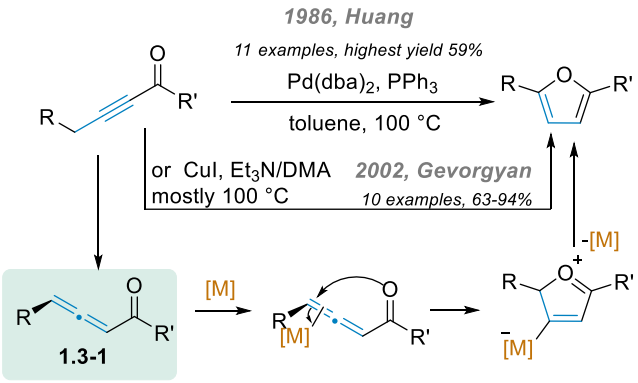

Highly electron-rich and hence reactive 2-aminofurans, devoid of stabilizing/ deactivating substituents,[33-37] are difficult to prepare despite the extensive applications of electron-rich 2-siloxy/alkoxyfurans.[38] A few scattered reports describing the access to a narrow subclass of these electron-rich are presented in the literature. These work have

established that those furans are unstable by exposure to air for a few hours[36] or decompose on silica gel column or upon recrystallization.[39]

In 1986, the Park group reported the synthesis of 5-aminofurans by reacting (aminocarbene)Iron complexes with alkynes.[39] In the proposed mechanism (**Scheme 9A**), the initial formation of a ferracyclobutene **(Scheme 9A**, **1.3-5)** could allow migratory insertion of CO and form the ferracyclopentenone/vinylketene **1.3-6**, subsequent α elimination and rearrangement of the dimethylamino unit results in a vinylcarbene complex (**1.3-7**), related to a ferracyclobutene (**1.3-8**). The latter intermediate reveals an iron-enolate

Scheme 9. Synthesis of Electron-rich Amino Furans

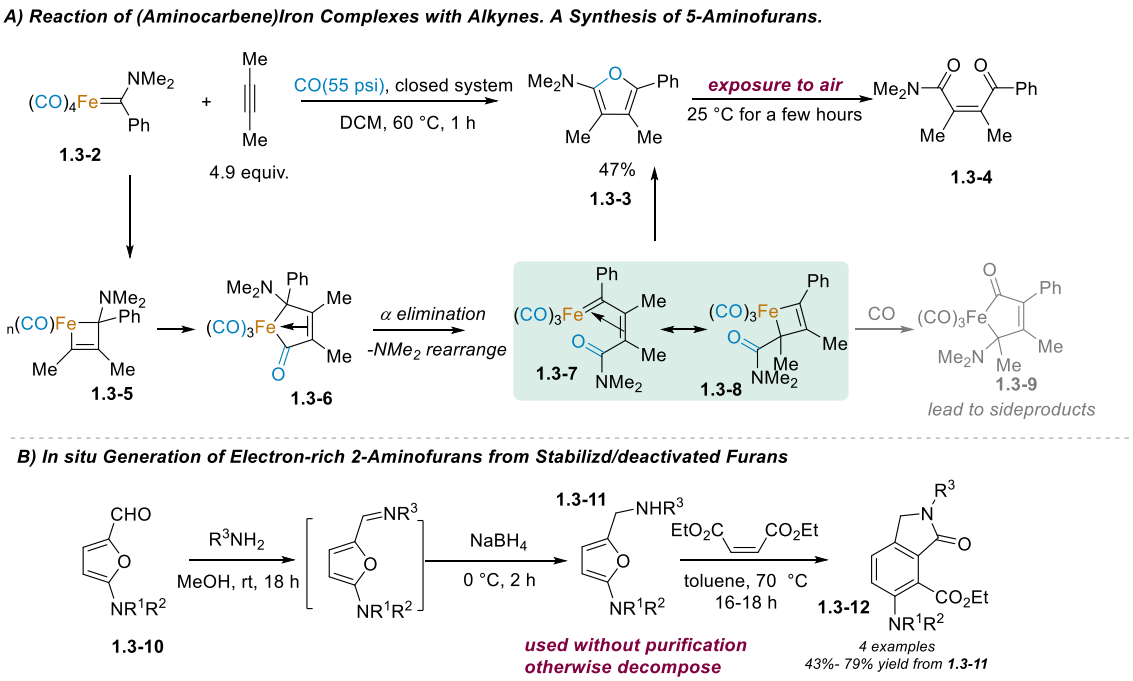

unit, coupling of the enolate oxygen with the original carbene carbon delivers the furan product **1.3-3**. The reaction yield of furan, however, suffered from side-product formation due to the incorporation of the reaction intermediate with multiple alkynes and carbon

monoxide. Except for the pre-mentioned low yielding, the synthetic utility was also largely limited by the use of toxic CO gas and the necessity of running reactions in a pressurized system for volatile substrates. Moreover, the author mentioned that the product **1.3-3** could undergo oxidation under air despite having a phenyl group acting as a deactivating/electron-withdrawing group, generating the diketone **1.3-4**. The other way to think about electron-rich furan synthesis is to start from a stabilized/non-electron-rich furan. For example, the Marque group reported the synthesis of 2-aminofurans starting from the parent 5-aminofuran-2-carbaldehydes **1.3-10**.[40] The author also mentioned that the in situ generated 2-aminofuran can easily undergo decomposition upon purification. Though the author performed one-pot synthesis starting from **1.3-10**, in most cases, only around 20% yield of the final adduct **1.3-12** could be obtained.

1.4. Designed Bifunctional Ligand Enabled Access to Electron-Rich Furans and Their Diels–Alder Reactions

1.4.1. Condition Study

In collaboration with our previous group member Dr. Xingguang Li, our group envisioned that the isomerization of acetylenic amide to allenylic amide could likewise (As shown in **Scheme 8**) be realized by a gold catalyst featuring our designed bifunctional ligands. As such, a sequence related to that in **Scheme 8** should permit for the first time access to highly electron-rich 2-aminofuran in a straightforward and expedient manner.

At the outset, the pyrrolidine-derived acetylenic amide **1.4-1a** was employed as the substrate for conditions optimization. We first tested the previously reported aniline ligand **L2**.[23] As shown in **Table 1**, entry 1, to our disappointment, the desired transformation did not occur

as expected. We attributed this to the deactivation of the gold catalyst by the initially formed electron-rich 2-amino furans. The 2-(1-pyrrolidino)furan product might be so electron-rich that it can trap and hence deactivate the gold catalyst. To circumvent this, 2.0 equivalent of *N*-phenylmaleiimide was added to trap the furan in situ via the Diels–Alder (D-A) reaction. To our delight, most of **1.4-1a** were consumed, and the bicyclic enamine **1.4-2a'** was formed in 23% NMR yield (entry 2). This product apparently results from the D-A adduct **1.4-4** of the anticipated 2-amino furans **1.4-3** and N-phenylmaleiimide as outlined in **Scheme 10**. Dehydrative aromatization of **1.4-4** would lead to the naphthalimide product **1.4-2a**, which, however, was barely detectable. Among our recently developed bifunctional ligands featuring a remote tertiary amino group (entries 3-5), L6 led to the best product yields, albeit a lower conversion, and in addition, the formation of **1.4-2a**. These results again highlighted the critical role of the positioning of the remote amino group, as previously mentioned in **Scheme 7**. Other typical gold catalysts (entries 6 and 7) and our previously developed amide-functionalized phosphine WangPhos give no desired product, revealing the critical effect of the basic ligand amino group. To promote dehydration for the reaction in entry 5, 3 Å molecular sieves were added, but the reaction was inhibited. With the addition of 2 equivalents of Boc_2O, the reaction was substantially improved to afford **1.4-2a** in 72% NMR yield along with 26% of **1.4-2a'** (entry 10). Running reaction under Ar had little impact on the reaction yield (entry 11). With extended reaction time, i.e., 30 hours (entry 12). **1.4-2a** was formed in 91% NMR yield and isolated in 86% yield, whilst no **1.4-2a**' remained.

Table 1. Condition Optimization

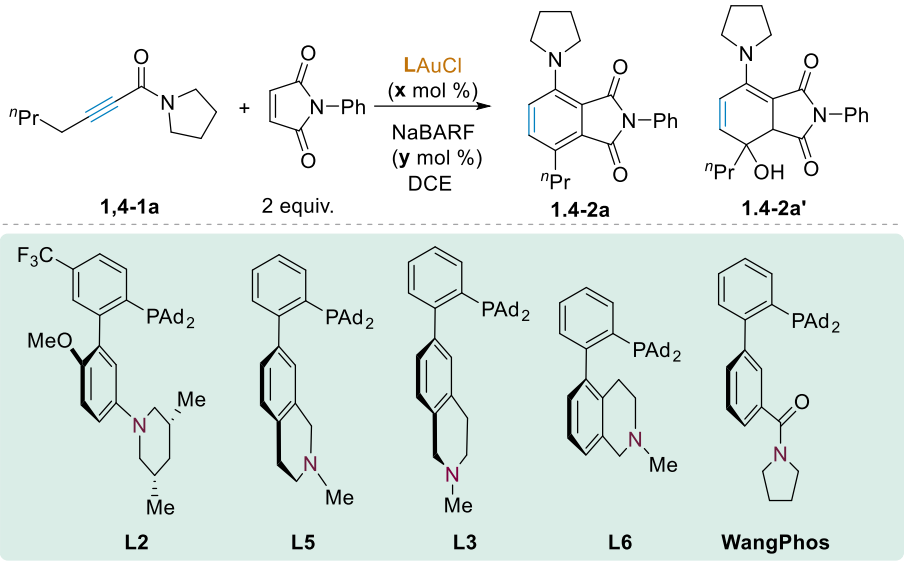

Entry	L	x(%)/y(%)	temp/time	additive	conversion	**1.4-2a/2a'**[b]
1[c]	**L2**	5/10	80 ˚C /15 h	-	7%	-
2	**L2**	5/10	80 ˚C /15 h	-	76%	<2%/23%
3	**L5**	5/10	80 ˚C /15 h	-	21%	-
4	**L3**	5/10	80 ˚C /15 h	-	20%	<2%/8%
5	**L6**	5/10	80 ˚C /15 h	-	54%	18%/35%
6	PPh_3	5/10	80 ˚C /15 h	-	20%	-
7	Johnphos	5/10	80 ˚C /15 h	-	20%	-
8	WangPhos	5/10	80 ˚C /15 h	-	20%	-
9	**L6**	5/10	80 ˚C /15 h	3Å MS	25%	-
10	**L6**	5/10	80 ˚C /15 h	Boc_2O[d]	100%	72%/26%
11[e]	**L6**	5/10	80 ˚C /15 h	Boc_2O[d]	100%	73%/26%
12	**L6**	5/10	80 ˚C /30 h	Boc_2O[d]	100%	91%[f]/0%

[a] All the reactions were run in 1,2-dichloroethane (DCE, 0.05M) in sealed vials. [b] Yield determined by NMR spectroscopy using triisopropylbenzene as the internal reference. [c] No N-phenylmaleiimide was added. [d] 2 equiv used. [e] Reaction run under Ar. [f] 86% yield of isolated product. M.S.=molecular sieves.

Scheme 10. Proposed Mechanism for the Formation of 1.4-2a and 1.4-2a'

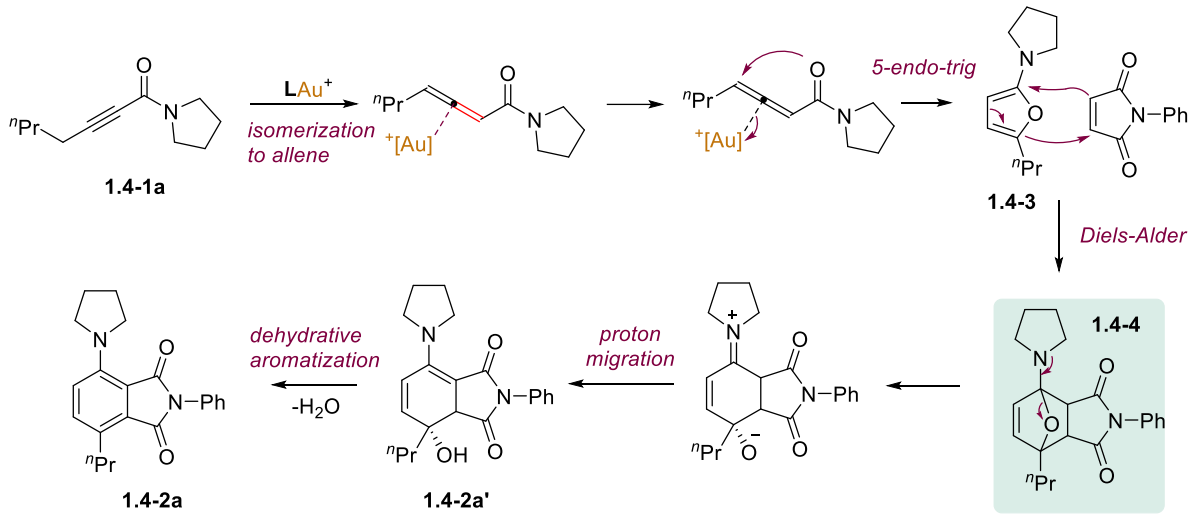

1.4.2. Sequential Cycloisomerization and Intermolecular D-A reaction

With the optimized reaction conditions in hand, we next examined the scope of this sequential gold-catalyzed cycloisomerization and intermolecular D-A reaction was studied by using *N*-phenylmaleiimide as the dienophile.

As shown in **Figure 3** (**1.4-2b** to **1.4-2g**), the ynamides can readily accommodate various *N*-substituents, including dimethylamino (**1.4-1b**), dibenzylamino (**1.4-1c**), piperidin-1-yl (**1.4-1d**), *N*-morpholinyl (**1.4-1e**), methyl(phenyl)amino (**1.4-1f**), and diphenylamino (**1.4-1g**), giving good to excellent yields ranging from 80 to 97%. Notably, N-phenyl substrates (**1.4-1f** and **1.4-1g**) exhibit better efficiencies. This phenomenon is consistent with phenyl being more electron-withdrawing, therefore lowering the basicity/electron-richness of the furan intermediate. However, the *N*,*N*-dibenzylynamides possessing a 6-OTIPS (**1.4-1h**), a 6-OAc (**1.4-1i**), a 6-*N*(Boc)Ts (**1.4-1j**), and a 5-OTBS group (**1.4-1k**) are less reactive than the nonfunctionalized counterpart **1.4-1c**. Despite requiring longer reaction times and higher catalyst loadings, the reactions still exhibited

Figure 3. Sequential Cycloisomerization and Intermolecular D-A reaction with N-Phenylmaleiimide.

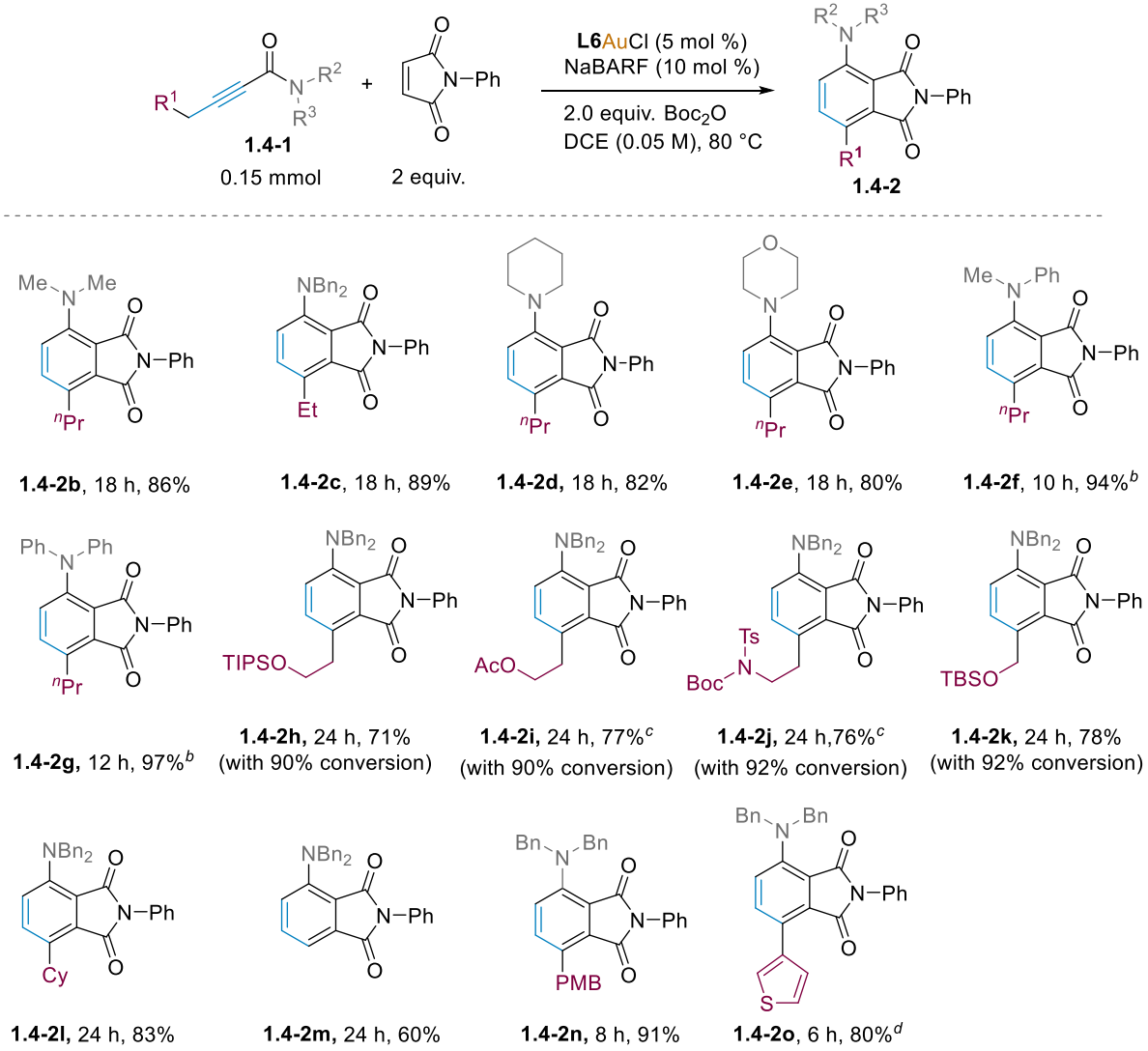

[b] Used 30 mg 3Å M.S. [c] Used 10 mol % **L4**AuCl and 20 mol % of NaBARF. [d] One equivalent of *N*-phenylphthalimide used.

good efficiencies. The alkynamide **1.4-1l**, featuring a sterically more hindered cyclohexyl group α to the C-C triple bond, underwent this tandem transformation smoothly, delivering **1.4-2**l in 83% yield. The substrate **1.4-1m** bearing no γ-substituent also reacted smoothly, providing the 3-amino substituted *N*-phenyl-phthalimide **1.4-2m** in a synthetically useful

yield. Substrates containing electron-donating aryl substituents at the γ-position reacted successfully, affording the biaryl products **1.4-2n** and **1.4-2o** in good to excellent yields.

The reactions of **1.4-1** bearing dialkyl or dibenzyl amino groups with less reactive dienophiles resulted in mostly little conversion, which is likely due to the inhibition of the gold catalysis by the electron-rich furan intermediate given the slow Diels-Alder reactions.

Scheme 11. Reactions of the Alkynamide 1.4-1f with Other Dienophiles

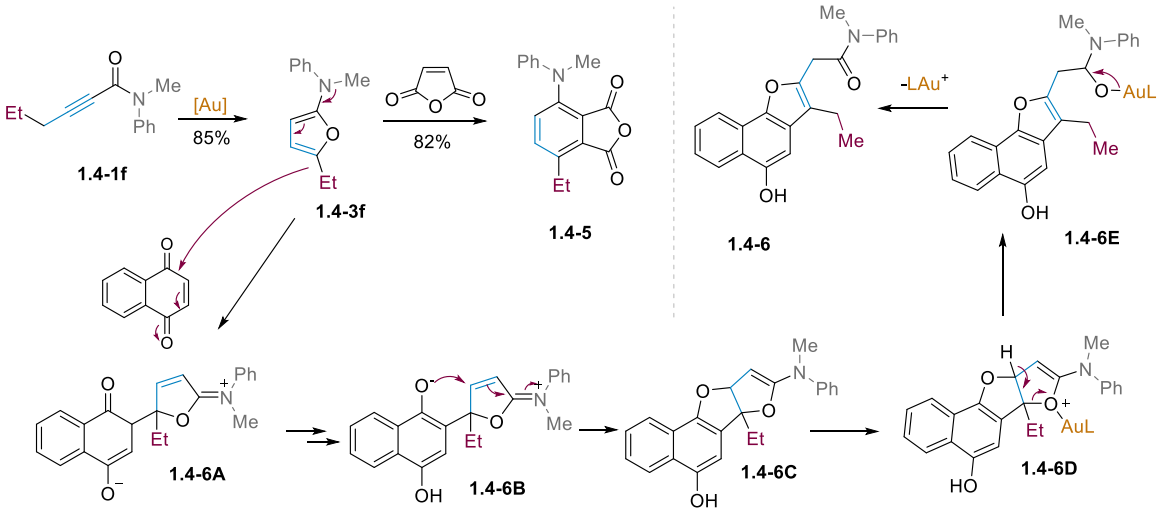

However, the comparatively less electron-rich 2-aminofuran **1.4-3f** could be generated from the *N*-phenyl-*N*-methylamide **1.4-1f** without any dienophile in 85% NMR yield (Scheme 11). Despite **1.4-3f** being sensitive to air and acid, we were able to purify it, albeit in 35% yield, by basic alumina column chromatography under an inert atmosphere, and fully characterize it. This result accredits our reaction design and supports the anticipated reaction mechanism. One-pot trapping of **1.4-3f** by maleic anhydride at room temperature afforded the anticipated phthalic anhydride **1.4-5** in 82% yield (Scheme 11). Notably, later in another project, one of our group members found our maleic anhydride has partial hydrolysis. The inhibition of the

gold-catalyzed cycloisomerization in the presence of maleic anhydride might also be attributed to the protonation of the amino group moiety on the ligand by the maleic acid inpurity. And Because of that, the soft propargylic deprotonation and subsequent cycloisomerization could not occur.

On the other hand, the one-pot reaction of **1.4-3f** with naphthoquinone led to no Diels-Alder adduct but the formation of the naphtho[1,2-b]furan **1.4-6** in 85% yield. A mechanism is proposed to rationalize its formation (**Scheme 11**). First, the nucleophilic Michael-type attack of the electron-rich **1.4-3f** on the naphthoquinone results in intermediate **1.4-6A**, which further undergoes aromatization to generate intermediate **1.4-6B**. Subsequently, the naphtholate oxygen undertakes another intramolecular attack, furnishing intermediate **1.4-6C**. With the help of Lewis acidic gold catalyst, the ring-opening of the intermediate **1.4-6C** finally leads to the product **1.4-6**.

1.4.3. Sequential Cycloisomerization and Intramolecular D-A reaction

The potential of rapid increase of molecular complexity by combining this furan formation with the intramolecular Diels-Alder reaction is also demonstrated. And in theory, facile intramolecular D-A reactions would permit the participation of a broader range of dienophiles. This is indeed the case. As shown in Scheme **12A**, the maleate-decorated *N*,*N*-dibenzylynamide **1.4-7a** was directly converted into the benzene-fused bicyclic lactone **1.4-8a** in a 75% isolated yield. On the contrary, the related intermolecular reaction between diethyl maleate and **1.4-1c** had little conversion. With a cinnamate moiety attached to the propynamide nitrogen atom (**1.4-7b** to **7d**), the tandem gold-catalyzed cycloisomerization, the Diels–Alder reaction, and dehydrative aromatization occurred with excellent efficiency (Scheme **12b** to **d**). The corresponding carbazole-4-carboxylate was formed more than 90%

yield upon isolation, delivering products with additional substitutions at the 3-position (**1.4-8c** and **1.4-8d**). Notably, in these reactions, no additive was needed, and the cinnamate moiety as a weak dienophile participated in the IMDA smoothly. Treatment of **1.4-8d** with TBAF leads to a tetracyclic structure **1.4-9** within 20 min.

Scheme 12. Scope Involving Intramolecular D-A Reactions

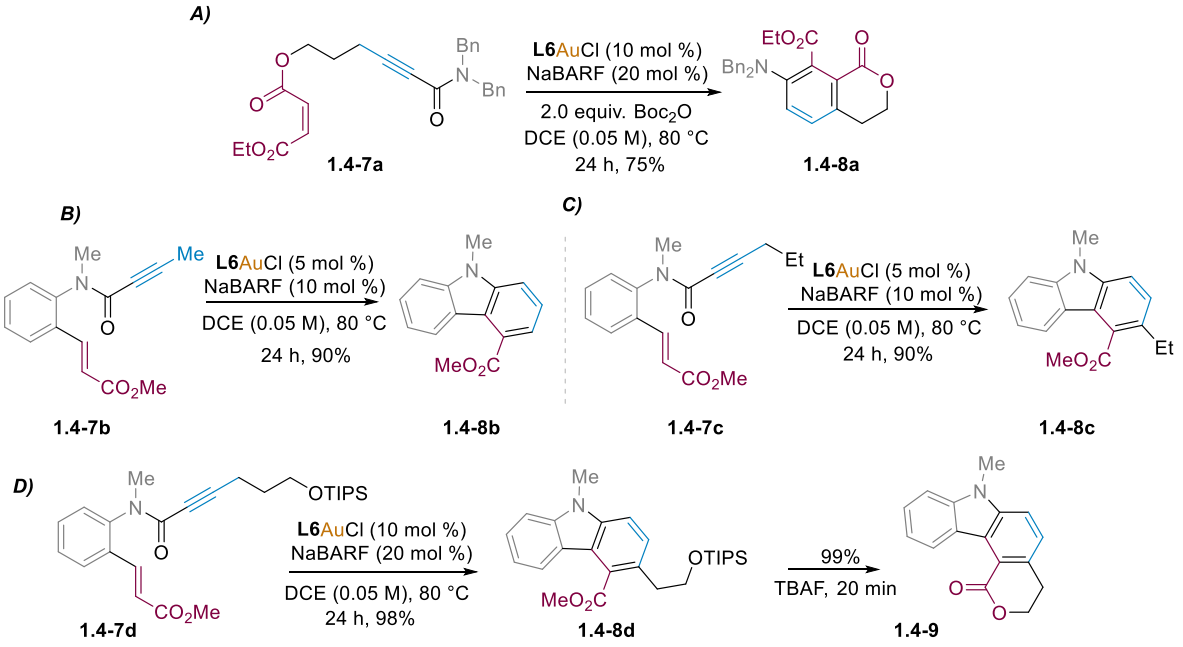

1.4.4. Conclusion

To sum up, we developed a gold-catalyzed in situ access to 2-aminofurans. The highly electron-rich nature of this class of furans makes it difficult to prepare them by other means but endows them with exceptional synthetic value. With bifunctional phosphine ligands specifically designed for cooperative gold catalysis, acetylenic amides are efficiently transformed into 2-aminofurans in a single step, which are further converted into functional

products in one pot. Combined with the ease of substrate preparation, this chemistry permits expedient studies of the synthetic utilities of these highly electron-rich and hence reactive furans.

1.5. Experimental Section

General. Ethyl acetate (ACS grade), hexanes (ACS grade) and diethyl ether (ACS grade) were purchased from Fisher Scientific and used without further purification. Anhydrous dichloromethane (HPLC grade), 1,2-dichloroethane (HPLC grade) were purified by distillation over calcium hydride. Toluene was distilled over sodium/benzophenone. Commercially available reagents were used without further purification. Reactions were monitored by thin layer chromatography (TLC) using Silicycle precoated silica gel plates. Flash column chromatography was performed over Silicycle silica gel (230-400 mesh). ^{1}H NMR and ^{13}C NMR spectra were recorded on Varian 400 MHz, 500 MHz and 600 MHz spectrometers using residue solvent peaks as internal standards ($CHCl_3$, ^{1}H: 7.26 ppm; ^{13}C: 77.16 ppm). Infrared spectra were recorded with a Perkin Elmer FT-IR spectrum 2000 spectrometer and are reported in reciprocal centimeter (cm^{-1}). Mass spectra were recorded with Xevo G2-XS QTOF Quadrupole Time-of-Flight Mass Spectrometry using electron spray ionization.

Preparation of Selected Substrates:

6-(Dibenzylamino)-6-oxohex-4-yn-1-yl ethyl maleate (1.4-7a)

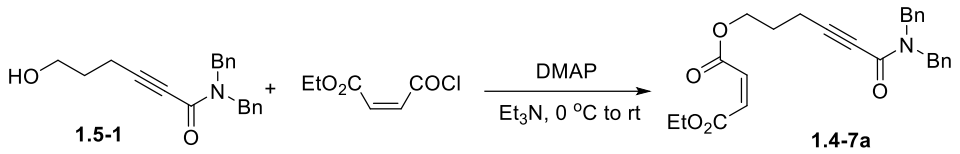

Ethyl (*Z*)-4-chloro-4-oxobut-2-enoate 1.4-**7a** was prepared according to the procedure for (*E*)-4-chloro-4-oxobut-2-enoate.[41] At 0 ˚C, to the solution of **1.5-1** (0.7 mmol) in DCM (10 mL) was added ethyl (Z)-4-chloro-4-oxobut-2-enoate (0.7 mmol), then Et_3N (1.5 equiv.) and DMAP (0.1 equiv.) were added subsequently. The mixture was stirred at rt for 2 h before adding brine (10 mL). The organic phase was dried with $MgSO_4$ and condensed. Further purification by chromatography gave the product 1.4-**7a** (166 mg, 55%). ^{1}H NMR (500 MHz, Chloroform-*d*) δ 7.43 – 7.14 (m, 10H), 6.81 (s, 2H), 4.66 (s, 2H), 4.50 (s, 2H), 4.34 – 4.19 (m, 4H), 2.49 (t, *J* = 7.1 Hz, 2H), 2.00 – 1.89 (m, 2H), 1.31 (t, *J* = 7.2 Hz, 2H). ^{13}C NMR (126 MHz, $CDCl_3$) δ 164.88, 164.80, 154.89, 136.32, 136.15, 134.12, 133.11, 128.93, 128.75, 128.51, 127.98, 127.70, 127.58, 91.70, 74.88, 63.59, 61.47, 51.40, 46.41, 26.91, 15.88, 14.19. IR (neat): 2982, 2938, 1721, 1631, 1496, 1423, 1260, 1030, 978, 733. MS-ESI (*m/z*): $[M+H]^+$ calcd. for $[C_{26}H_{28}NO_5]^+$, 434.1962; found 434.1948.

Methyl (E)-3-(2-(N-methylbut-2-ynamido)phenyl)acrylate (1.4-7b)

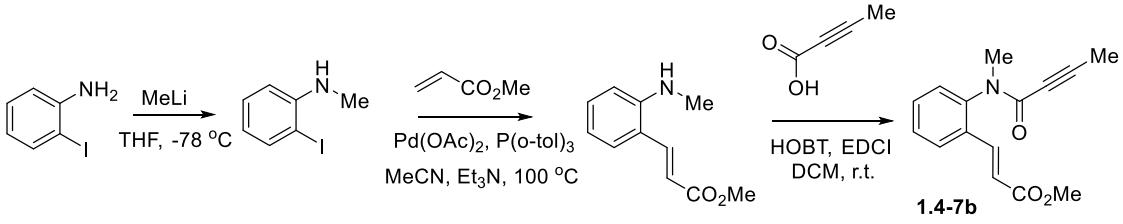

N-methyl-2-iodoaniline was prepared according to the procedure previously reported.[42] A mixture of N-methyl-2-iodoaniline (3.0g, 12.87 mmol) methylacrylate (1.33g, 15.44mmol), $Pd(OAc)_2$ (143.7 mg, 0.64 mmol), Et_3N (2.135 ml, 15.44 mmol), and $P(o\text{-}tol)_3$ (292mg, 0.96

mmol) in anhydrous CH_3CN (20 ml) was heated for 6 hrs in a tightly capped culture tube under Ar atmosphere. The mixture was portioned using Et_2O and a 1:1 mixture of 3 N HCl and brine. The crude product was purified by flash column chromatography, gave methyl (E)-3-(2-(dimethylamino) phenyl) acrylate (1.87g, 71%). 2-butynoic acid (168 mg, 2.0 mmol), EDCI (1.2 eq) and HOBT (0.1 eq) were added to a solution of methyl (E)-3-(2-(dimethylamino) phenyl) acrylate (1.0 eq) in DCM (0.25 M) at room temperature. The resulting solution was stirred at room temperature for 20 hours, quenched with $NaHCO_3$ (aq.) and extracted twice with DCM. The combined organic layers were washed with water and brine, dried over Na_2SO_4, concentrated in vacuo and purified by flash chromatography on silica gel to afford 1.4-**7b** in 62% yield (320 mg). ^{1}H NMR (500 MHz, Chloroform-d)(Major rotamer) δ 7.70 – 7.56 (m, 2H), 7.47 – 7.31 (m, 2H), 7.27 – 7.16 (m, 1H), 6.43 (d, J = 16.0, 1H), 3.79 (s, 3H), 3.23 (s, 3H), 1.65 (s, 3H). ^{13}C NMR (126 MHz, Chloroform-d) δ 166.86, 154.69, 142.53, 139.11, 132.81, 131.12, 129.53, 128.98, 127.46, 120.92, 90.54, 73.98, 51.99, 36.54, 3.93. IR (neat): 2998, 2225, 1702, 1624, 1364, 1270, 981, 775, 735, 594. $[M+Na]^+$ calcd. for $[C_{15}H_{15}NNaO_3]^+$, 280.0944; found 280.0953.

Methyl (E)-3-(2-(N-methylhex-2-ynamido)phenyl)acrylate (1.4-7c)

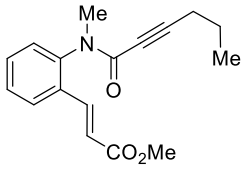

1.4-7c

Compound 1.4-**7c** was prepared according to the procedure for 1.4-7b by using 2-hexynoic acid (224 mg, 2 mmol) in the last step. Compound 1.4-**7c** was afforded in 65% yield (372 mg). ^{1}H NMR (500 MHz, Chloroform-d)) (Major rotamer) δ 7.71 – 7.56 (m, 2H), 7.46 – 7.31 (m, 2H), 7.27 – 7.15 (m, 1H), 6.42 (d, J = 16.0 Hz, 1H), 3.78 (s, 3H), 3.24 (s, 3H), 1.98

(t, J = 6.9 Hz, 2H), 1.16 (h, J = 7.2 Hz, 2H), 0.60 (t, J = 7.4 Hz, 3H). ^{13}C NMR (126 MHz, Chloroform-d) δ 166.81, 154.72, 142.67, 139.08, 132.90, 131.10, 129.55, 128.93, 127.37, 120.89, 94.55, 74.93, 51.95, 51.95, 36.42, 20.96, 20.68, 13.11. IR (neat): 2964, 2223, 1716, 1634, 1272, 1171, 1036, 763, 733, 589. [M+Na] $^{+}$ calcd. for [$C_{17}H_{19}NNaO_3$] $^{+}$, 308.1257; found 308.1255.

Methyl (E)-3-(2-(N-methyl-6-((triisopropylsilyl)oxy)hex-2ynamido)phenyl) acrylate (1.4-7d)

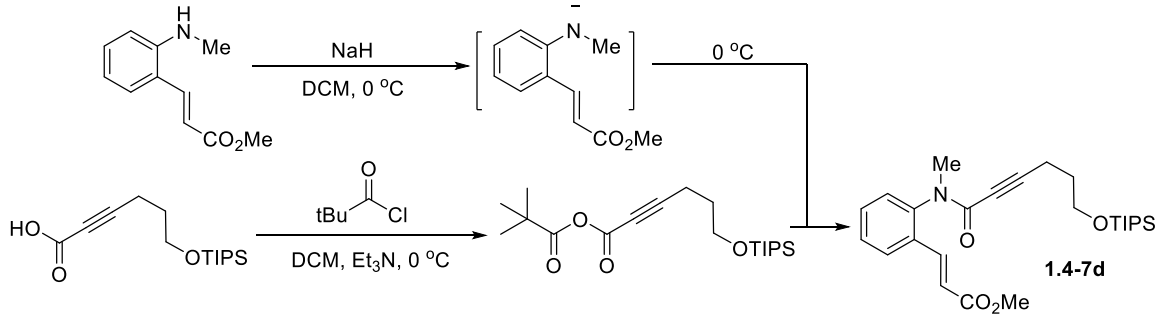

1.0 equiv. N-methyl-2-iodoaniline methylacrylate (235mg, 1.23 mmol) was dissolved in 6 ml DCM under Ar atmosphere, NaH 60% in oil (73.8mg, 1.84 mmol) was added at 0 ˚C, the reaction mixture was stirring at room temperature for another 45 minutes. 2.0 equiv. 6-((triisopropylsilyl)oxy) hex-2-ynoic acid (700 mg, 2.46 mmol) was dissolved in 6 ml DCM under Ar in a flame-dried round-bottomed flask, Et_3N (273 mg, 2.70 mmol), pivaloyl chloride (326 mg, 2.70 mmol) was added subseqyently. The reaction mixture was stirring for 20 minutes. After that, the mixture was cooled to 0 ˚C, then deprotonated N-methyl-2-iodoaniline methylacrylate solution was transferred to the reaction via cannula at 0 ˚C. The reaction was stirred overnight. 1.4-**7d** (350 mg, 62%) was obtained by flash chromatography. ^{1}H NMR (500 MHz, Chloroform-d) (Major rotamer) δ 7.72 – 7.57 (m, 2H), 7.48 – 7.35 (m, 2H), 7.26 (m, 1H), 6.44 (d, J = 16.0, 1H), 3.80 (s, 3H), 3.39 (t, J = 5.8 Hz, 2H), 3.25 (s, 3H),

2.15 (t, J = 7.0 Hz, 2H), 1.40 – 1.29 (m, 2H), 1.11 – 1.04 (m, 3H), 0.99 (d, J = 3.2 Hz, 18H). ^{13}C NMR (126 MHz, Chloroform-d) δ 166.75, 154.63, 142.67, 139.01, 132.84, 131.03, 129.59, 128.92, 127.32, 120.89, 94.58, 74.68, 61.26, 51.94, 36.42, 31.00, 18.10, 18.03, 18.02, 15.17, 11.96. IR (neat): 2943, 2865, 2225, 1719, 1640, 1171, 1104, 882, 733, 680. . [M+Na] $^{+}$ calcd. for [$C_{26}H_{39}NNaO_4Si$] $^{+}$, 480.2541; found 480.2537.

Gold-Catalyzed Intermolecular Ynamide Isomerization and D-A Reactions with Dienophiles

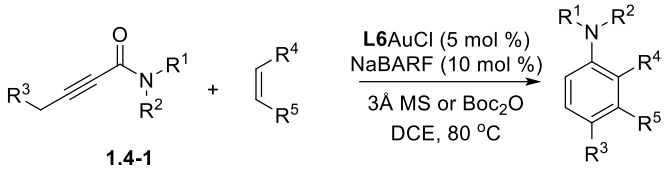

1.4-1 1.4-2

General procedure A: To a dried, Ar protected Schlenk tube were added sequentially 0.15 mmol ynamide **1.4-1,** 0.30 mmol dienophile (2 equiv.), 0.0075/0.0150 mmol **L6**AuCl (5 mol % or 10 mol % for some cases), 3Å molecular sieves, or 2.0 equiv. of Boc_2O, and 3 mL anhydrous DCE. 0.015 or 0.030 mmol NaBARF (10 mol % or 20 mol % for some cases) was added last. The reaction was then sealed and heated at 80 ˚C for 12-24 h. The reaction progress was monitored by TLC or NMR. After completion, the reaction mixture was concentrated under reduced pressure. Pure product 1.4-2 was obtained through silica gel flash chromatography.

Characterization Data for Selected Products:

2-Phenyl-4-propyl-7-(pyrrolidin-1-yl)isoindoline-1,3-dione (1.4-2a)

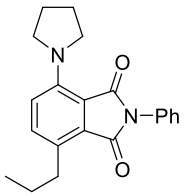

1.4-2a

Compound 1.4-**2a** was prepared by following general procedure A. The reaction was heated at 80 ˚C for 18 h using **L6AuCl** (5 mol %), NaBARF (10 mol %) and Boc_2O (2 equiv.) to give 1.4-**2a** (36.6 mg) in 73% yield. ^{1}H NMR (500 MHz, Chloroform-*d*) δ 7.52 – 7.45 (m, 2H), 7.45 – 7.40 (m, 2H), 7.38 – 7.33 (m, 1H), 7.30 (d, *J* = 8.8 Hz, 1H), 6.96 (d, *J* = 8.7 Hz, 1H), 3.64 – 3.54 (m, 4H), 3.07 – 2.96 (m, 2H), 2.03 – 1.94 (m, 4H), 1.72 – 1.61 (m, 2H), 0.98 (t, *J* = 7.3 Hz, 3H). ^{13}C NMR (126 MHz, $CDCl_3$) δ 168.04, 166.93, 145.52, 137.14, 132.49, 131.86, 129.72, 128.97, 127.66, 127.13, 120.91, 111.45, 51.91, 32.75, 25.93, 24.33, 14.14. IR (neat): 2960, 2929, 2869, 1702, 1642, 1501, 1375, 1190, 1115, 939, 765. MS-ESI (*m/z*): $[M+H]^+$ calcd. for $[C_{21}H_{23}N_2O_2]^+$, 335.1754; found 335.1741.

4-Hydroxy-2-phenyl-4-propyl-7-(pyrrolidin-1-yl)-3a,4-dihydro-1H-isoindole-1,3(2H)-dione (1.4-2a')

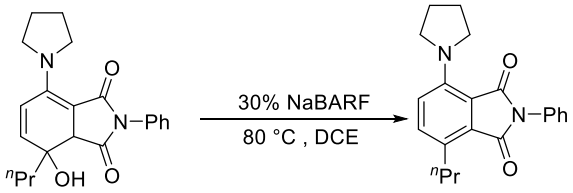

1.4-2a' 1.4-2a

Compound 1.4-2a' was separated from compound 1.4-2a by column chromatography. Compound **2a'** was converted to Compound **2a** with 30% NaBARF as an additive at 80 ˚C in DCE overnight. This result shows 1.4-2a can be obtained via dehydrative aromatization from 1.4-2a'.

4-Ethyl-7-(methyl(phenyl)amino)-2-phenylisoindoline-1,3-dione (1.4-2f)

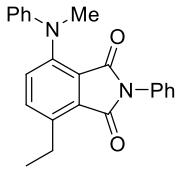

1.4-2f

Compound **2f** was prepared following general procedure A. The reaction was heated at 80 ˚C for 12 h using **L6AuCl** (5 mo l%), NaBARF (10 mol %) and 3Å molecular sieves to give **2f** (50.2 mg) in 94% yield. ^{1}H NMR (400 MHz, Chloroform-*d*) ^{1}H NMR (400 MHz, Chloroform-*d*) δ 7.53 – 7.32 (m, 7H), 7.30 – 7.21 (m, 2H), 6.98 – 6.94 (m, 3H), 6.93 – 6.89 (m, 3H), 3.45 (s, 2H), 3.17 (q, *J* = 7.5 Hz, 3H), 1.33 (t, *J* = 7.5 Hz, 3H). ^{13}C NMR (101 MHz, cdcl$_3$) δ 167.55, 165.44, 148.12, 145.35, 140.46, 136.46, 132.58, 131.93, 129.60, 129.21, 129.05, 127.94, 126.87, 122.88, 120.58, 117.35, 41.05, 24.39, 15.08. IR (neat): 2966, 2931, 1708, 1643, 1493, 1379, 1188, 893,746. MS-ESI (*m/z*): $[M+Na]^+$ calcd. for $[C_{23}H_{20}N_2O_2Na]^+$, 379.1417; found 379.1418.

4-(Diphenylamino)-2-phenyl-7-propylisoindoline-1,3-dione (1.4-2g)

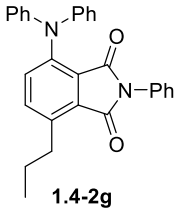

1.4-2g

Compound 1.4-**2g** was prepared following general procedure A. The reaction was heated at 80 ˚C for 12 h using **L6AuCl** (5 mol %), NaBARF (10 mol %) and 3Å molecular sieves to give 1.4-**2g** (62.9 mg) in 97% yield. ^{1}H NMR (400 MHz, Chloroform-*d*) δ 7.48 – 7.37 (m,

3H), 7.35 – 7.22 (m, 8H), 7.13 – 7.01 (m, 6H), 3.19 – 3.02 (m, 2H), 1.83 – 1.67 (m, 2H), 1.05 (t, *J* = 7.3 Hz, 3H). ^{13}C NMR (101 MHz, $CDCl_3$) δ 167.47, 164.28, 147.85, 143.37, 139.09, 137.40, 133.52, 131.86, 129.88, 129.31, 128.92, 127.73, 126.78, 123.65, 123.47, 123.45, 33.19, 24.23, 14.21. IR (neat): 3035, 2931, 1765, 1715, 1588, 1487, 1376, 1296, 1193, 1114, 753. MS-ESI (*m/z*): $[M+H]^+$ calcd. for $[C_{29}H_{25}N_2O_2]^+$, 433.1880; found 433.1881.

4-(Dibenzylamino)-2-phenylisoindoline-1,3-dione (1.4-2m)

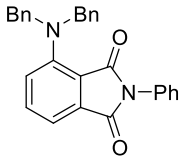

1.4-2m

Compound 1.4-**2m** was prepared following general procedure A. The reaction was heated at 80 ˚C for 24 h using **L6AuCl** (5 mol %), NaBARF (10 mol %) and Boc_2O (2 equiv.) to give 1.4-**2m** (37.6 mg) in 60% yield. ^{1}H NMR (500 MHz, Chloroform-d) δ 7.54 – 7.15 (m, 18H), 4.64 (s, 4H). ^{13}C NMR (126 MHz, Chloroform-d) δ 167.44, 166.95, 149.73, 137.63, 135.13, 134.73, 132.13, 129.15, 128.66, 128.07, 128.03, 127.45, 127.01, 125.41, 117.04, 115.37, 56.58. IR (neat):2923, 1701, 1612, 1484, 1377, 1112,736, 690. MS-ESI (*m/z*): $[M+H]^+$ calcd. for $[C_{28}H_{23}N_2O_2]^+$, 419.1754; found 419.1746.

4-(Dibenzylamino)-7-(4-methoxyphenyl)-2-phenylisoindoline-1,3-dione (1.4-2n)

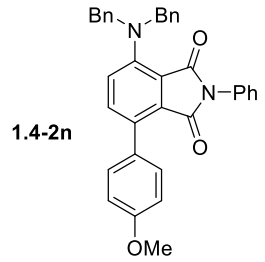

1.4-2n

Compound 1.4-**2n** was prepared following general procedure A. The reaction was heated at 80 ˚C for 8 h using **L6AuCl** (5 mol %), NaBARF (10 mol %) and Boc_2O (2 equiv.) to give 1.4-**2n** (70 mg) in 91% yield. ^{1}H NMR (500 MHz, Chloroform-d) δ 7.46 (m, 7H), 7.33 – 7.20 (m, 12H), 6.99 – 6.88 (m, 2H), 4.62 (s, 4H), 3.84 (s, 3H). ^{13}C NMR (126 MHz, cdcl3) δ 166.99, 166.42, 159.72, 148.71, 137.76, 137.45, 133.17, 132.10, 130.92, 129.05, 128.98, 128.95, 128.66, 128.17, 127.88, 127.44, 127.10, 125.91, 118.28, 113.50, 56.79, 55.41. IR (neat): 1706, 1607, 1376, 1178, 765, 739,692. MS-ESI (*m/z*): $[M+Na]^+$ calcd. for $[C_{35}H_{28}N_2NaO_3]^+$, 547.1992; found 549.1976.

4-Ethyl-7-(methyl(phenyl)amino)isobenzofuran-1,3-dione (1.4-5)

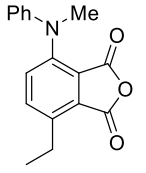

1.4-5

To a dried, Ar protected schlenk tube were added sequentially 0.15 mmol ynamide 1.4-**1f**, 0.0075 mmol **L6**AuCl (5 mol %), 0.015 mmol NaBARF (10 mol %) and 3 mL anhydrous DCE as solvent. The reaction was then heated at 80 ˚C for 10 h. Maleic anhydride (2 equiv.) was added and stirred for another 5 h at room temperature. The reaction was concentrated under reduced pressure. The residue was purified through silica gel flash chromatography to deliver **1.4-5** (34.6 mg) in 82% yield. ^{1}H NMR (500 MHz, Chloroform-*d*) δ 7.32 – 7.25 (m,

8H), 7.23 – 7.19 (m, 2H), 7.16 (d, *J* = 8.2 Hz, 1H), 7.10 (d, *J* = 8.2 Hz, 1H), 4.56 – 4.36 (m, 4H), 4.16 (s, 4H), 2.95 (t, *J* = 6.0 Hz, 2H), 1.35 (t, *J* = 7.2 Hz, 3H). ^{13}C NMR (126 MHz, $CDCl_3$) δ 168.40, 163.31, 148.43, 137.68, 135.50, 135.08, 129.14, 128.75, 128.35, 128.25, 127.23, 123.45, 67.10, 61.99, 57.96, 27.79, 14.01. IR (neat): 3038, 2971, 2934, 1834, 1766, 1597, 1495, 1210, 910, 755. MS-ESI (*m/z*): $[M+H]^+$ calcd. for $[C_{17}H_{16}NO_3]^+$, 282.1125; found 282.1132.

5-Ethyl-N-methyl-N-phenylfuran-2-amine (1.4-3f)

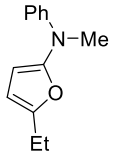

1.4-3f

To a dried, Ar protected Schlenk tube were added sequentially 0.15 mmol ynamide **1f**, 0.0075 mmol **L4**AuCl (5 mol%), 0.015 mmol NaBARF (10 mol%) and 3 mL anhydrous DCE as solvent. The reaction was then heated at 80 ˚C for 12 h. After cooling to room temperature. 0.05 mmol 1,3,5-trimethoxy benzene solution was injected under Ar as an internal reference. The NMR tube was pumped with Ar in advance and sealed with PTFE tape after loading the sample. The given NMR yield is 85%. The same reaction was performed again to get the purified product, and it was also finished in 12 hrs. Silica gel was added upon completion, and the solvent was removed under a vacuum. A chromatography under Ar gives the oxygen-sensitive furan intermediate **1.4-3f** in about 30% isolated yield due to inevitable air exposure during the process. ^{1}H NMR (500 MHz, Chloroform-*d*) δ 7.23 (t, J = 7.5 Hz, 2H), 6.87 – 6.81 (m, 3H), 5.95 (d, J = 1.8 Hz, 1H), 5.78 (d, J = 3.1 Hz, 1H), 3.25 (s, 3H), 2.60 (q, J = 7.6 Hz, 2H), 1.22 (t, J = 7.5 Hz, 3H). ^{13}C NMR (126 MHz, $CDCl_3$)

δ 153.00, 152.67, 148.11, 129.04, 119.44, 114.95, 104.78, 99.32, 39.17, 21.65, 12.24. 2D NMR COSY, HSQC, and HMBC are also attached. IR (neat): 2920, 1498, 1127, 749, 691, 497. MS-ESI (m/z): $[M+H]^+$ calcd. for $[C_{13}H_{16}NO]^+$,202.1226; found 202.1232.

2-(3-Ethyl-5-hydroxynaphtho[1,2-*b*]furan-2-yl)-*N*-methyl-*N*-phenylacetamide (1.4-6)

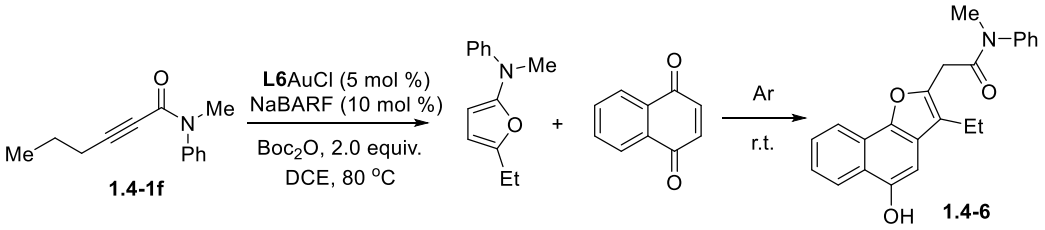

To a dried, Ar protected schlenk tube were added sequentially 0.15 mmol ynamide 1.4-**1f**, 0.0075 mmol **L6**AuCl (5 mol %), 0.015 mmol NaBARF (10 mol%), Boc_2O and 3 mL anhydrous DCE. The reaction was heated at 80 ˚C for 12 h, and was allowed to be cooled to room temperature, 0.30 mmol naphthalene-1,4-dione (2 equiv.) was added subsequently under Ar atmosphere. After 2 more hours at room temperature. The reaction was concentrated under reduced pressure. The residue was purified through silica gel flash chromatography to give **6** (45.8 mg) in 85% yield. ^{1}H NMR (500 MHz, Chloroform-d) δ 8.18 (d, J = 8.3 Hz, 1H), 8.00 (d, J = 8.1 Hz, 1H), 7.52 – 7.30 (m, 8H), 6.55 (s, 1H), 3.65 (s, 2H), 3.41 (s, 3H), 2.15 (q, J = 7.6 Hz, 2H), 0.97 (t, J = 7.6 Hz, 3H). ^{13}C NMR (126 MHz, Chloroform-d) δ 169.87, 147.91, 145.41, 144.36, 143.74, 130.11, 128.38, 127.56, 126.05, 123.78, 123.68, 123.08, 122.96, 121.33, 120.30, 119.71, 38.22, 32.70, 16.70, 14.60. IR (neat): 3269 (broad peak), 2965, 1634, 1421, 1247, 1223, 1125, 1071, 765, 699, 557. MS-ESI (*m/z*): $[M+Na]^+$ calcd. for $[C_{23}H_{21}NNaO_3]^+$,382.1414; found 382.1415.

Gold Catalyzed Intramolecular Ynamide Isomerization and D-A reactions

General procedure B: To a dried, Ar protected Schlenk tube were added sequentially 0.15 mmol ynamide **1.4-7**, 0.0075-0.0150 mmol **L6**AuCl (5 mol % or 10 mol % in some cases), 0.015-0.030 mmol NaBARF (10 mol% or 20 mol % in some cases), Boc_2O (2.0 equiv. in some cases) and 3 mL anhydrous DCE as the solvent. The reaction was then heated at 80 ˚C for 24 h and monitored by TLC or NMR. The reaction was concentrated under reduced pressure. The residue was purified through silica gel flash chromatography to yield pure product 7-**8**.

7-(Dibenzylamino)-8-ethylisochroman-1-one (1.4-8a)

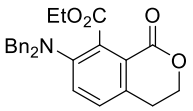

1.4-8a

Compound 1.4-**8a** was prepared following general procedure B. The reaction was heated at 80 ˚C for 24 h using **L6AuCl** (10 mol %), NaBARF (20 mol %) and Boc_2O (2 equiv.), furnishing 1.4-**8a** (46.7 mg) in 75% yield. ^{1}H NMR (500 MHz, Chloroform-*d*) ^{1}H NMR (500 MHz, Chloroform-*d*) δ 7.31 – 7.26 (m, 8H), 7.21 (t, *J* = 6.7 Hz, 2H), 7.16 (d, *J* = 8.3 Hz, 1H), 7.10 (d, *J* = 8.2 Hz, 1H), 4.50 – 4.45 (m, 4H), 4.16 (s, 4H), 2.95 (t, *J* = 6.0 Hz, 2H), 1.35 (t, *J* = 7.2 Hz, 3H). ^{13}C NMR (126 MHz, $CDCl_3$) δ 168.40, 163.31, 148.43, 137.68, 135.50, 135.08, 129.14, 128.75, 128.35, 128.25, 127.23, 123.45, 67.10, 61.99, 57.96, 27.79, 14.01. IR (neat): 3063, 3029, 2984, 1728, 1632, 1495, 1283, 1127, 1027, 961, 742. MS-ESI (*m/z*): $[M+H]^+$ calcd. for $[C_{26}H_{26}NO_4]^+$, 416.1856; found 416.1861.

Methyl 9-methyl-9H-carbazole-4-carboxylate (1.4-8b)

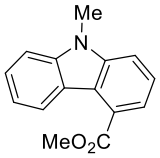

1.4-8b

Compound 1.4-**8b** was prepared following general procedure B. The reaction was heated at 80 ˚C for 24 h using **L6AuCl** (5 mol %) and NaBARF (10 mol %), Compound 1.4-**8b** (32.3 mg) was obtained in 90% yield. ^{1}H NMR (500 MHz, Chloroform-d) δ 8.89 (dt, J = 8.2, 1.0 Hz, 1H), 7.87 (dd, J = 7.5, 1.0 Hz, 1H), 7.60 (dd, J = 8.3, 1.0 Hz, 1H), 7.54 (ddd, J = 8.2, 7.0, 1.2 Hz, 1H), 7.50 (dd, J = 8.2, 7.5 Hz, 1H), 7.42 (dt, J = 8.3, 0.9 Hz, 1H), 7.29 (ddd, J = 8.1, 7.0, 1.1 Hz, 1H), 4.08 (s, 3H), 3.86 (s, 3H). ^{13}C NMR (126 MHz, Chloroform-d) δ 168.59, 141.84, 141.78, 126.83, 125.74, 125.37, 124.68, 122.21, 121.49, 121.48, 119.39, 112.74, 108.33, 52.26, 29.27. IR (neat): 2921, 1711, 1439, 1255, 1074, 742, 719. MS-ESI (*m/z*): $[M+H]^+$ calcd. for $[C_{15}H_{14}NO_2]^+$, 240.1019; found 240.1038.

Methyl 3-ethyl-9-methyl-9H-carbazole-4-carboxylate (1.4-8c)

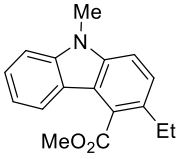

1.4-8c

Compound 1.4-**8c** was prepared following general procedure B. The reaction was heated at 80 ˚C for 24 h using **L6AuCl** (5 mol %) and NaBARF (10 mol %) to deliver 1.4-**8c** (44.8 mg) in 90% yield. ^{1}H NMR (400 MHz, Chloroform-d) δ 7.92 (dt, J = 8.0, 1.2 Hz, 1H), 7.48 (ddd, J = 8.2, 7.1, 1.2 Hz, 1H), 7.41 – 7.30 (m, 3H), 7.21 (ddd, J = 8.1, 7.1, 1.1 Hz, 1H), 4.12 (s, 3H), 3.80 (s, 3H), 2.84 (q, J = 7.6 Hz, 2H), 1.32 (t, J = 7.6 Hz, 3H). ^{13}C NMR (151 MHz, Chloroform-d) δ 170.64, 141.55, 139.51, 132.27, 126.63, 126.12, 125.73, 121.64, 121.03,

119.21, 119.15, 110.24, 108.66, 52.37, 29.18, 26.75, 16.84. IR (neat): 2962, 1716, 1467, 1253, 1086, 818, 744, 725. MS-ESI (*m/z*): $[M+Na]^+$ calcd. for $[C_{17}H_{17}NNaO_2]^+$, 290.1151; found 290.1167.

Methyl 9-methyl-3-(2-((triisopropylsilyl)oxy)ethyl)-9H-carbazole-4-carboxylate (1.4-8d)

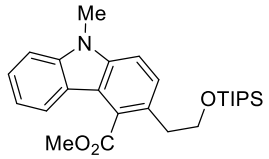

1.4-8d

Compound **1.4-8d** was prepared following general procedure B. The reaction was heated at 80 ˚C for 24 h using **L6AuCl** (10 mol %) and NaBARF (20 mol %) to deliver 1.4-**8d** (64.6 mg) in 98% yield. ^{1}H NMR (600 MHz, Chloroform-d) δ 7.90 (d, J = 7.9 Hz, 1H), 7.53 – 7.46 (m, 1H), 7.43 – 7.37 (m, 3H), 7.23 – 7.19 (m, 1H), 4.11 (s, 3H), 3.94 (t, J = 7.5 Hz, 2H), 3.83 (s, 3H), 3.07 (t, J = 7.5 Hz, 2H), 1.19 – 0.95 (m, 21H). ^{13}C NMR (151 MHz, Chloroform-d) δ 170.44, 141.52, 139.82, 128.30, 126.84, 126.57, 126.18, 121.66, 121.04, 119.28, 119.24, 109.96, 108.70, 65.24, 52.46, 37.40, 29.23, 18.16, 12.13. IR (neat): 2944, 2865, 1720, 1465, 1257, 1091, 882, 816, 741, 683, 641. MS-ESI (m/z): [M+Na]+ calcd. for $[C_{26}H_{37}NNaO_3Si]$+, 462.2435; found 462.2444.

1.6 References

1. Hashmi, A. S. K., Gold-catalyzed organic reactions. *Chemical Reviews* **2007,** *107* (7), 3180-3211.

2. Norman, R. O.; Parr, W. J.; Thomas, C. B., The reactions of alkynes, cyclopropanes, and benzene derivatives with gold (III). *Journal of the Chemical Society, Perkin Transactions 1* **1976,** (18), 1983-1987.

3. Fukuda, Y.; Utimoto, K., Effective transformation of unactivated alkynes into ketones or acetals with a gold (III) catalyst. *The Journal of Organic Chemistry* **1991,** *56* (11), 3729-3731.

4. Teles, J. H.; Brode, S.; Chabanas, M., Cationic gold (I) complexes: highly efficient catalysts for the addition of alcohols to alkynes. *Angewandte Chemie International Edition* **1998,** *37* (10), 1415-1418.

5. Gimeno, M. C.; Laguna, A., Three-and four-coordinate gold (I) complexes. *Chemical Reviews* **1997,** *97* (3), 511-522.

6. Kumar, M.; Jasinski, J.; Hammond, G. B.; Xu, B., Alkyne/Alkene/Allene‐Induced Disproportionation of Cationic Gold (I) Catalyst. *Chemistry–A European Journal* **2014,** *20* (11), 3113-3119.

7. Carreras, J.; Gopakumar, G.; Gu, L.; Gimeno, A.; Linowski, P.; Petuskova, J.; Thiel, W.; Alcarazo, M., Polycationic ligands in gold catalysis: synthesis and applications of extremely π-acidic catalysts. *Journal of the American Chemical Society* **2013,** *135* (50), 18815-18823.

8. Gaggioli, C. A.; Ciancaleoni, G.; Biasiolo, L.; Bistoni, G.; Zuccaccia, D.; Belpassi, L.; Belanzoni, P.; Tarantelli, F., Anomalous ligand effect in gold (I)-catalyzed

intramolecular hydroamination of alkynes. *Chemical Communications* **2015,** *51* (27), 5990-5993.

9. Iwai, T.; Okochi, H.; Ito, H.; Sawamura, M., Construction of Eight-Membered Carbocycles through Gold Catalysis with Acetylene-Tethered Silyl Enol Ethers. *Angewandte Chemie International Edition* **2013,** *52* (15), 4239-4242.

10. Ito, H.; Ohmiya, H.; Sawamura, M., Construction of Methylenecycloheptane Frameworks through 7-Exo-Dig Cyclization of Acetylenic Silyl Enol Ethers Catalyzed by Triethynylphosphine− Gold Complex. *Organic Letters* **2010,** *12* (19), 4380-4383.

11. Luo, Y.; Ji, K.; Li, Y.; Zhang, L., Tempering the reactivities of postulated α-oxo gold carbenes using bidentate ligands: Implication of tricoordinated gold intermediates and the development of an expedient bimolecular assembly of 2, 4-disubstituted oxazoles. *Journal of the American Chemical Society* **2012,** *134* (42), 17412-17415.

12. Lu, B.; Li, C.; Zhang, L., Gold-Catalyzed Highly Regioselective Oxidation of C− C Triple Bonds without Acid Additives: Propargyl Moieties as Masked α, β-Unsaturated Carbonyls. *Journal of the American Chemical Society* **2010,** *132* (40), 14070-14072.

13. Ji, K.; Zhao, Y.; Zhang, L., Optimizing P, N-Bidentate Ligands for Oxidative Gold Catalysis: Efficient Intermolecular Trapping of α-Oxo Gold Carbenes by Carboxylic Acids. *Angewandte Chemie* **2013,** *125* (25), 6636-6640.

14. Alcarazo, M.; Stork, T.; Anoop, A.; Thiel, W.; Fürstner, A., Steering the Surprisingly Modular π-Acceptor Properties of N-Heterocyclic Carbenes: Implications for Gold Catalysis. *Angewandte Chemie International Edition* **2010,** *49* (14), 2542-2546.

15. Ding, D.; Mou, T.; Feng, M.; Jiang, X., Utility of ligand effect in homogenous gold catalysis: enabling regiodivergent π-bond-activated cyclization. *Journal of the American Chemical Society* **2016,** *138* (16), 5218-5221.

16. Vreeken, V.; Broere, D. L.; Jans, A. C.; Lankelma, M.; Reek, J. N.; Siegler, M. A.; van der Vlugt, J. I., Well‐Defined Dinuclear Gold Complexes for Preorganization‐Induced Selective Dual Gold Catalysis. *Angewandte Chemie* **2016,** *128* (34), 10196-10200.

17. Ito, Y.; Sawamura, M.; Hayashi, T., Catalytic asymmetric aldol reaction: reaction of aldehydes with isocyanoacetate catalyzed by a chiral ferrocenylphosphine-gold (I) complex. *Journal of the American Chemical Society* **1986,** *108* (20), 6405-6406.

18. Jia, M.; Bandini, M., Counterion effects in homogeneous gold catalysis. *ACS Catalysis* **2015,** *5* (3), 1638-1652.

19. Kennedy-Smith, J. J.; Staben, S. T.; Toste, F. D., Gold (I)-catalyzed Conia-ene reaction of β-ketoesters with alkynes. *Journal of the American Chemical Society* **2004,** *126* (14), 4526-4527.

20. Gorin, D. J.; Toste, F. D., Relativistic effects in homogeneous gold catalysis. *Nature* **2007,** *446* (7134), 395-403.

21. LaLonde, R. L.; Brenzovich Jr, W. E.; Benitez, D.; Tkatchouk, E.; Kelley, K.; Goddard III, W. A.; Toste, F. D., Alkylgold complexes by the intramolecular aminoauration of unactivated alkenes. *Chemical Science* **2010,** *1* (2), 226-233.

22. Wang, Y.; Wang, Z.; Li, Y.; Wu, G.; Cao, Z.; Zhang, L., A general ligand design for gold catalysis allowing ligand-directed anti-nucleophilic attack of alkynes. *Nature Communications* **2014,** *5* (1), 1-8.

23. Wang, Z.; Wang, Y.; Zhang, L., Soft propargylic deprotonation: designed ligand enables au-catalyzed isomerization of alkynes to 1, 3-dienes. *Journal of the American Chemical Society* **2014,** *136* (25), 8887-8890.

24. Basak, A.; Chakrabarty, K.; Ghosh, A.; Das, G. K., Theoretical study on the isomerization of propargyl derivative to conjugated diene under Au (I)-catalyzed reaction: A DFT study. *Computational and Theoretical Chemistry* **2016,** *1083*, 38-45.

25. Li, X.; Wang, Z.; Ma, X.; Liu, P.-n.; Zhang, L., Designed bifunctional phosphine ligand-enabled gold-catalyzed isomerizations of ynamides and allenamides: Stereoselective and regioselective formation of 1-amido-1, 3-dienes. *Organic Letters* **2017,** *19* (21), 5744-5747.

26. Wang, Z.; Ying, A.; Fan, Z.; Hervieu, C.; Zhang, L., Tertiary amino group in cationic gold catalyst: tethered frustrated lewis pairs that enable ligand-controlled regiodivergent and stereoselective isomerizations of propargylic esters. *ACS Catalysis* **2017,** *7* (5), 3676-3680.

27. Gilchrist, T. L., Synthesis of aromatic heterocycles. *Journal of the Chemical Society, Perkin Transactions 1* **1999,** (20), 2849-2866.

28. Hou, X. L.; Cheung, H. Y.; Hon, T. Y.; Kwan, P. L.; Lo, T. H.; Tong, S. Y.; Wong, H. N., Regioselective syntheses of substituted furans. *Tetrahedron* **1998,** *54* (10), 1955-2020.

29. Méndez-Andino, J.; Paquette, L. A., Convergent regiodirected assembly of 2, 3-disubstituted furans. *Organic Letters* **2000,** *2* (25), 4095-4097.

30. Marshall, J. A.; Wallace, E. M.; Coan, P. S., Total Synthesis of the Pseudopterane (.+-.)-Kallolide B. *The Journal of Organic Chemistry* **1995,** *60* (4), 796-797.

31. Brown, T.; Armitage, M.; Blakemore, R.; Blurton, P.; Durant, G.; Ganellin, C.; Ife, R.; Parsons, M.; Rawlings, D.; Slingsby, B., Isocytosine H2-receptor histamine antagonists. III. The synthesis and biological activity of lupitidine (SK&F 93479) and related compounds. *European journal of medicinal chemistry* **1990,** *25* (3), 217-226.

32. Lee, C.-F.; Yang, L.-M.; Hwu, T.-Y.; Feng, A.-S.; Tseng, J.-C.; Luh, T.-Y., One-pot synthesis of substituted furans and pyrroles from propargylic dithioacetals. New annulation route to highly photoluminescent oligoaryls. *Journal of the American Chemical Society* **2000,** *122* (20), 4992-4993.

33. Padwa, A.; Crawford, K. R.; Rashatasakhon, P.; Rose, M., Several convenient methods for the synthesis of 2-amido substituted furans. *The Journal of Organic Chemistry* **2003,** *68* (7), 2609-2617.

34. Padwa, A.; Brodney, M. A.; Satake, K.; Straub, C. S., Cycloaddition− Rearrangement Sequence of 2-Amido Substituted Furans as a Method of Synthesizing Hexahydroindolinones. *The Journal of Organic Chemistry* **1999,** *64* (13), 4617-4626.

35. Padwa, A.; Dimitroff, M.; Waterson, A. G.; Wu, T., Diels− alder reaction of 2-amino-substituted furans as a method for preparing substituted anilines. *The Journal of Organic Chemistry* **1997,** *62* (12), 4088-4096.

36. Cochran, J. E.; Wu, T.; Padwa, A., Synthesis of polysubstituted anilines using the Diels-Alder reaction of methyl 5-aminofuroate. *Tetrahedron Letters* **1996,** *37* (17), 2903-2906.

37. Chatani, N.; Hanafusa, T., Reaction of cyclopropenones with trimethylsilyl cyanide with the aid of transition metal complexes or phosphines. A new synthesis of 5-amino-2-furancarbonitriles. *The Journal of Organic Chemistry* **1987,** *52* (19), 4408-4409.

38. Boukouvalas, J.; Sperry, J.; Brimble, M. A., 2-Trimethylsilyloxyfuran. *Encyclopedia of Reagents for Organic Synthesis* **2001**.

39. Semmelhack, M.; Park, J., Reaction of (aminocarbene) iron complexes with alkynes. A synthesis of 5-aminofurans. *Organometallics* **1986,** *5* (12), 2550-2552.

40. Medimagh, R.; Marque, S.; Prim, D.; Chatti, S., 5-Amino-2-furylmethylamines-Appealing Precursors of Aminoisoindolinones? *Synthesis* **2010,** *2010* (05), 770-774.

41. Martinez-Cuezva, A.; Lopez-Leonardo, C.; Bautista, D.; Alajarin, M.; Berna, J., Stereocontrolled synthesis of β-lactams within [2] rotaxanes: showcasing the chemical consequences of the mechanical bond. *Journal of the American Chemical Society* **2016,** *138* (28), 8726-8729.

42. Le, C. M.; Sperger, T.; Fu, R.; Hou, X.; Lim, Y. H.; Schoenebeck, F.; Lautens, M., Stereoselective synthesis of methylene oxindoles via palladium (II)-catalyzed intramolecular cross-coupling of carbamoyl chlorides. *Journal of the American Chemical Society* **2016,** *138* (43), 14441-14448.

2. Catalytic S_N2 Glycosylations toward 1,2-*cis*-Glycopyranosides

2.1 Glycosylation: History and Challenges

Carbohydrates serve essential biological functions such as energy storage, structural components, and primary metabolites and play critical roles in a broad range of biological processes such as signal transduction, fertilization, metathesis, cell-cell adhesion, and immune responses.[1-5] In recent studies, oligosaccharides, and glycoconjugates have also demonstrated great potential in disease diagnosis, bioimaging, and immunotherapies.[6-10]

The exceptional structural complexity of oligosaccharides themselves or in conjugation with other biomolecules such as natural products, lipids, and proteins poses significant challenges to their synthesis and hinders the study of their biological functions. Natural glycans' low abundance and structural microheterogeneity make it challenging to get the pure isolates, let alone characterizing these molecules. Although scientists have successfully isolated and characterized certain types of natural carbohydrates, the growing demand for significant quantities of pure compounds still cannot be satisfied. Consequently, the scientific community often relies on chemical synthesis to systematically study these molecules and their unnatural counterparts. Over the past decades, various chemical glycosylation methods have been developed and extensively reviewed.[11-24]

Among different types of glycosides, the *O*-glycosides are the most abundant in nature and attract the most attention from scientists. Except for 2-deoxysugars, these molecules are commonly classified into two categories, namely, 1,2-*cis*- and 1,2-*trans*-glycosides (**Figure 4A and B**).

Figure 4. Examples of Common Monosaccharide Residues in Glycosides

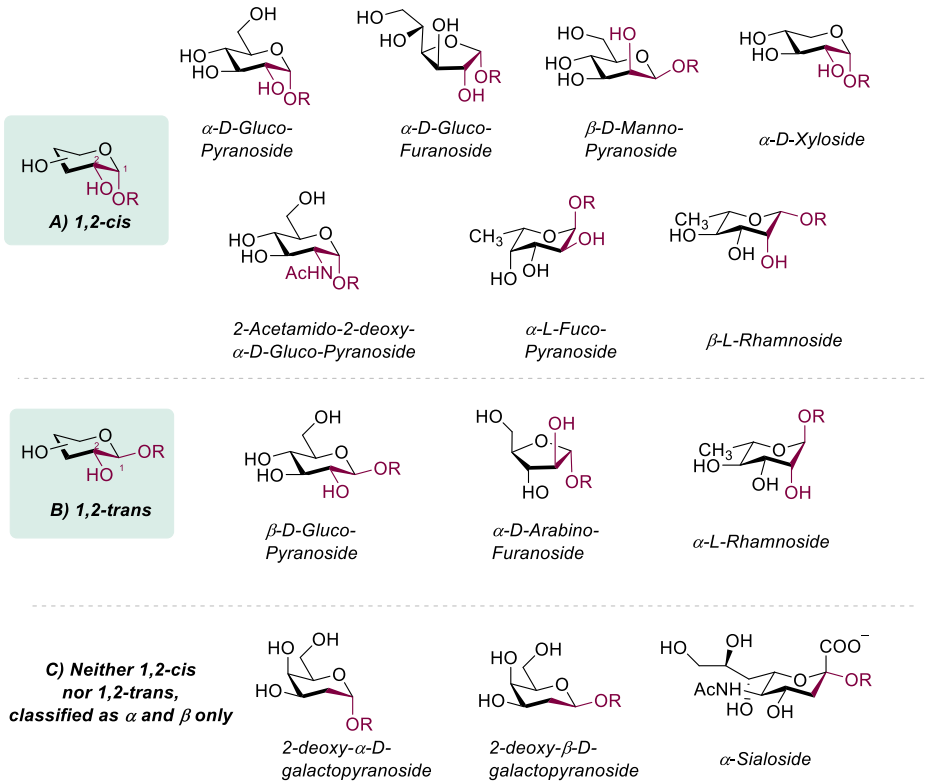

For some common types of glycosides without the neighboring substituent to the anomeric center, these compounds can only be referred to as α- and β- glycosides, as shown in **Figure 4C**. Among these classes of glycosidic linkages, the major obstacle for synthetic chemists is the selective formation of 1,2-*cis* glycosidic bonds.

Chemical glycosylation is arguably one of the longest-standing challenges in the field of organic chemistry. In general, a glycosyl donor with a leaving group at its anomeric position undergoes activation by a promoter to react with a glycosyl acceptor (**Scheme 13**, **2.1-1**), delivering the corresponding glycoside products. Upon activation, a glycosyl cation (**Scheme 13**, **2.1-3 or 2.1-6**) is generated by the promoter-assisted departure of the leaving group, which is stabilized due to the resonance contribution of an oxocarbenium

intermediate (**Scheme 13**, **2.1-5 or 2.1-7**). If the 2-position on the donor is a participating group, for example, an acyloxy group, the oxacarbenium ion can be further be converted into a bicyclic acyloxonium intermediate (**Scheme 13**, **2.1-4**). The ensuing nucleophilic attack by a glycosyl acceptor can only proceed through the convex face (**Scheme 13**, **path c**) since the concave face is blocked. This approach provides access to 1,2-*trans* glycosides with very high or complete selectivity, although occasionally orthoester byproducts or trace1,2-*cis* products are formed (**Scheme 13**, **path d, e**).

Scheme 13. General Pathways for Chemical Glycosylation Reactions

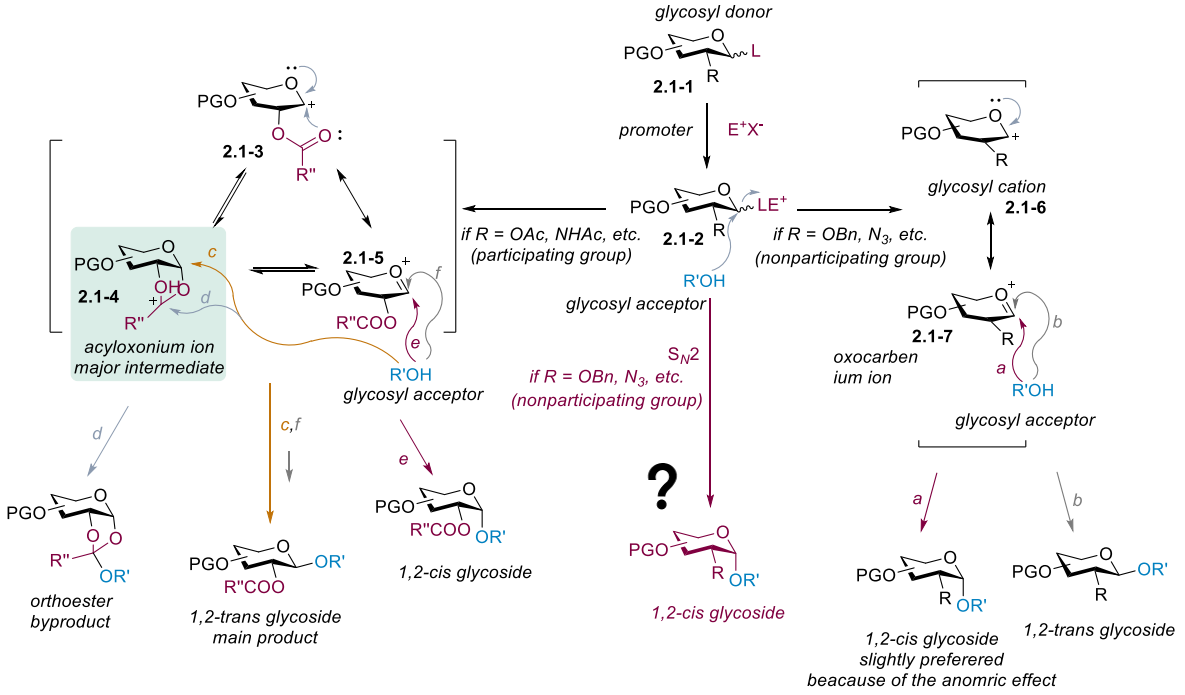

On the other hand, with a non-participating group at the 2-position, the nucleophilic attack can happen either from the top face (**Scheme 13**, **path a**) or bottom face (**Scheme 13**, **path b**) of the flattened ring of the oxocarbenium moiety. These uncontrolled reactions usually lead to a mixture of diastereomers with the selectivity slightly favoring 1,2-*cis* in the

cases of glucosides and galactosides due to the anomeric effect. To date, a generally applicable and highly stereoselective construction of 1,2-*cis* glycosidic bonds remains an unsolved problem in carbohydrate chemistry.

2.2 Selected Strategies for the Synthesis of 1,2-cis Glycopyranosides

Several known factors, including temperature, solvent, type of donor used, type of acceptor used, amount and type of promoter used, protecting groups, etc., are able to affect the stereochemical outcome and yield in glycosylation reactions. Since the methods of 1,2-cis glycopyranosides have already been reviewed extensively,[24-27] only representative approaches, and the most recent advances in this field will be discussed in this part.

2.2.1 Effect of Reaction conditions

The temperature profiles are probably the most manageable condition in a reaction. Generally speaking, lower temperature reactions usually favor the formation of the kinetically controlled product, i.e., the β-glycoside.[28, 29] Due to the anomeric effect, the thermodynamically favored α-glycoside is preferred at higher temperatures.

On the other hand, the effect of reaction solvent on the selectivity of the glycosylation reaction has been comprehensively investigated. In general, for non-participating nonpolar solvents like toluene and DCM, glycosylation may favor the S_N2 reaction. Polar reaction solvents with the ability to promote charge separation and stabilize the oxocarbenium species through solvation exhibit more S_N1 characteristics.

Scheme 14. Effect of the Reaction Solvent and its Application in Oligosaccharide Synthesis

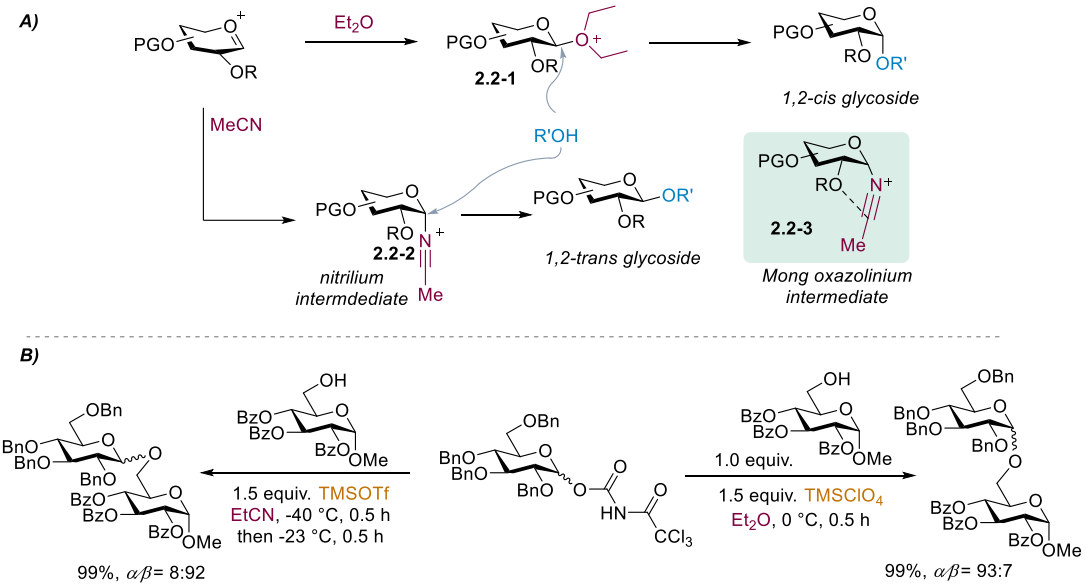

On the contrary, participating solvents have a more decisive influence on the stereoselective selectivity of the glycosidic bond formation. Previous reports have shown that ethereal solvents tend to promote glycosylation in an α-selective manner, whereas nitrile solvents tend to favor β-glycosylation. This tendency was later rationalized as follows: for ethereal solvents like tetrahydrofuran, diethyl ether, and 1,4-dioxane, the equatorial β-onium adduct **2.2-1** was suggested to be formed and is much more reactive than its α-counterpart.[30, 31] As a result, the preferential attack of it by an acceptor results in the selective formation of the α- product. The directing effect of polar nitrile solvent has been studied since the 1970s, but it was not until 1990 when the Fraser-Reid group achieved the first correct assignment of the α glucosyl nitrilium ion **(Scheme 14, 2.2-2)**.[32] Although the α- intermediate is more stable than its β- counterpart due to the anomeric effect, the Mong group recently proposed

an oxazolinium intermediate **2.2-3** via 2-*O* participation, which further stabilizes the *α*-intermediate.[33] The subsequent S_N2 attack at **2.2-2** or **2.2-3** will furnish the *β*- product selectively. For example, in a study by the Omura group in 2010, the selectivity was totally reversed (**Scheme 14B**) by changing the solvent.[34] This strategy has been widely used with glucosyl, galactosyl, 2-azido glucosyl, and Kdo types of donors.[35-39]

Scheme 15. Effect of DMF as the Reaction Co-solvent

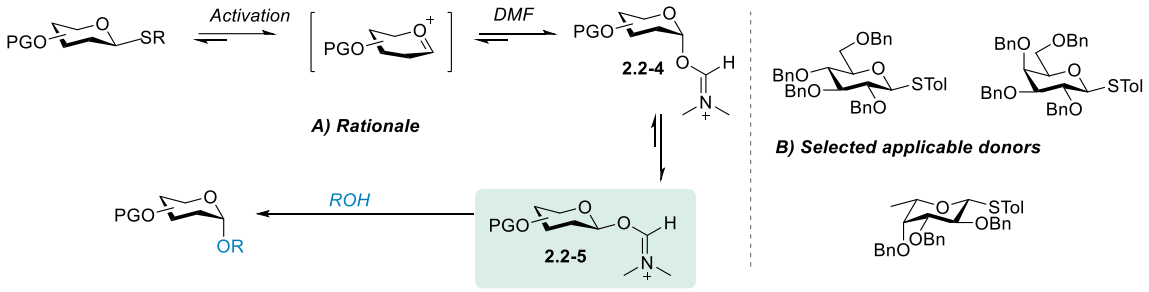

The Mong group further investigated the solvent effect by using DMF as a co-solvent.[40] The author showed that the increase in the equivalents of DMF in the reaction system was translated to a significant improvement of *α*-selectivity. The observation was rationalized as follows, the oxocarbenium ion generated upon activation is trapped by DMF, giving an equilibrating mixture of cationic *α/β*-glycosyl *O*-imidates. The more reactive *β*-form (**Scheme 15, 2.2-5**) reacts faster with acceptors in an S_N2 fashion, Consequently, the reaction is selectively funneled through the *β*-intermediate, leading to the *α*-glycoside selectively. However, this strategy only applies to the formation of 1,2-*cis* glucosides or galactosides.

Other Factors, like promoters, additives can also affect selectivity substantially. For example, in 2012, Demchenko and co-workers demonstrated a method involving bromine as the promoter.[41] The only reactive intermediate in this reaction is the *β*-bromide. By adopting

a superdisarmed α-thioglycoside as substrate, initially, the β-bromide (**Scheme 16, 2.2-6**) was generated with high selectivity. The disarmed nature of the donor makes isomerization of the glycosyl bromide slower, providing enough time for the nucleophilic attack, delivering the stereo-inverted product with complete selectivity. The overall stereochemical outcome is stereoretention. However, the yields with secondary alcohols are low due to their weak nucleophilicity and the competitive isomerization of the reactive β-bromide towards unreactive α-bromide. The α-bromide can be reactivated with mercury (II) bromide additive, leading to higher yields with secondary acceptors at the cost of α-stereoselectivity.

Scheme 16. Stereoselective Glycosidation of Superdisarmed Thioglycoside

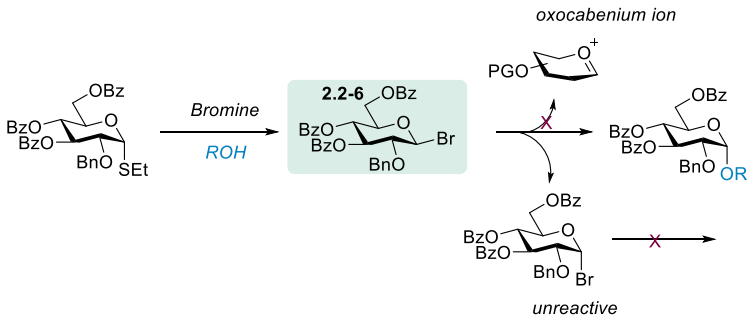

2.2.2 Strategies Based on Structural Modifications on the Sugar Ring

2.2.2.1 Neighboring Group Participation

As prementioned in **Scheme 13**, acyl-type neighboring protecting groups offer a reliable and highly stereoselective approach to the 1,2-*trans*-glycosides. In 2004, Boons and co-workers developed a strategy in which the donors were functionalized with a participating nucleophilic group capable of blocking the face of the cyclic oxocarbenium intermediate

opposite to the 2-*O*, which could lead to 1,2-*cis* glycosides selectively.[42] As depicted in **Scheme 17A**, it is envisioned that a specifically designed donor with a nucleophilic chiral auxiliary group attached to its 2-position could form a six-membered ring system upon activation. In the case of an *S*-configured version, the formation of the *trans*-decaling-like intermediate **2.2-8** results in a more favorable equatorial placement of the chiral substituent, which will also have less gauche interactions in the bicyclic structure. On the other hand, the formation of *cis*-decaling-like intermediate **2.2-7** leads to an axial placement of the chiral substituent, which in turn leads to an unfavorable 1,3-diaxial repulsion. Consequently, the *S*-configuration auxiliary group results in 1,2-*cis*-glycoside formation by forming the *trans*-decalin-like intermediate **2.2-8** selectively. According to a similar rationale, the *R*-configured auxiliary is envisioned to favor 1,2-*trans* glycoside formation through a *cis*-decalin intermediate (**2.2-9**). In the first successful implementation of this design (**Scheme 17B**), an ethoxy carbonyl benzyl moiety is installed at the 2-position by reacting ethyl mandelate (**2.2-12**) with Cerny epoxide (**2.2-11**). The resulting **2.2-13** further undergoes acetolysis of the 1,6-anhydro-bridge. Both trichloroacetimidate donors (*S*)-**2.2-14** and (*R*)-**2.2-14** were prepared because both the enantiomers of ethyl mandelate **(2.2-12)** are readily available. As shown in **Scheme 17B**, when the donor (*S*)-**2.2-14** was glycosylated with the acceptor **2.2-15**, disaccharide **2.2-16** was obtained with high α-selectivity. On the contrary, when the donor (*R*)-**2.2-14** was used, a reversal of anomeric selectivity was observed. Using sodium methoxide in methanol followed by a birch reduction, acyl groups, and benzyl groups, including the chiral auxiliary, could be deprotected, furnishing disaccharide **2.2-17**.

Scheme 17. Chiral Auxiliaries Designed to Form *cis*- or *trans*-Decalin-like Intermediates to Afford 1,2-*trans* or 1,2-*cis*-Glycosides

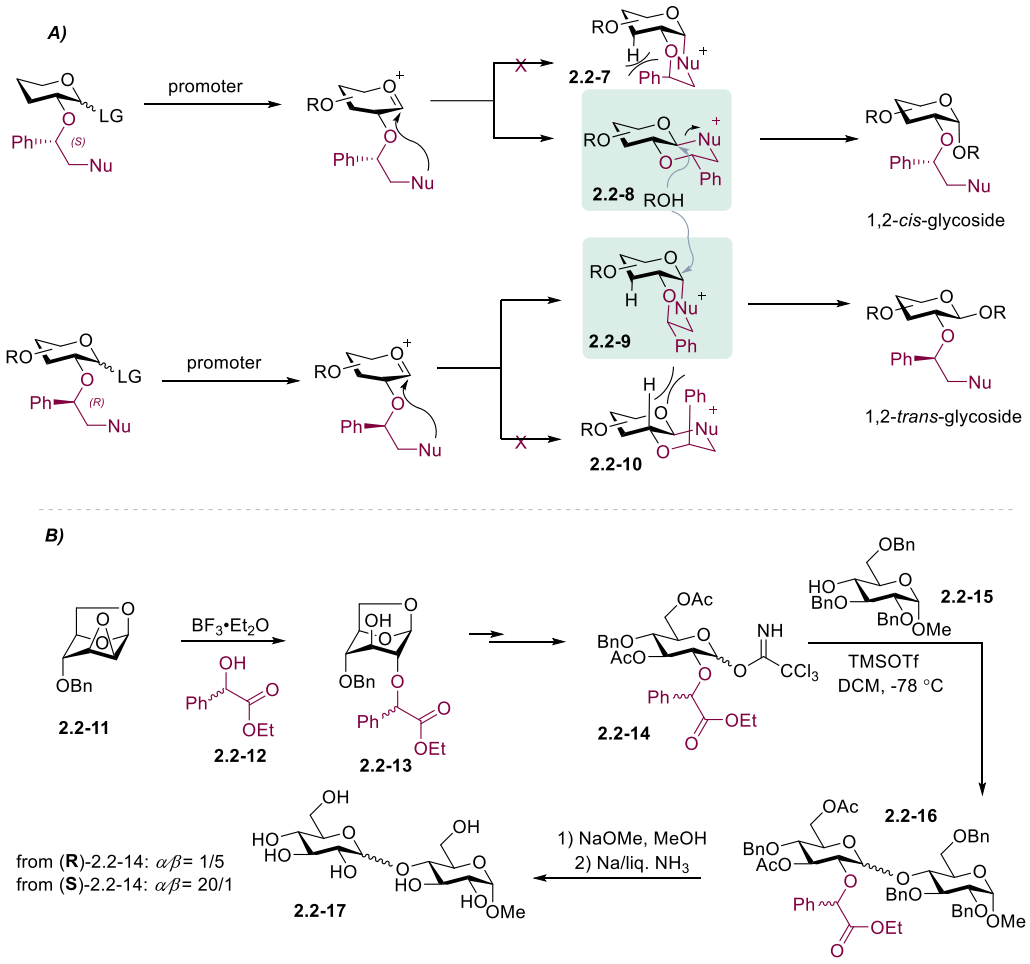

However, for these donors with an ethoxy carbonyl benzyl moiety, in some cases where less electron-withdrawing *O*-protecting groups are employed, for example, using an allyl group at 3-position in replacement of an acyl group, the 1,2-*cis* selectivity is substantially lower. The erosion of selectivity was attributed to the the participation of oxocarbenium intermediate. Later, the Boons group developed a second-generation auxiliary by installing an (*S*)-phenylthiomethylbenzyl ether moiety at the 2-position of a glycosyl donor.[43] It was

assumed that the neighboring group participation could be enhanced by increasing the nucleophilicity of the participating moiety and reducing conformational flexibility of the auxiliary. The (*S*)-(phenylthiomethyl)benzyl moiety was stereoselectively introduced by reacting the alcohol **2.2-19** with (*S*)-1-phenyl-2-(phenylthio)ethan-1-ol **2.2-18** in the presence of Lewis acid (**Scheme 18A**). The reaction proceeds via an episulfonium intermediate **2.2-20** formed by anchimeric assistance of the thiophenyl group. The stereochemistry of **2.2-18** is retained overall due to the double inversion in the process. This modification significantly improved 1,2-*cis* stereoselectivities and provided 1,2-*cis*-glycosides exclusively. However, the stereo-inversion does not apply to donors functionalized with *(R)*-(phenylthiomethyl)benzyl moiety. This method was further applied to the solid-supported synthesis of a biologically important branched α-glucan from *Aconitum carmichaeli*.[44]

Scheme 18. Second Generation Chiral Auxiliary

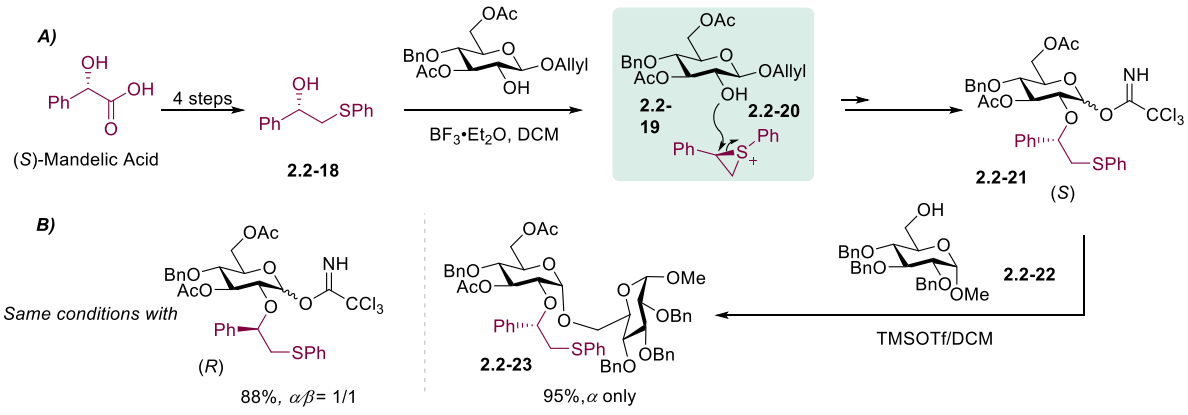

Scheme 19. Efforts to Simplify the Donor Synthesis

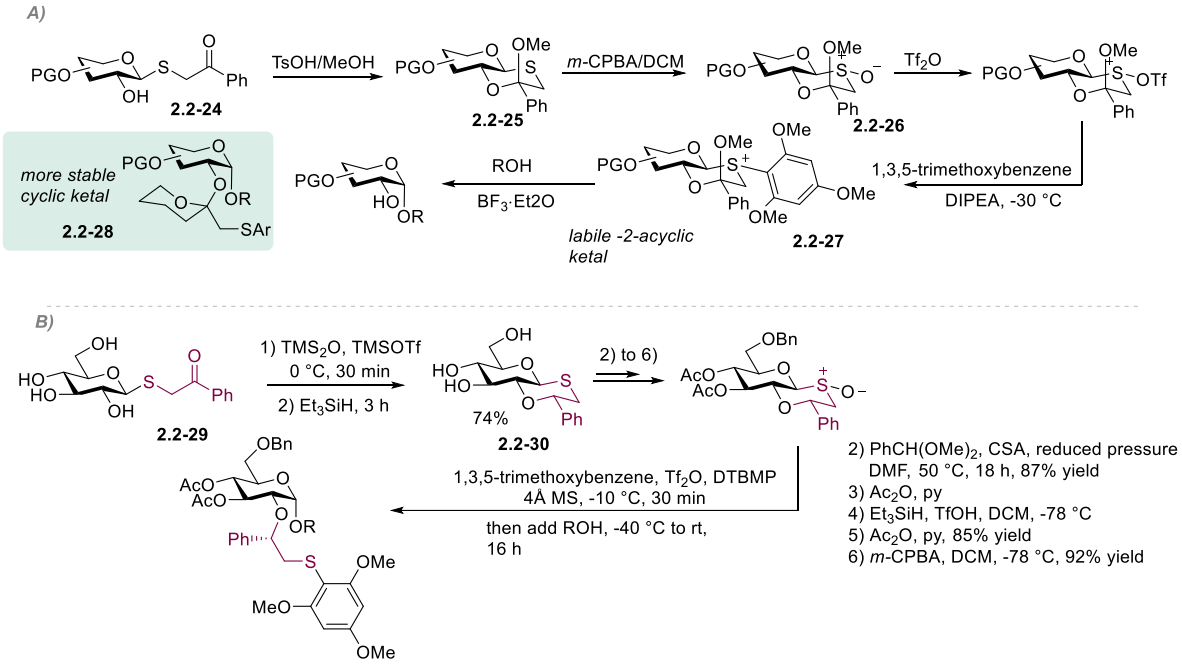

The major drawback of the previous approach is the difficulties for the installation of the auxiliary group at the 2-position. In 2009, Turnbull et al. developed an elegant synthesis starting from thioglycoside **2.2-25**, which has an anomeric α-directing group and is easy to prepare.[45] The ketone moiety of the tetraol thioglycoside **2.2-25**, upon exposure to MeOH in the presence of TsOH, cyclized regio- and stereoselectively to give methyl ketal **2.2-25**, in which the bulky phenyl group adopts an equatorial position and the methoxy group can also benefit from anomeric stabilization. Oxidation of these sulfides with *m*-CPBA gave the corresponding sulfoxide **2.2-26** as the equatorial isomer. The subsequent electrophilic aromatic substitution would give rise to in situ generated donor **2.2-27**. The selectivity with this donor is complete, albeit with moderate yield in some cases. The major drawback of this approach is the lability of the ketal auxiliary group, especially for less reactive disarmed donors. In these cases, MeOH was released from the ketal auxiliary group during the glycosylation reaction, giving methyl glycoside as a sideproduct. Later in 2012, the Turnbull group developed a new type of donor adopting a more stable cyclic ketal moiety, which

improved the performance.[46] In the same year, the Boons group solved the lability problem by adopting a 1,3-oxathiane moiety.[47] The oxathiane **2.2-30**, stable under acidic, basic, and reductive conditions, was prepared by a one-pot, two-step process involving a trimethylsilyl acetal intermediate, followed by reduction by Et_3SiH.

Scheme 20. Applications of Neighboring Group Participation Strategy towards Mannosylations

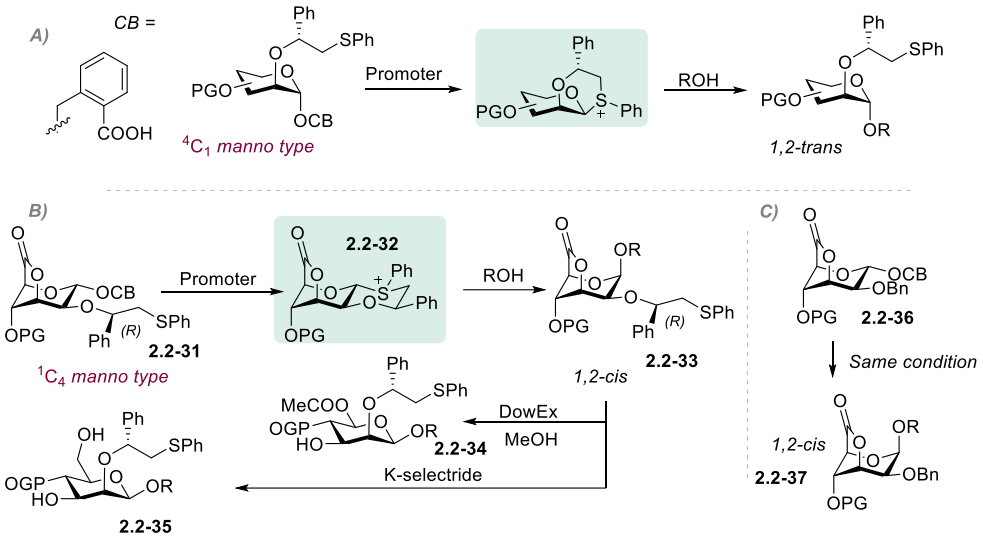

More recently, The Boltje group further applied this strategy toward mannosylation.[48] The 1,2-*trans* mannosylation reactions are innately preferred, and exhibit no problem with this strategy (**Scheme 20 A**). For the 1,2-*cis* mannosylations, the author took advantage of conformationally $^1C_4$ locked mannosides using a 3,6-lactone bridge (**Scheme 20B**). It was envisioned that the formation of a trans-decalin intermediate **2.2-32** is possible with an (*R*)-configured auxiliary as the phenyl group occupies the equatorial position. The donor **2.2-32** indeed gave 1,2-*cis* products with high selectivity.Further transformation of the glycoside products **2.2-33** could lead to ring-opening product **2.2-34** or the corresponding mannose

analog **2.2-35**. However, even with a simple Bn group at *O*-2, the corresponding donor **2.2-36** reacted to deliver the 1,2-*cis* mannoside **2.2-37** with similar selectivity under the same reaction conditions.

Scheme 21. Proposed Remote Participation in the Mannuronic Acid Lactones

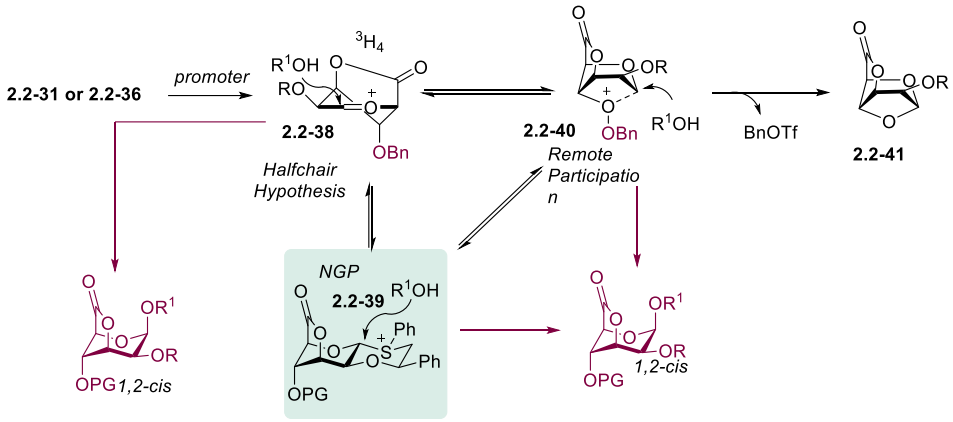

The author further performed VT-NMR experiments to investigate the mechanism and found **2.2-41** was formed without adding acceptors, whether using donors with the auxiliary group or without. This result clearly indicated the C4 benzyl group participation (**2.2-40**). On the other hand, the expected $^{3}H_{4}$ oxocarbenium ion **2.2-38** may also lead to the *β*-product formation. However, although **2.2-41** was ultimately formed with the auxiliary group, VT-NMR experiments showed that the sulfonium ion formation was highly favored at the reaction temperature, making the pathway shown in **Scheme 20B** the most possible.

2.2.2.2 Conformation-Restraining Cyclic Protecting Groups

As shown in **Scheme 21**, torsional effects induced by cyclic protecting groups may have decisive impacts on the stereoselectivity of glycosylation. This strategy is widely applied in

the synthesis of 1,2-*cis* mannosides. The first direct *β*-mannosylation was achieved in 1961 by Gorin et al.,[49] using the mannosyl bromide **2.2-42** as donors with silver oxide as the promoter. The presence of 2,3-di-*O*-carbonyl group seems to be critical for the *β*-selectivity. Later in 1974, the same donor was used by Bebault and Dutton to prepare disaccharide **2.2-45**, which corresponds to a disaccharide segment of biologically important glycans on the cell surface (**Scheme 22A**).[50]

Scheme 22. History of Using Conformation-Restraining Cyclic Protecting Groups

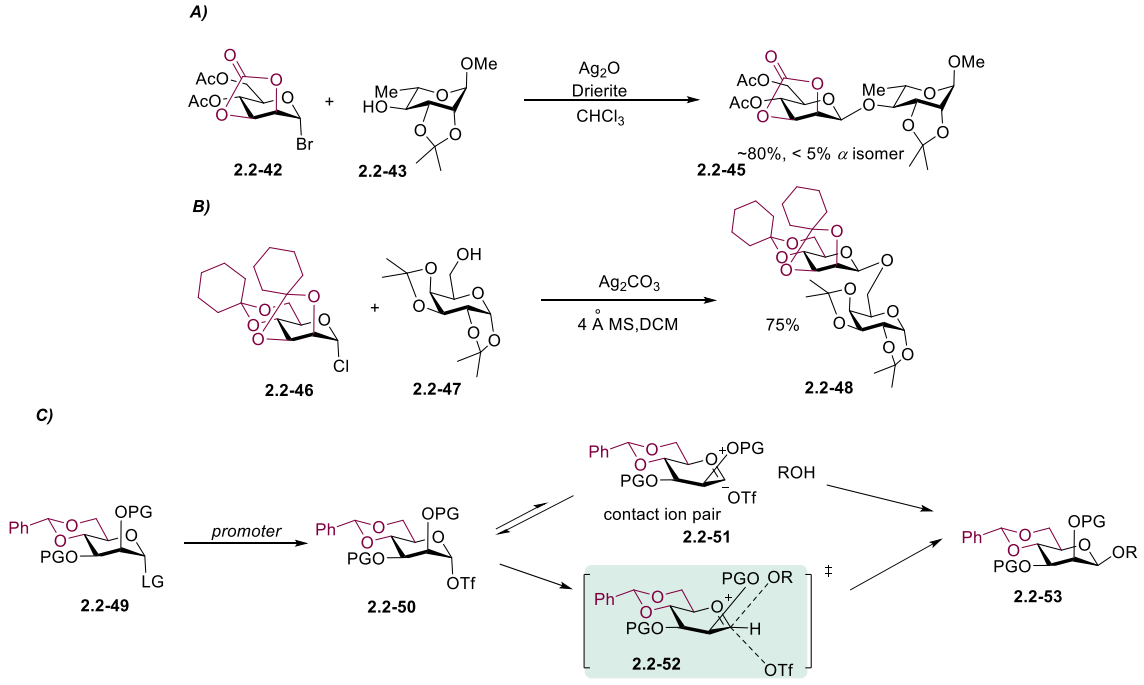

In 1979, Garegg and Iversen demonstrated mannosyl chloride **2.2-46** with 2,3-4,6-di-*O*-cyclohexylidene protection would undergo *β*-mannosylation with primary alcohol 2.2-47 in good yield (**Scheme 22B**).[51] However, the performance of this reaction is poor with secondary alcohol acceptors.

The best β-mannosylation using this strategy is the work by Crich and co-workers (**Scheme 22C**).[52, 53] It has been demonstrated that 4,6-O-benzylidene-protected mannosyl donors give superior β- selectivity in comparison to donors lacking this type of protection. Several mechanism studies have shown the formation of the α-triflate **2.2-50,** which exists in dynamic equilibrium with the contact ion pair **2.2-51**.[18, 54-56] The presence of mannosyl triflate intermediates in mannosylation was widely recognized with 4,6-benzylidene acetal protected mannosyl donors possessing different leaving groups.[57-63] A mechanistic study based on KIE suggested that the reaction proceeds via an oxocarbenium ion-like intermediate, although the covalent α-triflate **2.2-50** was detected by NMR.[53] The stereoselectivity observed was attributed to the shielding effect of the α-face of the flattened ring imposed by a closely associated triflate counterion, which would lead to β-selective glycosylation. A similar conclusion was drawn from KIE experiments with mannosyl iodides.[64] The disarming effect of the 4,6-*O*-benzylidene protection on glycoside reactivity was found to be a combination of electronic withdrawal effect and torsional strain.[65]

However, poor selectivity is observed continuously for the 4,6-*O*-benzylidene-protected mannosyl donors possessing a bulky group at *O*-3.[66, 67] The loss of β-selectivity is attributed to that the bulky group on *O*-3 would push the benzyl group on *O*-2 towards the anomeric center, therefore blocking the β- face.

Scheme 23. The Use of the Sterically Minimal Propargyl Group at *O*-2 in Mannosyl Donors

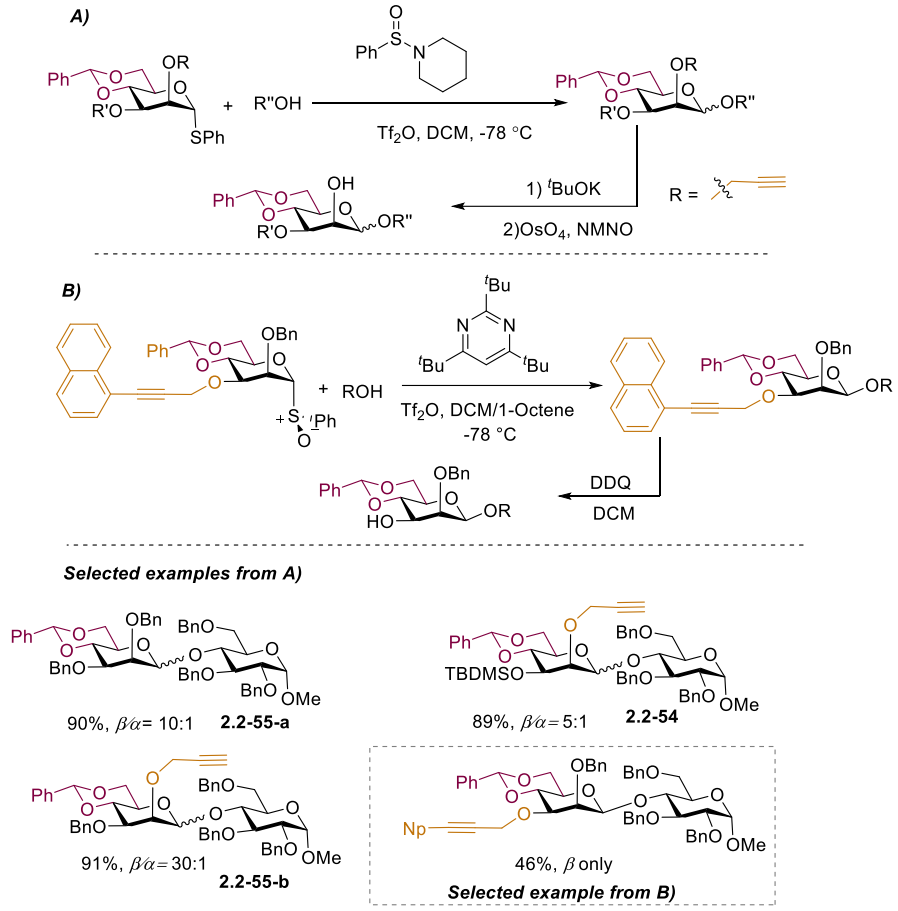

To overcome the poor stereoselectivity, the Crich group employed the sterically minimal 2-*O*-propargyl as the protecting group.[68, 69] As shown in **Scheme 23**, when R' = TBDMS, a moderate *β*-selectivity was observed (**2.2-54**). Instead, with R' = Bn, the β/α selectivity is improved to 30/1 (**2.2-55-a**). Moreover, this selectivity is also notably better than that with the corresponding 2,3-*O*-dibenzyl donor(**2-55-b**). However, to remove the propargyl ether protecting group, a two-step deprotection protocol is required, i.e., an initial treatment with base followed by catalytic osmoylation of the resulting allenyl ether. To find a better approach, later in 2016, the Crich group introduced (1-naphthyl)propargyl group as a

sterically unobtrusive alcohol protecting group, and their cleavage can be achieved in a single step by exposure to dichlorodicyanoquinone in wet DCM.[70]

Scheme 24. Stereodirecting Effect of 4,6-O-Benzylidene Acetal with Glucosyl Donors

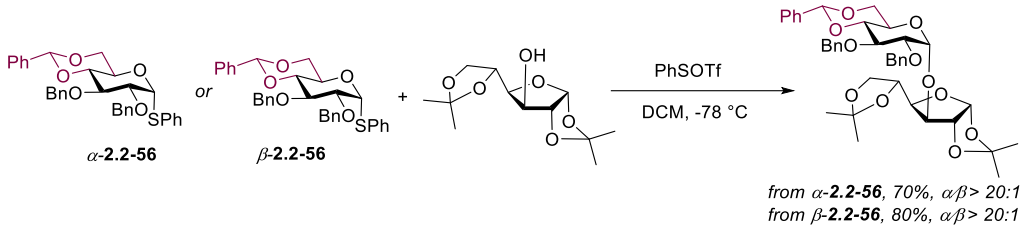

The glycosylation selectivity of 4,6-*O*-benzylidene protected glucopyranosyl donors has also been investigated.[52] As shown in **Scheme 24**, high α-selectivity is obtained from either the α or β thioglycoside donor, and it was rationalized by that the resulting triflate intermediate upon activation undergoes equilibrium between the α-intermediate anomer and its more reactive β-anomer. The α-glucoside is preferentially formed from the latter triflate instead of a discrete oxocarbenium intermediate.

Besides the 4,6-benzylidene protecting groups, various cyclic protecting groups have been deployed to achieve stereoselective construction of specific types of glycosidic bonds. For instance, 2,3-*trans*-oxazolidinone is employed for the construction of 1,2-*cis* glucosaminyl glycosides[71-82] and 4,6-silylene[83] and 2,6-lactones[84] for β mannosylation.

2.2.2.3 Remote Protecting Groups

Compared to the neighboring group participation by the 2-*O*-protecting groups, the influence from remote *O*-protecting groups has long been underestimated. However, the idea

of remote participating groups has attracted the carbohydrate community's attentions in recent years.

Table 2. Directing Effect of Electron-withdrawing Groups at *O*-3, *O*-4, and *O*-6 Positions of Mannosyl Donors

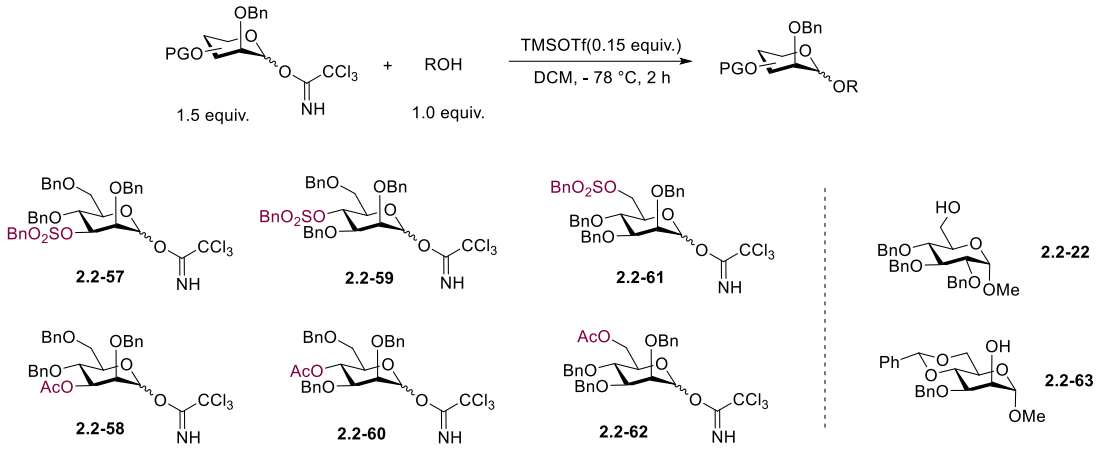

ratio (β/α), yield %	***EWG at O-3***		***EWG at O-4***		***EWG at O-6***	
Donor	***2.2-57***	***2.2-58***	***2.2-59***	***2.2-60***	***2.2-61***	***2.2-62***
Acceptor **2.2-22**	*15.9/1, 95%*	*1/25.9 91%*	*10.7/1 80%*	*4.0/1 85%*	*13.8/1 76%*	*α only 84%*
Acceptor **2.2-63**	*10.2/1 93%*	*1/39 94%*	*5.0/1 86%*	*4.1/1 87%*	*9.1/1 85%*	*1/2.2 85%*

In 2009, The Kim group presented a systematic study on mannosylations with donors possessing an electron-withdrawing group at *O*-3, *O*-4, or *O*-6 positions.[85] As shown in Table 2, strongly electron-withdrawing benzylsulfonyl groups at *O*-3 of mannosyl donors (**Table 2**, **2.2-57**) are highly *β*-directing, while all acyl groups including acetyl (**Table 2**, **2.2-58**), benzoyl, and *p*-nitrobenzoyl at *O*-3 were *α*-directing, Among these three acyl groups, the *α*-directing effect of *p*-nitrobenzoyl is the weakest, whereas the acetyl group exhibited the most potent *α*-directing effect. As depicted in **Scheme 25B**, it was reasoned

that the participation of 3-*O*-acyl groups would generate relatively stable bicyclic six-membered ring dioxocarbenium ion intermediate **2.2-67**, and mannosylation with this type of donors would occur predominantly through acceptor attacking the *α*-face of the mannose ring, which is in a $^1C_4$ conformation. On the other hand, all electron-withdrawing protecting groups including benzylsulfonyl and acyl groups, promoted *β*-selective mannosylation when attached at 4-*O* position. It was also observed that donors with strongly electron-withdrawing groups (e.g. **2.2-59**) at 4-*O* position exhibited stronger *β*-directing effect than the corresponding donors with weakly electron-withdrawing groups (e.g., **2.2-60**). The non-participation of the 4-O-acyl group could be rationalized by the unfavorable formation of the seven-membered ring dioxocarbenium ion **2.2-69**, forcing the sugar ring to adopt a boat conformation. For mannosyl donors possessing electron-withdrawing groups at *O*-6, benzylsulfonyl, *p*-nitrobenzoyl, and benzoyl groups all exerted the *β*-directing effect, and the *β*-selectivitywas again more pronounced for strongly electron-withdrawing benzylsulfonyl group (**2.2-61**) than for weakly electron-withdrawing *p*-nitrobenzoyl and benzoyl groups. Interestingly, the acetyl group at *O*-6 of mannosyl donors (**2.2-62**) led to α-selectivities. The proposed pathway involves a seven-membered dioxocarbenium ion **2.2-68**, which would lead to *α*-disaccharides. This pathway could account for the inferior *β*-selectivity observed with 6-*O*-benzoyl and the 6-*O*-*p*-nitrobenzoyl groups.

Low-temperature NMR studies revealed the formation of the corresponding *α*-mannosyl triflates intermediate **2.2-66** at -60 °C when mannosyl trichloroacetimidate donors bearing either a benzylsulfonyl group or benzoyl group at *O*-3, *O*-4, or *O*-6 positions were reacted with 1.0 equivalent of TMSOTf. On the contrary, the NMR spectra showed no sign of the generation of the triflate intermediate at the same temperature when the tetra-*O*-benzylmannosyl donor was used. A mechanism was therefore proposed for the origin of the

β-directing effect (**Scheme 25A**). Activation of donor **2.2-64** with TMSOTf would lead to mannosyl oxocarbenium ion **2.2-65**, which is in equilibrium with the α-mannosyl triflate **2.2-66**. The electron-withdrawing group on the sugar ring would destabilize **2.2-65** but might stabilize **2.2-66** so that the equilibrium would shift toward the covalent **2.2-66**. **2.2-66** or its contact ion pair with the triflate anion blocking the α-face would react with acceptor in an S_N2-like manner to deliver the β- mannoside product.

Scheme 25. Mechanisms Considerations for the Directing Effect in Mannosylation Reactions

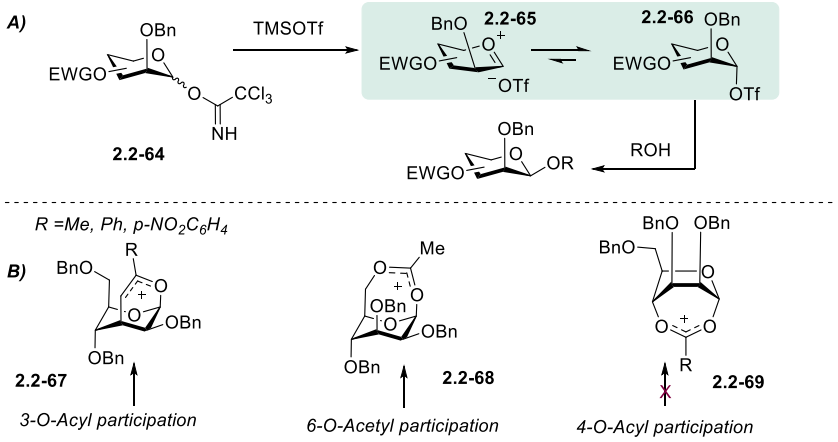

A distinct stereo-directing method enabled by remote protecting groups was reported by Demchenko and co-workers. In this approach, a remote picolinyl (Pic) or a picoloyl (Pico) protecting groups was employed (**Table 3**).[86] Although a picolinyl group at *C*-2 acts as an arming participating group and gives 1,2-*trans* glycosides via the thus-formed six-membered ring intermediate,[87] a remote picolinyl group could not bond directly to the anomeric center. Instead, it tends to form a hydrogen bond with the incoming acceptor (e.g., **2.2-71**) and hence delivers it to the same side of the sugar ring. This strategy can lead to the formation of 1,2-*cis* glycosides. This directing effect is more pronounced with a picoloyl substituent (**2.2-**

70). It was demonstrated that under more diluted conditions (5 mM), the 4-*O*-picoloyl or picolinyl glucosyl donors react faster and exhibit higher *cis*-selectivities than under more concentrated conditions (50 mM). This strategy was further applied to galactosyl donors (e.g., **2.2-72**) and rhamnosyl donors (e.g., **2.2-73**) for *β*-glycosides synthesis (e.g., **2.2-77** and **2.2-78**). Later, the Demchenko group extended this strategy to mannoside synthesis and showed that the presence of a 3-*O*-picoloyl group in mannosyl donor **2.2-74** could deliver *β*-mannoside (**2.2-79**) effectively at room temperature. However, the selectivities are moderate with more challenging secondary acceptors.[88]

Table 3. Hydrogen-Bond-Mediated Aglycone Delivery (HAD)

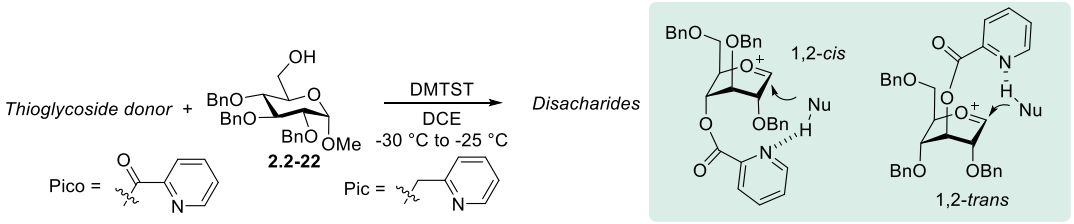

Entry	Donor	Conc. (acceptor)	Time	Product(yield)	$\alpha\beta$ ratio
1	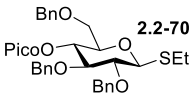 **2.2-70**	5 mM	4 h	**2.2-75**, 73%	> 25/1
2	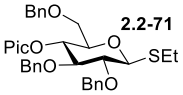 **2.2-71**	5 mM	5 h	**2.2-76**, 86%	5.3/1
3	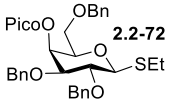 **2.2-72**	5 mM	1 h	**2.2-77**, 95%	<1/25
4	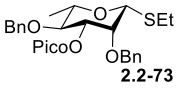 **2.2-73**	50 mM	15 min	**2.2-78**, 94%	<1/25
5	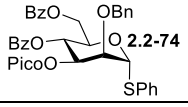 **2.2-74**	5 mM	2.5 h, rt	**2.2-79**, 91%	1/18.5

Figure 5. Enhance the *α*-Selectivity by Steric Shielding of the *β*-Face

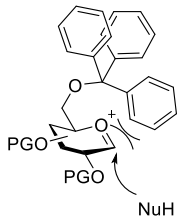

The shielding of the top face of the ring by sterically bulky *O*-protecting group, particularly at 6-*O* position, has been harnessed for 1,2-*cis* glucosylation and galactosylation reactions. For example, the bulky *O*-6 trityl group leads to improved *α*-selectivity in **Figure 5.**[89, 90]

2.2.2.4 Intramolecular Aglycone Delivery (IAD)

The idea of intramolecular glycosylation was first employed by Barresi and Hindsgaul to achieve *β*-mannosides synthesis.[91] Later, further improvements were made, including the introduction of silicon-mediated aglycone delivery [92, 93] and the allyl-mediated strategy,[94] affording high yields and complete stereoselectivities for 1,2-*cis* glucosylation and mannosylation. In 2008, The Ito group reported a naphthylmethyl ether (NAP)-mediated intramolecular aglycone delivery that generally provides higher yields in comparison to those of previous approaches. It allows for the stereoselective access to various 1,2-*cis* linkages, such as *β*-mannosides, *β*-arabinosides, and *α*-galactosides. For example, 2-*O*-NAP-protected glycosyl sulfide **2.2-80** was reacted with the acceptor **2.2-81** in the presence of DDQ, generating the tethered intermediate **2.2-82.**The MeOTf-promoted intramolecular and *cis* delivery of the acceptor moiety followed by acetylation deliver the 1,2-*cis* mannoside **2.2-83** in 90% yield and with complete *β*-selectivity.

Scheme 26. *β*-Mannosylation via NAP-tether Mediated IAD.

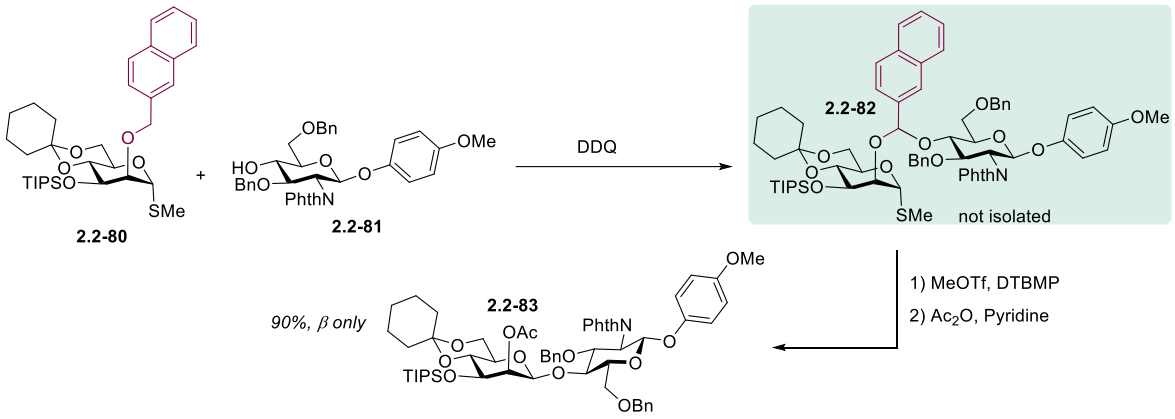

2.2.2.5 Boron-mediated Aglycon Delivery (BMAD)

1,2-Anhydro sugars are versatile glycosylating agents. For example, the peracetylated 1,2-anhydro glucose, known as Brigl's anhydride,[95] was used for noncatalytic, thermal glycosylations with simple alcohols in the early 20th century.[96, 97]

In 2015, the Toshima group developed a powerful approach for 1,2-*cis* glycosides synthesis using 1,2-anhydro sugars in the presence of boronic acid catalysts.[98] This approach is reminiscent of intramolecular aglycone delivery. However, it is catalytic. As shown in **Scheme 27**, a boronic acid catalyst **2.2-84** would react with diol glycosyl acceptor **2.2-85**, giving rise to the formation of the boronic ester **2.2-86**. Subsequently, this ester could activate the 1,2-anhydro glycosyl donor **2.2-87** owing to its Lewis acidity, leading to the oxonium cation intermediate **2.2-88** featuring a tetracoordinate boronate at 2-*O* position. The intramolecular aglycon delivery of the less-hindered alkoxy moiety in the boronate leads to the desired 1,2-*cis* glycosyl linkage. Transesterification between the thus-formed boronic ester and **2.2-85** would deliver the 1,2-*cis* glycoside product and regenerate **2.2-86**.

Scheme 27. Boronic Acid-Catalyzed Regio- and Stereoselective Glucosylation.

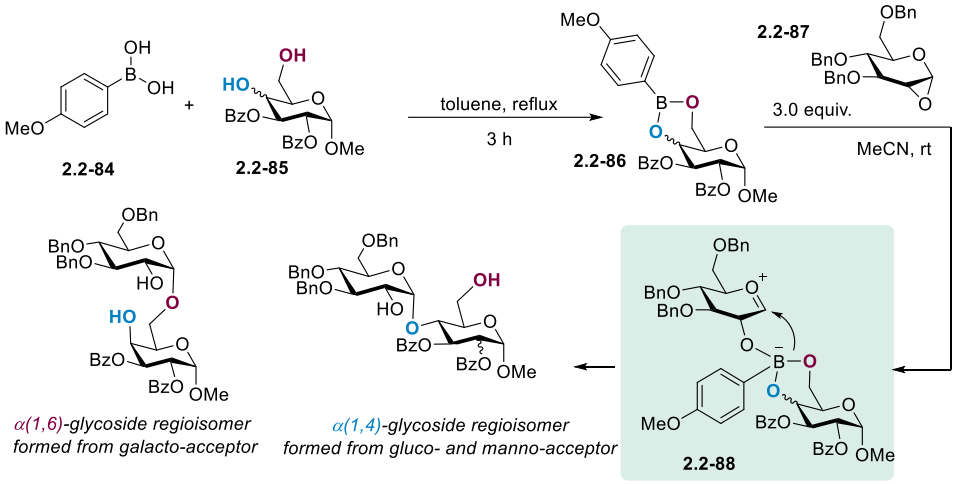

It was found that the selectivity for 1,2-*cis*-glycosides is very high, and this method exhibits high chemoselectivity towards one of the alcohol functionalities of the acceptor. As depicted in **Scheme 27**, glucose- and mannose-derived acceptors lead exclusively to α-1,4-glycosides, whereas galactose acceptors furnish α-1,6-glycosides with complete chemo- and stereoselectivity.

By introducing a *p*-nitro boronic acid catalyst, Nishi et al. extended the same principle of regio- and stereoselective glycosylation to β-mannosylation.[99] It was shown that, with the original *p*-methoxy boronic acid catalyst, the reaction is nonstereoselective, giving ~ 1:1 α-/β-mixtures. The result suggests that the electron-donating group in the boronic acid reduces the Lewis acidity of the boron atom, causing a weak activation of the donor, resulting in possible intermolecular S_N2 type substitution of the acceptor from the α-face of the intermediate (**Scheme 28B**). In contrast, the nitro group in the boronic acid **2.2-89** increases the Lewis acidity of the boron atom, which causes a better activation of the donor, leading to the formation of the oxonium cation and S_N1 type intramolecular nucleophilic attack from the β-face of the oxocarbenium intermediate (**Scheme 28A**).

Scheme 28. Boronic Acid-Catalyzed Regioselective *β*-Mannosylations

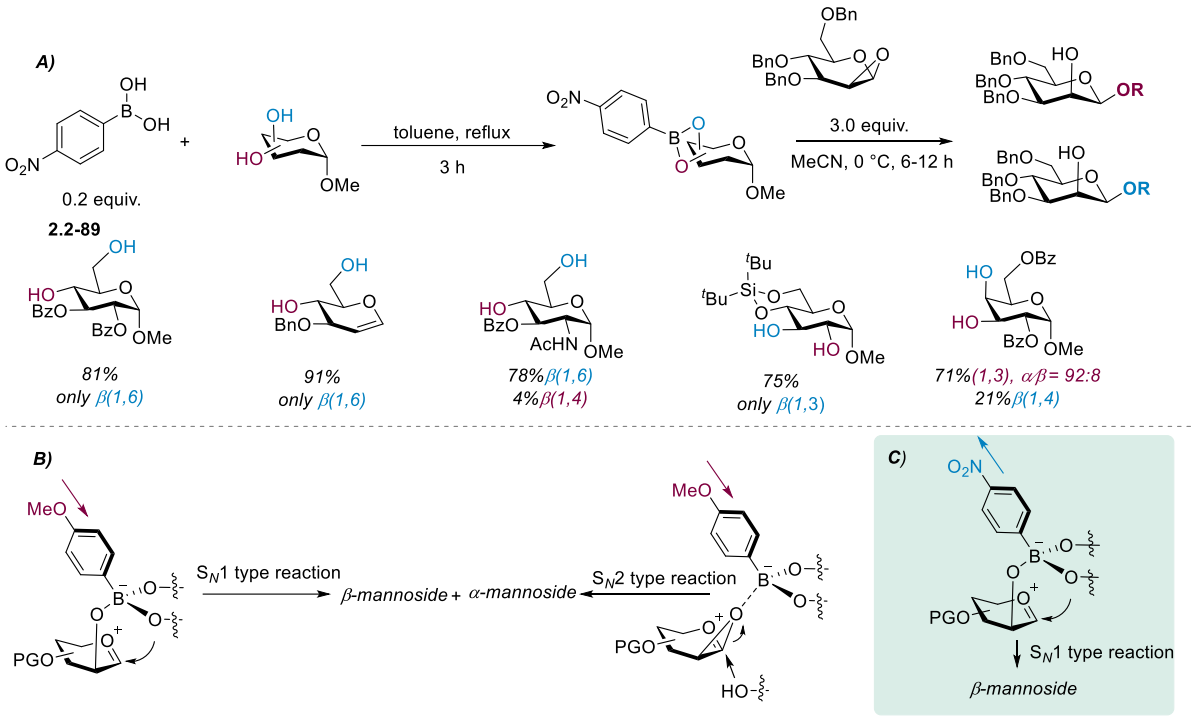

Another variant of this glycosylation strategy was reported by Tanaka et al. with Mono-ol acceptors,[100, 101] which employed the modified boronic acid catalyst **2.2-90** (**Scheme 29**). Notably, this approach does not require the pretreatment of the acceptor with the catalyst in refluxing toluene. With electron-donating substituents on the phenyl ring of the boronic acid catalyst, more α-selectivity was observed, indicating a competing S_N2 pathway. Interestingly, exclusive formation of the undesired 1,2-*trans*-glycoside was obtained when using toluene or DCM as the solvent, suggesting the involvement of the solvent, i.e., MeCN. For sterically more demanding secondary acceptors, stochiometric amount of the boronic acid is required to realize synthetically useful yield. The same reaction protocol was later used to synthesize 1,2-*cis*-glucosides and 1,2-*cis*-galactosides in THF.[101]

Scheme 29. Boronic Acid-Catalyzed 1,2-*cis*-Stereoselective Glycosylation with Mono-ol Acceptors

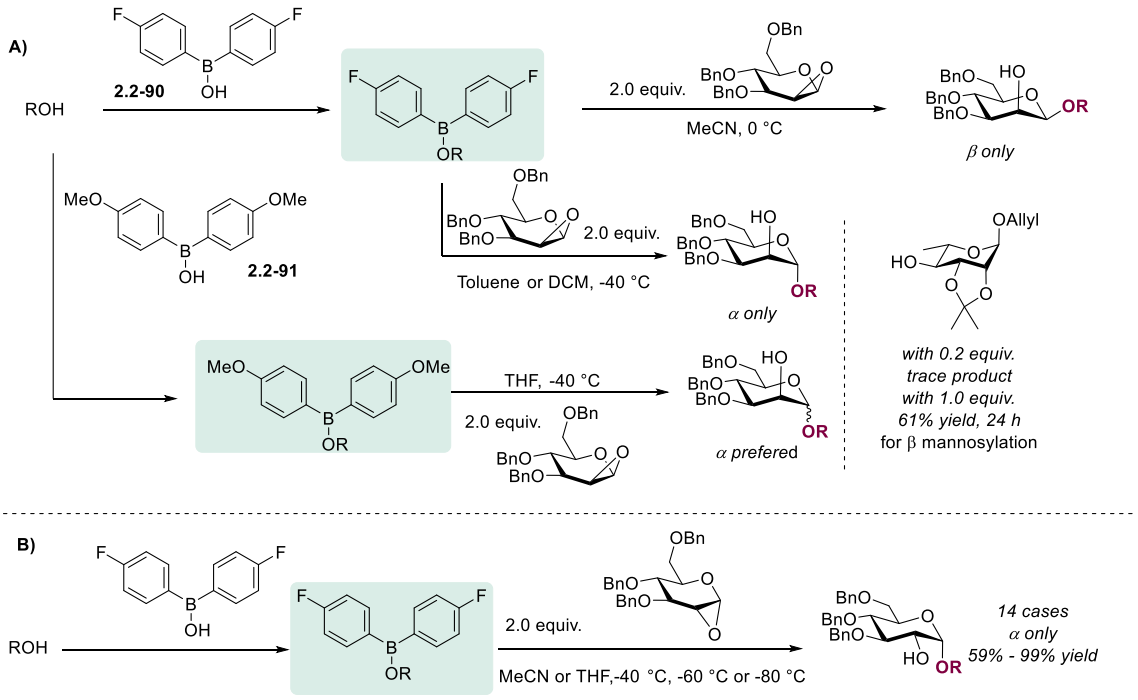

Later, in 2018, the Toshima group applied the same strategy to the stereospecific *β*-l-rhamnosylation using 1,2-anhydro-L-rhamnose donor with mono-ol or 4,6-diol sugar acceptors in the presence of **2.2-90** or **2.2-89,** respectively. The protocol was applied to synthesize a trisaccharide derived from the antigen of *S. pneumoniae* serotypes 7B, 7C, and 7D.[102]

Scheme 30. Boronic Acid-Catalyzed 1,2-*cis*-Stereoselective Glycosylation with Unprotected Sugar Acceptors and *trans*-1,2-Diols

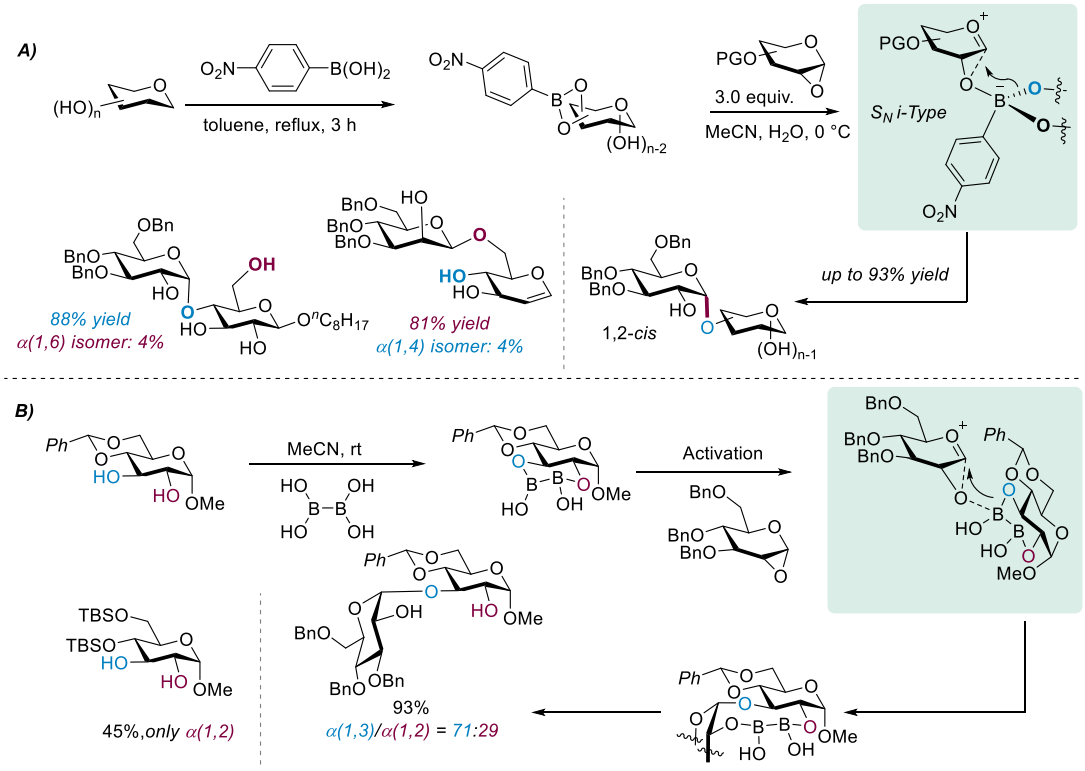

Another application of this strategy is the 1,2-*cis*-stereoselective glycosylation with unprotected sugar acceptors, in which the *p*-nitrophenylboronic acid was used as the catalyst in the presence of water. Mechanistic studies using the KIE experiments and DFT calculations indicated that a highly dissociative concerted S_N i mechanism is involved (**Scheme 30A**). Later in 2020, *trans*-1,2-Diol sugar acceptors in the presence of a diboron catalyst are also applicable to this approach.[103] Notably, different chemoselectivity can be achieved by tuning the steric bulkiness near the hydroxyl groups **(Scheme 30B**).

2.2.3 Other Approaches and Special Methods

2.2.3.1 Stereoselective Glycosylation Enabled by Cooperative Catalysis

Scheme 31. Phosphoric Acid/Thiourea-Catalyzed Glycosylations by the Schmidt Group

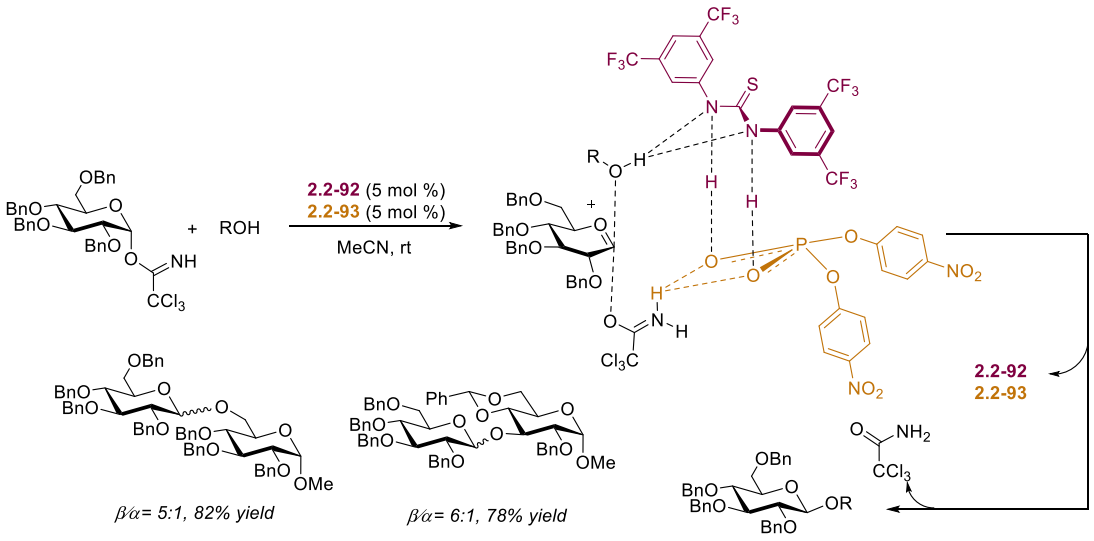

In 2013, the Schmidt group introduced a new concept of cooperative catalysis in which a thiourea cocatalyst **2.2-92** was shown to increase the reaction rate and *β*-selectivity in glycosylations catalyzed by phosphoric acids. Control experiments demonstrated that the Brønsted acid **2.2-93** alone functioned as a very weak activator of the donor in the absence of the thiourea **2.2-92**. Besides, NMR experiments clearly indicated the protons of the cocatalyst **2.2-92** were involved in precomplexation. Therefore, the proposed mechanism involved a transition state with the cooperative activation of the leaving group and the incoming acceptor, as depicted in **Scheme 31**. The reaction proceeds well with high yield and selectivity for simple alcohol acceptors. However, when a slightly larger acceptor like *L*-menthol was employed, the selectivity was moderate (for example, using *L*-menthol as the acceptor, α/β = 4:1). The loss of selectivity could be attributed to the more crowded

transition state. Although comparable β-selectivities were still observed with more hindered 6-OH and 4-OH glycosyl acceptors, it is likely due to the participation of the MeCN solvent (**Scheme 14**). This protocol was applied to gluco-, galacto-, and xylo- TCA donors.

Scheme 32. Glycosylation Catalyzed by Macrocyclic Bis-thioureas

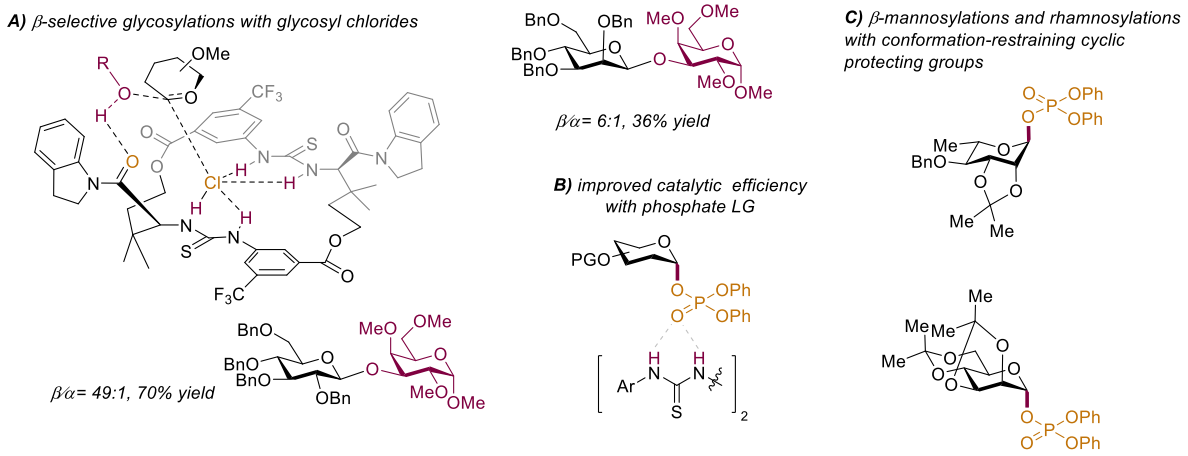

In 2017, the Jacobsen group developed a β-selective glycosylation reaction catalyzed by macrocyclic bis-thioureas, which also features a cooperative mechanism. [104] As shown in Scheme 32A, the macrocyclic bis-thioureas catalyst activates the leaving group and promotes the nucleophilic attack by hydrogen bonding at the same time, leading to stereochemical inversion at the anomeric center. However, for sterically more hindered secondary acceptors, the yield and selectivity of β-mannosylation are low. Further improvements include using a phosphate leaving group that endows stronger hydrogen bonding interaction[105] and using conformation-restraining cyclic phosphate for β-mannosylations and rhamnosylations.[106]

2.2.3.2 Gold(I)-Catalyzed Glycosylation with Glycosyl *o*-Alkynylbenzoates as Donors

In 2008, the Yu group first introduced glycosyl *ortho*-alkynylbenzoates as donors under the catalysis of $Ph_3PAuOTf$.[107] Later in 2013, the Yu group further studied the reaction by crossover experiments, revealing an exogenous anomerization mechanism.[108] As depicted in **Scheme 33A**, all the intermediates are reversible during the reaction. The addition of the isochromen-4-yl gold(I) complex **2.2-99** onto a sugar oxocarbenium could lead to the formation of **2.2-96**, which subsequently undergoes elimination of LAu^+ to regenerate the donor without controlling the anomeric configuration. Interestingly, the donor anomerization was inhibited when additional vinyl gold(I) complex **2.2-99** was added into the reaction. An NMR study was performed to provide a rationale for the observation, revealing the formation of an isochromen-4-yl-gem-digold(I) complex **2.2-97**. This geminal gold complex **2.2-97** was found to be unreactive in catalysis but in equilibrium with the mono-gold(I) complex and the catalytic LAu^+. Moreover, the proposed glycosyloxypyrylium intermediate **2.2-96** was successfully trapped via a cycloaddition reaction by using *n*-butyl vinyl ether as the dienophile. With the formation of intermediate **2.2-96** confirmed, S_N2-like reaction of **2.2-96** in the presence of large excess of accetpors (i.e., 10.0 equivalents) was observed with both donor anomers, leading to stereoselective formation of the dissacharide **2.2-103** with inverted anomeric configuration when a reactive acceptor was employed. However, with a more hindered and less nucleophilic acceptor, no inversion was observed with the α-donor, but the reaction still yielded more β-product than that starting from the β-donor (**2.2-104**)

Scheme 33. Mechanism of *Ortho*-Alkynylbenzoate Activation and S_N2-Like Inversion in the Presence of Large Excess of Acceptor

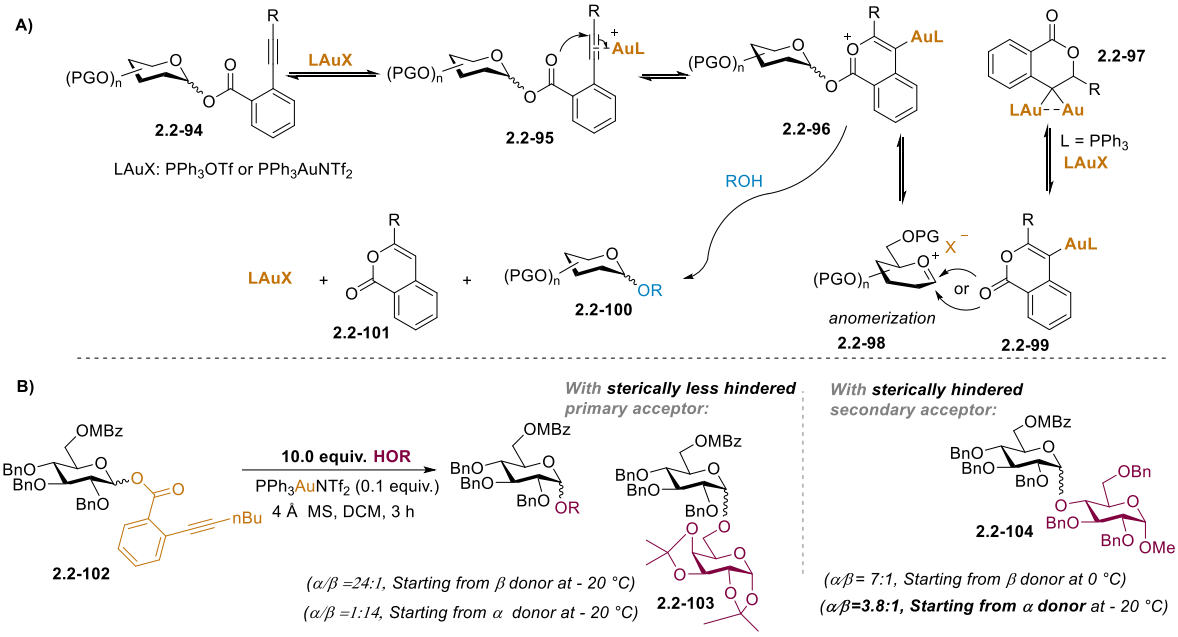

Scheme 34. *β*-Rhamnopyranosylation via Gold(I)-Catalyzed Glycosylation with 2-Alkynyl-4-Nitro-Benzoate Donors

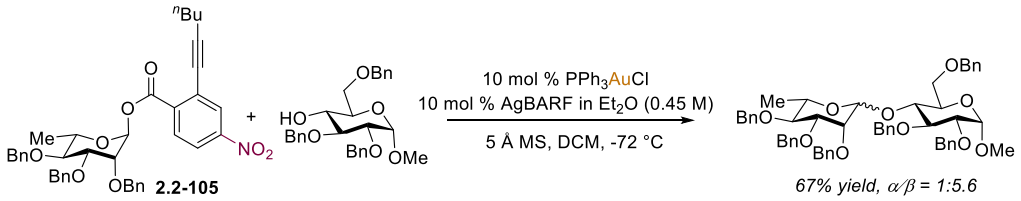

Later in 2015, The Yu group extended this strategy to *β*-mannosylation with the Crich-type 4,6-*O*-benzylidene donors.[109] Moreover, in a more recent study, they further used this strategy to synthesize *β*-rhamnosides.[110] However, for the reactions with the original unsubstituted leaving group, less reactive secondary acceptors failed to trap the glycosyloxypyrylium intermediate effectively at low temperatures. To circumvent this, the nitro-substituted donor **2.2-105** with enhanced nucleofugality was employed, and moderate stereoinversion was achieved even with steric demanding acceptors (**Scheme 34)**.

2.3 Donor Design and Reaction Discovery

As discussed in the previous section, various innovative methods have been developed and partially addressed the challenges in the formation of 1,2-*cis* glycosidic bonds. Those strategies, however, suffer from several common drawbacks/limitations: a) the need to match sugar types and specific O-protecting groups (PG) diminish their generality; b) the need to install a specific PG, which is often special and distinct from common PGs, inevitably complicates donor synthesis with regard to protecting group installation/manipulation and diminish synthetic flexibility and step economy; c) such a protecting group is carried into the glycoside product, which may complicate subsequent glycosylation or require additional PG manipulation. Alternative strategies toward 1,2-*cis* glycosides relying on solvent effects or halide ion catalysis are also limited by applicable scope.

Figure 6. Our General Design

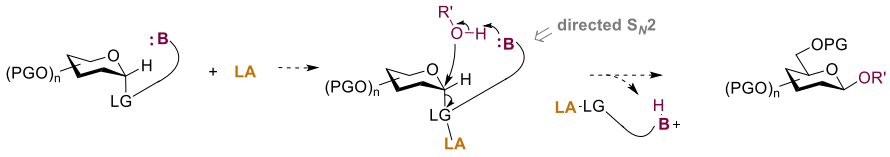

We envisioned a glycosylation strategy that employs a basic group-assisted delivery of acceptor (**Figure 6**). The key feature of this design that would conceptually accommodate any sugar donors, regardless of their configurations and protecting group patterns, and is distinct from all reported strategies is that the basic directing group is to be installed on the glycosyl leaving group and hence traceless in the glycoside product upon reaction. This design necessitates a S_N2-type glycosylation in order to harness the directing effect. By using 1,2-*trans* glycosyl donors, this strategy would lead to a general solution to the challenging construction of 1,2-*cis* glycosides.

The challenges in implementing this traceless directing group design are several folds: a) designing the appropriate structural feature in the leaving group that permits efficient backend delivery of the donor; b) easy access to such a structural feature, c) catalytic LG activation, and d) avoiding the detrimental Lewis pairing between the basic group and LA activator. In practice, we decided to engineer the LG based on the *ortho*-alkynylbenzoates used in Yu's glycosylation chemistry.[111]

Table 4. Initial Trials with Amide Directing Groups

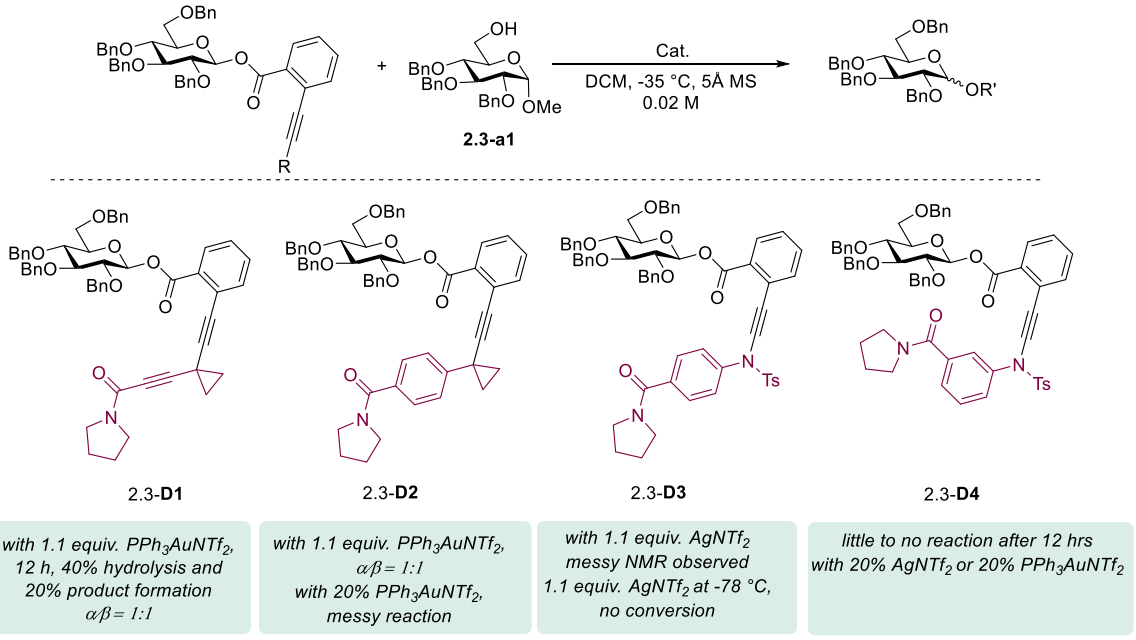

At the outset, we decided to install the amides directing groups on the leaving group, as shown in **Table 4**. Although we didn't perform systematic investigations with different conditions, for the limited conditions we tried, no α-selectivity was observed. The reaction was either messy or showed a selectivity around 1:1. At that time, we attribute this to the intramolecular amide group attack at the anomeric position, therefore messing up the

reaction and selectivity. However, there could also be some lab technique issues back to that time since we didn't know the best way to perform this kind of glycosylation reaction. A more reasonable explanation might be the intermolecular participation from the initially generated byproduct. According to our experience with the latter systems, a compatible solvent that could precipitate the byproduct might be crucial for a clean reaction, and DCM might not be the first choice.

Next, we moved our interest towards other basic directing groups, donor **2.3-D5**, **2.3-D7**, **2.3-D8** bearing benzoxazole, 1,2,3-triazole, 2-phenyl oxazole moieties were prepared. As shown in Table 5, the initial trial of the donor **2.3-D5** with acceptor **2.3-a1** showed a moderate α- selectivity with 1.1 equivalent of PPh_3AuNTf_2, albeit low conversion (entry 1). With a bulkier gold catalyst, under the same conditions, the ratio was improved to 8:1. However, only 50% conversion and 10% desired product were observed (entry 2). The reaction was slow even at room temperature (entry 3). With donor **2.3-D6** devoid of any directing group, the reaction was finished within 12 hours, giving only a 1:1 ratio of the desired product (entry 6), this indicates that donor **2.3-D5**, although inefficient, might still have some directing ability. The reaction of the donor with a triazole directing group was very slow with 1.0 equiv. of $P(o\text{-tol})_3AuNTf_2$ and totally no conversion with 5% catalyst (entry 6-7). Donor **2.3-D8** had a very clean reaction with the acceptor in the presence of 1.0 equiv. of $P(o\text{-tol})_3AuNTf_2$ (entry 8). However, the selectivity is still low. With sterically less hindered PPh_3AuNTf_2, the selectivity is even lower (entry 9).

Table 5. Initial Trials with Other Directing Groups

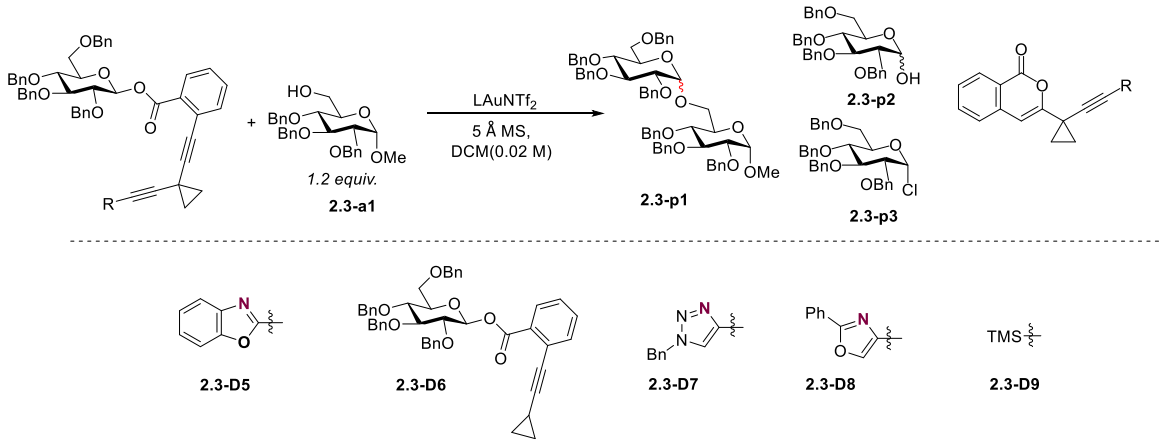

Entry	Donor	Catalyst	Cat. loading (%)	Temp. (°C)	Time (h)	Conversion %	p1/p2/p3 (%/%/%)	Selectivity (α/β)
1	D5	PPh_3AuNTf_2	110	-35	12	32	12/0/20	4.5:1.0
2	D5	$P(o\text{-}tol)_3AuNTf_2$	110	-35	12	50	10/20/20	8.0:1.0
3	D5	PPh_3AuNTf_2	110	r.t.	12	70	20/50/0	2.3:1.0
4	D6	PPh_3AuNTf_2	110	-35	12	100	50/20/0	1.0:1.0
6	D7	$P(o\text{-}tol)_3AuNTf_2$	100	-35	22	30	0/16/14	N/A
7	D7	$P(o\text{-}tol)_3AuNTf_2$	5	-35	22	0	N/A	N/A
8	D8	$P(o\text{-}tol)_3AuNTf_2$	100	-35	12	73	70/0/0	2.5:1.0
9	D8	PPh_3AuNTf_2	100	-35	12	100	79/21/0	1.5:1.0
10	D8	PPh_3AuNTf_2	20	-35	24	100	98/0/0	11:1.0
11	D9	PPh_3AuNTf_2	20	-35	12	100	95/0/0	1.5:1.0
12	D8	PPh_3AuNTf_2	50	-35	24	100	97/0/0	2.8:1

*All reactions were quenched with 1.0 equiv. TBACl before stopped.

To our surprise, with 20% of PPh_3AuNTf_2, the reaction of donor **2.3-D8** proceeded smoothly with *α/β* ratio being > 10:1. Donor **2.3-D9** possessing a hindered TMS group showed no selectivity with the same catalyst loading (entry 11). We further tried the reaction with donor **2.3-D8** in the presence of 50% PPh_3AuNTf_2, and the reaction went smoothly with an *α/β* selectivity of 2.8:1. The comparison between entries 9, 10, and 12 revealed a trend: the selectivity is poorer if more gold catalyst was employed. We reasoned that the

cationic gold(I) binds to the oxazole nitrogen and thereby removes it from directing/facilitating the acceptor's backend attack (**Figure 7A**). As a result, the beneficial role of oxazole appeared to be eliminated (entries 9 vs. 11).

Figure 7. Coordination of Gold(I) Catalyst with the Basic Directing Site

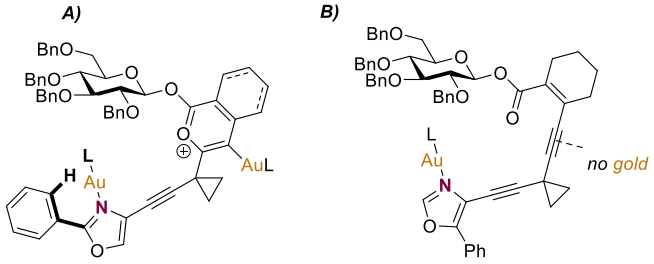

Scheme 35. Synthesis and Initial Trial Reactions of Glycosyl Ynenoate Donor

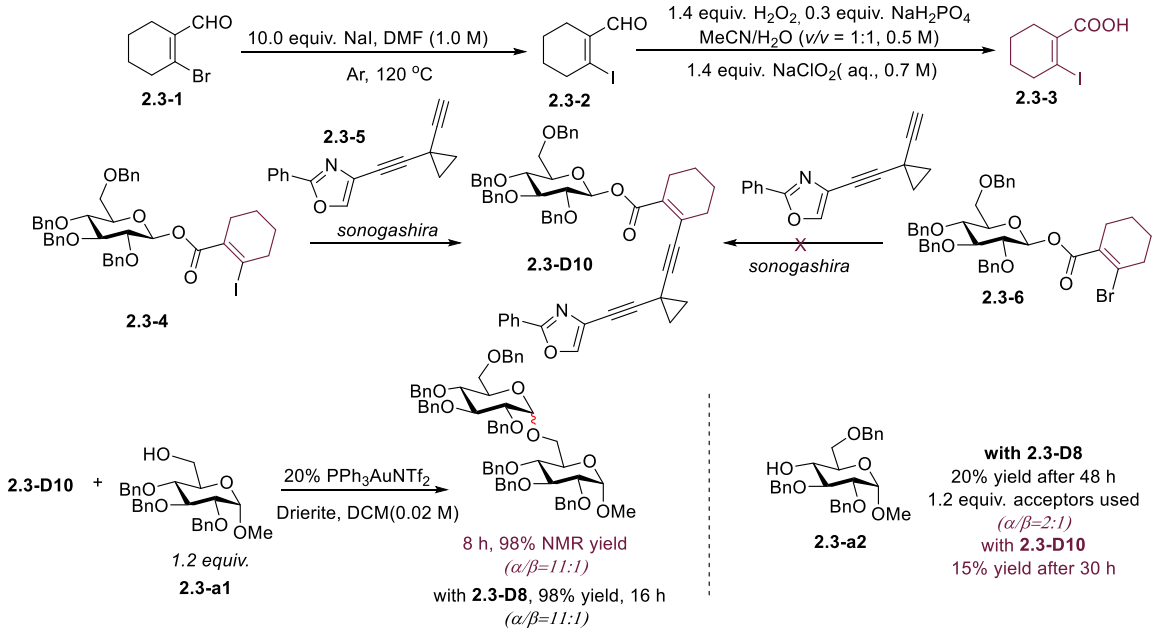

Next, we tried to prepare a donor with an ynenoate leaving group. According to a study our group previously reported, [112] we believe there would be several advantages for this type of donors over Yu's glycosyl *ortho*-alkynylbenzoates donors. A rationale was proposed as

follows: Upon activation, the pyrylium ring in the intermediate should enjoy more aromaticity than isochromenylium ring in Yu's intermediate, in line with the fact that benzene enjoys more aromaticity (36 kcal mol^{-1} resonance energy) than the second benzene ring in naphthalene (61–36 = 25 kcal mol^{-1} resonance energy). Because of that, the pyrylium intermediate could be formed more readily and is a less reactive donor, which might offer the following advantages: a) enabling more efficient catalysis, hence shorter reaction time; b) the increased preference of S_N2 over S_N1 in the glycosidic bond formation process. However, we encountered difficulty in the donor synthesis, i.e., the glycosyl ester bearing a bromo-functionality (**2.3-6**) did not undergo the Sonogashira coupling with the diyne **2.3-5**. To solve this problem, as shown in **Scheme 35**, our previous group member, Dr. Zhitong Zheng, developed a route to access 2-iodocyclohex-1-ene-1-carboxylic acid **2.3-3** by a Finkelstein reaction of the aldehyde **2.3-1** followed by an oxidation with the resulting compound **2.3-2**. The corresponding glycosyl ester bearing an iodo-functionality did undergo the Sonogashira reaction smoothly, delivering the donor **2.3-D10.** With donor **2.3-D10** in hand, we first tested the reaction with primary sugar acceptor **2.3-a1**. To our delight, the reaction finished in 8 hours with similar selectivity. However, the reaction is still slow and only moderate selective with the more challenging secondary acceptor **2.3-a2**.

We initially reasoned that the 2-phenyl group on the oxazole ring is too bulky to direct sterically more demanding acceptors efficiently. To circumvent that, a donor **(2.3-D12)** with an oxazole moiety devoid of the 2-position substitution was prepared. Disappointingly, there's no reaction observed under the same conditions as those show in **Table 5, entry 10**. Increasing the reaction temperature to 0 ˚C did not help, either. Further investigation showed that the reaction would happen when more than 100% catalyst was used, albeit with low selectivity. In the former case, the gold catalyst appeared to be largely sequestered because

of its coordination with the unhindered oxazole. As rationalized in Figure **7B**, since the binding effect is so strong that no catalyst could escape, little to no conversion was observed if less than a stoichiometric amount of catalyst was used. Further modifications, including lowering the basicity of the unhindered directing site (**2.3-D11**) and using a little more hindered isopropyl substitution next to the nitrogen (**2.3-D13**), were found incompetent. Later on, we found that the donor (**2.3-D15**) with a *tert*-butyl substitution at the oxazole 2-position could undergo glycosylation with primary acceptor **2.3-a1** smoothly with higher selectivity (α/β = 14:1) than previous result with donor **2.3-D10** (α/β = 11:1). However, the reaction took almost one day to finish with less hindered **2.3-a1**, let alone with sterically more demanding acceptor **23-a2**. Donor **2.3-D14** with a methyl group at 5-position gave only marginally better selectivity but prolonged reaction time. The general trend of different oxazole directing groups is depicted in **Scheme 36**. To this end, we decided to stay on the original design using the 2-phenyl oxazole as the directing group.

We further turned our eyes on the modification of the glycosyl ester linkages. As shown in **Scheme 37**, the donor **2.3-D17** was prepared. We reasoned that the newly added methyl group might be able to offer beneficial conformational control. However, this modification leads to a longer reaction time and worse selectivity compared to that from the donor **2.3-D8** under the same set of conditions. Another variant we tested was the donor **2.3-D18**. We reasoned that the oxygen next to the alkene moiety should stabilize the glycosidic bond, thereby permitting more S_N2 characteristics in the reaction (**Scheme 37B**). To our disappointment, with this donor, we observed the donor anomeric epimerization even at -25 ˚C, leading to an inferior α/β ratio. Moreover, a significant amount of chlorination sideproduct was formed upon quenching by tetrabutylammonium chloride. In this case, the oxygen might significantly increase the nucleophilicity of the carbonyl group on the

byproduct, leading to isomerization of the intermediate. The chlorination might be generated from the not-so-reactive α-glycosyl pyrylium intermediate, which might cause the erosion of selectivity.

Scheme 36. The General Trend of Donors with Different Oxazole Directing Groups

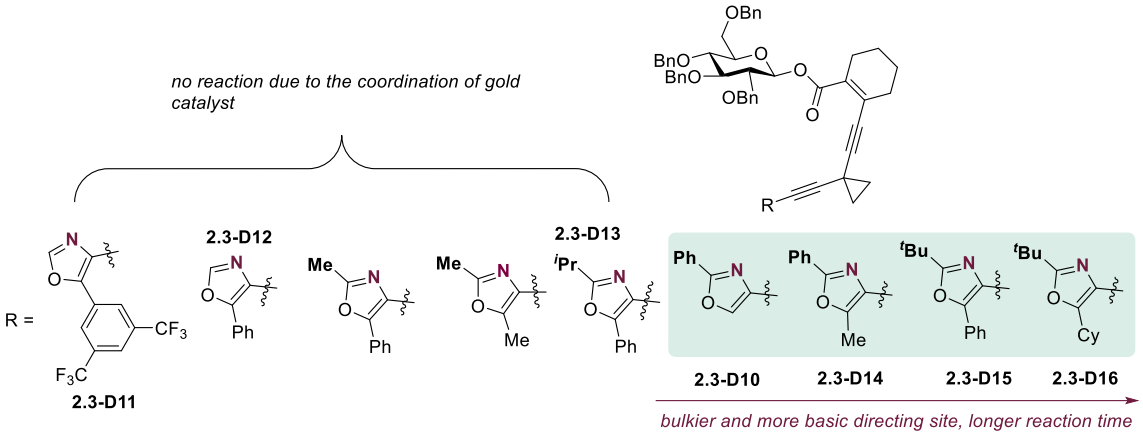

Scheme 37. Other Structural Modifications.

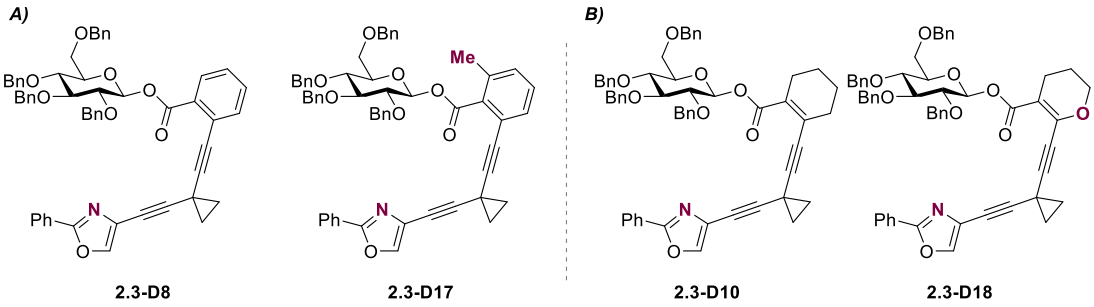

Scheme 38. Selected Reactivity Profiles of Glycosyl Ynenoate Donor

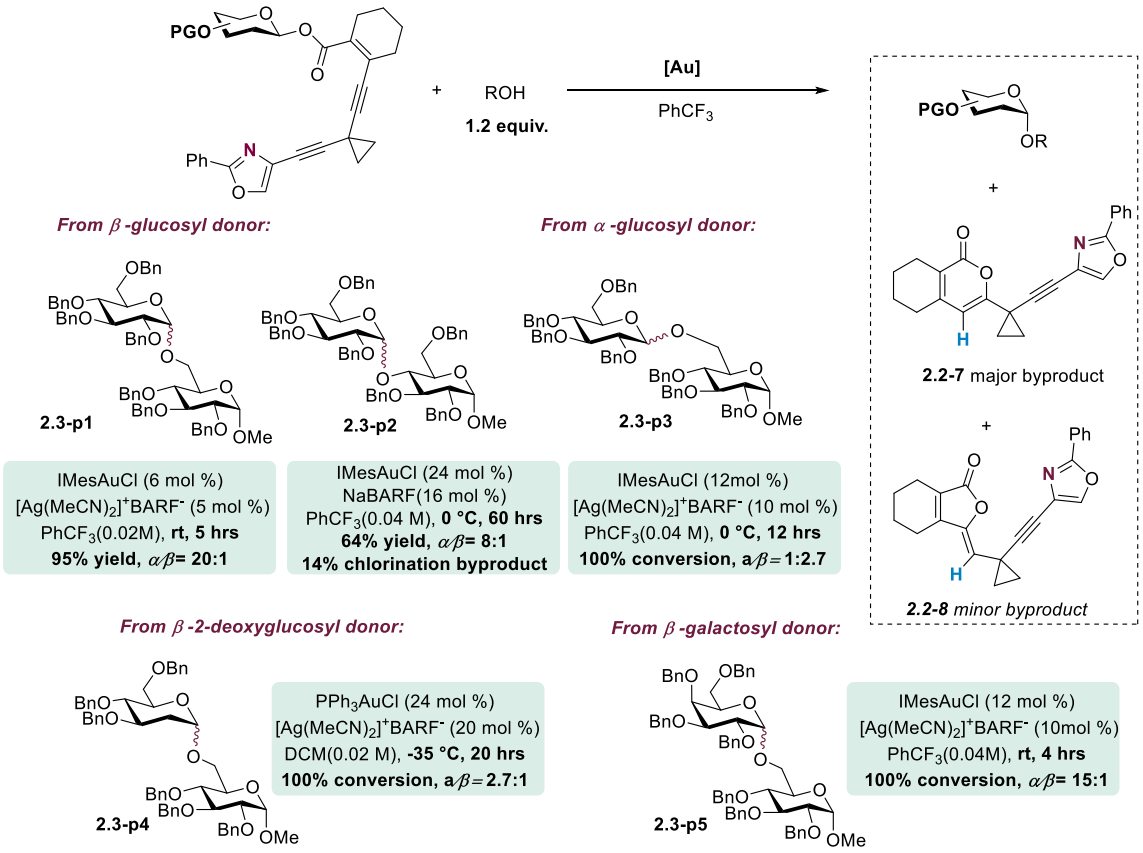

Besides the two donors I prepared, our former group member, Dr. Zhitong Zheng, also prepared a different type of donors replacing the cyclohexene ring in donor **2.3-D10** with a cyclopentene ring. However, no noticeable improvement in terms of selectivity and rate was observed.

Later, a systematic conditions study was performed with the donor **2.3-D10.** Among nonpolar solvents such as DCM, toluene, fluorobenzene, and trifluorotoluene, trifluorotoluene provides the best reaction rate and selectivity. Coincidentally, We found $IMesAu^+$ catalyst gave much superior selectivity than all the other catalysts we tried, albeit with a longer reaction time. To our surprise, **2.3-p1** was obtained in 95% yield with 20:1 α/β selectivity even at room temperature. Besides, the reaction is finished in 5 hours. Encouraged by this promising result, we examined the system with several challenging

acceptors and donors. Disappointingly, with the sterically demanding secondary acceptor **2.3-2a**, the best *α/β* selectivity we can get is 8:1 with an impractically long reaction time (**Scheme 38, 2.3-p2**). Perbenzylated *β*-galactosyl donor reacts smoothly with the primary acceptor at room temperature as well, showing excellent *α*-selectivity (**Scheme 38, 2.3-p5**). However, the reactions with *β*-2-deoxyglucosyl donor and *α*-glucosyl donor could only deliver the corresponding disaccharides with moderate inversions (**Scheme 38, 2.3-p4, 2.3-p3**). Moreover, we were initially confused by the fact that the integrations of product peaks were larger than those of the byproduct peaks in crude NMR spectra. Surprisingly, we found there was the unexpected formation of the 5-membered ring byproduct (**2.2-8**), although in small quantities in most cases running at low temperatures. This indicates a competing 5-exo-dig cyclization in addition to the thermodynamically more favored 6-endo-dig pathway. The resulting glycosyl intermediate featuring a 5-membered ring might lead to non-selective glycosylation, which could be attributed to the low selectivities in some cases.

Frustrated by those results, we decided to explore some new strategies. Although a lot of strategies were tried, one strategy we tried finally led to the discovery of a new type of donor with dimethoxy substitutions. We envisioned that we could use a stoichiometric amount of cheap electrophiles to activate the donor at -78 ˚C, generating the activated intermediate **2.3-9** quantitatively. Hopefully, the intermediate **2.3-9** is stable at low temperature, therefore allowing an S_N2 type of displacement. If successful, this strategy would allow us to use more basic directing groups without worrying about the metal coordination and steric issues we previously encountered (**Scheme 39A**). However, despite various activating reagents and conditions were tried, none of them gave us a clean product

Scheme 39. The Story of the Introduction of Donors with Dimethoxy Moiety

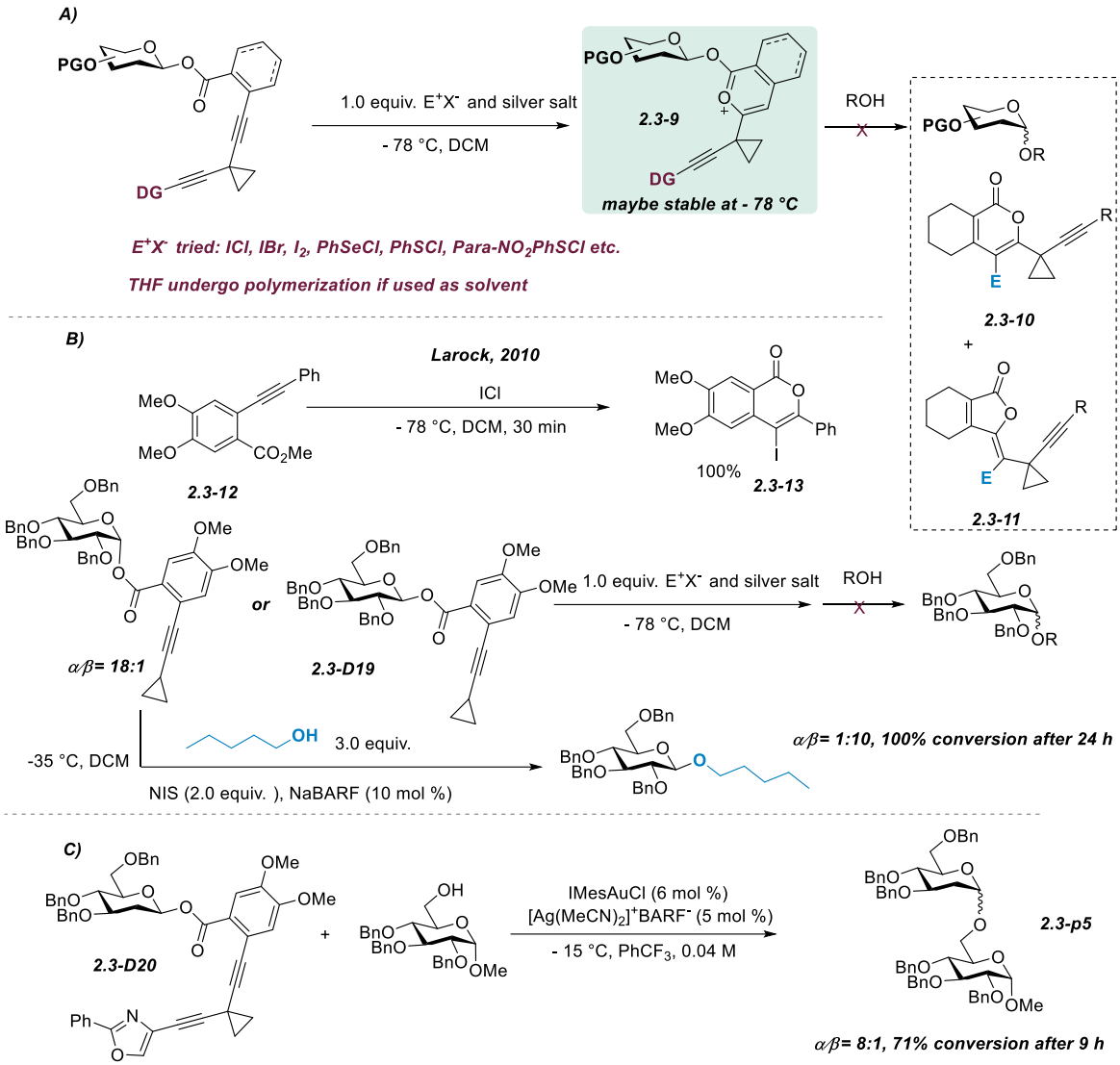

formation with an obvious inversion. Moreover, a nearly 1:1 ratio of both byproducts, **2.3-10** and **2.3-11** formed when some electrophilic iodine reagent was used. Later, we found that the Larock group reported a case in which methyl 4,5-dimethoxy-2-(phenylethynyl)benzoate **2.3-12** could undergo cyclization in the presence of 1.2 equiv. ICl, generating isochromenone **2.3-13** with quantitative yield within 30 mins at -78 ˚C (**Scheme 39B**).[113] Encouraged by the literature results, we prepared both anomers of **2.3-D19**. However, no clean generation of the disaccharide could be observed with the donor *β*-**2.3-D19**. In contrast,

the reaction of α-**2.3-D19** with 1-hexanol in the presence of NIS and 10 mol % NaBARF at -35 ˚C led to encouraging inversion at the anomeric position. At the same time, I prepared the corresponding β-2-deoxyglucosyl donor **2.3-D20**, and its reaction with primary sugar acceptor at -15 ˚C showed a significantly better selectivity (α/β = 8:1, **Scheme 39C**) than the best selectivity (α/β = 2.7:1) we could obtain from the corresponding ynenoate donor (see **Scheme 38**). Moreover, with the new donor, no 5-exo-dig cyclization could be observed. To this end, we decided to investigate this type of donors further.

2.4 Catalytic S_N2 Glycosylation toward 1,2-cis-Glycopyranosides

2.4.1 The Formal Condition Optimizations

We performed a formal conditions optimization as shown in **Table 6** by performing the synthesis of methyl $_D$-glucopyranosyl-(1→6)-α-D-glucopyranoside **2.4-2a** from the β-$_D$-glucopyranosyl donors and the acceptor methyl α-D-glucopyranoside **2.4-1a**. Initial experiments began with the β-$_D$-glucopyranosyl ester donor **D1** (Figure 2C), which contains a 2-phenyl group on the oxazole ring. To our delight, **2.4-2a** was obtained with a respectable α/β ratio of 11:1 in the presence of 20 mol % of PPh_3AuNTf_2 in DCM at -35 ˚C (entry 1). In comparison, the donor **2.4-D2** devoid of oxazole led to little stereoselectivity (entry 2), revealing the critical role of the basic heterocycle in enabling anomeric configuration inversion. This conclusion is further supported by the outcomes when the amount of the gold catalyst was varied. For example, the α/β ratio was lowered to 2.8:1 in the case of 50% PPh_3AuNTf_2 (entry 3) and further to 1.5:1 in the case of one equivalent of the gold catalyst (entry 4). These results are consistent with the directing role played by the oxazole nitrogen as the cationic gold(I) increasingly binds to it and hence diminishes its designed function.

This detrimental binding of oxazole to Au(I) is even more pronounced with the donor **2.4-D3**, of which the oxazole is devoid of substitution at its C2 position and hence presents an unhindered ring nitrogen for coordination. In this case, the gold catalyst appeared to be largely sequestered (entry 5). Upon further donor and conditions optimization, we discovered that the donor **2.4-D4** bearing two methoxy groups on its benzoate permits a faster reaction while maintaining similar *α*-selectivity (entry 6). With $IMesAu^+$ generated from IMesAuCl/$[Ag(MeCN)_2]^+$ $BARF^-$ as the catalyst in 5 mol %, the reaction was sluggish at 0˚C due to the decreased acidity and the lower loading of the catalyst. With 62% conversion after 16 h, the *α/β* selectivity was, however, improved to >20:1 (entry 7). Changing the reaction solvent from DCM to trifluorotoluene led to near quantitative yield while maintaining excellent *α*-selectivity (entry 8). Lowering the reaction temperature led to an even better selectivity but at the cost of conversion (entry 9). As evident from entries 7 and 8, the solvent effect was further examined. We discovered that the isochromen-1-one byproduct **2.4-3** (R' = 3,4-$(MeO)_2$) is crystalline and has significantly higher solubility in DCM (>0.02 M at -15 ˚C) than in $PhCF_3$ (~0.0056 M at -15 ˚C). It is reasoned that the slower reaction rate in DCM is partly due to the coordination of Au(I) by the oxazole nitrogen of **2.4-3**. On the contrary, in $PhCF_3$, most of **2.4-3** precipitate out from the reaction. To this end, with a mixture of $PhCF_3$ and even less dissolving cyclohexane (*v/v* = 4:1) and at an increased concentration (0.08 M), the reaction was substantially accelerated and proceeded to completion in 15 h at -15 ˚C (entry 10). The reaction was again quantitative and highly *α*-selective. In comparison, under these optimized conditions, **2.4-D2** again resulted in a poor *α/β* ratio of 3.1/1 (entry 11).

Table 6. The Formal Condition Optimizations

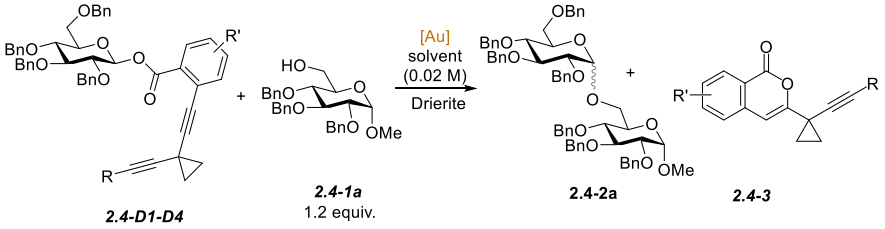

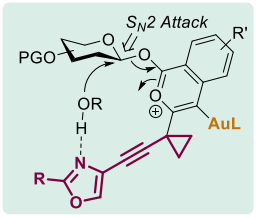

Entry	Donor	Catalyst[a] (equiv.)	Solvent (conc.)	Temp. /Time	Yield(a/b)[b]
1	**D1**	A	DCM	-35 °C/24 h	95% (11:1)
2	**D2**	A	DCM	-35 °C/24 h	95% (1.5:1)
3	**D1**	A[c]	DCM	-35 °C/12 h	95% (2.8:1)
4	**D1**	A[d]	DCM	-35 °C/12 h	96% (1.5:1)
5	**D3**	A	DCM	-35 °C/24 h	<5% (N/A)[e]
6	**D4**	A	DCM	-35 °C/5 h	96% (11:1)
7	**D4**	B	DCM	0 °C/16 h	62% (>20:1)[e]
8	**D4**	B	$PhCF_3$	0 °C/16 h	>99% (>20:1)
9	**D4**	B	$PhCF_3$	-15 °C/24 h	41% (>30:1)[e]
10	**D4**	B	[f]	-15 °C/15 h	>99%[g] (27:1)
11	**D2**	B	[f]	-15 °C/10 h	92%[h] (3.1:1)

[a] A: $Ph_3PAuNTf_2$ (20 mol %); B: IMesAuCl (6 mol %)/ $[Ag(MeCN)_2]^+$ $BARF^-$ (5 mol %). [b] Combined NMR yield and anomeric ratio determined by NMR. [c] 50 mol % catalyst instead. [d] 1 equiv. of catalyst instead. [e] Conversion is nearly the same as yield. [f] $PhCF_3$ and cyclohexane (v/v = 4:1) were used as the solvent and the initial substrate concentration is 0.08 M. [g] 97% yield of isolated product. [h] 93% conversion.

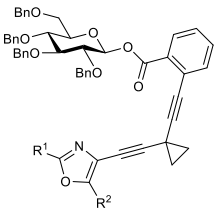

2.4-D1 *(R^1 = Ph, R^2 = H)*
2.4-D3 *(R^1 = H, R^2 = Ph)*

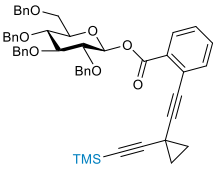

2.4-D2

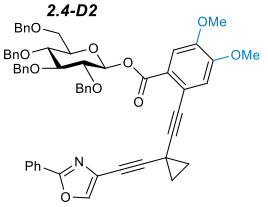

2.4-D4

2.4.2 Reaction Scope with *β*-D-Glucopyranosyl Donors

Figure 8. Reaction Scope with Perbenzylated *β*-*D*-Glucopyranosyl Donors

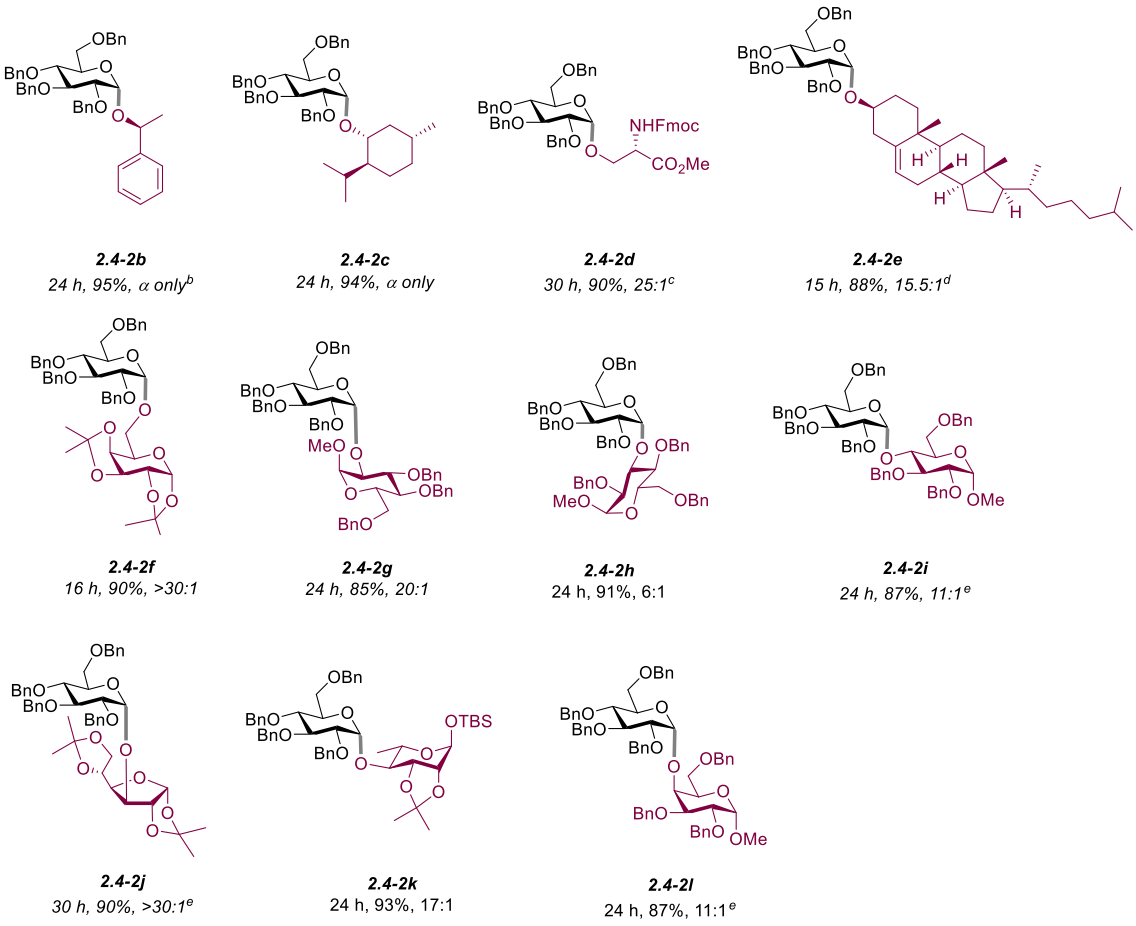

[a] Standard condition. [b] Concentration: 0.02 M. Reaction was stirred at 0 °C with 12% IMesAuCl and 10% $[Ag(MeCN)_2]^+BARF^-$. [c] Concentration: 0.08 M. DCM and cyclohexane (v/v = 1:1) were used as solvent. Reaction was running at 0 °C. [d] Concentration: 0.04 M. Reaction was stirred at -15 °C with 12% IMesAuCl and 10% $[Ag(MeCN)_2]^+BARF^-$. $PhCF_3$ and cyclohexane (v/v = 1:1) were used as solvent. [e] 2.0 equiv. of acceptors were used.

Our optimized reaction conditions (i.e., **Table 6**, entry 10) were applied to a range of acceptors by using **2.4-D4** as the donor. As shown in **Figure 8**, chiral alcohols such as (*R*)-1-phenylethanol and *L*-menthol reacted with excellent yields and exclusive *α* selectivities (**Figure 8**, **2.4-2b** and **2.4-2c**). *L*-Serine esters and cholesterol were running at different solvents due to their poor solubility in the mixed solvent system. The reaction with *L*-serine ester was slow and hence performed at 0 ˚C for 30 hours. Nevertheless, the yields and *α*-

selectivities remained high (**2.4-2d** and **2.4-2e**). The reaction of the galactopyranose-based primary alcohol acceptor proceeded in 90% yield and with >30:1 *α/β* ratios (**2.4-2f**). We then examined tri-*O*-benzylated D-pyranoglucose acceptors with an unprotected secondary hydroxy group at 2-,3-, or 4-position, respectively (**2.4-2g-2j**). While the yields were all high, the *α*-selectivity ranged from 20:1 for the 1→2 linkage, 11:1 for the 1→4 linkage to 6:1 for the 1→3 linkage. The D-glucofuranose and L-rhamnopyranose-derived acceptors also reacted well, exhibiting excellent yields and selectivities (**2.4-2j** and **2.4-2k**), while the reaction with methyl *α*-*O*-2,3,6-tribenzylgalactopyranoside displayed a respectable 11:1 preference for the *α*-glycosidic linkage (**2.4-2l**).

Figure 9. Reaction Scope with Structurally Modified *β*-D-Glucopyranosyl Donors

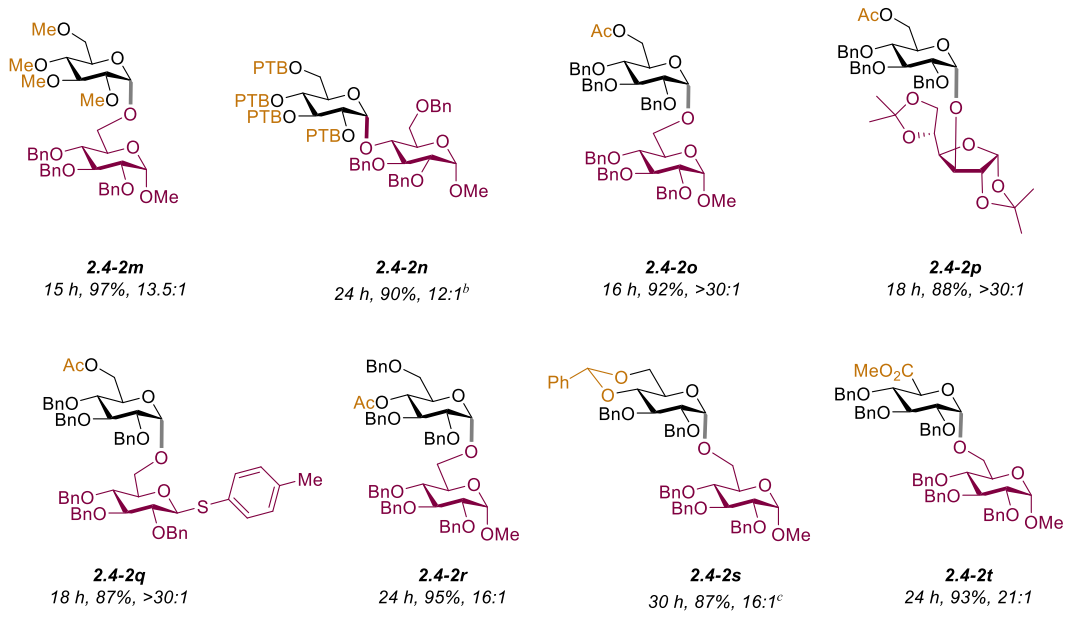

[a] Standard condition. [b] Concentration: 0.02 M. Reaction was stirred at 0 °C with 12% IMesAuCl and 10% $[Ag(MeCN)_2]^+BARF^-$. [c] 2.0 equiv. of acceptors were used.

With methyl groups replacing the benzyl groups in **2.4-D4**, the selectivity was diminished to 13.5:1 (**2.4-2m**). We attribute this to the fact that methyl is less inductively electron-withdrawing than benzyl. Consequently, the methylated donor has a higher tendency of participating in the S_N1 pathway. We also prepared the 4-*t*-butylbenzyl counterpart of the donor **2.4-D4**, which shall be more soluble in the mixed nonpolar solvent system, but the improvement on yield and selectivity was marginal (**2.4-2n**). With readily removable acetyl replacing the *O*-6-benzyl group in **2.4-D4**, generally higher selectivity was observed (**2.4-2o-2q**). It is noteworthy that this gold catalysis accommodates a thioglycoside as the acceptor (**2.4-2q**) and thus permit downstream glycosylation via thioglycoside activation. In addition, replacing the *O*-4-benzyl group of **2.4-D4** with acetyl posed no problem, and **2.4-2r** was formed in 95% yield and an α/β ratio of 16:1, which is only marginally lower than that with **2.4-D4**. Further modifying **2.4-D**4 by installing *O*-4,6-benzylidene protection or oxidizing it into methyl gluconate was inconsequential, as the products from reacting with **1a**, i.e., **2.4-2s** and **2,4-2t**, were formed in excellent yields and with high α-selectivities.

2.4.3 Reaction Scope with Other 1,2-*trans* Monosaccharide Donors

We then applied this design to the synthesis of other 1,2-*cis*-pyranosides. The reaction of the corresponding β-$_D$-galactopyranosyl donor with a primary or secondary alcohol donor also exhibited excellent α selectivities, affording the 1,2-*cis*-galactoside **2.4-2u** and **2.4-2v** in excellent yields (**Figure 10A)**. The reaction of the xylopyranosyl donor was also highly α-selective and efficient (**Figure 10B**). We then explored this S_N2 glycosylation using α-mannosyl donors. As shown in **Figure 10C**, only a moderate inversion of the anomeric configuration was detected in the case of **2.4-2x**. To our delight, with the 4,6-benzylidene-

protected α-donor,[114] the reactions exhibited exclusive S_N2 characteristics regardless of the nature of the donor, and both **2.4-2y** and **2.4-2z** were formed only in the β-forms. In comparison, with a donor without the oxazole group, **2.4-2y** was formed with an α/β ratio of 1:13, and **2.4-2z** in a literature report[115] of 1:12, revealing the beneficial directing effect in addition to the inherent selectivity. A reported drawback[66] of employing 4,6-*O*-benzylidenemannosyl donors[116] is the substantially diminished selectivities caused by adverse steric buttressing of bulky 3-*O* groups. Despite subsequent improvements via using sterically minimal propargyl as the 2-*O* protecting group[69] or employing Yu's *o*-alkynylbenzoate system,[115] the issue remains when bulky acceptors are employed. For example, the mannoside **2.4-2ab** containing a bulky 3-*O*-TBS group and formed from the sterically demanding secondary glucoside acceptor exhibited as a ≤7:1 β/α mixture. Using our strategy, **2.4-2ab** was formed with an improved β/α ratio of 13:1. Remarkably, the reaction was run at ambient temperature, which is advantageous over literature cryogenic conditions (e.g., -20 °C[115] and -78 °C[69]). This strategy was also successfully applied to the synthesis of **2.4-2aa**.

2.4.4 Synthesis of Oligosaccharides

To demonstrate the utility of this strategy, we applied it to oligosaccharide synthesis. As shown in **Scheme 40A**, using methyl 2,3,4-tri-*O*-benzyl-$_D$-glucopyranoside as the initial acceptor and the 6-acetate analog of **2.4-D4** (i.e., **2.4-D5**) as the donor, an iterative process consisting of glycosylation and basic hydrolysis delivered the protected isomaltotetraose **2.4-4c** in 78% overall yield and excellent α-selectivities after three iterations. Alternatively, the related maltotriose derivative **2.4-4d** can be accessed in one step from the α-maltose-derived donor 2.4-**D6** in 88% yield and with good α-selectivity (**Scheme 40B**). In addition,

as shown in **Scheme 40C**, we examined chemoselectivity by employing methyl 2,3-di-*O*-benzyl-α-$_D$-glucopyranoside as the acceptor. Its reaction with **2.4-D4** indeed selectively glycosylated the more accessible 6-OH group to afford the disaccharide **2.4-2ac** with excellent α-selectivity and in 92% yield. It was then reacted with the mannose-derived donor **2.4-D7** to afford the branched trisaccharide **2.4-4e** in 89% yield and with an β/α ratio of >20:1. This two-step sequence was also run successfully in one-pot.

Figure 10. Reaction Scope with Other 1,2-*trans* Monosaccharide Donors

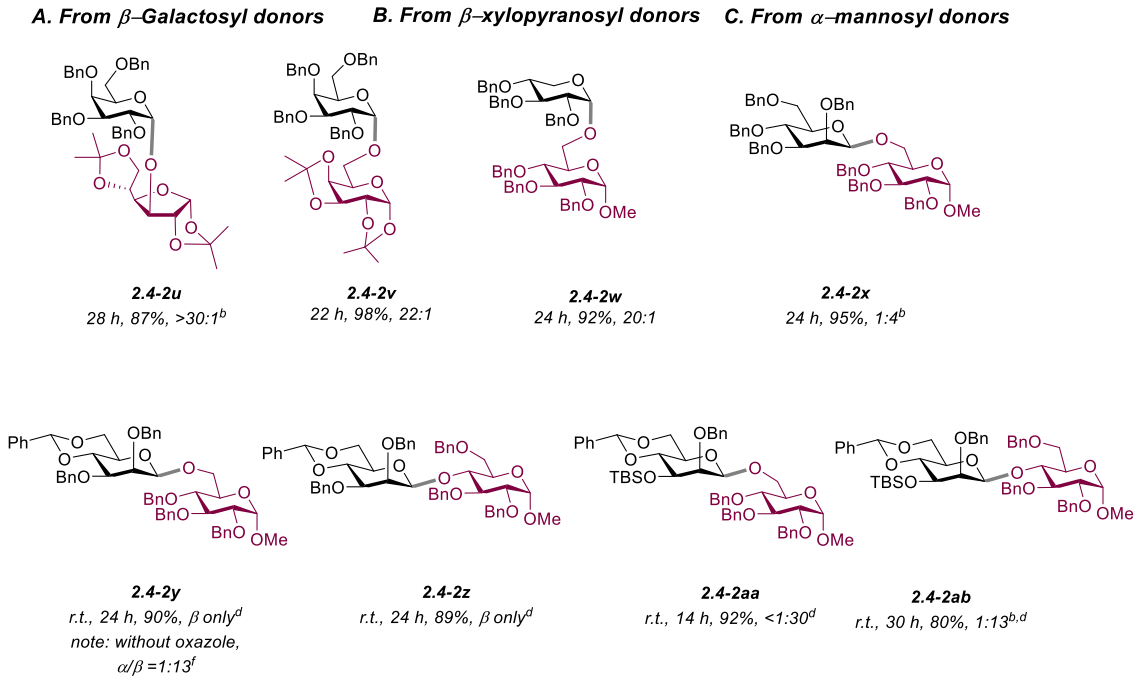

[a] *Standard condition.* [b] *2.0 equiv. of acceptors were used.* [c] *Reaction was running in 0.02 M $PhCF_3$ with 1.2 equiv. of acceptors using 10 mol % PPh_3AuNTf_2 as catalyst at -25 °C.* [d] *Reaction was running at r.t.* [e] *NMR yield.* [f] *See experiment details.*

Scheme 40. Synthesis of Oligosaccharides

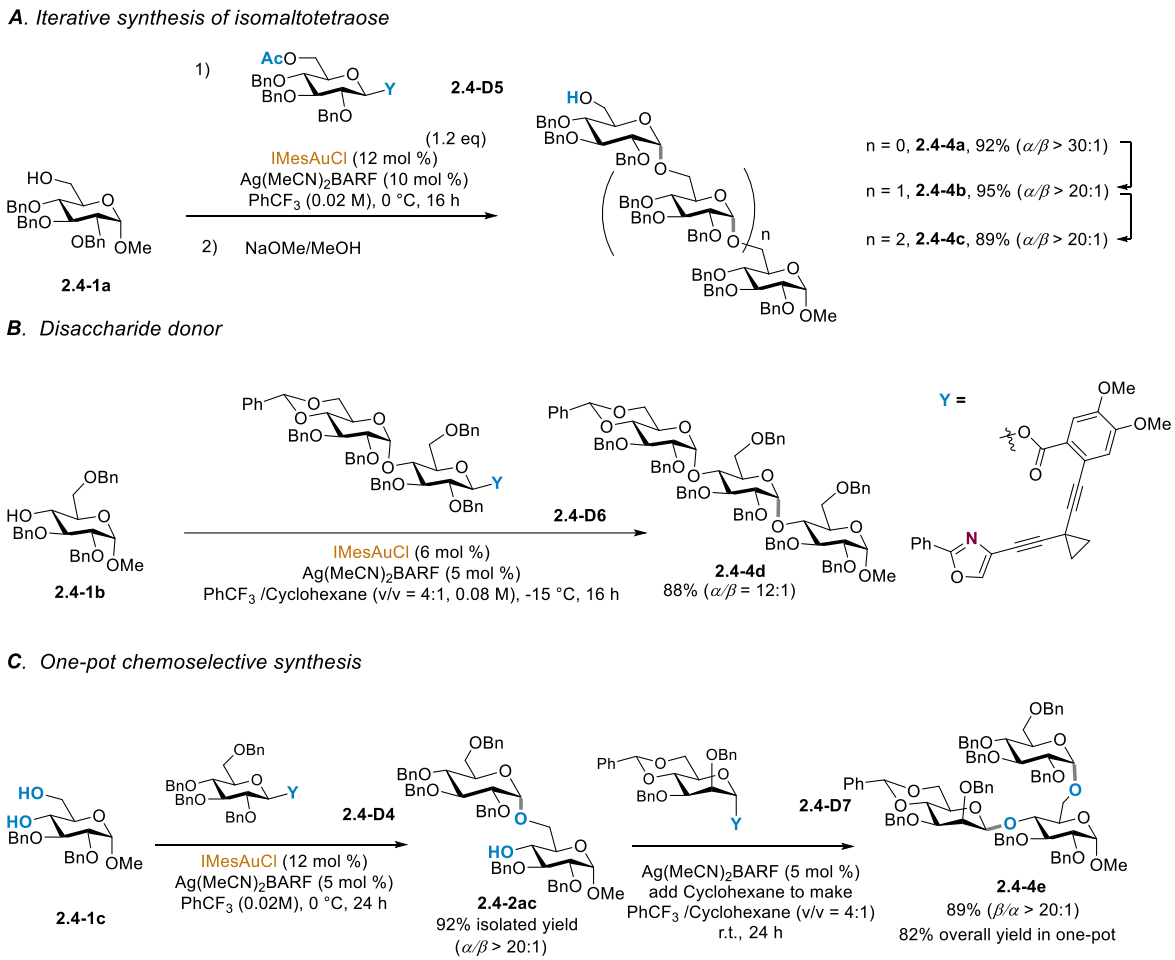

2.4.5 Computational Details

To offer insight into the high levels of stereospecificity in the formation of 1,2-cis glycosidic bonds, we performed density functional theory (DFT) calculations to study the S_N1 and S_N2 pathways of the glycosylation of *O*-methylated analog of **2.4-D4** using MeOH as a model acceptor (**Figure 11**). The overall catalytic cycle (**Figure 12**) involves a facile Au(I)-catalyzed cyclization of the ortho-alkynylbenzoate to form the isochromenylium intermediate **7** with the twist-boat conformation, which is 2.2 kcal/mol more stable than its chair conformation **7a**, followed by a rate- and stereoselectivity-determining glycosylation

step. Glycosylation via the concerted S_N2-transition state (**TS2**) requires lower activation energy than the leaving group dissociation (**TS1**) in the unimolecular S_N1 pathway ($\Delta G^{\ddagger}$ = 14.1 and 16.8 kcal/mol, respectively). These results suggest that the stereospecific S_N2 reaction with the *β*-donor is faster than the formation of oxocarbenium ion in an S_N1-type process. To support this finding experimentally, the reaction of the per-methylated counterpart of **2.4-D4** (**10** in **Figure 12**) with MeOH under the computed reaction conditions (i.e., **Table 6**, entry 9) yielded permethylated yielded the permethylated glucose **9** with *α/β* > 50:1.

We then analyzed factors that promote the S_N2-like transition state (**TS2**). **TS2** features a loose structure with relatively long C^1–O^{LG} and C^1–O^{Nu} distances (2.41 and 2.42 Å, respectively), which alleviate the 1,2-*cis* steric repulsion between C^2–OMe and the alcohol acceptor. The isochromenylium leaving group (LG) requires relatively small distortion energy (ΔE_{dist} = 9.7 kcal/mol with respect to the dissociated leaving group, and -2.9 kcal/mol with respect to the LG in **7**) to orient the oxazole ring in the sidearm to form a strong hydrogen bond with the alcohol acceptor (*d*(N–H) = 1.83 Å). In addition, the isochromenylium ring is oriented perpendicular to the C6 oxygen lone pair. This geometry enables stabilizing lone pair/π interactions with the positively charged isochromenylium ring [see **Figure 13** for the NCI (noncovalent interaction) plot visualization of the stabilizing interactions]. Finally, the lone pair/π interactions between the C6 oxygen and the isochromenylium promote the pyranose ring in the ground state of **7** to adopt a twist boat conformation, which minimizes the distortion of the pyranose ring to achieve the half-chair conformation ($^4H_3$) in the S_N2 transition state.

Figure 11. Computational Mechanistic Studies.

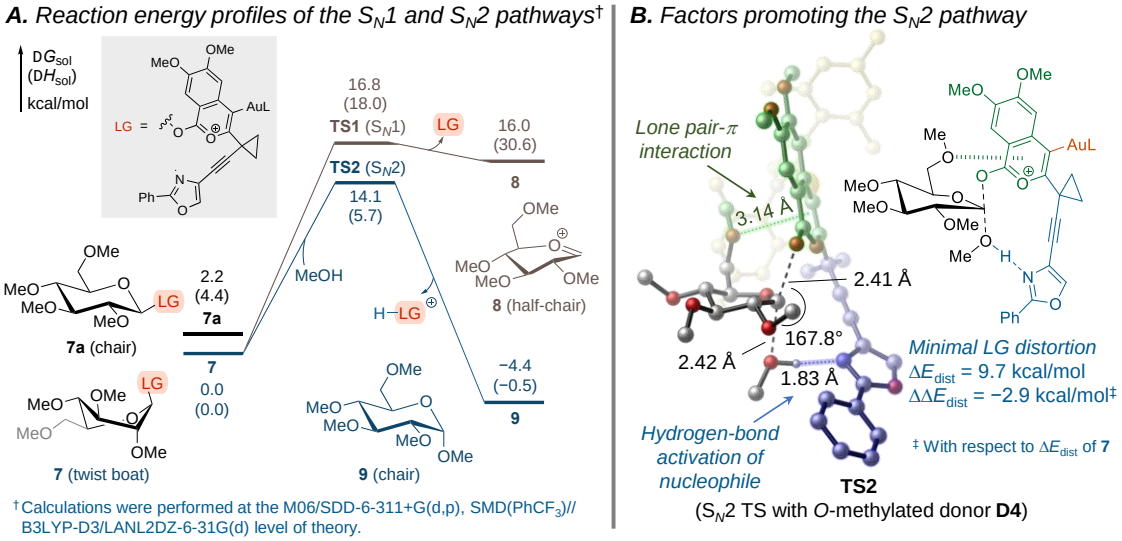

2.4.6 Conclusion

In conclusion, gold-catalyzed S$_N$2 glycosylation is developed to achieve general access to challenging 1,2-*cis*-glycosidic linkages, a long-standing problem in carbohydrate synthesis. This chemistry is enabled by a unique directing-group-on-leaving-group strategy, in which a 'traceless' basic oxazole moiety is appended to the anomeric leaving group and engineered to direct the backend attack at the anomeric center by a glycosyl acceptor. Under exceptionally mild conditions, the reactions exhibit mostly excellent yields and good to outstanding 1,2-*cis*-selectivities. Notably, sterically demanding secondary glycosyl acceptors are readily allowed. The utilities of this strategy in oligosaccharide synthesis are successfully demonstrated.

Figure 12. Reaction Energy Profiles

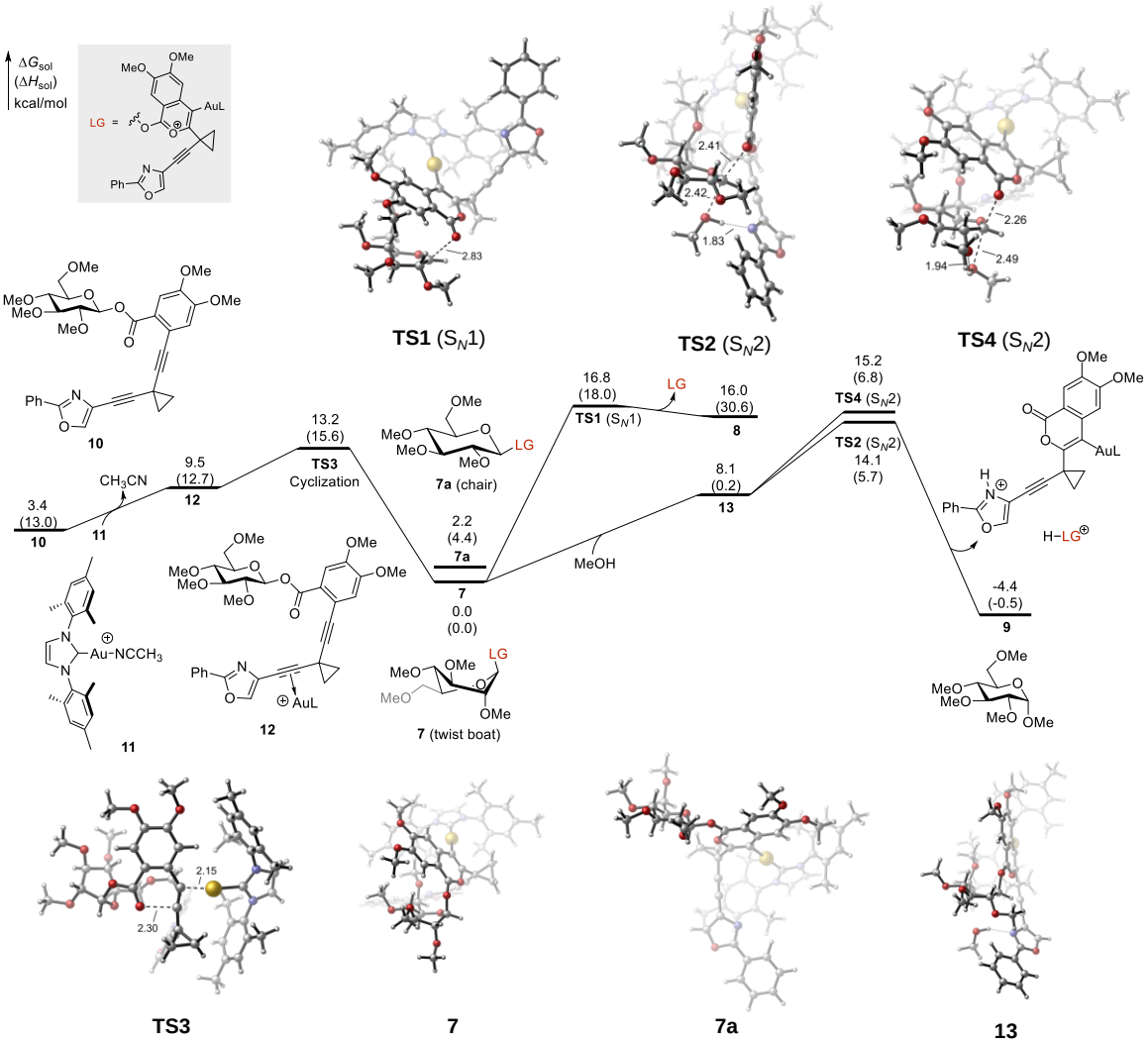

*Reaction Energy Profiles of the Au-Catalyzed Cyclization and Glycosylation of 10 with MeOH as the acceptor. All energies Are with Respect to 7, in kcal/mol。

Figure 13. NCI Plots

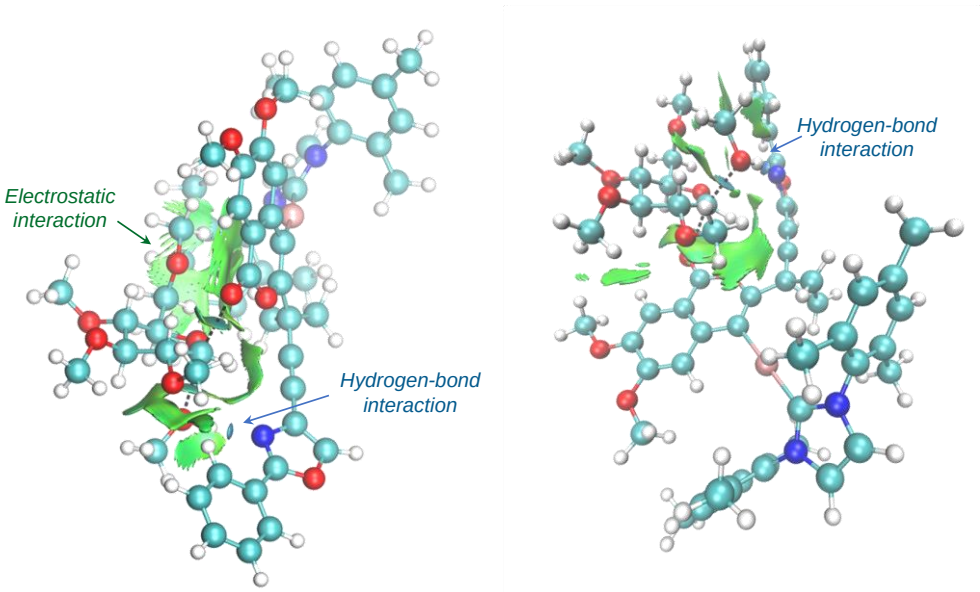

* NCI Plots to Visualize the Through-space Electrostatic Interactions between the C6-OMe Group and the Isochromenylium and the Hydrogen Bond Interactions between the MeOH and the Oxazole Group in the Concerted S_N2 Transition States.

2.5 Experimental Section

General. Ethyl acetate (ACS grade), hexanes (ACS grade), and cyclohexane (ACS grade) were purchased from Fisher Scientific and used without further purification. Anhydrous dichloromethane (HPLC grade) was purified by distillation over calcium hydride. Anhydrous trifluorotoluene was purchased from Sigma Aldrich and was used without further purification. Commercially available 2-iodo-4,5-dimethoxy-benzoic acid, if showing reddish color, was purified by basic aluminum oxide column. Reactions were monitored by thin-layer chromatography (TLC) using Silicycle precoated silica gel plates. Flash column

chromatography was performed over Silicycle silica gel (230-400 mesh). ^{1}H NMR and ^{13}C NMR spectra were recorded on Bruker 400 MHz, Bruker 500 MHz, Varian 400 MHz, 500 MHz, and 600 MHz spectrometers using residue solvent peaks as internal standards ($CHCl_3$, ^{1}H: 7.26 ppm; ^{13}C: 77.00 ppm). Mass spectra were recorded with Xevo G2-XS QTOF Quadrupole Time-of-Flight Mass Spectrometry using electron spray ionization.

Anomerically pure glycosyl *o*-iodobenzoates were obtained either through column purification or recrystallization mostly in Et_3N and in some cases in EtOH. In some cases, the reaction of the Schmidt glycosyl trichloroimidates with the benzoic acid afforded excellent anomeric selectivity. Alternatively, direct coupling between the benzoic acid and the protected reducing monosaccharides using DCC/DMAP can also give predominantly 1,2-*trans* glycosyl esters. The anomeric purities of glycosides were determined by different chemical shifts of the anomeric hydrogens on ^{1}H NMR, which also exhibit different coupling constants. For glycosides documented in the literature, the ^{1}H NMR, ^{13}C NMR, and HRMS data of our products match those reported. For glycosides without literature precedent, the decoupled HSQC spectra were obtained, and the anomeric configurations were determined based on the ^{1}JC-H value. The value of a β-anomer is ~170 Hz, and that of an α-anomer is ~160 Hz.

Sidearm Synthesis:

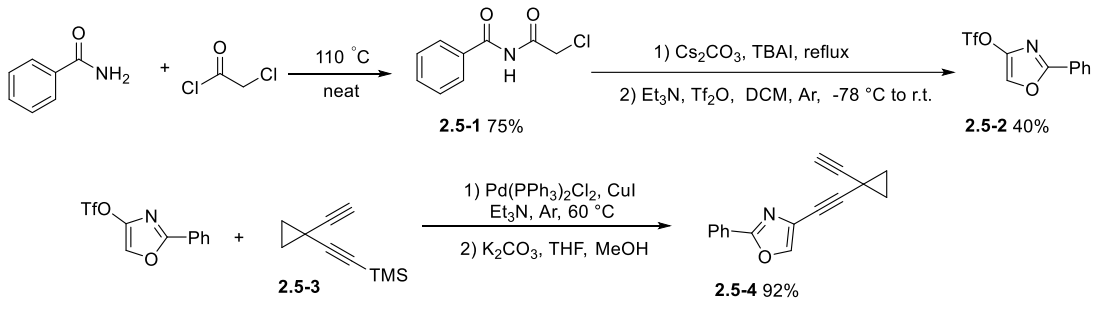

Compound **2.5-1** N-(choloroacetyl) benzamide was prepared in 75% yield according to reported procedure.[117] A flame-dried round-bottomed flask was charged with finely ground **2.5-1** powder (40 mmol, 8.0 g), followed by the addition of Cs_2CO_3 (2.0 equiv., 80 mmol, 26.0 g), TBAI (5 mol %, 2.0 mmol, 745 mg), and MTBE (160 mL). The flask was heated to reflux for 24 h. The reaction mixture was then cooled to room temperature, diluted by DCM, and filtered through a 3-cm thick Celite® pad twice to fully remove Cs_2CO_3. The Rf value of the oxazolone product is a little bit lower than that of **2.5-1**, and the crude NMR indicates about 54% conversion. A quick silica gel column chromatography was applied to remove the reddish color of the mixture by using PE/EA=5:1 to 3:1 as eluent. The yellowish mixture (about a 1:1 molar ratio of **2.5-1** and oxazolone) was directly subjected to the next step without separation. **2.5-2** (4.7 g) was then obtained according to the reported procedure.[118] The combined yield of the two steps is 40%. **2.5-3** was prepared on a large scale from cyclopropyl acetylene in 70% overall yield according to the previously reported procedure. [119] The Sonogashira coupling between **2.5-3** (18 mmol, 2.9 g) and **2.5-2** (16 mmol, 4.7 g) with $Pd(PPh_3)_2Cl_2$ (5 mol %, 560 mg) and CuI (7.5 mol %, 228 mg) under Argon in 50 mL degassed Et_3N reached completion in 24h at 60 °C upon flash column chromatography, the product was then subjected to the removal of TMS group by using K_2CO_3 (1.5 equiv., 24 mmol, 3.3 g) in 1:1 volume ratio of THF and MeOH (40 mL). **2.5-4** was obtained in 92% yield (3.4 g) upon flash column chromatography.

2.5-4: ^{1}H NMR (500 MHz, $CDCl_3$) δ 8.07 – 7.99 (m, 2H), 7.79 (s, 1H), 7.50 – 7.41 (m, 3H), 2.01 (s, 1H), 1.44 – 1.39 (m, 2H), 1.39 – 1.34 (m, 2H). ^{13}C NMR (126 MHz, $CDCl_3$) δ 161.44, 141.26, 130.79, 128.79, 126.71, 126.56, 124.69, 93.94, 84.51, 66.83, 65.00, 20.50, 3.00. MS-ESI (m/z): $[M+Na]^+$ calcd. for $[C_{11}H_{16}NNaO]^+$, 256.0733; found 256.0743.

Preparation of Selected Donors:

General procedure A:

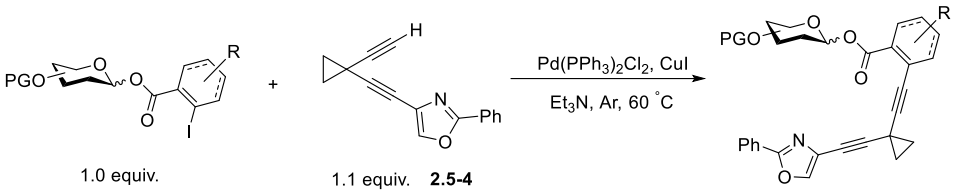

To a flame dried Schlenk flask were added the glycosyl ester (1.0 equiv.), **2.5-4** (1.05 equiv.), $Pd(PPh_3)_2Cl_2$ (5 mol %) and CuI (7.5 mol %). The flask was vacuumed and filled with Argon three times before adding degassed Et_3N (to make a ~0.05 M solution or using THF/Et_3N mixed solvent if better solubility is needed). The mixture was left at 60 °C oil bath for 12 h. The product is bluish under UV light and can be purified by a flash column. After the column, the donors should be stored in the refrigerator. It is noteworthy that after being washed with saturated Na_2CO_3 aqueous solution, the donors are bench stable for a couple of months.

Donor **2.4-D4:**

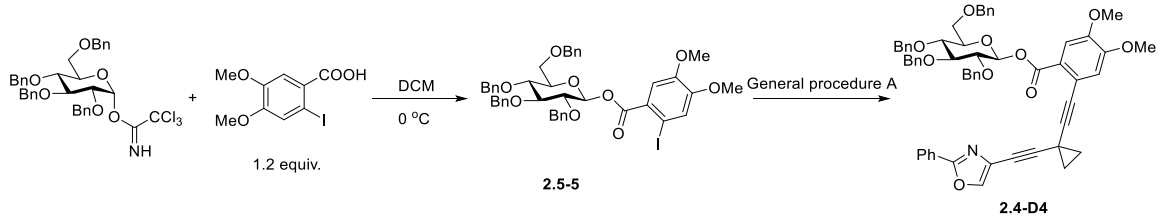

Anomerically pure 2,3,4,6-tetra-*O*-benzyl-α-D-glucopyranosyl trichloroacetimidate was prepared according to the reported procedures.[120] To a flame-dried flask were added commercially available 2-iodo-4,5-dimethoxy-benzoic acid (1.2 equiv., 6 mmol, 1.85 g) and DCM. The reaction was then cooled to a 0 o C by an ice-water bath. The shown trichloroacetimidate (1.0 equiv., 5 mmol, 3.43g) was added to the reaction mixture. The

reaction was allowed to gradually warm to room temperature overnight. Upon routine workup, anomerically pure **2.5-5** (β/α > 100/1, 3.12 g, 75% yield) was obtained by collecting the later 80% fractions during column chromatography.^{1}H NMR (500 MHz, Chloroform-*d*) δ 7.50 (s, 1H), 7.45 (s, 1H), 7.36 – 7.25 (m, 13H), 7.24 – 7.13 (m, 7H), 5.94 – 5.85 (m, 1H), 4.92 (d, *J* = 11.0 Hz, 1H), 4.89 – 4.83 (m, 2H), 4.81 (s, 2H), 4.66 (d, *J* = 12.1 Hz, 1H), 4.59 (d, *J* = 10.7 Hz, 1H), 4.52 (d, *J* = 12.1 Hz, 1H), 3.94 (s, 3H), 3.89 – 3.78 (m, 8H), 3.67 (dt, *J* = 9.5, 2.6 Hz, 1H).^{13}C NMR (126 MHz, Chloroform-*d*) δ 162.95, 152.19, 148.31, 138.14, 137.76, 137.60, 137.55, 128.17, 128.13, 127.96, 127.74, 127.66, 127.58, 127.57, 127.52, 127.51, 127.47, 127.46, 123.91, 113.91, 94.59, 85.85, 84.68, 80.58, 77.09, 76.63, 75.38, 75.35, 74.77, 74.65, 73.31, 67.76, 56.05, 55.77. MS-ESI (m/z): $[M+Na]^+$ calcd. for $[C_{43}H_{43}INaO_9]^+$, 853.1844, found 853.1862.

Donor **2.4-D4** (2.7 g, 96% yield) was prepared by following the general procedure A (3 mmol scale).^{1}H NMR (600 MHz, Chloroform-*d*) δ 8.08 – 7.97 (m, 2H), 7.75 (s, 1H), 7.50 – 7.41 (m, 4H), 7.36 – 7.23 (m, 13H), 7.22 – 7.12 (m, 7H), 7.03 (s, 1H), 5.92 (d, *J* = 7.4 Hz, 1H), 4.92 (d, *J* = 11.0 Hz, 1H), 4.89 – 4.79 (m, 4H), 4.63 (d, *J* = 12.0 Hz, 1H), 4.56 (d, *J* = 10.7 Hz, 1H), 4.51 (d, *J* = 12.0 Hz, 1H), 1.61 – 1.45 (m, 4H). ^{13}C NMR (101 MHz, Chloroform-*d*) δ 163.52, 161.31, 151.96, 148.19, 141.38, 138.41, 138.03, 137.88, 137.86, 130.72, 128.77, 128.35, 128.32, 128.29, 127.94, 127.90, 127.84, 127.81, 127.71, 127.64, 127.61, 126.72, 126.51, 124.77, 123.20, 118.42, 116.31, 113.02, 94.60, 94.56, 84.83, 81.07, 75.64, 75.57, 75.55, 74.97, 73.47, 68.13, 66.60, 56.17, 56.04, 21.35, 21.32, 4.25. MS-ESI (m/z): $[M+Na]^+$ calcd. for $[C_{59}H_{53}NNaO_{10}]^+$, 958.3562, found 958.3558.

Donor **2.4-D5:**

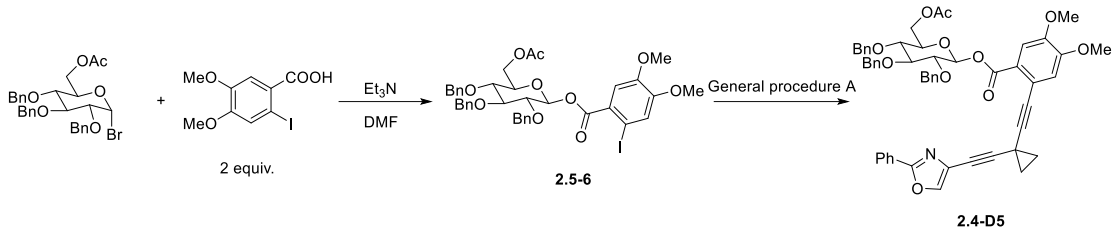

6-O-acetyl-2,3,4-tri-O-benzyl-α-D-glucopyranosyl bromide was prepared according to the reported procedure. [121] 5 Å molecular sieves (100 mg) was added to a flame-dried flask, Et3N (2 mL) and DMF (10 mL) was then added, glucopyranosyl bromide (0.54 mmol, 300 mg) and carboxylic acid (2.0 equiv., 340 mg) were added at last. The reaction was stirred overnight. **2.5-6** (*β/α* > 40:1,270 mg, 64% yield) was collected and can be separated by column with PE/EA=3:1. ^{1}H NMR (600 MHz, $CDCl_3$) δ 7.47 (s, 1H), 7.44 (s, 1H), 7.36 – 7.25 (m, 10H), 7.22 (m, 5H), 5.91 (dd, J = 7.8, 1.2 Hz, 1H), 4.94 (d, J = 10.9 Hz, 1H), 4.87 (dd, J = 14.0, 10.9 Hz, 2H), 4.81 (s, 2H), 4.60 (d, J = 10.9 Hz, 1H), 4.35 – 4.26 (m, 2H), 3.93 (s, 3H), 3.84 (t, J = 8.7 Hz, 1H), 3.80 – 3.73 (m, 2H), 3.78 (s, 3H), 3.66 (t, J = 9.3 Hz, 1H), 2.03 (s, 3H). ^{13}C NMR (126 MHz, $CDCl_3$) δ 170.62, 163.00, 152.47, 148.52, 138.09, 137.59, 137.44, 128.50, 128.43, 128.38, 128.13, 128.09, 128.04, 127.80, 127.78, 127.68, 124.15, 124.00, 114.09, 94.52, 86.08, 84.81, 80.76, 76.93, 75.56, 74.95, 74.86, 73.75, 62.74, 56.26, 55.91, 20.83. MS-ESI (m/z): $[M+Na]^+$ calcd. for $[C_{38}H_{39}INaO_{10}]^+$, 805.1480, found 805.1489.

Donor **2.4-D5** (1.57 g, 89% yield). was synthesized by following the general procedure A (2 mmol scale).^{1}H NMR (600 MHz, $CDCl_3$) δ 8.05 – 8.00 (m, 2H), 7.75 (s, 1H), 7.48 – 7.43 (m, 4H), 7.36 – 7.27 (m, 8H), 7.25 – 7.18 (m, 7H), 7.01 (s, 1H), 5.96 – 5.88 (m, 1H), 4.94 (d, J = 10.9 Hz, 1H), 4.88 (d, J = 11.1 Hz, 1H), 4.85 – 4.80 (m, 3H), 4.54 (d, J = 10.8 Hz, 1H), 4.30 (qd, J = 12.1, 3.5 Hz, 2H), 3.94 (s, 3H), 3.85 (s, 3H), 3.83 – 3.80 (m, 2H), 3.75 (ddd, J = 10.0, 4.6, 2.3 Hz, 1H), 3.63 – 3.55 (m, 1H), 2.03 (s, 3H), 1.65 – 1.50 (m, 4H). ^{13}C NMR

(126 MHz, cdcl3) δ 170.59, 163.48, 161.31, 152.03, 148.25, 141.41, 138.16, 137.75, 137.50, 130.72, 128.74, 128.41, 128.35, 128.31, 128.28, 127.95, 127.91, 127.84, 127.80, 127.69, 127.67, 126.64, 126.46, 124.67, 123.01, 118.30, 116.28, 113.05, 94.48, 94.39, 94.34, 84.72, 81.02, 76.94, 75.61, 75.56, 74.94, 74.88, 73.71, 66.67, 62.82, 56.12, 55.94, 21.25, 21.20, 20.77, 4.22. MS-ESI (m/z): $[M+Na]^+$ calcd. for $[C_{54}H_{49}NNaO_{11}]^+$, 910.3198, found 910.3207.

Donor **2.4-D6:**

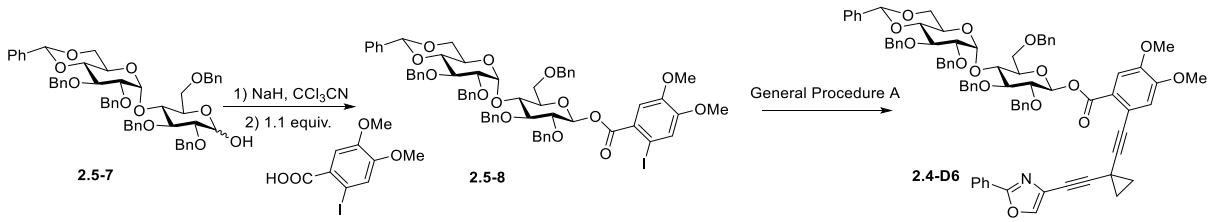

2.5-7 was synthesized according to the reported procedure. [122] **2.5-8** was synthesized by following a procedure similar to that for **2.5-5.** Compound **2.5-8:** ^{1}H NMR (500 MHz, $CDCl_3$) δ 7.51 (d, J = 6.7 Hz, 3H), 7.44 (s, 1H), 7.43 – 7.34 (m, 5H), 7.33 – 7.18 (m, 21H), 7.16 (dd, J = 7.3, 2.2 Hz, 2H), 6.08 (d, J = 6.9 Hz, 1H), 5.66 (d, J = 3.8 Hz, 1H), 5.55 (s, 1H), 4.93 (d, J = 11.1 Hz, 1H), 4.84 – 4.73 (m, 4H), 4.73 – 4.56 (m, 5H), 4.40 (dd, J = 9.9, 8.2 Hz, 1H), 4.10 (dd, J = 10.2, 4.8 Hz, 1H), 4.04 (t, J = 9.3 Hz, 1H), 3.98 – 3.83 (m, 5H), 3.93 (s, 3H), 3.80 (dd, J = 11.1, 2.0 Hz, 1H), 3.69 (s, 3H), 3.62 (q, J = 10.1, 9.7 Hz, 2H), 3.55 (dd, J = 9.4, 3.8 Hz, 1H). ^{13}C NMR (126 MHz, $CDCl_3$) δ 163.21, 152.36, 148.55, 138.59, 138.16, 138.06, 137.89, 137.49, 137.44, 128.80, 128.36, 128.30, 128.28, 128.24, 128.17, 128.13, 127.94, 127.81, 127.80, 127.77, 127.67, 127.54, 127.51, 127.37, 127.35, 126.84, 126.01, 124.26, 124.05, 114.21, 101.12, 97.14, 94.12, 85.74, 84.82, 82.26, 79.82, 78.72, 78.64, 75.21, 74.57, 74.14, 73.80, 73.43, 71.61, 68.81, 68.27, 63.25, 56.24, 55.82. MS-ESI (m/z): $[M+Na]^+$ calcd. for $[C_{63}H_{63}INaO_{14}]^+$, 1193.3155, found 1193.3149.

2.4-D6 (270 mg, 85% yield) was synthesized by following the general procedure A (0.25 mmol scale).^{1}H NMR (500 MHz, $CDCl_3$) δ 8.08 – 8.01 (m, 2H), 7.74 (s, 1H), 7.55 – 7.50 (m, 3H), 7.46 (dd, J = 5.2, 2.0 Hz, 3H), 7.43 – 7.38 (m, 3H), 7.36 (ddd, J = 7.7, 3.5, 1.6 Hz, 4H), 7.33 – 7.16 (m, 21H), 7.05 (s, 1H), 6.07 (d, J = 7.1 Hz, 1H), 5.69 (d, J = 3.8 Hz, 1H), 5.55 (s, 1H), 4.94 (d, J = 11.2 Hz, 1H), 4.88 (dd, J = 11.4, 9.2 Hz, 2H), 4.80 (d, J = 11.2 Hz, 1H), 4.75 (dd, J = 11.4, 7.3 Hz, 3H), 4.66 (d, J = 12.1 Hz, 1H), 4.61 (dd, J = 12.0, 5.7 Hz, 2H), 4.35 (dd, J = 9.8, 8.1 Hz, 1H), 4.11 (dd, J = 10.2, 4.8 Hz, 1H), 4.05 (t, J = 9.3 Hz, 1H), 3.99 – 3.86 (m, 5H), 3.96 (s, 3H), 3.84 – 3.80(m, 1H), 3.80 (s, 3H), 3.67 – 3.58 (m, 2H), 3.55 (dd, J = 9.5, 3.8 Hz, 1H), 1.67 – 1.51 (m, 4H). ^{13}C NMR (126 MHz, $CDCl_3$) δ 163.44, 161.29, 151.97, 148.24, 141.31, 138.58, 138.32, 138.03, 137.89, 137.59, 137.47, 130.67, 128.76, 128.71, 128.26, 128.24, 128.22, 128.21, 128.12, 128.09, 127.95, 127.90, 127.87, 127.71, 127.67, 127.64, 127.59, 127.53, 127.50, 127.46, 127.34, 127.24, 126.75, 126.71, 126.49, 125.98, 124.71, 123.22, 118.34, 116.29, 113.05, 101.09, 97.16, 94.57, 94.47, 93.99, 84.84, 82.23, 80.43, 78.74, 78.57, 75.52, 75.15, 74.79, 74.42, 73.69, 73.60, 73.37, 71.82, 68.80, 68.45, 66.63, 63.23, 56.11, 55.89, 21.33, 4.24. MS-ESI (m/z): $[M+Na]^+$ calcd. for $[C_{79}H_{73}NNaO_{15}]^+$, 1298.4872, found 1298.4878.

Donor **2.4-D7:**

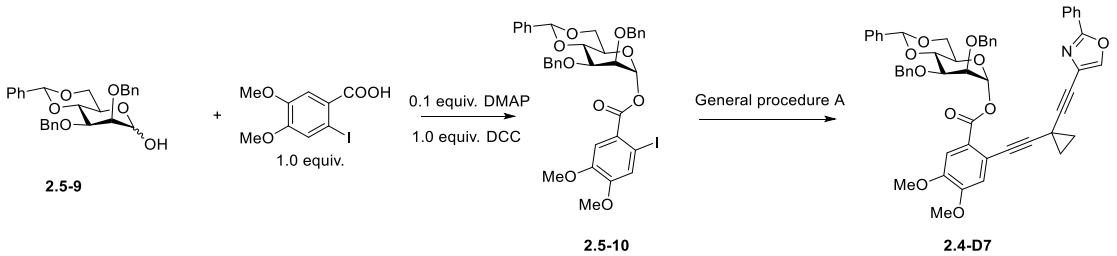

2.5-9 was synthesized according to the previously reported procedure. [123] **2.5-10** can be

obtained by coupling **2.5-9** (10 mmol, 4.49 g) with commercially available 2-iodo-4,5-dimethoxy-benzoic acid (10 mmol, 3.08 g) in the presence of 4-dimethylaminopyridine (0.1 equiv., 1 mmol, 122.17 mg) and *N*, *N*'-dicyclohexylcarbodiimide (10 mmol, 2.06 g). The product is a white solid with α/β ratio >10:1. The pure α anomer (5.3 g) was recrystallized from Et3N. The yield after recrystallization is 72%.^{1}H NMR (500 MHz, $CDCl_3$) δ 7.54 – 7.50 (m, 2H), 7.50 – 7.44 (m, 2H), 7.42 – 7.36 (m, 6H), 7.35 – 7.26 (m, 7H), 6.38 (d, J = 1.7 Hz, 1H), 5.68 (s, 1H), 4.88 (s, 2H), 4.82 (d, J = 12.8 Hz, 1H), 4.73 (d, J = 12.7 Hz, 1H), 4.39 (t, J = 9.7 Hz, 1H), 4.29 (dd, J = 10.1, 4.6 Hz, 1H), 4.20 (dd, J = 10.1, 3.4 Hz, 1H), 4.01 (dd, J = 3.4, 1.8 Hz, 1H), 3.96 (td, J = 9.8, 4.6 Hz, 1H), 3.90 (s, 3H), 3.87 (t, J = 10.2 Hz, 1H), 3.82 (s, 3H). ^{13}C NMR (126 MHz, $CDCl_3$) δ 163.71, 152.38, 148.74, 138.48, 137.58, 137.45, 128.89, 128.48, 128.41, 128.38, 128.20, 127.97, 127.72, 127.63, 127.52, 126.01, 125.57, 123.79, 114.76, 101.50, 93.72, 84.49, 78.59, 75.39, 74.82, 73.66, 72.56, 68.48, 66.75, 56.31, 56.03. MS-ESI (m/z): $[M+Na]^+$ calcd. for $[C_{36}H_{35}INaO_9]^+$, 761.1218, found 761.1224.

Donor **2.4-D7** (742 mg, 88% yield) was synthesized according to the general procedure A (1 mmolscale). ^{1}H NMR (500 MHz, $CDCl_3$) δ 8.02 – 7.96 (m, 2H), 7.62 (s, 1H), 7.55 – 7.49 (m, 2H), 7.44 (ddd, J = 9.3, 5.2, 2.9 Hz, 5H), 7.39 – 7.29 (m, 9H), 7.28 – 7.21 (m, 3H), 7.02 (s, 1H), 6.42 (d, J = 1.6 Hz, 1H), 5.69 (s, 1H), 4.88 (d, J = 12.1 Hz, 1H), 4.85 (s, 2H), 4.74 (d, J = 12.1 Hz, 1H), 4.40 (t, J = 9.8 Hz, 1H), 4.35 (dd, J = 10.3, 4.8 Hz, 1H), 4.16 (dd, J = 10.0, 3.3 Hz, 1H), 4.05 (dd, J = 3.4, 1.8 Hz, 1H), 4.02 (dd, J = 9.7, 4.7 Hz, 1H), 3.95 (s, 3H), 3.90 (t, J = 10.3 Hz, 1H), 3.82 (s, 3H), 1.58 – 1.46 (m, 4H). ^{13}C NMR (126 MHz, $CDCl_3$) δ 163.61, 161.31, 152.11, 148.45, 141.36, 138.40, 137.70, 137.47, 130.72, 128.80, 128.74, 128.39, 128.26, 128.22, 128.13, 128.05, 127.82, 127.46, 127.39, 126.70, 126.51, 126.01, 124.66, 123.12, 118.03, 116.91, 112.79, 101.47, 94.65, 94.31, 93.39, 78.62, 75.83, 75.64,

75.62, 73.50, 72.95, 68.58, 66.89, 66.71, 56.20, 56.04, 21.48, 21.45, 4.20. MS-ESI (m/z): $[M+Na]^+$ calcd. for $[C_{52}H_{45}NNaO_{10}]^+$, 866.2936, found 866.2949.

Gold-catalyzed Stereoselective Glycosylation:

General procedure B:

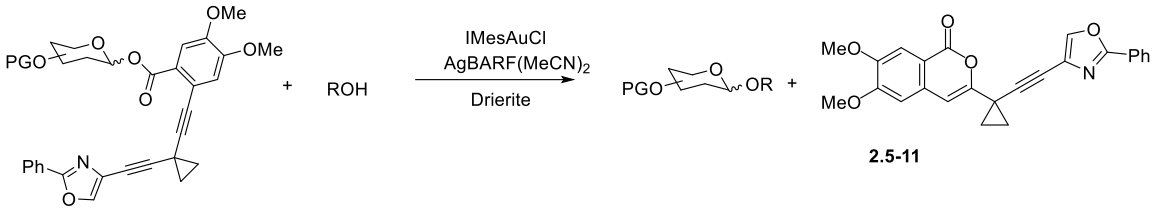

2.5-11

A donor (1.0 equiv., 0.06 mmol), an acceptor (1.2 equiv., 0.072 mmol), IMesAuCl (6 mol %, 0.0036 mmol, 1.93 mg) and 30 mg ground white drierite® were added subsequently to a glass vial (purchased from VWR®, Catalog Number: 66011-085). Trifluorotoluene (0.45 mL) andcyclohexane (0.15 mL) were subsequently injected. The vial was capped with an open-top screw cap with a silicone liner (purchased from Wheaton™), sealed with parafilm, Shaked, and then cooled to -15 °C. Meanwhile, a trifluorotoluene solution of [Ag(MeCN)2]+BARF- (0.02 M, 0.15 mL, 5 mol %, 0.0030 mmol) was injected into the vial. The reaction progress was monitored by TLC. After the reaction, a DCM solution of TBACl was used to quench the reaction at -15 °C, and the reaction mixture was filtered through a Celite® pad before column chromatography.

The byproduct **2.5-11** was separated and characterized: ^{1}H NMR (500 MHz, $CDCl_3$) δ 8.10 – 8.03 (m, 2H), 7.88 (s, 1H), 7.59 (s, 1H), 7.51 – 7.44 (m, 3H), 6.86 (s, 1H), 6.81 (s, 1H), 3.98 (s, 3H), 3.96 (s, 3H), 1.78 (q, J = 4.4 Hz, 2H), 1.55 – 1.49 (q, J = 4.4 Hz, 2H). ^{13}C NMR

(126 MHz, $CDCl_3$) δ 162.02, 161.72, 155.34, 153.76, 149.31, 141.48, 133.45, 130.96, 128.88, 126.66, 126.62, 124.71, 112.67, 109.44, 105.90, 102.66, 93.55, 69.91, 56.28, 56.26, 18.47, 15.49. MS-ESI (m/z): $[M+Na]^+$ calcd. for $[C_{25}H_{19}NNaO_5]^+$, 436.1155, found 436.1168.

Characterization Data for Selected Glycosides:

2.4-2n:

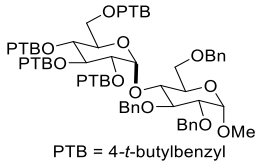

2.4-2n was prepared according to the general procedure B but with 2 equiv. acceptors employed. The reaction was finished after 24 h and afforded the product in 90% yield (65 mg) with α/β = 12:1. The anomers could not be separated. For the α anomer. ^1H NMR (500 MHz, $CDCl_3$) δ 7.37 – 7.18 (m, 27H), 7.17 – 7.12 (m, 2H), 7.09 – 7.04 (m, 2H), 5.71 (d, J = 3.6 Hz, 1H), 5.02 (d, J = 11.5 Hz, 1H), 4.87 (t, J = 11.7 Hz, 2H), 4.77 (t, J = 10.3 Hz, 2H), 4.71 (d, J = 12.1 Hz, 1H), 4.65 – 4.49 (m, 7H), 4.37 (d, J = 10.4 Hz, 1H), 4.25 (d, J = 12.0 Hz, 1H), 4.10 (t, J = 8.9 Hz, 1H), 4.05 (t, J = 8.9 Hz, 1H), 3.91 (dd, J = 9.8, 8.6 Hz, 1H), 3.88 – 3.80 (m, 2H), 3.73 – 3.62 (m, 3H), 3.60 (dd, J = 9.2, 3.5 Hz, 1H), 3.52 (dd, J = 10.1, 3.2 Hz, 2H), 3.41 – 3.39 (m, 1H), 3.38 (s, 3H), 1.33 (s, 9H), 1.32 (s, 9H), 1.28 (s, 9H), 1.27 (s, 9H). ^{13}C NMR (126 MHz, $CDCl_3$) δ 150.53, 150.48, 150.39, 138.95, 138.22, 138.03, 135.83, 135.54, 135.00, 134.91, 128.39, 128.21, 128.18, 128.17, 127.97, 127.90, 127.87, 127.85, 127.64, 127.29, 127.21, 127.07, 126.91, 125.24, 125.18, 125.14, 125.11, 97.77, 96.68, 82.13, 82.00, 80.22, 79.25, 77.47, 77.25, 77.00, 76.75, 75.40, 74.71, 74.46, 73.38,

73.19, 73.09, 73.08, 72.19, 70.97, 69.54, 69.54, 68.99, 67.96, 55.08, 34.49, 34.48, 34.44, 34.43, 31.35, 31.33, 31.31, 31.29. 31.33, 31.31, 31.29. The anomeric $^{1}J_{C\text{-}H}$ is 175Hz (see attached decoupled HSQC), which supports the major anomer being *α*. MS-ESI (m/z): $[M+Na]^{+}$ calcd. for $[C_{78}H_{98}NaO_{11}]^{+}$, 1233.7001, found 1233.6980.

2.4-2q:

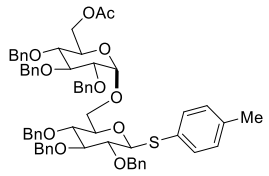

2.4-2q was prepared according to the general procedure B. The reaction was finished after 18 h and afforded the product in 93% yield (57 mg) with *α/β* > 30:1. The *β* product was not obvious on crude NMR. All spectra were run using deuterated acetone due to its instability in $CDCl_3$. For the α anomer, ^{1}H NMR (600 MHz, Acetone) δ 7.52 (d, J = 8.1 Hz, 2H), 7.51 – 7.48 (m, 2H), 7.42 – 7.38 (m, 4H), 7.37 – 7.23 (m, 24H), 7.17 (d, J = 7.9 Hz, 2H), 5.20 (d, J = 3.5 Hz, 1H), 5.04 (d, J = 11.1 Hz, 1H), 4.94 – 4.85 (m, 6H), 4.83 (d, J = 10.8 Hz, 1H), 4.80 (d, J = 11.3 Hz, 1H), 4.76 (d, J = 5.6 Hz, 1H), 4.74 (d, J = 7.6 Hz, 1H), 4.69 (d, J = 10.7 Hz, 1H), 4.65 (d, J = 11.1 Hz, 1H), 4.30 (dd, J = 11.9, 2.2 Hz, 1H), 4.22 (dd, J = 11.9, 4.7 Hz, 1H), 4.03 (t, J = 9.2 Hz, 1H), 3.99 – 3.91 (m, 2H), 3.88 (dd, J = 12.1, 1.7 Hz, 1H), 3.81 (t, J = 9.4 Hz, 1H), 3.75 (t, J = 8.9 Hz, 1H), 3.64 (ddd, J = 9.6, 4.3, 1.6 Hz, 1H), 3.60 (dd, J = 9.6, 3.5 Hz, 1H), 3.54 (dd, J = 10.1, 8.8 Hz, 1H), 3.29 (dd, J = 9.9, 8.6 Hz, 1H), 2.25 (s, 3H), 2.01 (s, 3H).^{13}C NMR (126 MHz, Acetone) δ 170.81, 140.13, 139.92, 139.77, 139.73, 139.59, 139.57, 138.29, 133.05, 131.36, 130.65, 129.24, 129.09, 129.07, 129.04, 129.02, 129.00, 128.81, 128.78, 128.74, 128.71, 128.66, 128.53, 128.40, 128.38, 128.33, 128.31, 128.21, 128.19, 128.16, 97.64, 88.46, 87.33, 82.37, 81.99, 81.38, 79.68, The anomeric $^{1}J_{C\text{-}H}$

is around 172 Hz (see attached decoupled HSQC) which proves the major anomer being *α*. MS-ESI (m/z): $[M+Na]^+$ calcd. for $[C_{63}H_{66}NaO_{11}S]^+$, 1053.4218, found 1053.4236.

2.4-4c:

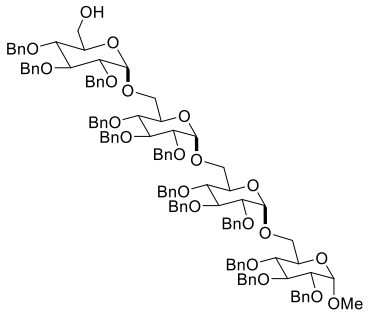

Anomerically pure **2.4-4c** (94 mg, 89% yield) was isolated. ^{1}H NMR (600 MHz, $CDCl_3$) δ 7.36 – 7.16 (m, 62H), 5.00 (d, J = 3.5 Hz, 1H), 4.97 – 4.88 (m, 9H), 4.87 (d, J = 11.1 Hz, 1H), 4.81 (d, J = 10.9 Hz, 1H), 4.79 – 4.73 (m, 3H), 4.66 (ddd, J = 13.5, 11.7, 6.5 Hz, 5H), 4.61 (dd, J = 11.5, 6.7 Hz, 2H), 4.58 – 4.49 (m, 6H), 4.00 – 3.93 (m, 4H), 3.85 – 3.57 (m, 15H), 3.52 – 3.44 (m, 2H), 3.40 (ddd, J = 12.7, 9.6, 3.5 Hz, 3H), 3.32 (s, 3H). ^{13}C NMR (126 MHz, cdcl3) δ 138.85, 138.82, 138.72, 138.64, 138.60, 138.50, 138.47, 138.46, 138.37, 138.26, 138.19, 128.40, 128.37, 128.35, 128.32, 128.31, 128.25, 128.02, 127.99, 127.96, 127.95, 127.93, 127.80, 127.79, 127.76, 127.69, 127.61, 127.52, 127.50, 127.48, 127.44, 127.40, 127.36, 98.00, 97.18, 97.08, 97.05, 82.08, 81.58, 81.46, 80.36, 80.28, 80.17, 80.14, 77.71, 77.53, 77.42, 77.41, 75.66, 75.47, 75.41, 75.40, 74.99, 74.94, 74.92, 74.87, 73.37, 72.36, 72.30, 72.21, 70.87, 70.80, 70.75, 70.53, 65.80, 65.71, 65.44, 61.87, 55.13. All three anomeric $^1J_{C-H}$ value are around 171Hz (see decoupled HSQC attached) which proves it's the structure with α linkages shown above. MS-ESI (m/z): $[M+Na]^+$ calcd. for $[C_{109}H_{116}NaO_{21}]^+$, 1783.7901, found 1783.7906.

2.4-4d:

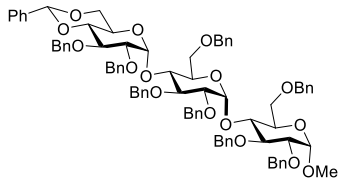

2.4-4d was prepared according to the general procedure B but in the presence of 2 equiv. acceptors. The diastereoselectivity of the reaction was determined by ^{1}H NMR analysis of the unpurified reaction mixture. The major α anomer (70 mg, 88% yield) was separated from the minor β anomer by flash column chromatography. ^{1}H NMR (500 MHz, $CDCl_3$) δ 7.53 – 7.46 (m, 2H), 7.42 – 7.08 (m, 43H), 5.71 (d, J = 3.9 Hz, 1H), 5.59 (d, J = 3.5 Hz, 1H), 5.54 (s, 1H), 5.04 (d, J = 11.6 Hz, 1H), 4.92 (d, J = 11.6 Hz, 1H), 4.84 (dd, J = 17.2, 11.4 Hz, 2H), 4.75 – 4.65 (m, 4H), 4.64 – 4.41 (m, 9H), 4.15 – 4.02 (m, 5H), 3.98 (t, J = 9.3 Hz, 1H), 3.85 (m, 4H), 3.71 – 3.57 (m, 5H), 3.55 – 3.47 (m, 3H), 3.39 (s, 3H). ^{13}C NMR (126 MHz, $CDCl_3$) δ 139.01, 138.84, 138.67, 138.27, 138.13, 138.03, 138.02, 137.69, 137.61, 128.80, 128.42, 128.34, 128.26, 128.24, 128.22, 128.20, 128.17, 128.14, 127.90, 127.85, 127.82, 127.61, 127.59, 127.55, 127.51, 127.49, 127.48, 127.41, 127.34, 127.09, 127.05, 126.77, 126.59, 126.05, 101.13, 97.81, 97.21, 96.12, 82.30, 81.88, 81.75, 80.02, 79.67, 79.00, 78.66, 75.07, 74.39, 73.91, 73.42, 73.36, 73.34, 73.14, 72.93, 72.83, 71.97, 70.49, 69.56, 68.96, 68.72, 63.16, 55.18. Two anomeric $^{1}J_{C\text{-}H}$ values are around 178 Hz (see decoupled HSQC attached) which proves it's the structure with two α linkages as shown above. MS-ESI (m/z): $[M+Na]^{+}$ calcd. for $[C_{82}H_{86}NaO_{16}]^{+}$, 1349.5808, found 1349.5817.

2.4-4e:

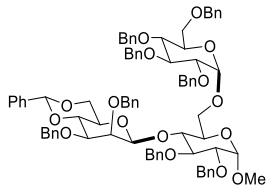

To a glass vial were added donor **2.4-D4** (0.1 mmol, 93.6 mg), the diol acceptor (0.1 mmol, 37.4 mg), IMesAuCl (012mmol, 6.5 mg), 150 mg drierite, and $PhCF_3$ (4.75 mL) sequentially. The vial was capped with an open-top screw cap with a silicone liner (purchased from Wheaton™), sealed with parafilm, shaked, and then cooled to 0 °C. A trifluorotoluene solution of $[Ag(MeCN)_2]^+BARF^-$ (0.02 M, 0.25 mL, 0.005 mmol) was then injected into the vial. The reaction was allowed to run for 24 h. After that, the reaction was warmed to room temperature, donor **2.4-D7** (0.1 mmol, 84.4 mg) was added, and another $[Ag(MeCN)_2]^+BARF^-$ (0.005 mmol, 0.24 mL of 0.02 M solution) was injected. Cyclohexane (1.3 mL) was then added to precipitate more byproduct out. The reaction was allowed to run for another 24 h. The reaction was quenched by a DCM solution of TBACl. A flash column chromatography was then performed, furnishing 108 mg product (82% yield). It should be noted that the molar ratio of **2.4-D4**: **2.4-1c**: **2.4-D7** should be 1: 1: 1, or there could be side product formation which resulted from 2 molecules of **2.4-D4** reacts with 1 molecule of **2.4-1c**. Stepwise procedures gave similar ratio and yield. ^1H NMR (600 MHz, $CDCl_3$) δ 7.40 – 7.13 (m, 43H), 7.12 – 7.07 (m, 2H), 5.50 (s, 1H), 5.12 (s, 1H), 5.11 (d, J = 7.2 Hz, 1H), 4.93 (d, J = 10.8 Hz, 1H), 4.91 – 4.84 (m, 2H), 4.84 – 4.79 (m, 2H), 4.74 (ddd, J = 13.7, 12.1, 7.0 Hz, 4H), 4.66 (d, J = 11.6 Hz, 1H), 4.59 (t, J = 11.8 Hz, 2H), 4.55 (d, J = 12.1 Hz, 1H), 4.53 – 4.49 (m, 2H), 4.45 (dd, J = 11.5, 8.5 Hz, 2H), 4.10 (dt, J = 17.3, 9.6 Hz, 2H), 3.92 – 3.86 (m, 4H), 3.76 (d, J = 12.5 Hz, 1H), 3.72 (dq, J = 10.2, 1.9 Hz, 1H), 3.69 – 3.57 (m, 6H), 3.53 (dd, J =

9.6, 3.4 Hz, 1H), 3.48 (t, J = 10.3 Hz, 1H), 3.38 (s, 3H), 3.41 – 3.35 (m, 1H), 3.25 (td, J = 9.7, 4.8 Hz, 1H). ^{13}C NMR (101 MHz, $CDCl_3$) δ 139.56, 138.62, 138.54, 138.28, 138.11, 138.01, 137.90, 137.67, 128.66, 128.44, 128.35, 128.33, 128.32, 128.29, 128.21, 128.06, 128.01, 128.00, 127.96, 127.92, 127.90, 127.87, 127.85, 127.81, 127.73, 127.72, 127.68, 127.63, 127.47, 127.40, 127.35, 127.31, 127.14, 126.12, 101.57, 101.30, 98.19, 96.78, 82.07, 80.28, 80.08, 79.20, 78.96, 78.89, 77.46, 77.28, 77.20, 77.14, 75.71, 75.18, 75.10, 75.01, 73.66, 73.41, 72.85, 72.83, 70.62, 70.38, 68.56, 68.46, 67.56, 64.60, 55.31. Attached decoupled HSQC showed one α linkage and one β glycosidic linkage. MS-ESI (m/z): $[M+Na]^+$ calcd. for $[C_{82}H_{86}NaO_{16}]^+$, 1349.5808, found 1349.5813.

2.6 References

1. Rademacher, T.; Parekh, R.; Dwek, R., Glycobiology. *Annual review of biochemistry* **1988,** *57* (1), 785-838.

2. Paulson, J. C., Glycoproteins: what are the sugar chains for? *Trends in biochemical sciences* **1989,** *14* (7), 272-276.

3. Kobata, A., Structures and functions of the sugar chains of glycoproteins. *EJB Reviews* **1993**, 207-225.

4. Varki, A., Biological roles of oligosaccharides: all of the theories are correct. *Glycobiology* **1993,** *3* (2), 97-130.

5. Ohtsubo, K.; Marth, J. D., Glycosylation in cellular mechanisms of health and disease. *Cell* **2006,** *126* (5), 855-867.

6. Dube, D. H.; Bertozzi, C. R., Glycans in cancer and inflammation—potential for therapeutics and diagnostics. *Nature reviews Drug discovery* **2005,** *4* (6), 477-488.

7. Nahálka, J.; Shao, J.; Gemeiner, P., Oligosaccharides, neoglycoproteins and humanized plastics: their biocatalytic synthesis and possible medical applications. *Biotechnology and applied biochemistry* **2007,** *46* (1), 1-12.

8. Fukase, K.; Tanaka, K., Bio-imaging and cancer targeting with glycoproteins and N-glycans. *Current opinion in chemical biology* **2012,** *16* (5-6), 614-621.

9. Niederhafner, P.; Reiniš, M.; Šebestík, J.; Ježek, J., Glycopeptide dendrimers, Part III—a review: use of glycopeptide dendrimers in immunotherapy and diagnosis of cancer and viral diseases. *Journal of peptide science: an official publication of the European Peptide Society* **2008,** *14* (5), 556-587.

10. Ulrich, S.; Dumy, P.; Boturyn, D.; Renaudet, O., Engineering of biomolecules for sensing and imaging applications. *Journal of Drug Delivery Science and Technology* **2013,** *23* (1), 5-16.

11. Toshima, K.; Tatsuta, K., Recent progress in O-glycosylation methods and its application to natural products synthesis. *Chemical reviews* **1993,** *93* (4), 1503-1531.

12. Yu, B.; Sun, J.; Yang, X., Assembly of naturally occurring glycosides, evolved tactics, and glycosylation methods. *Accounts of Chemical Research* **2012,** *45* (8), 1227-1236.

13. Yang, Y.; Yu, B., Recent advances in the chemical synthesis of C-glycosides. *Chemical reviews* **2017,** *117* (19), 12281-12356.

14. Wen, L.; Edmunds, G.; Gibbons, C.; Zhang, J.; Gadi, M. R.; Zhu, H.; Fang, J.; Liu, X.; Kong, Y.; Wang, P. G., Toward automated enzymatic synthesis of oligosaccharides. *Chemical reviews* **2018,** *118* (17), 8151-8187.

15. Panza, M.; Pistorio, S. G.; Stine, K. J.; Demchenko, A. V., Automated chemical oligosaccharide synthesis: novel approach to traditional challenges. *Chemical reviews* **2018,** *118* (17), 8105-8150.

16. Bennett, C. S.; Galan, M. C., Methods for 2-deoxyglycoside synthesis. *Chemical reviews* **2018,** *118* (17), 7931-7985.

17. Williams, R.; Galan, M. C., Recent advances in organocatalytic glycosylations. *European Journal of Organic Chemistry* **2017,** *2017* (42), 6247-6264.

18. Adero, P. O.; Amarasekara, H.; Wen, P.; Bohé, L.; Crich, D., The experimental evidence in support of glycosylation mechanisms at the SN1–SN2 interface. *Chemical reviews* **2018,** *118* (17), 8242-8284.

19. Leng, W.-L.; Yao, H.; He, J.-X.; Liu, X.-W., Venturing beyond donor-controlled glycosylation: new perspectives toward anomeric selectivity. *Accounts of Chemical Research* **2018,** *51* (3), 628-639.

20. Wang, H.-Y.; Blaszczyk, S. A.; Xiao, G.; Tang, W., Chiral reagents in glycosylation and modification of carbohydrates. *Chemical Society Reviews* **2018,** *47* (3), 681-701.

21. Nielsen, M. M.; Pedersen, C. M., Catalytic glycosylations in oligosaccharide synthesis. *Chemical reviews* **2018,** *118* (17), 8285-8358.

22. Kitamura, K.; Ando, Y.; Matsumoto, T.; Suzuki, K., Total synthesis of aryl C-glycoside natural products: strategies and tactics. *Chemical reviews* **2018,** *118* (4), 1495-1598.

23. McKay, M. J.; Nguyen, H. M., Recent advances in transition metal-catalyzed glycosylation. *ACS catalysis* **2012,** *2* (8), 1563-1595.

24. Takahashi, D.; Toshima, K., 1, 2-cis O-Glycosylation Methods. **2020**.

25. Nigudkar, S. S.; Demchenko, A. V., Stereocontrolled 1, 2-cis glycosylation as the driving force of progress in synthetic carbohydrate chemistry. *Chemical science* **2015,** *6* (5), 2687-2704.

26. Demchenko, A. V., 1, 2-cis O-Glycosylation: methods, strategies, principles. *Current Organic Chemistry* **2003,** *7* (1), 35-79.

27. Mensink, R. A.; Boltje, T. J., Advances in Stereoselective 1, 2‐cis Glycosylation using C‐2 Auxiliaries. *Chemistry–A European Journal* **2017,** *23* (70), 17637-17653.

28. Schmidt, R. R.; Rücker, E., Stereoselective glycosidations of uronic acids. *Tetrahedron Letters* **1980,** *21* (15), 1421-1424.

29. Dohi, H.; Nishida, Y.; Tanaka, H.; Kobayashi, K., o-Methoxycarbonylphenyl 1-Thio-β-d-Galactopyranoside, A Non-malodorous Thio Glycosylation Donor for the Synthesis of Globosyl α (1-4)-Linkages. *Synlett* **2001,** *2001* (09), 1446-1448.

30. Nishimura, D.; Hasegawa, A.; Nakajima, M., Solvent effect and anchimeric assistance on α-glycosylation. *Agricultural and Biological Chemistry* **1972,** *36* (10), 1767-1772.

31. Demchenko, A.; Stauch, T.; Boons, G.-J., Solvent and other effects on the stereoselectivity of thioglycoside glycosidations. *Synlett* **1997,** *1997* (07), 818-820.

32. Ratcliffe, A. J.; Fraser-Reid, B., Generation of α-D-glucopyranosylacetonitrilium ions. Concerning the reverse anomeric effect. *Journal of the Chemical Society, Perkin Transactions 1* **1990,** (3), 747-750.

33. Chao, C.-S.; Lin, C.-Y.; Mulani, S.; Hung, W.-C.; Mong, K.-k. T., Neighboring-group participation by C-2 ether functions in glycosylations directed by nitrile solvents. *Chemistry-A European Journal* **2011,** *17* (43), 12193-12202.

34. Shirahata, T.; Matsuo, J.-i.; Teruya, S.; Hirata, N.; Kurimoto, T.; Akimoto, N.; Sunazuka, T.; Kaji, E.; Ōmura, S., Improved catalytic and stereoselective glycosylation with glycosyl N-trichloroacetylcarbamate: application to various 1-hydroxy sugars. *Carbohydrate Research* **2010,** *345* (6), 740-749.

35. Schmidt, R. R.; Behrendt, M.; Toepfer, A., Nitriles as solvents in glycosylation reactions: highly selective β-glycoside synthesis1. *Synlett* **1990,** *1990* (11), 694-696.

36. Crich, D.; Li, W., α-Selective sialylations at− 78 C in nitrile solvents with a 1-adamantanyl thiosialoside. *The Journal of organic chemistry* **2007,** *72* (20), 7794-7797.

37. Pradhan, T. K.; Lin, C. C.; Mong, K.-K. T., Preparation of a protected 3-deoxy-D-manno-oct-2-ulosonate glycal donor for the synthesis of β-KDO-containing oligosaccharides. *Organic Letters* **2014,** *16* (5), 1474-1477.

38. Mannerstedt, K.; Ekelöf, K.; Oscarson, S., Evaluation of thioglycosides of Kdo as glycosyl donors. *Carbohydrate Research* **2007,** *342* (3-4), 631-637.

39. Koshiba, M.; Suzuki, N.; Arihara, R.; Tsuda, T.; Nambu, H.; Nakamura, S.; Hashimoto, S., Catalytic Stereoselective Glycosidation with Glycosyl Diphenyl Phosphates: Rapid Construction of 1, 2-cis-α-Glycosidic Linkages. *Chemistry–An Asian Journal* **2008,** *3* (8-9), 1664-1677.

40. Liu, C. Y. I.; Mulani, S.; Mong, K. K. T., Iterative One-Pot α-Glycosylation Strategy: Application to Oligosaccharide Synthesis. *Advanced Synthesis & Catalysis* **2012,** *354* (17), 3299-3310.

41. Kaeothip, S.; Yasomanee, J. P.; Demchenko, A. V., Glycosidation of thioglycosides in the presence of bromine: mechanism, reactivity, and stereoselectivity. *The Journal of organic chemistry* **2012,** *77* (1), 291-299.

42. Kim, J. H.; Yang, H.; Boons, G. J., Stereoselective glycosylation reactions with chiral auxiliaries. *Angewandte Chemie International Edition* **2005,** *44* (6), 947-949.

43. Kim, J.-H.; Yang, H.; Park, J.; Boons, G.-J., A general strategy for stereoselective glycosylations. *Journal of the American Chemical Society* **2005,** *127* (34), 12090-12097.

44. Boltje, T. J.; Kim, J.-H.; Park, J.; Boons, G.-J., Chiral-auxiliary-mediated 1, 2-cis-glycosylations for the solid-supported synthesis of a biologically important branched α-glucan. *Nature chemistry* **2010,** *2* (7), 552-557.

45. BruceáTurnbull, W., Stereoselective glycosylation using oxathiane glycosyl donors. *Chemical Communications* **2009,** (39), 5841-5843.

46. Fascione, M. A.; Webb, N. J.; Kilner, C. A.; Warriner, S. L.; Turnbull, W. B., Stereoselective glycosylations using oxathiane spiroketal glycosyl donors. *Carbohydrate Research* **2012,** *348*, 6-13.

47. Fang, T.; Mo, K.-F.; Boons, G.-J., Stereoselective assembly of complex oligosaccharides using anomeric sulfonium ions as glycosyl donors. *Journal of the American Chemical Society* **2012,** *134* (17), 7545-7552.

48. Elferink, H.; Mensink, R. A.; White, P. B.; Boltje, T. J., Stereoselective β-mannosylation by neighboring-group participation. *Angewandte Chemie* **2016,** *128* (37), 11383-11386.

49. Gorin, P.; Perlin, A., Configuration of glycosidic linkages in oligosaccharides: IX. Synthesis of α-and β-D-mannopyranosyl disaccharides. *Canadian Journal of Chemistry* **1961,** *39* (12), 2474-2485.

50. Bebault, G. M.; Dutton, G. G., Synthesis of 4-O-β-d-mannopyranosyl-l-rhamnopyranose. *Carbohydrate research* **1974,** *37* (2), 309-319.

51. Garegg, P. J.; Iversen, T., facile synthesis of beta-D-mannopyranosides. *Carbohydrate research* **1979**.

52. Crich, D.; Cai, W., Chemistry of 4, 6-O-benzylidene-d-glycopyranosyl triflates: contrasting behavior between the gluco and manno series. *The Journal of organic chemistry* **1999,** *64* (13), 4926-4930.

53. Crich, D.; Chandrasekera, N. S., Mechanism of 4, 6-O-Benzylidene-Directed β-Mannosylation as Determined by α-Deuterium Kinetic Isotope Effects. *Angewandte Chemie International Edition* **2004,** *43* (40), 5386-5389.

54. Huang, M.; Garrett, G. E.; Birlirakis, N.; Bohé, L.; Pratt, D. A.; Crich, D., Dissecting the mechanisms of a class of chemical glycosylation using primary 13 C kinetic isotope effects. *Nature chemistry* **2012,** *4* (8), 663-667.

55. Crich, D.; Sun, S., Direct synthesis of β-mannopyranosides by the sulfoxide method. *The Journal of organic chemistry* **1997,** *62* (5), 1198-1199.

56. Crich, D.; Sun, S., Are glycosyl triflates intermediates in the sulfoxide glycosylation method? A chemical and 1H, 13C, and 19F NMR spectroscopic investigation. *Journal of the American Chemical Society* **1997,** *119* (46), 11217-11223.

57. Crich, D.; Sun, S., Direct formation of β-mannopyranosides and other hindered glycosides from thioglycosides. *Journal of the American Chemical Society* **1998,** *120* (2), 435-436.

58. Weingart, R.; Schmidt, R. R., Can preferential β-mannopyranoside formation with 4, 6-O-benzylidene protected mannopyranosyl sulfoxides be reached with trichloroacetimidates? *Tetrahedron Letters* **2000,** *41* (45), 8753-8758.

59. Kim, K. S.; Kim, J. H.; Lee, Y. J.; Lee, Y. J.; Park, J., 2-(Hydroxycarbonyl) benzyl glycosides: a novel type of glycosyl donors for highly efficient β-mannopyranosylation and oligosaccharide synthesis by latent-active glycosylation. *Journal of the American Chemical Society* **2001,** *123* (35), 8477-8481.

60. Codée, J. D.; Hossain, L. H.; Seeberger, P. H., Efficient installation of β-mannosides using a dehydrative coupling strategy. *Organic letters* **2005,** *7* (15), 3251-3254.

61. Baek, J. Y.; Choi, T. J.; Jeon, H. B.; Kim, K. S., A Highly Reactive and Stereoselective β-Mannopyranosylation System: Mannosyl 4-Pentenoate/PhSeOTf. *Angewandte Chemie* **2006,** *118* (44), 7596-7600.

62. Kim, K. S.; Lee, Y. J.; Kim, H. Y.; Kang, S. S.; Kwon, S. Y., Glycosylation with glycosyl benzyl phthalates as a new type of glycosyl donor. *Organic & biomolecular chemistry* **2004,** *2* (17), 2408-2410.

63. Kim, K. S.; Fulse, D. B.; Baek, J. Y.; Lee, B.-Y.; Jeon, H. B., Stereoselective direct glycosylation with anomeric hydroxy sugars by activation with phthalic anhydride and trifluoromethanesulfonic anhydride involving glycosyl phthalate intermediates. *Journal of the American Chemical Society* **2008,** *130* (26), 8537-8547.

64. El-Badri, M. H.; Willenbring, D.; Tantillo, D. J.; Gervay-Hague, J., Mechanistic studies on the stereoselective formation of β-mannosides from mannosyl iodides using α-deuterium kinetic isotope effects. *The Journal of organic chemistry* **2007,** *72* (13), 4663-4672.

65. Jensen, H. H.; Nordstrøm, L. U.; Bols, M., The disarming effect of the 4, 6-acetal group on glycoside reactivity: torsional or electronic? *Journal of the American Chemical Society* **2004,** *126* (30), 9205-9213.

66. Crich, D.; Dudkin, V., An unusual example of steric buttressing in glycosylation. *Tetrahedron Letters* **2000,** *41* (30), 5643-5646.

67. Crich, D.; Li, W.; Li, H., Direct Chemical Synthesis of the β-Mannans: Linear and Block Syntheses of the Alternating β-(1→ 3)-β-(1→ 4)-Mannan Common to Rhodotorula glutinis, Rhodotorula mucilaginosa, and Leptospira biflexa. *Journal of the American Chemical Society* **2004,** *126* (46), 15081-15086.

68. Crich, D.; Jayalath, P., 2-O-Propargyl Ethers: Readily cleavable, minimally intrusive protecting groups for β-mannosyl donors. *Organic letters* **2005,** *7* (11), 2277-2280.

69. Crich, D.; Jayalath, P.; Hutton, T. K., Enhanced diastereoselectivity in β-mannopyranosylation through the use of sterically minimal propargyl ether protecting groups. *The Journal of organic chemistry* **2006,** *71* (8), 3064-3070.

70. Crich, D.; Wu, B., 1-Naphthylpropargyl ether group: A readily cleaved and sterically minimal protecting system for stereoselective glycosylation. *Organic letters* **2006,** *8* (21), 4879-4882.

71. Benakli, K.; Zha, C.; Kerns, R. J., Oxazolidinone protected 2-amino-2-deoxy-D-glucose derivatives as versatile intermediates in stereoselective oligosaccharide synthesis and the formation of α-linked glycosides. *Journal of the American Chemical Society* **2001,** *123* (38), 9461-9462.

72. Kerns, R. J.; Zha, C.; Benakli, K.; Liang, Y.-Z., Extended applications and potential limitations of ring-fused 2, 3-oxazolidinone thioglycosides in glycoconjugate synthesis. *Tetrahedron Letters* **2003,** *44* (44), 8069-8072.

73. Boysen, M.; Gemma, E.; Lahmann, M.; Oscarson, S., Ethyl 2-acetamido-4, 6-di-O-benzyl-2, 3-N, O-carbonyl-2-deoxy-1-thio-β-D-glycopyranoside as a versatile GlcNAc donor. *Chemical Communications* **2005,** (24), 3044-3046.

74. Wei, P.; Kerns, R. J., Factors affecting stereocontrol during glycosidation of 2, 3-oxazolidinone-protected 1-tolylthio-N-acetyl-D-glucosamine. *The Journal of organic chemistry* **2005,** *70* (10), 4195-4198.

75. Wei, P.; Kerns, R. J., Chemoselective deprotection and functional group interconversion of ring-fused 2N, 3O-oxazolidinones of N-acetyl-D-glucosamine. *Tetrahedron Letters* **2005,** *46* (40), 6901-6905.

76. Geng, Y.; Zhang, L.-H.; Ye, X.-S., Stereoselectivity investigation on glycosylation of oxazolidinone protected 2-amino-2-deoxy-D-glucose donors based on pre-activation protocol. *Tetrahedron* **2008,** *64* (22), 4949-4958.

77. Geng, Y.; Zhang, L.-H.; Ye, X.-S., Pre-activation protocol leading to highly stereoselectivity-controllable glycosylations of oxazolidinone protected glucosamines. *Chemical Communications* **2008,** (5), 597-599.

78. Yang, L.; Ye, X.-S., A highly α-selective glycosylation for the convenient synthesis of repeating α-(1→ 4)-linked N-acetyl-galactosamine units. *Carbohydrate research* **2010,** *345* (12), 1713-1721.

79. Olsson, J. D.; Eriksson, L.; Lahmann, M.; Oscarson, S., Investigations of glycosylation reactions with 2-N-acetyl-2 N, 3 O-oxazolidinone-protected glucosamine donors. *The Journal of organic chemistry* **2008,** *73* (18), 7181-7188.

80. Satoh, H.; Manabe, S.; Ito, Y.; Lüthi, H. P.; Laino, T.; Hutter, J. r., Endocyclic cleavage in glycosides with 2, 3-trans cyclic protecting groups. *Journal of the American Chemical Society* **2011,** *133* (14), 5610-5619.

81. Manabe, S.; Ishii, K.; Ito, Y., N-benzyl-2, 3-oxazolidinone as a glycosyl donor for selective α-glycosylation and one-pot oligosaccharide synthesis involving 1, 2-cis-glycosylation. *Journal of the American Chemical Society* **2006,** *128* (33), 10666-10667.

82. Manabe, S.; Ishii, K.; Ito, Y., N-Benzyl-2, 3-trans-Carbamate-Bearing Glycosyl Donors for 1, 2-cis-Selective Glycosylation Reactions. Wiley Online Library: 2011.

83. Heuckendorff, M.; Bendix, J.; Pedersen, C. M.; Bols, M., β-Selective mannosylation with a 4, 6-silylene-tethered thiomannosyl donor. *Organic letters* **2014,** *16* (4), 1116-1119.

84. Hashimoto, Y.; Tanikawa, S.; Saito, R.; Sasaki, K., β-Stereoselective mannosylation using 2, 6-lactones. *Journal of the American Chemical Society* **2016,** *138* (45), 14840-14843.

85. Baek, J. Y.; Lee, B.-Y.; Jo, M. G.; Kim, K. S., β-Directing effect of electron-withdrawing groups at O-3, O-4, and O-6 positions and α-directing effect by remote participation of 3-O-acyl and 6-O-acetyl groups of donors in mannopyranosylations. *Journal of the American Chemical Society* **2009,** *131* (48), 17705-17713.

86. Yasomanee, J. P.; Demchenko, A. V., Effect of remote picolinyl and picoloyl substituents on the stereoselectivity of chemical glycosylation. *Journal of the American Chemical Society* **2012,** *134* (49), 20097-20102.

87. Smoot, J. T.; Pornsuriyasak, P.; Demchenko, A. V., Development of an arming participating group for stereoselective glycosylation and chemoselective oligosaccharide synthesis. *Angewandte Chemie* **2005,** *117* (43), 7285-7288.

88. Pistorio, S. G.; Yasomanee, J. P.; Demchenko, A. V., Hydrogen-bond-mediated aglycone delivery: focus on β-mannosylation. *Organic letters* **2014,** *16* (3), 716-719.

89. Adinolfi, M.; Iadonisi, A.; Schiattarella, M., An approach to the highly stereocontrolled synthesis of α-glycosides. Compatible use of the very acid labile dimethoxytrityl protecting group with Yb (OTf) 3-promoted glycosidation. *Tetrahedron Letters* **2003,** *44* (34), 6479-6482.

90. Boons, G.-J.; Bowers, S.; Coe, D. M., Trityl ethers in oligosaccharide synthesis: A novel strategy for the convergent assembly of oligosaccharides. *Tetrahedron Letters* **1997,** *38* (21), 3773-3776.

91. Barresi, F.; Hindsgaul, O., Synthesis of. beta.-mannopyranosides by intramolecular aglycon delivery. *Journal of the American Chemical Society* **1991,** *113* (24), 9376-9377.

92. Stork, G.; Kim, G., Stereocontrolled synthesis of disaccharides via the temporary silicon connection. *Journal of the American Chemical Society* **1992,** *114* (3), 1087-1088.

93. Bols, M., Stereocontrolled synthesis of α-glucosides by intramolecular glycosidation. *Journal of the Chemical Society, Chemical Communications* **1992,** (12), 913-914.

94. Seward, C. M.; Cumpstey, I.; Aloui, M.; Ennis, S. C.; Redgrave, A. J.; Fairbanks, A. J., Stereoselective cis glycosylation of 2-O-allyl protected glycosyl donors by intramolecular aglycon delivery (IAD). *Chemical Communications* **2000,** (15), 1409-1410.

95. Brigl, P., Kohlenhydrate II. Über ein neues, das 1, 2-Anhydrid der Glucose. **1922**.

96. Hickinbottom, W. J., CCCCXV.—Glucosides. Part I. The formation of glucosides from 3: 4: 6-triacetyl glucose 1: 2-anhydride. *Journal of the Chemical Society (Resumed)* **1928**, 3140-3147.

97. Haworth, W. N.; Hickinbottom, W. J., CCCXCVI.—Synthesis of a new disaccharide, neo trehalose. *Journal of the Chemical Society (Resumed)* **1931**, 2847-2850.

98. Nakagawa, A.; Tanaka, M.; Hanamura, S.; Takahashi, D.; Toshima, K., Regioselective and 1, 2-cis-α-Stereoselective Glycosylation Utilizing Glycosyl-Acceptor-Derived Boronic Ester Catalyst. *Angewandte Chemie* **2015,** *127* (37), 11085-11089.

99. Nishi, N.; Nashida, J.; Kaji, E.; Takahashi, D.; Toshima, K., Regio-and stereoselective β-mannosylation using a boronic acid catalyst and its application in the synthesis of a tetrasaccharide repeating unit of lipopolysaccharide derived from E. coli O75. *Chemical Communications* **2017,** *53* (21), 3018-3021.

100. Tanaka, M.; Nashida, J.; Takahashi, D.; Toshima, K., Glycosyl-acceptor-derived borinic ester-promoted direct and β-stereoselective mannosylation with a 1, 2-anhydromannose donor. *Organic letters* **2016,** *18* (9), 2288-2291.

101. Tanaka, M.; Takahashi, D.; Toshima, K., 1, 2-cis-α-Stereoselective glycosylation utilizing a glycosyl-acceptor-derived borinic ester and its application to the total synthesis of natural glycosphingolipids. *Organic letters* **2016,** *18* (19), 5030-5033.

102. Nishi, N.; Sueoka, K.; Iijima, K.; Sawa, R.; Takahashi, D.; Toshima, K., Stereospecific β-l-Rhamnopyranosylation through an SNi-Type Mechanism by Using Organoboron Reagents. *Angewandte Chemie* **2018,** *130* (42), 14054-14058.

103. Tomita, S.; Tanaka, M.; Inoue, M.; Inaba, K.; Takahashi, D.; Toshima, K., Diboron-Catalyzed Regio-and 1, 2-cis-α-Stereoselective Glycosylation of trans-1, 2-Diols. *The Journal of organic chemistry* **2020,** *85* (24), 16254-16262.

104. Park, Y.; Harper, K. C.; Kuhl, N.; Kwan, E. E.; Liu, R. Y.; Jacobsen, E. N., Macrocyclic bis-thioureas catalyze stereospecific glycosylation reactions. *Science* **2017,** *355* (6321), 162-166.

105. Levi, S. M.; Li, Q.; Rötheli, A. R.; Jacobsen, E. N., Catalytic activation of glycosyl phosphates for stereoselective coupling reactions. *Proceedings of the National Academy of Sciences* **2019,** *116* (1), 35-39.

106. Li, Q.; Levi, S. M.; Jacobsen, E. N., Highly selective β-mannosylations and β-rhamnosylations catalyzed by bis-thiourea. *Journal of the American Chemical Society* **2020,** *142* (27), 11865-11872.

107. Li, Y.; Yang, Y.; Yu, B., An efficient glycosylation protocol with glycosyl ortho-alkynylbenzoates as donors under the catalysis of Ph3PAuOTf. *Tetrahedron Letters* **2008,** *49* (22), 3604-3608.

108. Tang, Y.; Li, J.; Zhu, Y.; Li, Y.; Yu, B., Mechanistic insights into the gold (I)-catalyzed activation of glycosyl ortho-alkynylbenzoates for glycosidation. *Journal of the American Chemical Society* **2013,** *135* (49), 18396-18405.

109. Zhu, Y.; Yu, B., Highly Stereoselective β-Mannopyranosylation via the 1-α-Glycosyloxy-isochromenylium-4-gold (I) Intermediates. *Chemistry–A European Journal* **2015,** *21* (24), 8771-8780.

110. Zhu, Y.; Shen, Z.; Li, W.; Yu, B., Stereoselective synthesis of β-rhamnopyranosides via gold (i)-catalyzed glycosylation with 2-alkynyl-4-nitro-benzoate donors. *Organic & biomolecular chemistry* **2016,** *14* (5), 1536-1539.

111. Yu, B., Gold (I)-catalyzed glycosylation with glycosyl o-alkynylbenzoates as donors. *Accounts of chemical research* **2018,** *51* (2), 507-516.

112. Dong, X.; Chen, L.; Zheng, Z.; Ma, X.; Luo, Z.; Zhang, L., Silver-catalyzed stereoselective formation of glycosides using glycosyl ynenoates as donors. *Chemical Communications* **2018,** *54* (62), 8626-8629.

113. Yao, T.; Larock, R. C., Synthesis of isocoumarins and α-pyrones via electrophilic cyclization. *The Journal of organic chemistry* **2003,** *68* (15), 5936-5942.

114. Crich, D.; Sun, S., Formation of β-mannopyranosides of primary alcohols using the sulfoxide method. *The Journal of Organic Chemistry* **1996,** *61* (14), 4506-4507.

115. Zhu, Y.; Yu, B., Highly Stereoselective β-Mannopyranosylation via the 1-α-Glycosyloxy-isochromenylium-4-gold(I) Intermediates. *Chemistry – A European Journal* **2015,** *21* (24), 8771-8780.

116. Crich, D., Chemistry of Glycosyl Triflates: Synthesis of β-Mannopyranosides. *Journal of Carbohydrate Chemistry* **2002,** *21* (7-9), 663-686.

117. Raheem, I. T.; Goodman, S. N.; Jacobsen, E. N., Catalytic asymmetric total syntheses of quinine and quinidine. *Journal of the American Chemical Society* **2004,** *126* (3), 706-707.

118. Ferrer Flegeau, E.; Popkin, M. E.; Greaney, M. F., Suzuki coupling of oxazoles. *Organic Letters* **2006,** *8* (12), 2495-2498.

119. Kawade, R. K.; Liu, R.-S., Gold-Catalyzed Oxidative Cyclization of 4-Allenyl-1-ynes with 8-Methylquinoline Oxide. *Organic Letters* **2013**.

120. Schmidt, R. R.; Michel, J., Facile synthesis of α-and β-O-glycosyl imidates; preparation of glycosides and disaccharides. *Angewandte Chemie International Edition in English* **1980,** *19* (9), 731-732.

121. Ng, K.; Shaktah, R.; Vardanyan, L.; Minehan, T. G., Total Synthesis of Alvaradoins E and F, Uveoside, and 10-epi-Uveoside. *Organic Letters* **2019,** *21* (22), 9175-9178.

122. Liu, L.; Pohl, N. L., Synthesis of a series of maltotriose phosphates with an evaluation of the utility of a fluorous phosphate protecting group. *Carbohydrate Research* **2013,** *369*, 14-24.

123. Worm‐Leonhard, K.; Larsen, K.; Jensen, K. J., 4, 6‐O‐Benzylidene Directed β‐Mannosylation Without Intermediate Triflate Formation? Comparison of Trichloroacetimidate and DISAL Donors in Microwave‐Promoted Glycosylations under Neutral Conditions. *Journal of Carbohydrate Chemistry* **2007,** *26* (7), 349-368.

3. Generally Applicable Catalytic S_N2 Glycosylation toward 1,2-*cis*-Furanosides

3.1 Chemical Synthesis of Furanosides

Furanosides are less abundant compared to their six-membered counterparts. Nevertheless, they are common structural constituents of polysaccharides in living organisms, such as plants, bacteria, parasites, and fungi.[1-4] For instance, bacteria's cell wall is coated with glycan structures consisting of furanosides motifs that play many essential roles, including modulating immune responses and serving as a permeability barrier to drugs. Some of the mycobacterial species could cause human disease, and one well-known example is *Mycobacterium tuberculosis*. Treatment of the infections caused by those species requires a molecular-level understanding of how mycobacterial cell wall glycans mediate these processes. Similar to pyranosides, the chemical synthesis of 1,2-*trans* furanosides can be reliably achieved by neighboring group participation, and because of that, the construction of 1,2-*cis* furanosides lies as the main challenge in the furanosides synthesis. On the other hand, 1,2-*cis* furanosides are widely existing structures in mycobacterial glycans. For example, the Ara6 motif consists of two 1,2-*cis* linkages (**Figure 14A**) is a common structure that can be found at the nonreducing terminus of both the mycolyl-arabinogalactan (AG) and lipoarabinomannan (LAM) complex.[5]

Compared to pyranosyl donors, The S_N2 type displacement is even more challenging for furanosyl donors. As shown in **Figure 14B**, first, a furanosyl oxocarbenium ion contains one less electron-withdrawing C−O bond than the corresponding pyranosyl system, which makes the leaving group more nucleofugal. Second, introducing a sp^2 center into a five-membered ring results in a significant loss of torsional strain, leading to relatively stable oxocarbenium

formation, whereas the opposite is true for six-membered rings. Therefore, furanoses are more prone than pyranoses to S_N1 pathways. Moreover, for those 1,2-*cis*-*β*- systems, thermodynamics always prefer the formation of *α*-products through the anomeric effect, making the synthesis of 1,2-*cis*-*β*-furanosides even more difficult than 1,2-*cis*-*α*- furanosides.

Figure 14. Chemical Synthesis of Furanosides: Challenges and Background

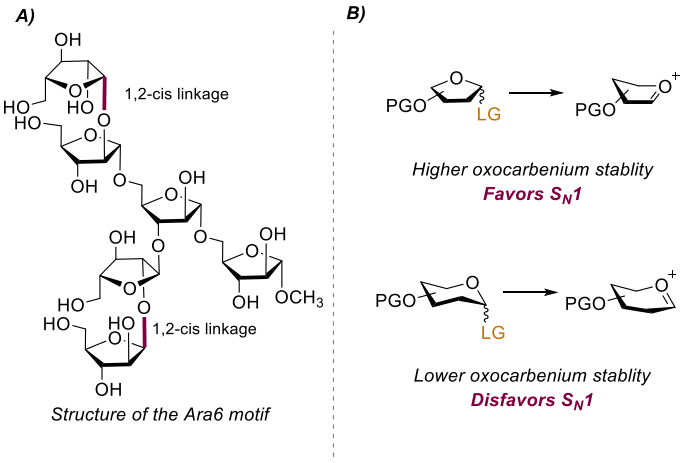

3.2 Previous Strategies for the Synthesis of 1,2-cis Furanosides

Despite the challenging nature of 1,2-*cis* furanosides synthesis, some innovative approaches to address these challenges have been developed. Several strategies employ similar rationales and principles to those in the 1,2 -*cis* pyranosides synthesis. For example, with the epoxide ring serving to impose conformational constraint, 2,3-anhydro furanosyl donors were used by the Lowary group to synthesize 2,3-anhydro-*β*-lyxofuranosyl glycosides.[6] Later, they extended this strategy to the construction of 2,3-anhydro-*β*-arabinofuranosyl linkages. which was followed by a regioselective (-)-sparteine-mediated nucleophilic epoxide ring-opening (**Scheme 41, 3.2-1**) to deliver the corresponding-*β*-arabinofuranosides (**Scheme 41A**).[7] Mechanistic study indicates a similar mechanism to the Crich *β*-mannosylation method,[8] which involves an intermediate *α*-glycosyl triflate. The

same strategy was further applied to the synthesis of α-galactofuranosides.[9, 10] Another approach relying on the conformational restrictions was reported by the Boons group[11] and soon after by the Ito group,[12] in which the silyl-based protecting groups bridge the *O*-3/*O*-5 of the arabinofuranose ring. As shown in **Scheme 41B**, the rationale for the stereoselectivity was explained via a previous model proposed by Woerpel and co-workers,[13] as depicted in **Scheme 41B 3.2-4** and **3.2-5**, the nucleophilic attack from the α-face is disfavored due to the 1,2-gauche interaction between the pseudoaxially oriented C-2 hydrogen and the incoming acceptor. Moreover, molecular modeling studies indicate that the β-product is thermodynamically favored over its α-counterpart. The β-product has a pseudoaxially oriented glycoside linkage (**3.2-6** and **3.2-7**), which may be favorable because of the anomeric effect. The author also mentioned that the donor **3.2-3** usually outperforms the donor **3.2-2** in terms of β-selectivity. This observation could be explained by the fact that a more distorted conformation needs to be formed to accommodate the attack for the six-five fused system **3.2-4** than its eight-five fused counterpart **3.2-5**. In the scope study, sterically more hindered acceptors also showed higher β-selectivity, suggesting that the steric factor plays an essential role in controlling the stereochemical outcome. Except for those strategies relying on the conformational restrictions, other strategies have also been reported including hydrogen-bond-mediated aglycone delivery (**Scheme 41C**),[14] and intramolecular aglycon delivery (**Scheme 41D**).[15]

Scheme 41. Common Strategies Used in the Synthesis of 1,2-*cis* Furanosides

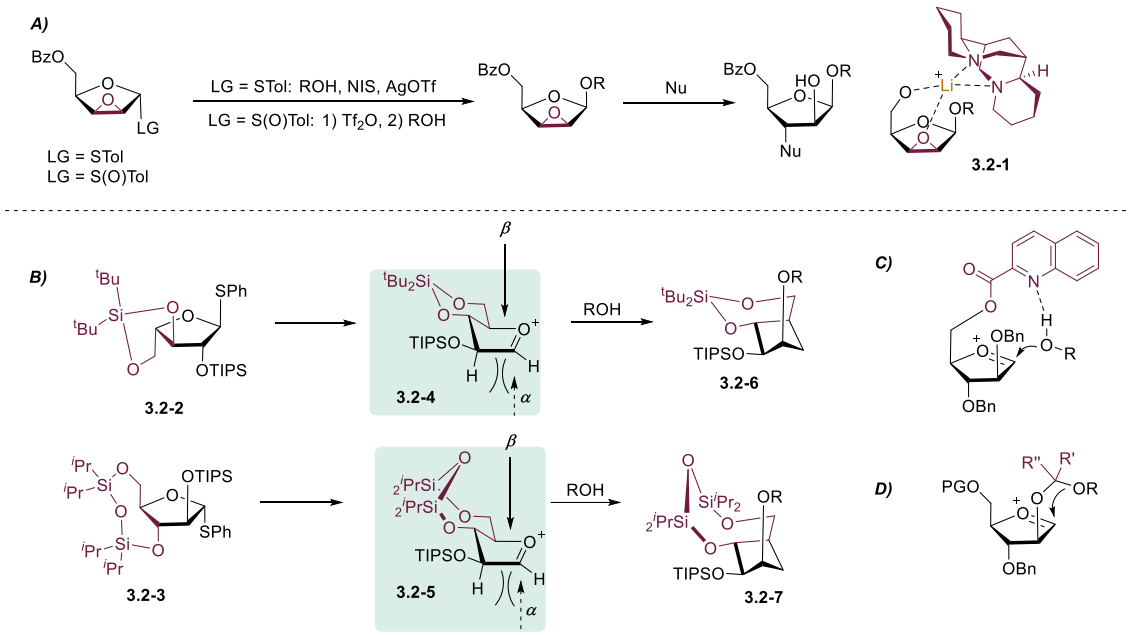

Scheme 42. Indirect Synthesis of 1,2-*cis* Furanosides

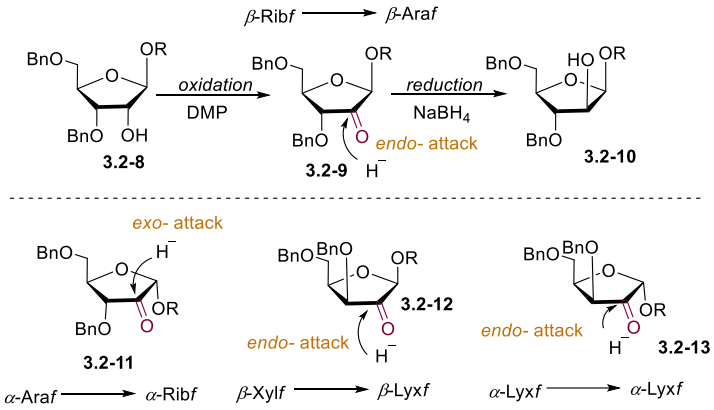

Another interesting strategy to prepare the 1,2-*cis* furanosides was reported by the Hotha group, in which the 1,2-*trans* furanosides were initially synthesized and later converted into 1,2-*cis* glycosides through oxidation−reduction reactions.[16] In this approach, the hydride

attack could only proceed from the less crowded face around the carbonyl group of the C2-ulose derivative, which is also the reason why this transformation could only happen in one direction. For example, 1,2-*cis* arabinofuranoside (**3.2-10**) was obtained from 1,2-*trans* ribofuranoside (**3.2-8**) through an *endo*-attack of the hydride to the carbonyl group (**3.2-9**). Similarly, 1,2-*cis* ribofuranosides and lyxofuranosides were prepared from the corresponding 1,2-*trans* arabinofuranosides and xylofuranosides respectively (**3.2-11** and **3.2-12**). However, in the case of 1,2-*trans* lyxofuranosides, the 3,5-di-O-benzyl groups make the *exo*-attack of the hydride on the ketone completely unavailable, giving back the starting material (**3.2-13**).

Scheme 43. Furanosylations Catalyzed by Bis-thiourea Hydrogen-Bond Donors

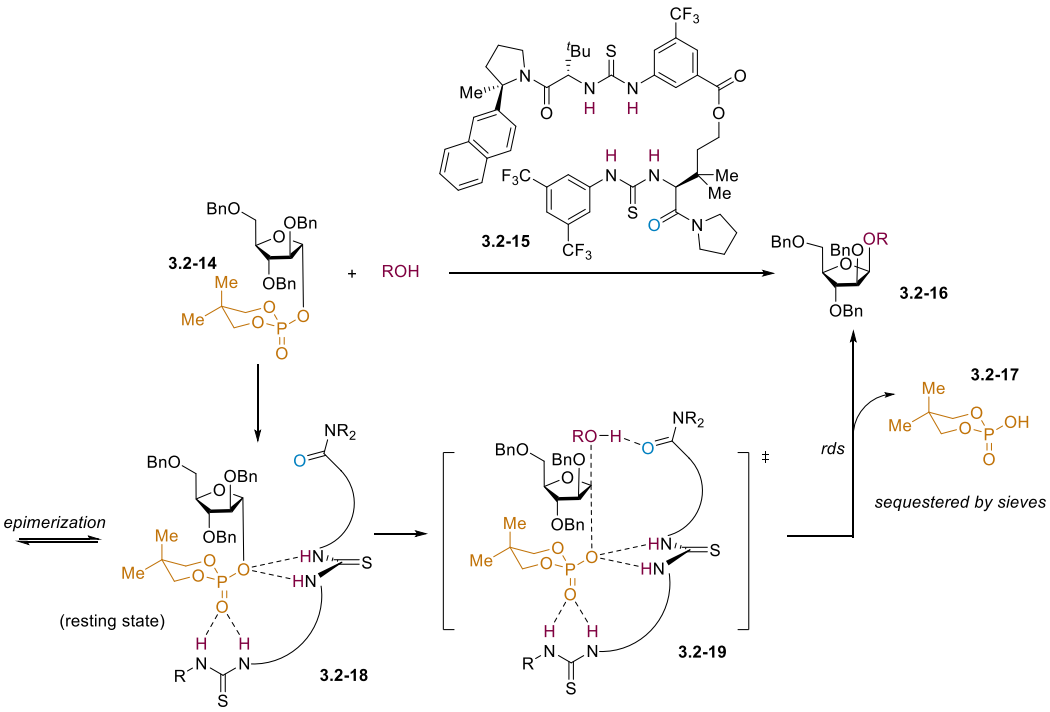

In 2020, the Jacobsen group reported one important work in furanosylation chemistry,[17] using a bis-thiourea catalyst to work on the furanosyl phosphate donor similar to the work they previously reported in pyranose chemistry (**Scheme 32)**. The author proposed a resting-

state bis-thiourea−glycosyl phosphate complex (**3.2-18**), which could further undergo stereospecific and rate-limiting substitution by the acceptors (**3.2-19**) to deliver the stereo-inverted product. This pathway competes with an epimerization pathway promoted by the catalyst (**3.2-15**) and an additional phosphate source (**3.2-17**). In some cases, the donors are more prone to epimerization due to the nature of different sugars. For example, under standard conditions, the 1,2-*trans* xylosylfuranosyl donor doesn't give stereo-inverted but the stereo-retained xyloside. Another major drawback of this strategy is that it seems the sterically more hindered secondary acceptors are not applicable, as the author summarized in their supporting information. Moreover, the formation of challenging 1,2-*cis* lyxofuranosides and glucofuranosides were not investigated.

3.3 A Generally Applicable S_N2 Strategy toward 1,2-cis-Furanosides

As discussed in the previous chapter, we developed an S_N2 strategy for stereoselective construction of 1,2-*cis*-pyranosidic linkage.[18] Our design is not limited to a particular type of sugar and can be of much-needed general applicability. In this chapter, we will demonstrate that the S_N2 approach enabled the directing-group-on-leaving-group (DGLG) strategy is also operative in furanoside synthesis and permits generally applicable, high yielding, and highly stereoselective construction of a broad range of 1,2-*cis*-furanosides.

Yu's glycosyl *ortho*-alkynylbenzoate strategy,[19, 20] featuring mild conditions and exhibits excellent efficiency, has been widely used to prepare pyranose-based oligo/polysaccharides and glycoconjugates in the past decade.[21,22,23] On the contrary, there are only scattered reports about its application in furanoside synthesis. Most of them are limited to *N*-furanosylation.[24, 25] *O*-furanosylations are only presented as single cases in the preparation of glycosylated natural products.[26, 27] Moreover, all these studies use armed donors and rely

on neighboring group participation to achieve 1,2-*trans*-furanosidic linkages,[24, 26, 27] or long-distance acyl group participation to access 1,3-*trans*-2-deoxyfuranosidic linkages.[25] To the best of our knowledge, there's no study for the armed and hence substantially more reactive and challenging furanosyl *ortho*-alkynylbenzoate donors. Moreover, the stereoselective construction of 1,2-*cis*-furanosides employing *ortho*-alkynylbenzoate donors has not yet been reported. To this end, we decided to also examine the corresponding armed furanosyl donors without the oxazole directing group to evaluate the role of the directing group and probe their utility in furanosylation.

3.3.1 The Preparation of 1,2-*trans* Furanosyl Donors

The major concern for the preparation of furanosyl donors is how to install the leaving groups stereoselectively. Based on our experience with the previous 1,2-*cis* pyranoside project, coupling the reducing sugar moiety with the benzoic acid under Steglich esterification conditions usually favors the formation of 1,2-*trans* glycosyl esters over their 1,2-*cis* counterparts. Therefore, we tested different furanosyl reducing sugars with standard Steglich esterification conditions initially. To our delight, all these reactions showed an exclusive or predominant formation of 1,2-trans fruanosyl esters. Although the reason is not clear, the 1,2-*trans* stereoselectivity might originate from steric considerations. As shown in **Table 7A**, in the cases of *D*-ribose and *D*-lyxose, in which all the substitutions are on the same face, the coupling reactions showed complete 1,2-*trans* selectivity.

Moreover, we found that the *L*-fucofuranosyl esters, *D*-arabinofuranosyl esters, and *D*-xylofuranosyl esters showing in **Table 7B** are all white crystalline solid. Therefore, we performed recrystallizations in ethanol. The mixture was dissolved in a minimal amount of ethanol at 75 °C. Subsequently, the temperature was gradually lowered to -10 °C. To our

delight, those pure crystalline 1,2-*trans* diastereomers crashed out as white needle-like solids with high yield. Moreover, for *D*-xylofuranosyl esters, the resulting two diastereomers on TLC are clearly separated spots. Therefore, the purification of 1,2-*cis* xylofuranosyl ester is also straightforward and can be done easily by column chromatography.

As shown in **Table 7C**, the *D*-galactofuranosyl esters and *D*-glucofuranosyl esters were obtained with moderate 1,2-*trans* selectivity as well. The diastereomers are not separable on TLC. But by using pure DCM as eluent, the pure 1,2-*trans* diastereomer could be collected. Usually, the former three-quarters fractions are pure, whereas the latter fractions are mixtures of both diastereomers (**Table 7C**).

Besides, we suspect that both isomers of *D*-ribofuranosyl esters might be separable by column chromatography, which could provide us with an opportunity to check the S_N2 characteristics of the 1,2-*cis* ribofuranosyl donors. In order to synthesize it, the benzoic acid was converted to the corresponding benzoyl chloride, then reacted with the ribosyl reducing sugar, giving an almost 1:1 ratio of the anomeric mixture. And indeed, the TLC showed two isomeric spots on TLC. On the other hand, the DCC/DMAP coupling can only provide 1,2-*trans* ribofuranosyl esters.

The following Sonogashira coupling reactions of the furanosyl esters and the alkyne moiety are always robust and efficient. The yields of the desired donors are constantly higher than 78% and could be up to 98%.

Table 7. The Preparation of 1,2-*trans* Furanosyl Esters

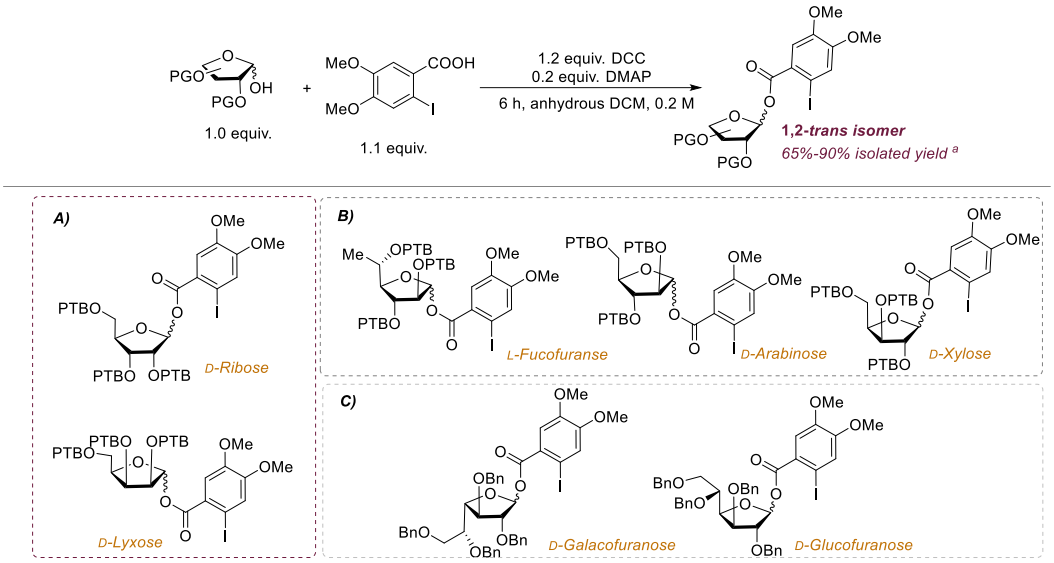

Entry	Reducing Sugar	Selectivity *1,2-trans/cis*	Yield of Isomeric Mixture [b]	Purification Method [a]	Yield of Pure 1,2-*trans* product [b]
1	*D*-ribo*f*	*trans* only	-	A	90%
2	*D*-lyx*of*	*trans* only	-	A	83%
3	*L*-fuco*f*	>20:1	85%	B	76%
4	*D*-arabino*f*	7:1	92%	B	74%
5	*D*-xylo*f*	4:1[c]	88%	B	66%
6	*D*-galacto*f*	6:1[d]	86%	C	65%
7	*D*-gluco*f*	7:1[d]	91%	C	68%

[a] A: Column chromatography (eluent: hexanes/ethyl acetate); B: Recrystallization (in ethanol); C: Column chromatography (eluent: DCM); [b] Yield based on the reducing sugar. [c] Both diastereoisomers are separable by column chromatography. [d] Only the major diastereoisomer is separable by column chromatography.

3.3.2 Conditions Optimizations

At the outset, we decided to study the synthesis of *D*-xylofuranosides and particularly the α-anomers,[28] which does not apply to the previously reported *bis*-urea-catalyzed S_N2 approach.[17] Seven xylosyl donors, including the α- and β-anomers of **3.3-D1**-**D3** and β-**3.3-D4,** were prepared. Donor α-**3.3-D4** could not be prepared pure and hence was not examined. As shown in the graphics of **Table 8**, **3.3-D1** possesses the optimized oxazole-functionalized 3,4-dimethoxybenzoate moiety along with 4-*tert*-butylbenzyl (PTB) as the *O*-protecting

group, which serves the purpose of improving the donor's solubility in apolar solvents. Comparing to **3.3-D1**, **3.3-D2** lacks the oxazole directing group, **3.3-D3** lacks the benzene ring methoxy groups, and **3.3-D4** lacks both. In the cases of the latter two donors, the absence of electron-donating MeO groups should enhance the nucleofugality of the gold-activated leaving groups. As such, the glycosylation may experience increased S_N1 characteristics. In addition, the *O*-protecting groups in **3.3-D3** are benzyl groups. These donors were reacted with methyl 2,3,4-tri-*O*-benzyl-α-$_D$-glycopyranoside (i.e., **3.3-2a**), and the results are shown in **Table 8**. Under the shown optimal reaction conditions with the prototypical and shelf-stable Gagosz complex $Ph_3PAuNTf_2$ as the catalyst,[29] the reaction of β-***3.3*-D1** exhibited a high level of stereoinversion, affording the α-xylofuranoside α-**3.3-3a** featuring a 1,2-*cis*-glycosidic linkage in nearly quantitative yield and with a ratio of 16.2:1 over its β-anomer (entry 1). Moreover, the reaction went to completion in 1 h. In comparison, the reaction of β-3.3-**D2** was slower and exhibited a lower α/β selectivity of 7.5/1 (entry 2), confirming the expected beneficial directing effect of the oxazole ring in both the α-selectivity and the reaction rate. Interestingly, little difference between β-**3.3- D3** and β-**3.3-D4** was detected in their reactions with **3.3-2a** (entries 3 and 4**)**. The lack of apparent directing effect here suggests the labile nature of the bonding between the activated LG and the xylofuranosyl moiety. These results reveal the importance of the benzene ring MeO groups in the case of β-**3.3-D1** in making the gold-activated LG less nucleofugal and hence being more prone to the directing group-promoted S_N2 attack. On the other hand, the moderate S_N2 characteristics exhibited by **3.3-D2** and **3.3-D3** reveals that the Yu's system, despite not studied previously with armed systems, can be synthetically serviceable and might involve contact ion pairs. When the reaction solvent was switched from $PhCF_3$/cyclohexane (v/v = 4:1) to DCM, the α-selectivities were consistently lower (entries

5-7). To rule out these observed α-selectivities are not inherent to the oxocarbenium intermediate in an S_N1 pathway, we studied the reactions of the α-donors under identical reaction conditions. Much to our delight, in all three cases (entries 8-10), configuration inversion at the anomeric position predominated. Moreover, the reaction of α-**3.3-D1** led to the best ratio of 10/1, favoring the β-xylofuranoside β-**3.3-3a**. These results support a predominant S_N2 pathway in the reaction of either of the **3.3-D1** anomers (entries 1 and 8).

Table 8. The Reactions of Xylofuranosyl Donors

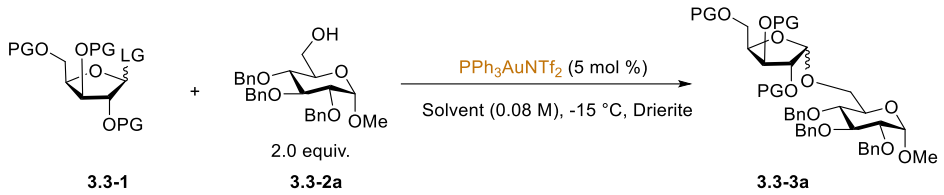

3.3-1 3.3-2a 3.3-3a

Entry	Donor	Solvent	Time	Conversion	Yield[a]	α/β
1	***β*-3.3-D1**	**Mixed[b]**	**-15 °C/1 h**	**100%**	**99%**	**16.2:1[c]**
2	*β*-3.3-**D2**	Mixed[b]	-15 °C/1 h	74%	72%	7.5:1
3	*β*-3.3-**D3**	Mixed[b]	-15 °C/0.5 h	100%	99%	8.8:1
4	*β*-3.3-**D4**	Mixed[b]	-15 °C/3 h	100%	98%	9.3:1
5	*β*-3.3-**D1**	DCM	-15 °C/3 h	47%	47%	10.8:1
6	*β*-3.3-**D2**	DCM	-15 °C/1 h	100%	97%	3.0:1
7	*β*-3.3-**D3**	DCM	-15 °C/0.5 h	100%	98%	3.0:1
8	***α*-3.3-D1**	**Mixed**	**-15 °C/0.5 h**	**100%**	**97%**	**1:10 [d]**
9	*α*-3.3-**D2**	Mixed	-15 °C/0.5 h	100%	90%	1:5.5
10	*α*-3.3-**D3**	Mixed	-15 °C/0.5 h	100%	99%	1:6.0

[a] Crude NMR yield. [b] $PhCF_3$/cyclohexane = 4:1 (v/v). [c] 97% isolated yield. [d] 94% isolated yield.

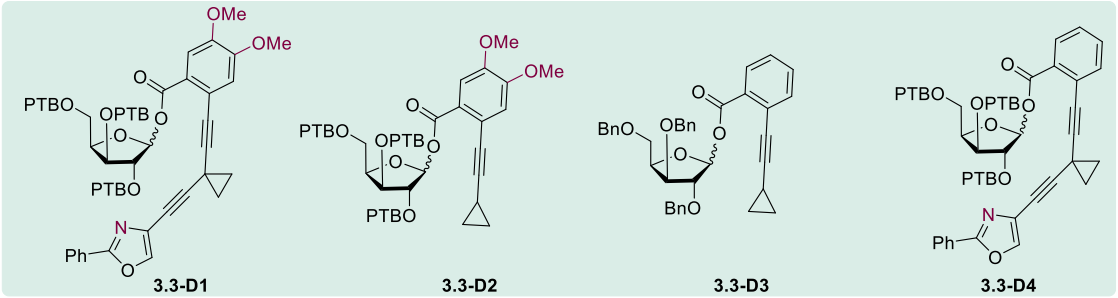

3.3-D1 3.3-D2 3.3-D3 3.3-D4

3.3.3 Scope Study with Pentofuranosides

Figure 15. The Stereoinvertive Synthesis of Xylofuranosides.

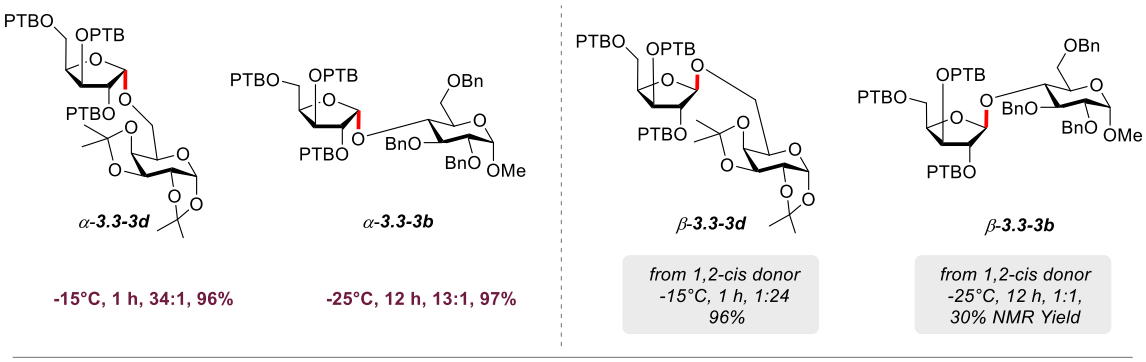

With 2.0 equiv. acceptors.

We then briefly explored the scope of the xylofuranosylation using representative acceptors. As shown in **Figure 15**, with the more reactive acetonide-protected galactoside acceptor (**3.3-2d**), the reaction of either *β*-**3.3-D1** or *α*-**3.3-D1** exhibited a higher level of stereoinversion than that with **3.3-2a**, leading to the formation of either of the **3.3-3d** anomers with excellent selectivity. For the hindered secondary glucoside acceptor, the formation of the 1,2-*cis*-xylofuranoside *α*-**3.3-3b** was still highly stereoinvertive at a lower temperature (i.e., -25 °C) and, moreover, nearly quantitative. On the other hand, the formation of *β*-**3.3-3b** is not stereoselective. Examination of the NMR spectra of the reaction mixture showed donor epimerization during the reaction process, revealing some limitation of this approach with the sterically demanding and hence challenging secondary acceptor **3.3-2b**.

Figure 16. Donors and Acceptors Involved in the Scope Study

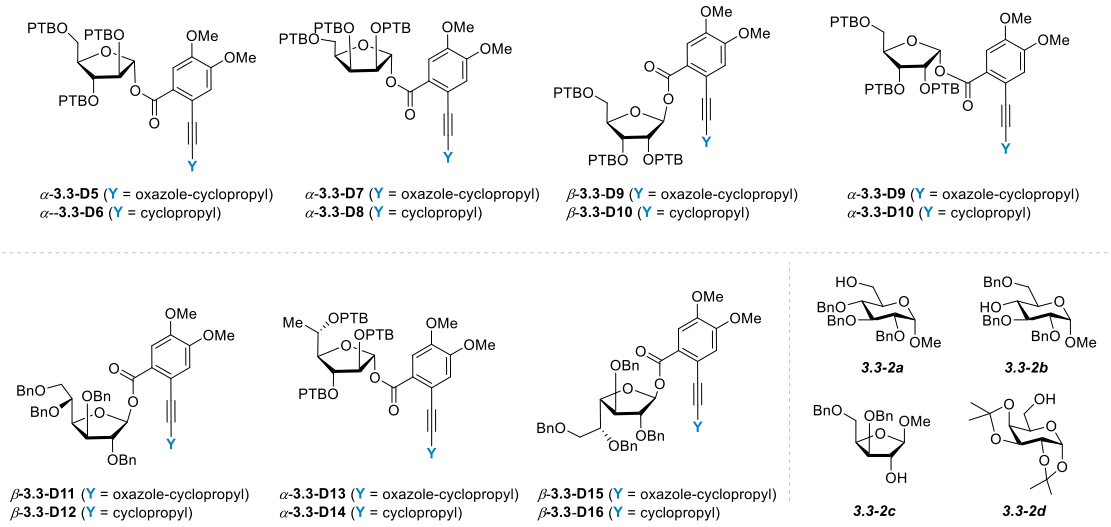

We then turned our attention to apply the gold catalysis to the synthesis of the other three *D*-pentofuranosides. A series of different donors and acceptors were prepared (see **Figure 16**). For the pentofuranosides, we limited the acceptors to the glucosides **3.3-2a** and more challenging secondary acceptor **3.3-2b**. The reactivity range outlined by these two acceptors should provide informative guidance when other acceptors are considered.

As shown in **Figure 17**, in the case of *D*-arabinose, the glycosylation of **3.3-2a** by *α*-**D5** possessing the oxazole directing group afforded the product *β*-**3.3-4a** with an excellent ratio of 16:1 favoring the 1,2-*cis*-glycosidic linkage. The reaction was also fast and highly efficient. In comparison, without the directing group, the donor *α*-**3.3-D6** led to a moderate *β*/*α* ratio of 6.3:1, confirming the directing effect in the reaction of *α*-**3.3-D5**. With the more hindered **3.3-2b** as the acceptor, by lowering the reaction temperature to -25 ˚C, the *β*/*α* selectivity was 8/1 with excellent yield. Again, the reaction with donor *α*-**3.3-D5** showed a similar level of enhancement in selectivity compared to that with donor *α*-**3.3-D6** under the same conditions (i.e., -15 ˚C). In the case of *D*-lyxose, the furanosylation of **3.3-2a** with the

α- donor with the oxazole directing group, i.e., α-**3.3-D7**, was highly β-selective and exhibited excellent efficiency, despite all four ring substituents in the furanoside β-**3.3-5a** being on the same side. Without the directing group in ***α*-3.3-D8**, the β/α selectivity was notably lower, i.e., 13/1 instead of 22/1, again revealing the usefulness of the directing strategy. On the other hand, with challenging **3.3-2b** as the acceptor, both α-donors afforded the 1,2-*cis*-lyxoside β-**3.3-5b** with moderate yet serviceable selectivities. In the formation of 1,2-*cis*-ribosides, we discovered that the directing group does not afford improved selectivity. For example, the furanosylation of **3.3-2a** with either β-donor, i.e., β-**3.3-D9** or β-**3.3-D10**, led to a similarly excellent level of α-preference and excellent efficiency. The same phenomenon was observed in the reaction of the more challenging **3.3-2b**. In this case, the level of stereoinversion, i.e., α/β = 17~18/1, is outstanding. With the α-anomers of **3.3-D9** and **3.3-D10** available in pure form, their reactions with **3.3-2a** were less stereoinvertive than the β-counterparts. However, the directing group offers notable benefit in this case as α-**3.3-D9** performed substantially better than α-**D10**. By lowering the reaction temperature to -25 ˚C, the 1,2-*trans*-ribofuranoside β-**3.3-6a** was formed from α-**3.3-D9** with an 8/1 selectivity with only 1.2 equiv. of acceptor over its α-counterpart and in an excellent combined yield.

Figure 17. The Reaction Scope with Other Pentofuranosyl Donors.

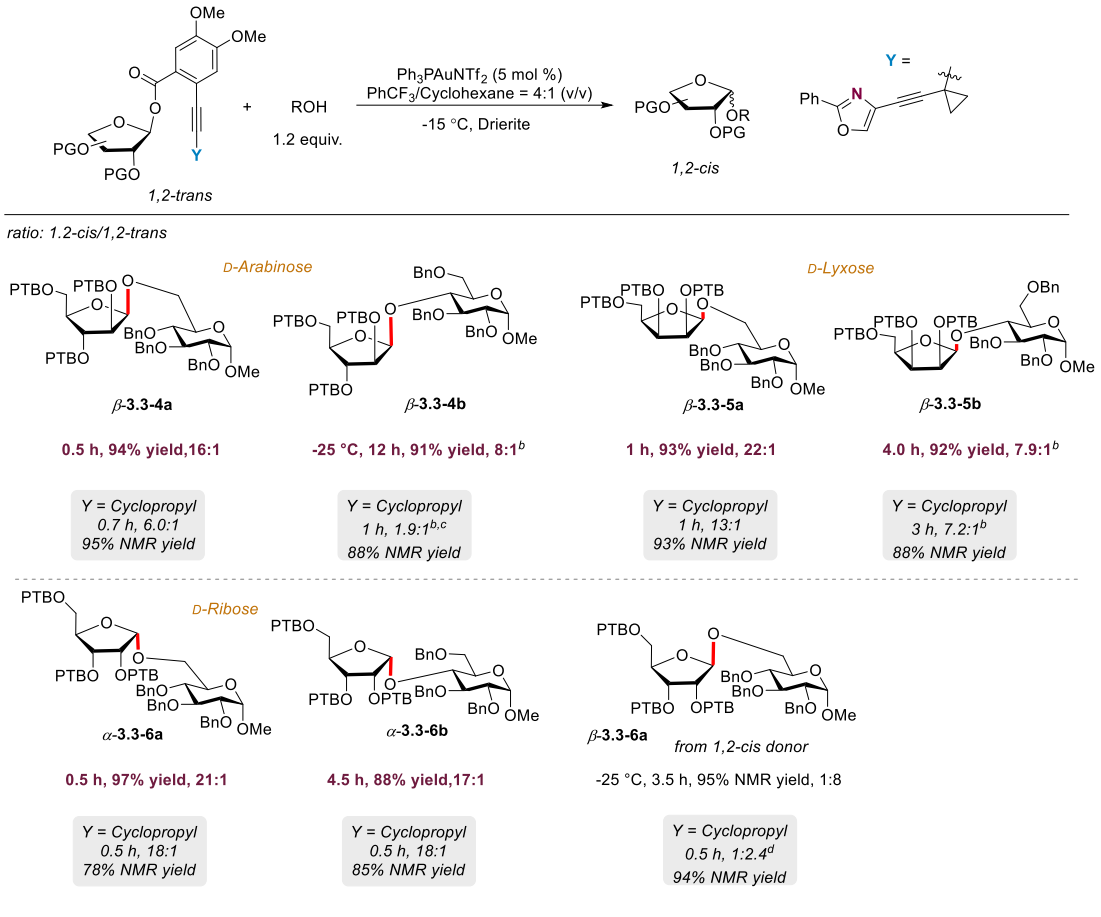

[a] *Standard conditions, with 1.2 equiv. acceptors* [b] *With 2.0 equiv. acceptors.*
[c] *With the oxazole functionalized donor at same temperature (i.e., -15 °C), 4.5 h, 91% NMR yield, 1,2-cis/1,2-trans = 6.5:1.*
[d] *With the oxazole functionalized donor at same temperature (i.e., -15 °C), 0.5 h, 91% NMR yield, 1,2-cis/1,2-trans = 1:5.5.*

3.3.4 Scope Study with Hexofuranosides

We also examined the reactions of several hexofuranosyl donors focusing on the challenging synthesis of 1,2-*cis*-furanosidic linkages. As shown in **Figure 18**, the D-glucofuranosyl donor *β*-**D11** reacted with the acceptor **3.3-2a** and **3.3-2b** smoothly to deliver the stereoinverted 1,2-*cis*-furanoside products *α*-**3.3-7a** and *α*-**3.3-7b** in excellent yields and with 12/1 and 18/1 preference, respectively. The inferior *α*/*β* ratios obtained by using *β*-**3.3-**

D12 lacking the oxazole directing group again indicates the oxazole group's beneficial directing effect in the furanosylation chemistry. The better selectivity in the latter case can be attributed to the increased equivalency of the acceptor **3.3-2b**. The same beneficial impacts of the directing group in stereoinvertive furanosylation were observed with $_L$-fucofuranosyl donors α-**3.3-D13** and α-**3.3-D14**. With the oxazole directing group, α-**3.3-D13** reacted with **3.3-2a** and the secondary xylosyl acceptor **3.3-2c** exceptionally well, affording the furanosides in ≥90% yields and with 35/1 and 18/1 β/α selectivities, respectively. In the absence of the directing group, the reactions were substantially less stereoinvertive, with the corresponding β-selectivities being 12/1 and 5.2/1, respectively. In the case of $_D$-galactofuranosyl donors β-**3.3-D15** and β-**3.3-D16**, more pronounced beneficial impacts by the directing group on stereoselectivity were observed. Notably, our approach delivered α-**3.3-9d** in a much better yield and selectivity than the previous work, which employed the same equivalency of acceptor **3,3-2d** (78% yield, 11:1). [17] this result further highlighted the efficiency of our approach.

3.3.5 Conclusion

In conclusion, generally applicable access to challenging 1,2-*cis*-glycosidic linkages in furanoside synthesis is achieved via gold-catalyzed furanosylation. The largely S_N2 nature of the glycosylation is supported by the highly stereoselective conversion of either donor anomer into the configurationally opposing product anomer in the cases of $_D$-xylose and $_D$-ribose. Mostly high levels of stereoinversion at the anomeric position of furanosyl donors are realized by employing the directing-group-on-leaving-group strategy, in which a basic oxazole moiety is appended to the anomeric leaving group and directs the backend attack at the anomeric center upon gold activation by a glycosyl acceptor. A broad range of furanoses

Figure 18. The Reaction Scope with Hexofuranosyl Donors.

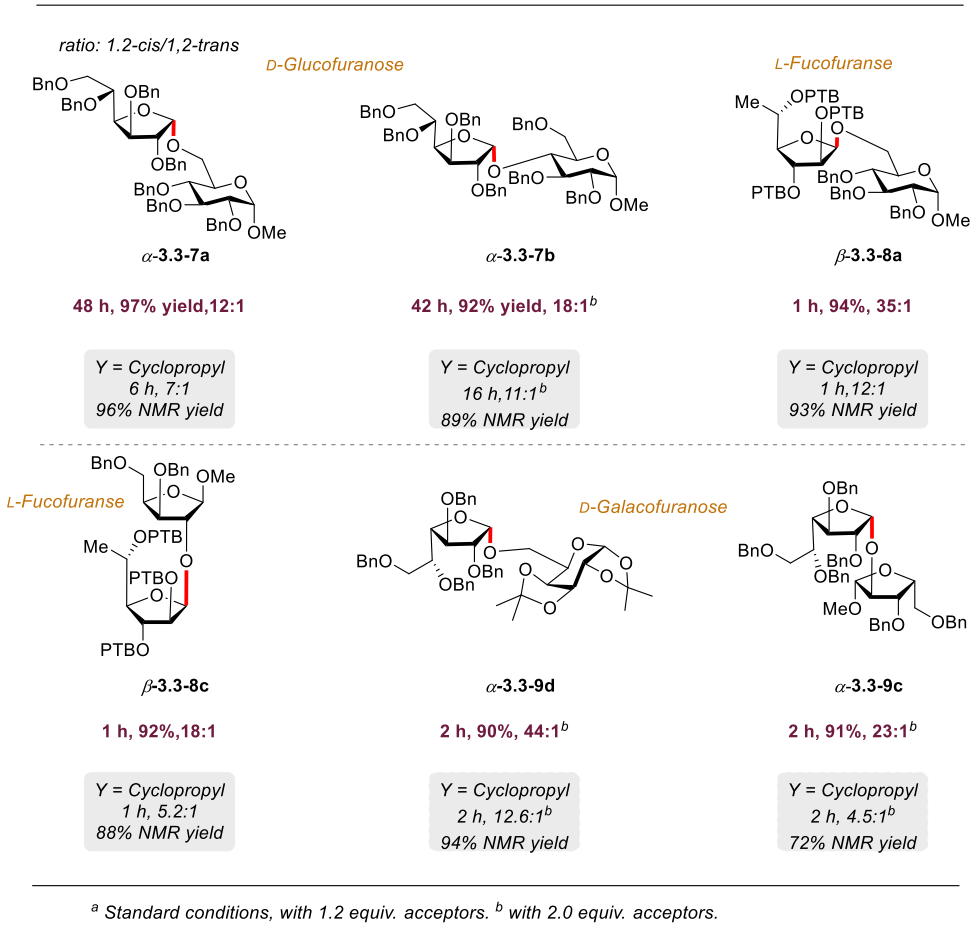

[a] *Standard conditions, with 1.2 equiv. acceptors.* [b] *with 2.0 equiv. acceptors.*

including all four *D*-pentofuranoses, *D*-glucofuranose, *L*-fucofuranose, and *D*-galactofuranose are suitable donor precusors. Except in the cases of *D*-ribose, the direct group strategy offers substantial improvement in reaction S_N2 characteristics among all other explored furanose types. Besides the high selectivities and general applicability toward 1,2-*cis*-furanosides, all the reactions are highly efficient, with yields routinely being >90%, and the reaction time is often between 30 min and 2 h.

3.4 Experimental Section

General. Ethyl acetate (ACS grade), hexanes (ACS grade), and cyclohexane (ACS grade) were purchased from Fisher Scientific and used without further purification. Anhydrous dichloromethane (HPLC grade) was purified by distillation over calcium hydride. Anhydrous trifluorotoluene was purchased from Sigma Aldrich and was used without further purification.Commercially available 2-iodo-4,5-dimethoxy-benzoic acid, if showing reddish color, was purified by basic aluminum oxide column. Reactions were monitored by thin-layer chromatography (TLC) using Silicycle precoated silica gel plates. Flash column chromatography was performed over Silicycle silica gel (230-400 mesh). ^{1}H NMR and ^{13}C NMR spectra were recorded on Bruker 400 MHz, Bruker 500 MHz, Varian 400 MHz, 500 MHz, and 600 MHz spectrometers using residue solvent peaks as internal standards ($CHCl_3$, ^{1}H: 7.26 ppm; ^{13}C: 77.00 ppm). Mass spectra were recorded with Xevo G2-XS QTOF Quadrupole Time-of-Flight Mass Spectrometry using electron spray ionization.

Anomerically pure furanosyl *o*-iodobenzoates were obtained either through column purification or recrystallization mostly in EtOH and in some cases in Et_3N. In all cases, direct coupling between the benzoic acid and the protected reducing monosaccharides using DCC/DMAP can give predominantly 1,2-*trans* or 1,2-*trans* only furanosyl esters. The anomeric purities of furanosides were determined by different chemical shifts of the anomeric hydrogens on ^{1}H NMR, which also exhibit different coupling constants. Generally, the 1,2-*trans* furanosides display smaller coupling constants at the anomeric position compared to that of the corresponding 1,2-*cis* furanosides.[30] For furanosides documented in the literature, the ^{1}H NMR, ^{13}C NMR, and HRMS data of our products match those reported. For those reactions with 4-*tert*-butylbenzyl (PTB) protected donors, the ^{1}HNMR data of the

isolated product are in good agreement with the corresponding benzyl protected ones reported in terms of the region between 3.0 ppm to 6.0 ppm.

Preparation of donors:

General procedure A:

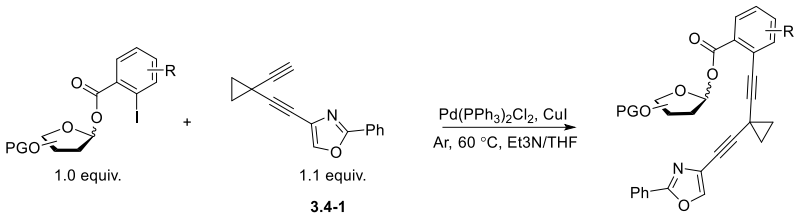

Compound **3.4-1** was prepared according to the reported procedure.[31] To a flame-dried Schlenk flask were added the furanosyl *o*-iodobenzoates (1.0 equiv.), **3.4-1 (**1.1 equiv.), $Pd(PPh_3)_2Cl_2$ (5 mol %) and CuI (7.5 mol %). The flask was vacuumed and filled with Argon three times before adding degassed Et_3N (to make a ~0.05 M solution or using THF/Et_3N mixed solvent if better solubility is needed). The mixture was left at 60 ˚C oil bath for 12 h. The product is bluish under UV light and can be purified by a flash column. After the column, the donors should be stored in the refrigerator. It is noteworthy that after being washed with saturated Na_2CO_3 aqueous solution, the donors are bench stable for a couple of months.

General procedure B:

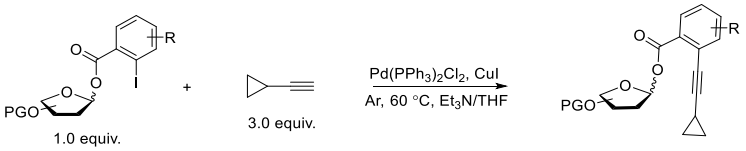

To a flame-dried Schlenk flask were added the furanosyl *o*-iodobenzoates (1.0 equiv.), $Pd(PPh_3)_2Cl_2$ (5 mol %) and CuI (7.5 mol %). The flask was vacuumed and filled with

Argon three times before adding degassed Et_3N (to make a ~0.05 M solution or using THF/Et_3N mixed solvent if better solubility is needed). Cyclopropyl acetylene (3.0 equiv.) was added subsequently via a syringe. The flask was then sealed by a glass stopper due to the volatility of cyclopropyl acetylene. The mixture was left at 60 ˚C oil bath for 12 h. The product is bluish under UV light and can be purified by a flash column. After the column, the donors should be stored in the refrigerator. It is noteworthy that after being washed with saturated Na_2CO_3 aqueous solution, the donors are bench stable for a couple of months.

Selected Donors Prepared:

Donor *β*-**3.3-D1**:

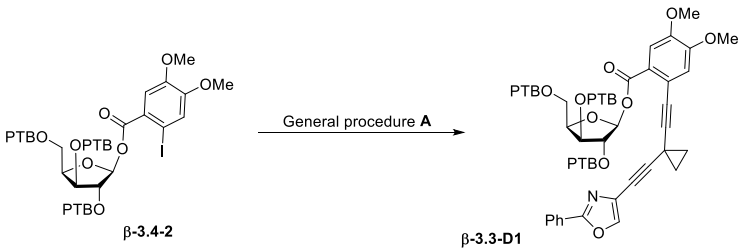

Donor *β*-**3.3-D1**(692 mg, 88% yield) was prepared by following the general procedure A (0.8 mmol scale). ^{1}H NMR (500 MHz, $CDCl_3$) δ 8.06 – 8.00 (m, 2H), 7.75 (s, 1H), 7.46 (tt, J = 6.0, 2.8 Hz, 3H), 7.39 – 7.21 (m, 11H), 7.16 (d, J = 8.0 Hz, 2H), 7.02 (s, 1H), 6.48 (s, 1H), 4.74 (d, J = 11.6 Hz, 1H), 4.68 (q, J = 5.9 Hz, 1H), 4.62 (d, J = 11.6 Hz, 1H), 4.57 (d, J = 11.9 Hz, 1H), 4.55 – 4.50 (m, 2H), 4.45 (d, J = 11.5 Hz, 1H), 4.35 (d, J = 1.6 Hz, 1H), 4.18 (dd, J = 5.6, 1.6 Hz, 1H), 3.93 (s, 3H), 3.92 – 3.88 (m, 1H), 3.81 (dd, J = 10.3, 6.8 Hz, 1H), 3.47 (s, 3H), 1.62 – 1.56 (m, 2H), 1.52 (dt, J = 5.1, 3.1 Hz, 2H), 1.31 (s, 9H), 1.30 (s, 9H), 1.29 (s, 9H). ^{13}C NMR (126 MHz, $CDCl_3$) δ 163.80, 161.33, 151.64, 150.91, 150.80, 150.40,

148.04, 141.23, 135.11, 134.55, 134.32, 130.70, 128.73, 127.63, 127.41, 126.72, 126.51, 125.36, 125.19, 125.15, 124.84, 123.98, 117.96, 116.12, 112.94, 100.36, 94.60, 94.36, 85.00, 82.31, 81.45, 75.44, 73.08, 72.26, 71.94, 68.94, 66.55, 56.06, 55.40, 34.49, 34.46, 34.41, 31.28, 31.26, 21.40, 21.36, 4.24. MS-ESI (m/z): $[M+Na]^+$ calcd. for $[C_{63}H_{69}NNaO_9]^+$, 1006.4865, found 1006.4879.

Donor α-**3.3-D1**:

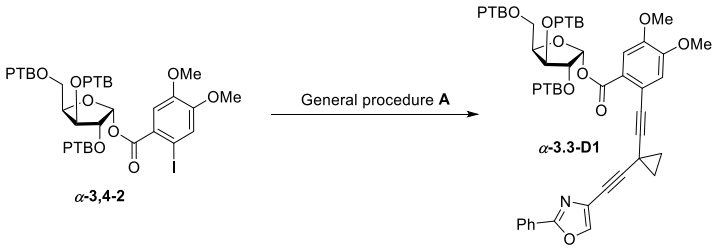

Donor α-**3.3-D1**(197 mg, 89% yield) was prepared by following the general procedure A (0.2 mmol scale). ^{1}H NMR (500 MHz, $CDCl_3$) δ 8.06 – 7.99 (m, 2H), 7.71 (s, 1H), 7.48 – 7.40 (m, 4H), 7.36 – 7.31 (m, 4H), 7.31 – 7.25 (m, 4H), 7.25 – 7.18 (m, 4H), 7.02 (s, 1H), 6.62 (d, J = 4.2 Hz, 1H), 4.67 (td, J = 6.3, 4.4 Hz, 1H), 4.62 (dd, J = 11.5, 3.7 Hz, 2H), 4.59 – 4.51 (m, 3H), 4.49 (d, J = 11.3 Hz, 1H), 4.40 (dd, J = 6.6, 5.2 Hz, 1H), 4.34 – 4.30 (m, 1H), 3.93 (s, 3H), 3.80 (dd, J = 10.5, 4.4 Hz, 1H), 3.76 (s, 3H), 3.69 (dd, J = 10.5, 6.1 Hz, 1H), 1.57 – 1.43 (m, 4H), 1.31 (s, 9H), 1.31 (s, 9H), 1.28 (s, 9H). ^{13}C NMR (126 MHz, $CDCl_3$) δ 164.27, 161.32, 151.64, 150.83, 150.63, 150.48, 148.19, 141.28, 135.13, 134.97, 134.51, 130.71, 128.75, 127.86, 127.60, 127.36, 126.76, 126.54, 125.22, 125.20, 124.85, 124.34, 117.86, 116.39, 113.00, 95.15, 94.65, 93.98, 83.74, 81.07, 78.49, 75.49, 73.32, 72.94, 72.32, 68.77, 66.54, 56.13, 55.88, 34.49, 34.48, 31.33, 31.32, 31.28, 21.36, 21.28, 4.24. MS-ESI (m/z): $[M+Na]^+$ calcd. for $[C_{63}H_{69}NNaO_9]^+$, 1006.4865, found 1006.4869.

Donor β-**3.3-D2**:

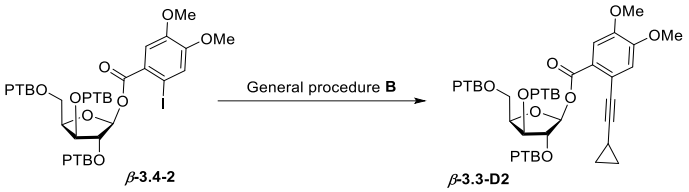

Donor β-**3.3-D2** (160 mg, 98% yield) was prepared by following the general procedure B (0.2 mmol scale). ^{1}H NMR (500 MHz, $CDCl_3$) δ 7.41 – 7.35 (m, 2H), 7.34 – 7.21 (m, 9H), 7.17 – 7.11 (m, 2H), 6.92 (s, 1H), 6.49 (s, 1H), 4.73 (d, J = 11.7 Hz, 1H), 4.67 (dt, J = 6.8, 5.5 Hz, 1H), 4.59 (d, J = 11.7 Hz, 1H), 4.56 (d, J = 11.9 Hz, 1H), 4.53 – 4.47 (m, 2H), 4.43 (d, J = 11.4 Hz, 1H), 4.31 (d, J = 1.6 Hz, 1H), 4.17 (dd, J = 5.7, 1.6 Hz, 1H), 3.95 – 3.85 (m, 1H), 3.90 (s, 3H), 3.80 (dd, J = 10.3, 6.8 Hz, 1H), 3.47 (s, 3H), 1.49 (tt, J = 8.0, 5.2 Hz, 1H), 1.31 (s, 9H), 1.29 (s, 9H), 1.28 (s, 9H), 0.86 (dddd, J = 11.0, 10.1, 8.1, 5.9 Hz, 4H). ^{13}C NMR (126 MHz, $CDCl_3$) δ 164.08, 151.68, 150.97, 150.85, 150.44, 147.71, 135.17, 134.58, 134.35, 127.69, 127.45, 125.41, 125.22, 125.19, 123.68, 118.96, 116.04, 113.00, 100.38, 98.09, 85.09, 82.33, 81.62, 74.65, 73.11, 72.32, 71.94, 69.00, 55.99, 55.43, 34.55, 34.50, 34.45, 31.32, 31.31, 31.30, 8.82, 8.80, 0.69.MS-ESI (m/z): $[M+Na]^+$ calcd. for $[C_{52}H_{64}NaO_8]^+$, 839.4493, found 839.4506.

Donor α-**3.3-D2**:

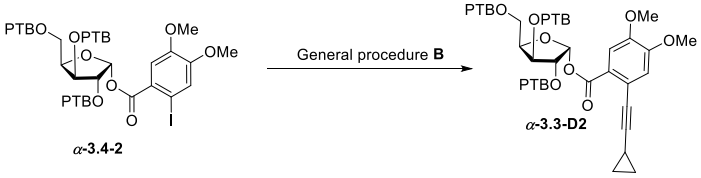

Donor α-**3.3-D2** (156 mg, 96% yield) was prepared by following the general procedure B (0.2 mmol scale). ^{1}H NMR (500 MHz, $CDCl_3$) δ 7.41 (s, 1H), 7.37 – 7.33 (m, 4H), 7.32 –

7.20 (m, 8H), 6.92 (s, 1H), 6.63 (d, J = 4.2 Hz, 1H), 4.67 – 4.45 (m, 7H), 4.37 (dd, J = 6.7, 5.3 Hz, 1H), 4.31 (t, J = 4.8 Hz, 1H), 3.91 (s, 3H), 3.80 (dd, J = 10.5, 4.5 Hz, 1H), 3.76 (s, 3H), 3.68 (dd, J = 10.5, 6.1 Hz, 1H), 1.47 (tt, J = 8.1, 5.0 Hz, 1H), 1.32 (s, 9H), 1.32 (s, 9H), 1.29 (s, 9H), 0.88 – 0.76 (m, 4H). ^{13}C NMR (126 MHz, $CDCl_3$) δ 164.56, 151.62, 150.81, 150.68, 150.50, 147.79, 135.13, 134.95, 134.51, 127.88, 127.61, 127.38, 125.24, 125.22, 125.20, 124.06, 118.83, 116.13, 113.00, 97.68, 94.99, 83.82, 80.94, 78.44, 74.65, 73.31, 72.89, 72.21, 68.73, 56.01, 55.86, 34.51, 34.49, 31.34, 31.33, 31.29, 8.71, 8.69, 0.69. MS-ESI (m/z): $[M+Na]^+$ calcd. for $[C_{52}H_{64}NaO_8]^+$, 839.4493, found 839.4517.

Donor *α*-**3.3-D5**:

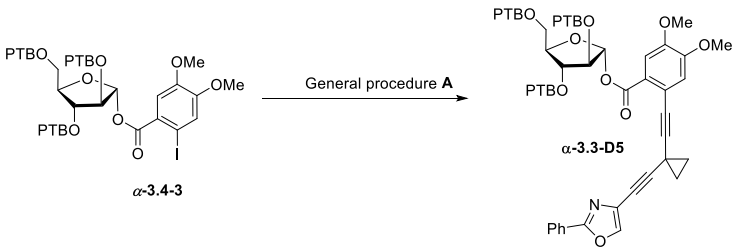

Donor *α*-3.3-**D5** (420 mg, 85% yield) was prepared by following the general procedure A (0.5 mmol scale). ^{1}H NMR (500 MHz, $CDCl_3$) δ 8.08 – 8.02 (m, 2H), 7.75 (s, 1H), 7.52 – 7.43 (m, 4H), 7.41 – 7.34 (m, 4H), 7.33 – 7.27 (m, 6H), 7.22 – 7.16 (m, 2H), 7.04 (s, 1H), 6.51 (s, 1H), 4.74 (d, J = 11.7 Hz, 1H), 4.65 – 4.60 (m, 1H), 4.56 (dd, J = 17.0, 5.1 Hz, 2H), 4.50 (dd, J = 10.2, 4.2 Hz, 3H), 4.33 (d, J = 2.1 Hz, 1H), 4.09 (dd, J = 5.5, 2.2 Hz, 1H), 3.96 (s, 3H), 3.71 (s, 3H), 3.72 – 3.64 (m, 2H), 1.58 (q, J = 3.8, 3.0 Hz, 2H), 1.51 (dt, J = 4.6, 2.8 Hz, 2H), 1.33 (s, 9H), 1.32 (s, 9H), 1.31 (s, 9H). ^{13}C NMR (126 MHz, $CDCl_3$) δ 163.95, 161.35, 151.75, 150.89, 150.79, 150.57, 148.19, 141.26, 135.02, 134.66, 134.38, 130.73, 128.77, 127.82, 127.64, 126.76, 126.54, 125.35, 125.25, 125.22, 124.86, 123.92, 118.06, 116.29, 112.96, 100.86, 94.65, 94.33, 86.86, 83.93, 83.55, 75.54, 73.27, 72.10, 71.89, 69.65,

66.53, 56.14, 55.79, 34.53, 34.50, 31.34, 31.31, 21.38, 21.34, 4.25. MS-ESI (m/z): $[M+Na]^+$ calcd. for $[C_{63}H_{69}NNaO_9]^+$, 1006.4865, found 1006.4871.

Donor α-3.3-**D6**:

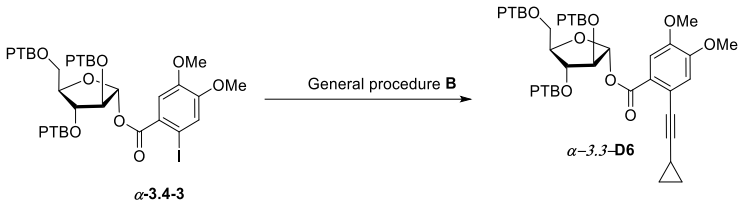

α-3.4-3

α–3.3–**D6**

Donor α-**D6** (156 mg, 96% yield) was prepared by following the general procedure B (0.2 mmol scale). ^{1}H NMR (500 MHz, $CDCl_3$) δ 7.43 (s, 1H), 7.39 – 7.33 (m, 4H), 7.31 – 7.24 (m, 6H), 7.18 – 7.12 (m, 2H), 6.91 (s, 1H), 6.51 (s, 1H), 4.71 (d, J = 11.8 Hz, 1H), 4.60 – 4.51 (m, 3H), 4.46 (d, J = 4.9 Hz, 3H), 4.29 (dd, J = 2.4, 0.8 Hz, 1H), 4.05 (dd, J = 5.9, 2.3 Hz, 1H), 3.90 (s, 3H), 3.71 (s, 3H), 3.68 (d, J = 5.1 Hz, 2H), 1.49 (tt, J = 8.2, 5.1 Hz, 1H), 1.31 (s, 9H), 1.31 (s, 9H), 1.29 (s, 9H), 0.88 – 0.75 (m, 4H). ^{13}C NMR (126 MHz, $CDCl_3$) δ 164.31, 151.77, 150.92, 150.80, 150.59, 147.85, 135.04, 134.68, 134.37, 127.88, 127.65, 127.61, 125.37, 125.25, 125.21, 123.66, 119.02, 116.10, 113.04, 100.84, 98.08, 87.01, 84.12, 83.37, 74.74, 73.28, 72.14, 71.88, 69.65, 56.04, 55.80, 34.55, 34.51, 31.35, 31.33, 31.31, 8.76, 0.67. MS-ESI (m/z): $[M+Na]^+$ calcd. for $[C_{52}H_{64}NaO_8]^+$, 839.4493, found 839.4502.

Gold-catalyzed Stereoselective Furanosylation

General procedure C:

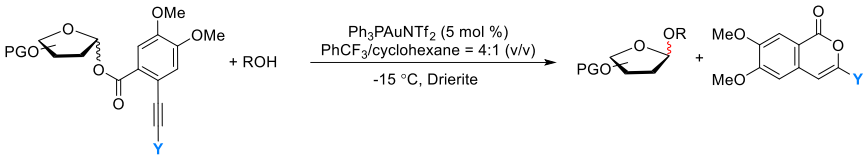

To a glass vial (purchased from VWR®, Catalog Number: 66011-085) equipped with a magnetic stir bar were added donors (56.1 mg, 0.06 mmol, 1.0 equiv.), acceptors (0.072 mmol, 1.2 equiv.), 90 mg grinded white drierite, trifluorotoluene (0.5 mL), and cyclohexane (0.15 mL). The vial was capped with an open top screw cap with silicon liner (purchased from Wheaton™) and sealed with parafilm. The vial was shaken and was then put into the -15 ˚C cooling bath. A 0.03 M solution of PPh_3AuNTf_2 in trifluorotoluene was prepared, and a 0.1 mL (2.2 mg, 0.003 mmol, 0.05 equiv.) of this solution was injected into the vial through the silicone liner via a 1 mL syringe. While injection, a small needle was punched through the silicone liner on the top of the vial to balance the pressure. The needle and the syringe were removed after the injection, and the cooling bath was covered with aluminum foil. When TLC indicated reaction completion, the TBACl/DCM solution was introduced to quench the reaction at -15 ˚C, and the reaction mixture was passed through a Celite® pad before running a column chromatography with hexanes/ethyl acetate as eluent.

Selected Characterization Data for Glycosides

***α*-3.3-3a:**

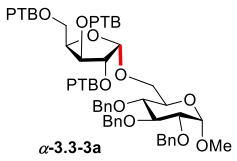

α-3.3-3a

α-**3a** was prepared from *β*-3.3-**D1** according to the general procedure C but with 2.0 equiv. acceptors employed. The reaction was finished after 1 h and afforded the product in 97% yield (60.2 mg) with *α/β* = 16.2:1. For the *α* anomer, ^{1}H NMR (600 MHz, $CDCl_3$) δ 7.39 – 7.22 (m, 25H), 7.18 (d, J = 8.2 Hz, 2H), 5.12 (d, J = 4.2 Hz, 1H), 4.97 (d, J = 10.9 Hz, 1H), 4.85 (t, J = 10.4 Hz, 2H), 4.76 (d, J = 12.0 Hz, 1H), 4.66 (dd, J = 14.2, 11.0 Hz, 2H), 4.62 – 4.58 (m, 3H), 4.54 (d, J = 12.0 Hz, 1H), 4.47 (dd, J = 13.8, 11.7 Hz, 3H), 4.40 (td, J = 6.9, 4.0 Hz, 1H), 4.27 (dd, J = 6.9, 5.6 Hz, 1H), 4.06 (dd, J = 11.6, 3.7 Hz, 1H), 4.04 – 3.96 (m, 2H), 3.77 – 3.66 (m, 4H), 3.58 (dd, J = 10.6, 6.9 Hz, 1H), 3.52 – 3.46 (m, 1H), 3.34 (s, 3H), 1.32 (s, 9H), 1.31 (s, 9H), 1.30 (s, 9H). ^{13}C NMR (101 MHz, $CDCl_3$) δ 150.66, 150.52, 150.40, 138.95, 138.34, 138.17, 135.25, 135.17, 135.00, 128.38, 128.33, 128.01, 127.99, 127.83, 127.80, 127.63, 127.58, 127.47, 127.39, 125.23, 125.20, 125.16, 100.57, 98.06, 83.72, 81.99, 81.62, 80.22, 77.84, 76.30, 75.64, 75.14, 73.50, 73.17, 72.23, 71.98, 70.28, 69.30, 66.47, 55.08, 34.50, 31.36, 31.34. MS-ESI (m/z): $[M+Na]^+$ calcd. for $[C_{66}H_{82}O_{10}Na]^+$,1057.5800, found 1057.5791.The NMR data of the isolated compound are in good agreement with those reported.[32]

β-**3.3-3a:**

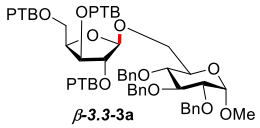

β-3.3-3a

β-**3.3-3a** was prepared from *α*-**3.3-D1** according to the general procedure C but with 2.0 equiv. acceptors employed. The reaction was finished after 1 h and afforded the product in 94% yield (58.3mg) with *α/β* = 1:10. For the *β* anomer, ^{1}H NMR (600 MHz, $CDCl_3$) δ 7.38 – 7.22 (m, 23H), 7.18 (dd, J = 15.4, 8.1 Hz, 4H), 5.06 (d, J = 1.8 Hz, 1H), 4.97 (d, J = 10.8 Hz, 1H), 4.86 (d, J = 10.9 Hz, 1H), 4.81 (d, J = 10.9 Hz, 1H), 4.78 (d, J = 12.1 Hz, 1H), 4.65 (d, J = 12.1 Hz, 1H), 4.59 (d, J = 11.0 Hz, 1H), 4.58 – 4.53 (m, 2H), 4.49 (t, J = 11.7 Hz, 2H), 4.46 – 4.38 (m, 4H), 4.07 – 3.96 (m, 4H), 3.79 (dt, J = 8.5, 4.3 Hz, 2H), 3.71 (dd, J = 10.3, 7.1 Hz, 1H), 3.65 (dd, J = 11.0, 5.6 Hz, 1H), 3.53 (dd, J = 9.6, 3.5 Hz, 1H), 3.49 (t, J = 9.5 Hz, 1H), 3.29 (s, 3H), 1.30 (s, 18H), 1.29 (s, 9H). ^{13}C NMR (126 MHz, $CDCl_3$) δ 150.81, 150.67, 150.41, 138.78, 138.21, 138.17, 135.38, 134.84, 134.49, 128.42, 128.38, 128.36, 128.08, 127.96, 127.86, 127.72, 127.65, 127.63, 127.58, 127.55, 127.49, 125.31, 125.24, 125.20, 107.49, 97.86, 86.86, 82.08, 81.76, 80.04, 79.93, 78.15, 75.75, 75.01, 73.37, 73.20, 71.86, 71.77, 70.07, 69.63, 66.89, 54.99, 34.51, 34.49, 31.36, 31.34, 31.31. MS-ESI (m/z): $[M+Na]^+$ calcd. for $[C_{66}H_{82}O_{10}Na]^+$,1057.5800, found 1057.5791. The NMR data of the isolated compound are in good agreement with those reported.[32]

α-**3.3-3d:**

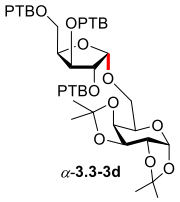

α-3.3-3d

α-**3.3-3d** was prepared from *β*-**D1** according to the general procedure C but with 2.0 equiv. acceptors employed. The reaction was finished after 1 h and afforded the product in 96% yield (47.8 mg) with *α*/*β* = 34:1. For the *α* anomer, ^{1}H NMR (600 MHz, $CDCl_3$) δ 7.38 – 7.28 (m, 8H), 7.28 – 7.24 (m, 2H), 7.19 (d, J = 8.1 Hz, 2H), 5.52 (d, J = 5.0 Hz, 1H), 5.08 (d, J = 4.1 Hz, 1H), 4.67 (d, J = 11.6 Hz, 1H), 4.62 – 4.54 (m, 3H), 4.54 – 4.46 (m, 3H), 4.42 (td, J = 6.7, 3.8 Hz, 1H), 4.34 – 4.26 (m, 3H), 4.04 (ddd, J = 8.0, 5.8, 1.8 Hz, 1H), 4.01 (t, J = 4.9 Hz, 1H), 3.88 (dd, J = 9.8, 5.9 Hz, 1H), 3.75 – 3.66 (m, 2H), 3.58 (dd, J = 10.7, 6.6 Hz, 1H), 1.51 (s, 3H), 1.45 (s, 3H), 1.35 – 1.28 (m, 33H). ^{13}C NMR (126 MHz, $CDCl_3$) δ 150.77, 150.51, 150.43, 135.27, 135.22, 134.86, 127.79, 127.65, 127.39, 125.28, 125.21, 125.19, 109.09, 108.51, 99.91, 96.34, 83.90, 81.63, 76.25, 73.19, 72.21, 71.83, 70.76, 70.69, 70.61, 69.28, 66.03, 65.58, 34.53, 34.50, 31.37, 31.36, 26.11, 26.06, 24.94, 24.55. MS-ESI (m/z): $[M+Na]^+$ calcd. for $[C_{50}H_{70}NaO_{10}]^+$, 853.4861, found 853.4856. The NMR data of the isolated compound are in good agreement with those reported.[17]

β-**3.3-3d:**

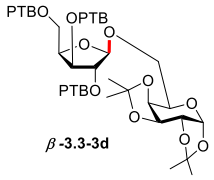

β-**3.3-3d** was prepared from *α*-**3.3-D1** according to the general procedure C but with 2.0 equiv. acceptors employed. The reaction was finished after 1 h and afforded the product in 96% yield (47.9 mg) with *α*/*β* = 1:24. For the *β* anomer, ^{1}H NMR (500 MHz, $CDCl_3$) δ 7.40 – 7.30 (m, 6H), 7.29 – 7.25 (m, 4H), 7.23 – 7.17 (m, 2H), 5.55 (d, J = 5.0 Hz, 1H), 5.13 (d, J = 1.5 Hz, 1H), 4.62 – 4.54 (m, 3H), 4.54 – 4.46 (m, 3H), 4.46 – 4.40 (m, 2H), 4.30 (dd, J =

5.0, 2.4 Hz, 1H), 4.20 (dd, J = 7.9, 1.8 Hz, 1H), 4.09 – 4.02 (m, 2H), 3.99 (ddd, J = 6.8, 4.5, 1.8 Hz, 1H), 3.94 (dd, J = 11.0, 4.4 Hz, 1H), 3.82 (dd, J = 10.3, 5.0 Hz, 1H), 3.73 (dd, J = 10.3, 7.0 Hz, 1H), 3.68 (dd, J = 10.9, 7.2 Hz, 1H), 1.52 (s, 3H), 1.43 (s, 3H), 1.33 (s, 3H), 1.32 (s, 9H), 1.31 (s, 9H), 1.31 (s, 9H), 1.29 (s, 3H). ^{13}C NMR (126 MHz, $CDCl_3$) δ 150.70, 150.56, 150.39, 135.46, 134.97, 134.74, 127.79, 127.56, 127.53, 125.27, 125.20, 109.23, 108.48, 107.39, 96.33, 86.46, 81.80, 80.06, 73.15, 71.72, 71.61, 71.22, 70.66, 70.59, 69.79, 67.78, 67.20, 34.52, 34.50, 34.49, 31.36, 31.34, 26.12, 26.01, 25.02, 24.39. MS-ESI (m/z): $[M+Na]^+$ calcd. for $[C_{50}H_{70}NaO_{10}]^+$, 853.4861, found 853.4843. The NMR data of the isolated compound are in good agreement with those reported.[17]

α-**3.3-3b:**

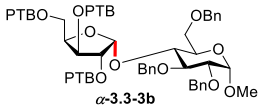

α-**3.3-3b**

α-**3.3-3b** was prepared from *β*-**3.3-D1** according to the general procedure C but with 2.0 equiv. acceptors employed. The reaction was finished within 12 h at -25 ˚C and afforded the product in 97% yield (60.2 mg) with *α/β* = 13:1. For the *α* anomer, ^{1}H NMR (500 MHz, $CDCl_3$) δ 7.37 – 7.19 (m, 23H), 7.19 – 7.14 (m, 2H), 7.12 – 7.07 (m, 2H), 5.59 (d, J = 4.4 Hz, 1H), 5.10 (d, J = 11.7 Hz, 1H), 4.75 (d, J = 11.7 Hz, 1H), 4.72 – 4.63 (m, 3H), 4.60 (d, J = 12.1 Hz, 1H), 4.56 (d, J = 11.8 Hz, 1H), 4.52 – 4.44 (m, 3H), 4.41 (dd, J = 11.7, 8.5 Hz, 2H), 4.35 (d, J = 11.8 Hz, 1H), 4.15 (q, J = 2.4, 1.4 Hz, 2H), 4.04 (t, J = 9.1 Hz, 1H), 3.94 – 3.86 (m, 2H), 3.81 (dd, J = 10.1, 8.7 Hz, 1H), 3.73 (dd, J = 10.5, 2.1 Hz, 1H), 3.65 – 3.59 (m, 2H), 3.56 (dd, J = 9.6, 3.5 Hz, 1H), 3.51 – 3.46 (m, 1H), 3.40 (s, 3H), 1.33 (s, 9H), 1.32 (s, 9H), 1.29 (s, 9H). ^{13}C NMR (126 MHz, $CDCl_3$) δ 150.60, 150.40, 139.07, 138.43, 137.94, 135.23,

135.04, 134.57, 128.40, 128.28, 128.19, 128.14, 127.87, 127.82, 127.68, 127.53, 127.39, 127.36, 127.12, 126.76, 125.22, 125.20, 125.14, 100.89, 97.64, 82.23, 81.73, 81.52, 80.24, 76.38, 74.80, 74.53, 73.32, 73.15, 72.57, 72.04, 69.52, 69.28, 55.02, 34.50, 34.47, 34.46, 31.35, 31.33, 31.30. MS-ESI (m/z): $[M+Na]^+$ calcd. for $[C_{66}H_{82}O_{10}Na]^+$,1057.5800, found 1057.5786. The NMR data of the isolated compound are in good agreement with those reported.[33]

***β*-3.3-3b:**

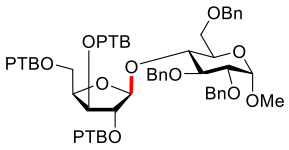

***β*-3.3-3b**

Donor *α*-**3.3-D1**(0.02 mmol) and acceptor **3.3-2b** (0.04 mmol, 2.0 equiv.) was subjected to the general procedure C but was running at -25 ˚C instead. The reaction was quenched after 12 h by a DCM solution of TBACl. The *α/β* ratio was determined to 1:1 by ^{1}H NMR analysis of the unpurified reaction mixture [The anomeric H of the *β* anomer: δ 5.27 (d, J = 1.8 Hz, 1H)]. The NMR yield is around 30%.

***β*-3.3-4a:**

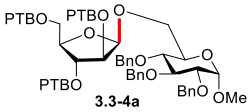

3.3-4a

β-**3.3-4a** was prepared from donor *α*-**3.3-D5** according to the general procedure C. The reaction was finished after 0.5 h and afforded the product in 94% yield (58.5 mg) with *α/β* =

1:16. To evaluate the role of the directing group, donor *α*-**3.3-D6** (0.02 mmol) and acceptor **2a** (0.024 mmol, 1.2 equiv.) was also subjected to the general procedure C. The reaction was quenched after 45 min by a DCM solution of TBACl. The *α/β* ratio was determined to 1:6 by ^{1}H NMR analysis of the unpurified reaction mixture. The NMR yield of this reaction is 95%. The reaction only gave 88% conversion if quenched after 0.5 h. For the β anomer, ^{1}H NMR (500 MHz, $CDCl_3$) δ 7.39 – 7.18 (m, 27H), 5.02 (d, J = 4.2 Hz, 1H), 4.98 (d, J = 10.9 Hz, 1H), 4.86 (d, J = 11.1 Hz, 1H), 4.81 (d, J = 7.7 Hz, 1H), 4.79 (d, J = 8.8 Hz, 1H), 4.67 (d, J = 12.1 Hz, 1H), 4.65 – 4.53 (m, 5H), 4.53 – 4.48 (m, 2H), 4.44 (d, J = 11.7 Hz, 1H), 4.15 – 4.09 (m, 2H), 4.07 (dq, J = 4.6, 2.6, 1.4 Hz, 1H), 4.02 – 3.94 (m, 2H), 3.80 (ddd, J = 10.1, 5.3, 1.7 Hz, 1H), 3.64 (dd, J = 11.1, 5.3 Hz, 1H), 3.59 (q, J = 5.5, 4.9 Hz, 2H), 3.57 – 3.51 (m, 2H), 3.31 (s, 3H), 1.35 – 1.30 (m, 18H), 1.30 (s, 9H). ^{13}C NMR (126 MHz, $CDCl_3$) δ 150.63, 150.55, 150.51, 138.83, 138.39, 138.23, 135.23, 135.17, 134.73, 128.41, 128.35, 128.34, 128.03, 127.89, 127.84, 127.63, 127.61, 127.59, 127.52, 127.49, 125.22, 125.19, 101.07, 97.92, 84.05, 83.67, 82.11, 80.75, 80.09, 78.03, 75.67, 74.84, 73.37, 73.09, 72.78, 72.07, 71.88, 70.20, 66.42, 55.09, 34.49, 31.34, 31.32. MS-ESI (m/z): $[M+Na]^+$ calcd. for $[C_{66}H_{82}O_{10}Na]^+$,1057.5800, found 1057.5813. The NMR data of the isolated compound are in good agreement with those reported.[32, 34]

β-3.3-**4b:**

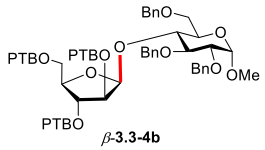

β-3.3-**4b**

β-3.3-**4b** was prepared from donor *α*-**3.3-D5** according to the general procedure C but with 2 equiv. acceptors employed. The reaction was finished within 12 h at -25 ˚C and afforded the

product in 91% yield (56.5 mg) with α/β = 1:8. To evaluate the role of the directing group, both donor α-**3.3-D5** and donor α-**3.3-D6** (0.02 mmol) with acceptor **3.3-2b** (0.024 mmol, 1.2 equiv.) were subjected to the general procedure C at -15 ˚C. The former reaction was finished after 4.5 h with 91% NMR yield, and the α/β ratio is equal to 1:6.5. The later reaction was finished after 0.5 h with 88% NMR yield, and the α/β ratio is equal to 1:1.9. For the β anomer, ^{1}H NMR (600 MHz, $CDCl_3$) δ 7.42 – 7.38 (m, 2H), 7.36 – 7.17 (m, 25H), 5.27 (d, J = 4.3 Hz, 1H), 4.98 (d, J = 10.1 Hz, 1H), 4.91 (d, J = 10.1 Hz, 1H), 4.75 (d, J = 12.1 Hz, 1H), 4.61 (d, J = 12.1 Hz, 1H), 4.60 – 4.56 (m, 2H), 4.56 – 4.48 (m, 3H), 4.46 (d, J = 11.7 Hz, 1H), 4.41 (d, J = 11.6 Hz, 1H), 4.35 (d, J = 12.1 Hz, 1H), 4.29 (d, J = 12.1 Hz, 1H), 4.05 (dt, J = 14.5, 5.6 Hz, 2H), 3.96 – 3.90 (m, 2H), 3.75 (ddd, J = 11.7, 6.2, 1.9 Hz, 2H), 3.68 – 3.56 (m, 4H), 3.53 (dd, J = 9.5, 3.5 Hz, 1H), 3.38 (s, 3H), 1.32 (s, 9H), 1.31 (s, 9H), 1.29 (s, 9H). ^{13}C NMR (126 MHz, $CDCl_3$) δ 150.64, 150.50, 150.39, 139.20, 138.33, 138.11, 135.23, 135.22, 134.86, 128.39, 128.18, 128.16, 128.13, 128.10, 127.83, 127.69, 127.63, 127.51, 127.50, 127.36, 127.26, 125.19, 125.16, 102.54, 97.79, 83.78, 83.53, 80.46, 80.38, 80.19, 77.49, 74.82, 73.28, 73.16, 72.99, 72.53, 72.08, 71.94, 69.98, 69.25, 55.14, 34.48, 34.46, 31.33, 31.32. MS-ESI (m/z): $[M+Na]^+$ calcd. for $[C_{66}H_{82}O_{10}Na]^+$,1057.5800, found 1057.5812. The major product was proved to be the β product according to the NOESY experiment. COSY, HMBC, HSQC and NOESY spectra are attached.

3.5 References

1. Lindberg, B., Components of bacterial polysaccharides. *Advances in carbohydrate chemistry and biochemistry* **1990,** *48*, 279-318.

2. Lowary, T. L., Twenty years of mycobacterial glycans: furanosides and beyond. *Accounts of chemical research* **2016,** *49* (7), 1379-1388.

3. Tefsen, B.; Ram, A. F.; van Die, I.; Routier, F. H., Galactofuranose in eukaryotes: aspects of biosynthesis and functional impact. *Glycobiology* **2012,** *22* (4), 456-469.

4. Peltier, P.; Euzen, R.; Daniellou, R.; Nugier-Chauvin, C.; Ferrieres, V., Recent knowledge and innovations related to hexofuranosides: structure, synthesis and applications. *Carbohydrate research* **2008,** *343* (12), 1897-1923.

5. Yin, H.; D'Souz, F. W.; Lowary, T. L., Arabinofuranosides from mycobacteria: synthesis of a highly branched hexasaccharide and related fragments containing β-arabinofuranosyl residues. *The Journal of organic chemistry* **2002,** *67* (3), 892-903.

6. Gadikota, R. R.; Callam, C. S.; Lowary, T. L., Stereocontrolled synthesis of 2, 3-anhydro-β-d-lyxofuranosyl glycosides. *Organic letters* **2001,** *3* (4), 607-610.

7. Gadikota, R. R.; Callam, C. S.; Wagner, T.; Del Fraino, B.; Lowary, T. L., 2, 3-Anhydro sugars in glycoside bond synthesis. Highly stereoselective syntheses of oligosaccharides containing α-and β-arabinofuranosyl linkages. *Journal of the American Chemical Society* **2003,** *125* (14), 4155-4165.

8. Crich, D., Mechanism of a chemical glycosylation reaction. *Accounts of chemical research* **2010,** *43* (8), 1144-1153.

9. Bai, Y.; Lowary, T. L., 2, 3-Anhydrosugars in glycoside bond synthesis. Application to α-d-galactofuranosides. *The Journal of organic chemistry* **2006,** *71* (26), 9658-9671.

10. Bai, Y.; Lowary, T. L., Synthesis of a pentasaccharide fragment of varianose, a cell wall polysaccharide from Penicillium varians. *The Journal of organic chemistry* **2006,** *71* (26), 9672-9680.

11. Zhu, X.; Kawatkar, S.; Rao, Y.; Boons, G.-J., Practical approach for the stereoselective introduction of β-arabinofuranosides. *Journal of the American Chemical Society* **2006,** *128* (36), 11948-11957.

12. Ishiwata, A.; Akao, H.; Ito, Y., Stereoselective synthesis of a fragment of mycobacterial arabinan. *Organic letters* **2006,** *8* (24), 5525-5528.

13. Larsen, C. H.; Ridgway, B. H.; Shaw, J. T.; Woerpel, K., A stereoelectronic model to explain the highly stereoselective reactions of nucleophiles with five-membered-ring oxocarbenium ions. *Journal of the American Chemical Society* **1999,** *121* (51), 12208-12209.

14. Liu, Q.-W.; Bin, H.-C.; Yang, J.-S., β-Arabinofuranosylation using 5-O-(2-quinolinecarbonyl) substituted ethyl thioglycoside donors. *Organic letters* **2013,** *15* (15), 3974-3977.

15. Cumpstey, I., Intramolecular aglycon delivery. *Carbohydrate research* **2008,** *343* (10-11), 1553-1573.

16. Thadke, S. A.; Mishra, B.; Hotha, S., Gold (III)-catalyzed glycosidations for 1, 2-trans and 1, 2-cis furanosides. *The Journal of organic chemistry* **2014,** *79* (16), 7358-7371.

17. Mayfield, A. B.; Metternich, J. B.; Trotta, A. H.; Jacobsen, E. N., Stereospecific Furanosylations Catalyzed by Bis-thiourea Hydrogen-Bond Donors. *Journal of the American Chemical Society* **2020,** *142* (8), 4061-4069.

18. Xu, C.; Rao, V. B.; Weigen, J.; Loh, C. C., A robust and tunable halogen bond organocatalyzed 2-deoxyglycosylation involving quantum tunneling. *Nature communications* **2020,** *11* (1), 1-17.

19. Li, Y.; Yang, Y.; Yu, B., An efficient glycosylation protocol with glycosyl ortho-alkynylbenzoates as donors under the catalysis of Ph3PAuOTf. *Tetrahedron Letters* **2008,** *49* (22), 3604-3608.

20. Yu, B., Gold(I)-Catalyzed Glycosylation with Glycosyl o-Alkynylbenzoates as Donors. *Accounts of Chemical Research* **2018,** *51* (2), 507-516.

21. Nicolaou, K. C.; Cai, Q.; Sun, H.; Qin, B.; Zhu, S., Total Synthesis of Trioxacarcins DC-45-A1, A, D, C, and C7″-epi-C and Full Structural Assignment of Trioxacarcin C. *Journal of the American Chemical Society* **2016,** *138* (9), 3118-3124.

22. Bai, Y.; Shen, X.; Li, Y.; Dai, M., Total Synthesis of (−)-Spinosyn A via Carbonylative Macrolactonization. *Journal of the American Chemical Society* **2016,** *138* (34), 10838-10841.

23. Wang, B.; Liu, Y.; Jiao, R.; Feng, Y.; Li, Q.; Chen, C.; Liu, L.; He, G.; Chen, G., Total Synthesis of Mannopeptimycins α and β. *Journal of the American Chemical Society* **2016,** *138* (11), 3926-3932.

24. Zhang, Q.; Sun, J.; Zhu, Y.; Zhang, F.; Yu, B., An Efficient Approach to the Synthesis of Nucleosides: Gold(I)-Catalyzed N-Glycosylation of Pyrimidines and Purines with Glycosyl ortho-Alkynyl Benzoates. *Angewandte Chemie International Edition* **2011,** *50* (21), 4933-4936.

25. Yang, F.; Zhu, Y.; Yu, B., A dramatic concentration effect on the stereoselectivity of N-glycosylation for the synthesis of 2'-deoxy-β-ribonucleosides. *Chem. Commun. (Cambridge, U. K.)* **2012,** *48* (56), 7097-7099.

26. Zhu, D.; Yu, B., Total synthesis of linckosides A and B, the representative starfish polyhydroxysteroid glycosides with neuritogenic activities. *Journal of the American Chemical Society* **2015,** *137* (48), 15098-15101.

27. Yang, W.; Sun, J.; Lu, W.; Li, Y.; Shan, L.; Han, W.; Zhang, W.-D.; Yu, B., Synthesis of Kaempferol 3-O-(3",6"-Di-O-E-p-coumaroyl)-β-D-glucopyranoside, Efficient Glycosylation of Flavonol 3-OH with Glycosyl o-Alkynylbenzoates as Donors. *J. Org. Chem.* **2010,** *75* (20), 6879-6888.

28. Zhang, L.; Shen, K.; Taha, H. A.; Lowary, T. L., Stereocontrolled Synthesis of α-Xylofuranosides Using a Conformationally Restricted Donor. *The Journal of Organic Chemistry* **2018,** *83* (15), 7659-7671.

29. Mézailles, N.; Ricard, L.; Gagosz, F., Phosphine Gold(I) Bis-(trifluoromethanesulfonyl)imidate Complexes as New Highly Efficient and Air-Stable Catalysts for the Cycloisomerization of Enynes. *Organic Letters* **2005,** *7* (19), 4133-4136.

30. Wang, X.; Woods, R. J., Insights into furanose solution conformations: beyond the two-state model. *Journal of biomolecular NMR* **2016,** *64* (4), 291-305.

31. Ma, X.; Zheng, Z.; Fu, Y.; Zhu, X.; Liu, P.; Zhang, L., A "Traceless" Directing Group Enables Catalytic SN 2 Glycosylation toward 1, 2-cis-Glycopyranosides. *Journal of the American Chemical Society* **2021,** *143* (31), 11908-11913.

32. Vidadala, S. R.; Gayatri, G.; Sastry, G. N.; Hotha, S., Propargyl/methyl furanosides as potential glycosyl donors. *Chemical Communications* **2011,** *47* (35), 9906-9908.

33. Mallick, A.; Mallikharjunarao, Y.; Rajasekaran, P.; Roy, R.; Vankar, Y. D., AuIII-Halide/Phenylacetylene-Catalysed Glycosylations Using 1-O-Acetylfuranoses and Pyranose 1, 2-Orthoesters as Glycosyl Donors. *European Journal of Organic Chemistry* **2016,** *2016* (3), 579-588.

34. Lee, Y. J.; Lee, K.; Jung, E. H.; Jeon, H. B.; Kim, K. S., Acceptor-dependent stereoselective glycosylation: 2 '-CB glycoside-mediated direct β-d-arabinofuranosylation

and efficient synthesis of the octaarabinofuranoside in mycobacterial cell wall. *Organic letters* **2005,** *7* (15), 3263-3266.

Appendix-NMR Spectra for Selected Compounds

NMR Spectra for Compounds in Chapter 1

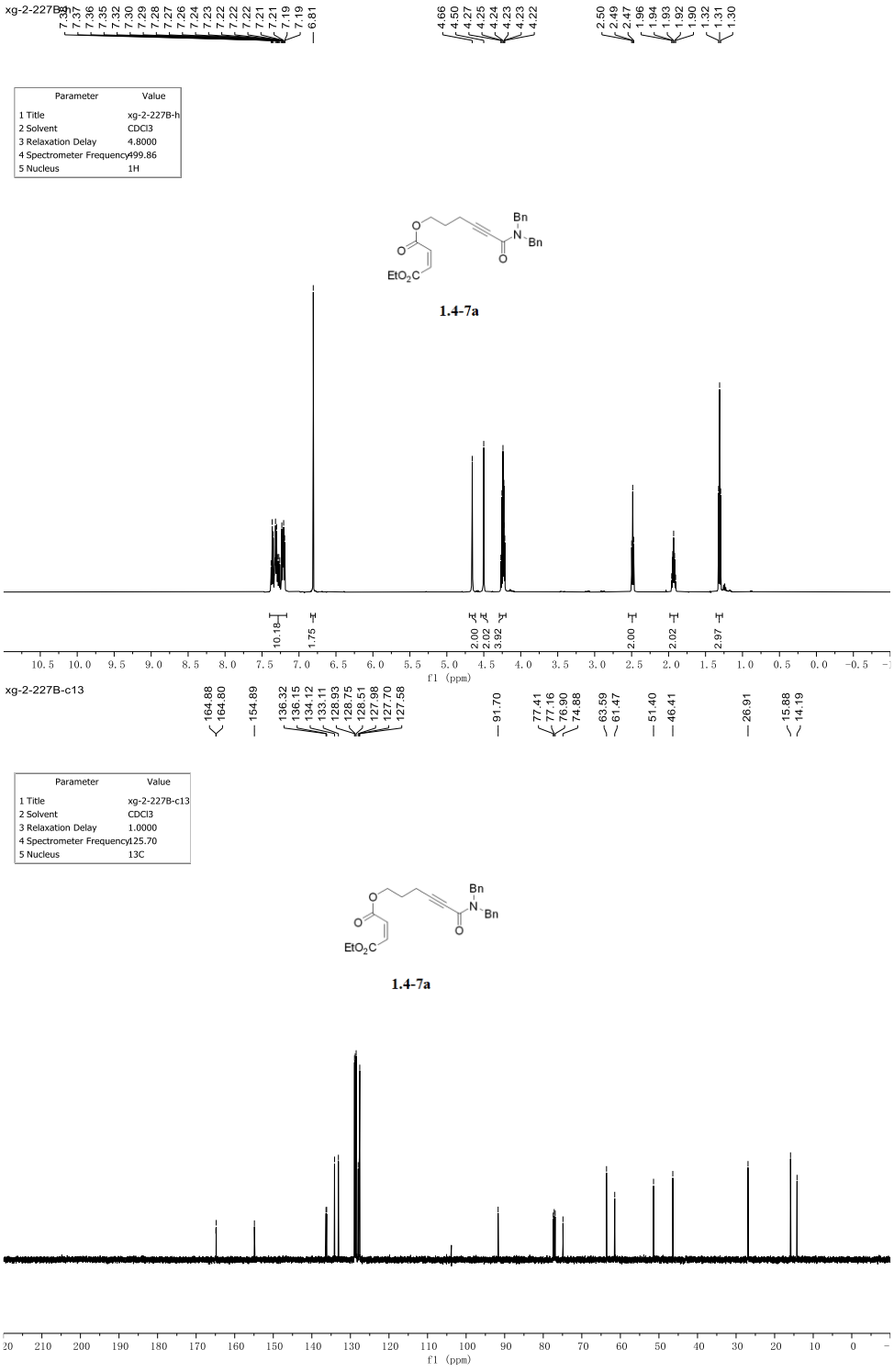

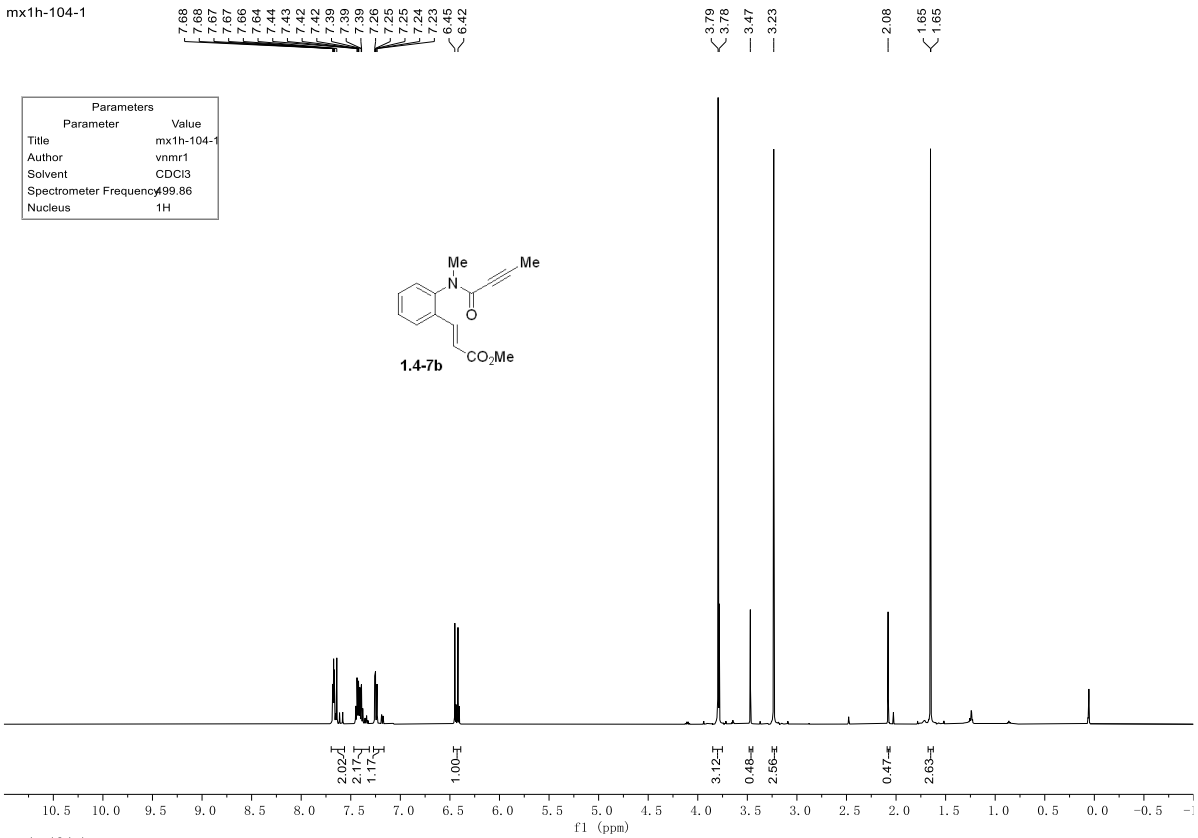
mx1h-104-1
7.68 7.68 7.67 7.67 7.66 7.64 7.44 7.43 7.42 7.42 7.39 7.39 7.39 7.26 7.25 7.25 7.24 7.23 6.45 6.42
3.79 3.78 3.47 3.23
2.08
1.65 1.65
Parameters
Parameter Value
Title mx1h-104-1
Author vnmr1
Solvent CDCl3
Spectrometer Frequency 499.86
Nucleus 1H
Me
N
Me
O
CO2Me
1.4-7b
2.02 2.17 1.17 1.00 3.12 0.48 2.56 0.47 2.63
10.5 10.0 9.5 9.0 8.5 8.0 7.5 7.0 6.5 6.0 5.5 5.0 4.5 4.0 3.5 3.0 2.5 2.0 1.5 1.0 0.5 0.0 -0.5
f1 (ppm)

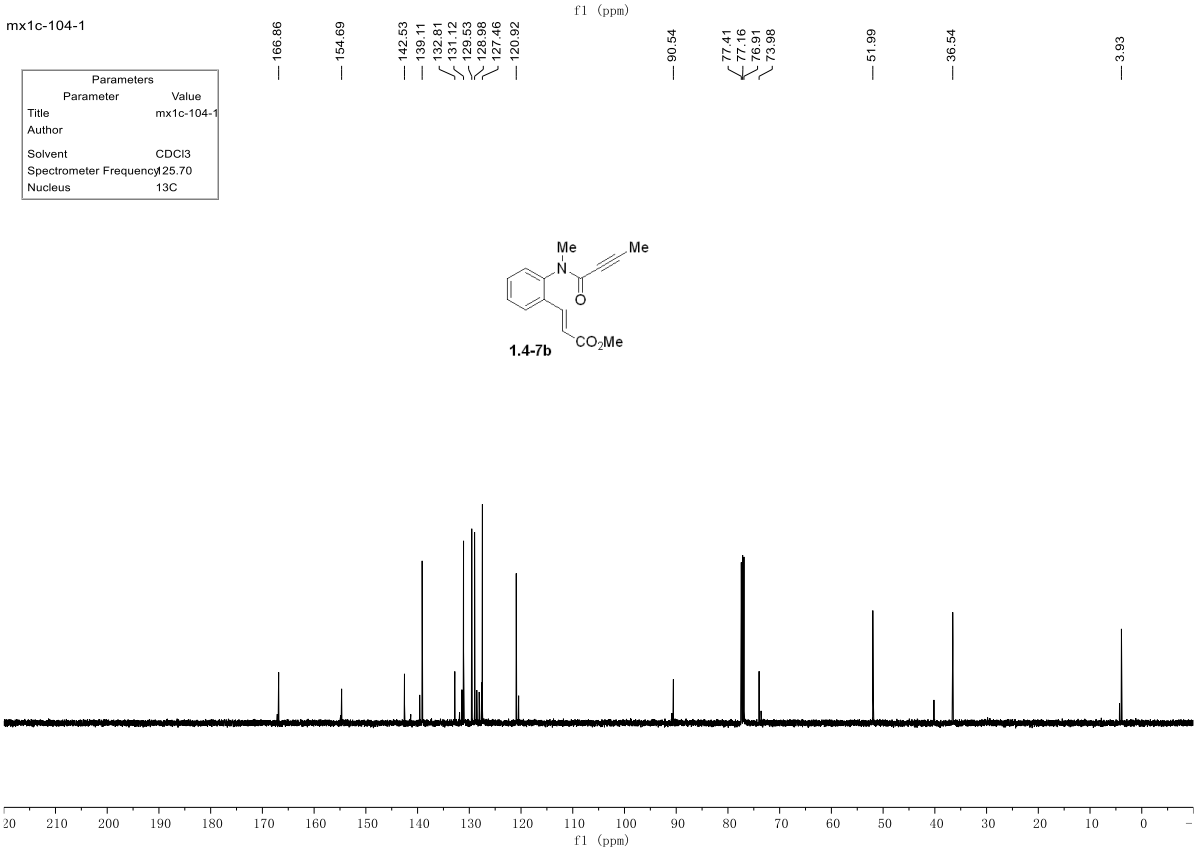
mx1c-104-1
166.86 154.69 142.53 139.11 132.81 131.12 129.53 129.98 127.46 120.92
90.54
77.41 77.16 76.91 73.98
51.99
36.54
3.93
Parameters
Parameter Value
Title mx1c-104-1
Author
Solvent CDCl3
Spectrometer Frequency 125.70
Nucleus 13C
Me
N
Me
O
CO2Me
1.4-7b
220 210 200 190 180 170 160 150 140 130 120 110 100 90 80 70 60 50 40 30 20 10 0
f1 (ppm)

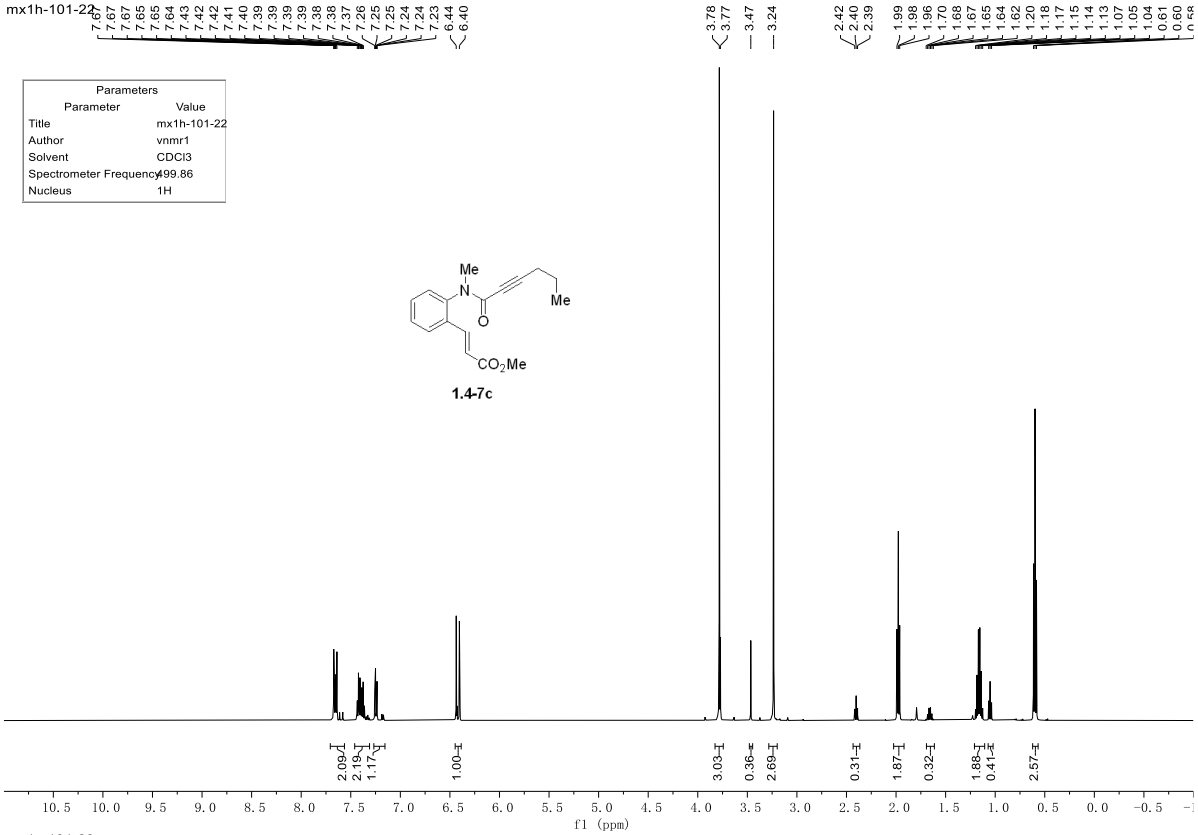
mx1h-101-22
Parameters
Parameter Value
Title mx1h-101-22
Author vnmr1
Solvent CDCl3
Spectrometer Frequency 499.86
Nucleus 1H
Me
N
O
Me
CO2Me
1.4-7c
f1 (ppm)

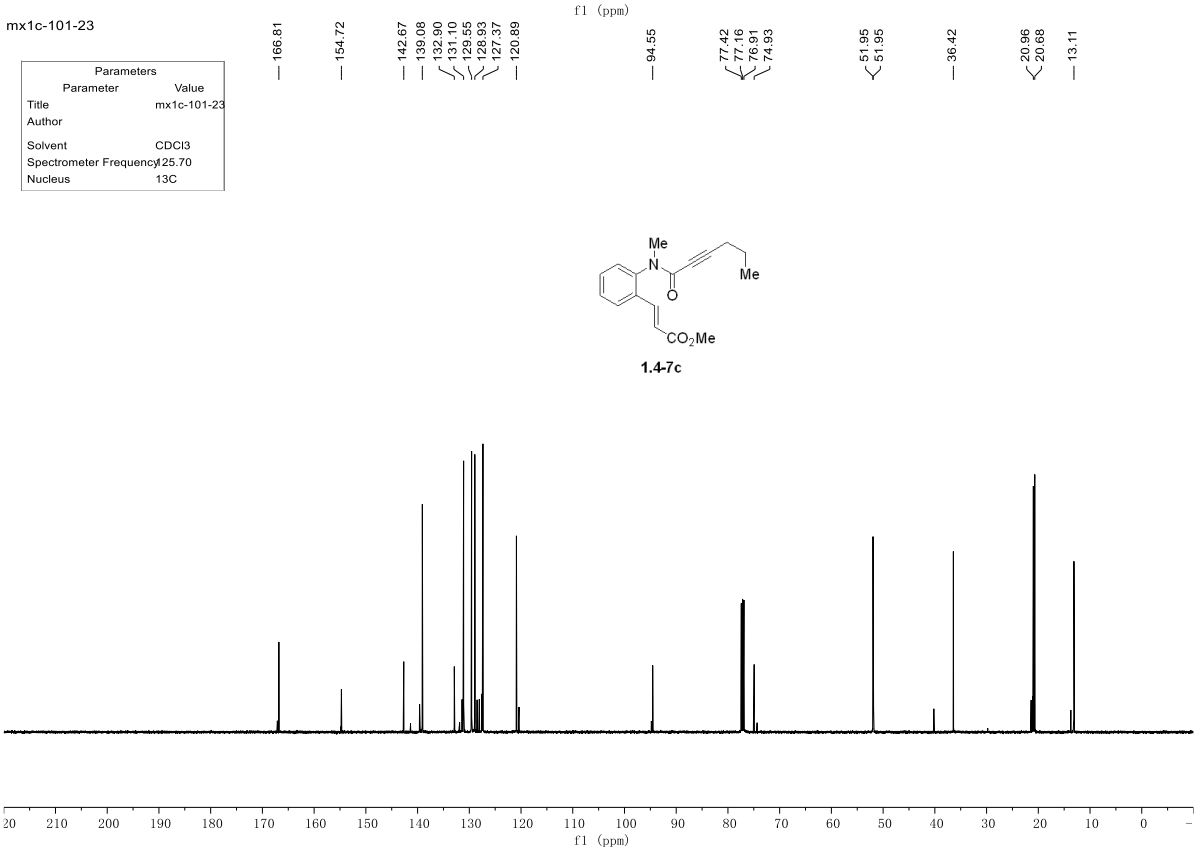
mx1c-101-23
Parameters
Parameter Value
Title mx1c-101-23
Author
Solvent CDCl3
Spectrometer Frequency 125.70
Nucleus 13C
Me
N
O
Me
CO2Me
1.4-7c
f1 (ppm)

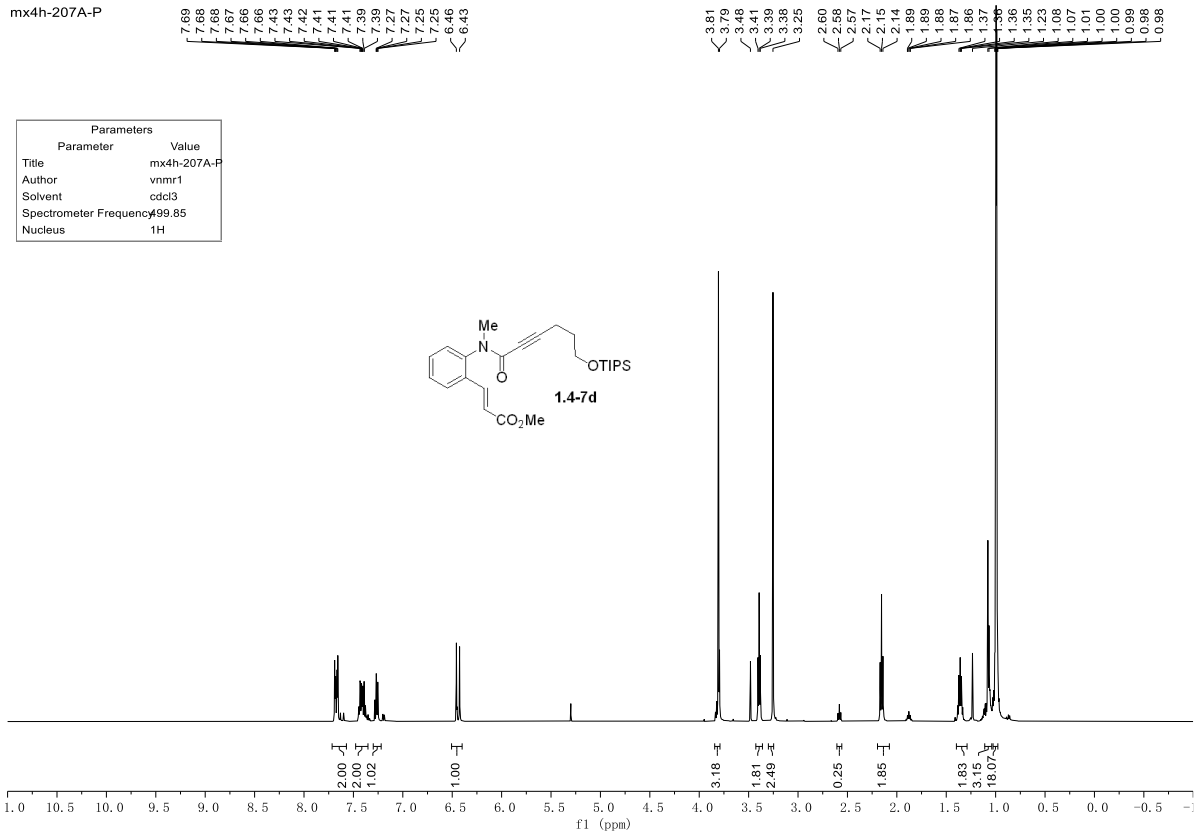
mx4h-207A-P
Parameters
Parameter Value
Title mx4h-207A-P
Author vnmr1
Solvent cdcl3
Spectrometer Frequency 499.85
Nucleus 1H
Me
N
O
OTIPS
CO2Me
1.4-7d
f1 (ppm)

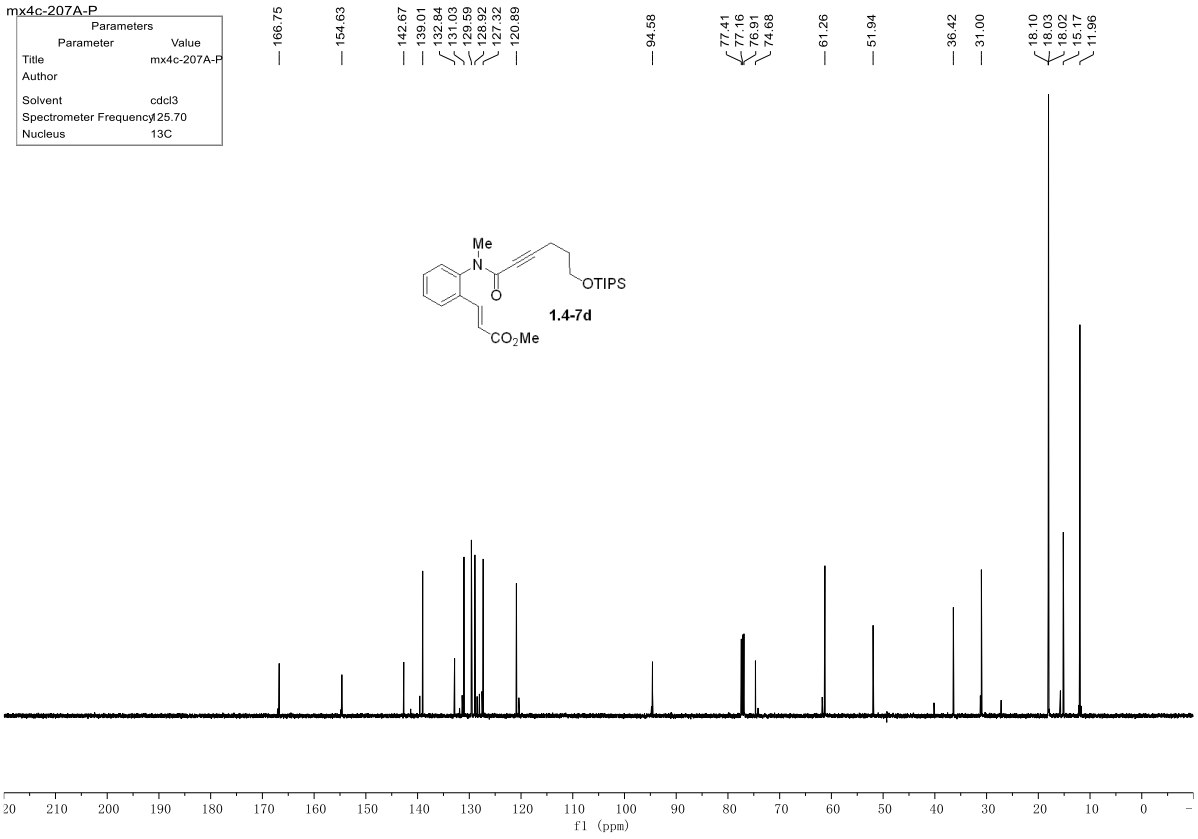
mx4c-207A-P
Parameters
Parameter Value
Title mx4c-207A-P
Author
Solvent cdcl3
Spectrometer Frequency 125.70
Nucleus 13C
Me
N
O
OTIPS
CO2Me
1.4-7d
f1 (ppm)

xg-2-222A-h

7.49 7.48 7.48 7.46 7.43 7.43 7.42 7.41 7.41 7.37 7.37 7.37 7.36 7.36 7.35 7.34 7.34 7.34 7.31 7.29 7.26 6.97 6.95

3.60 3.60 3.59 3.59 3.58 3.03 3.01 3.00 2.00 1.99 1.99 1.98 1.98 1.98 1.97 1.70 1.69 1.67 1.66 1.64 1.63 1.00 0.98 0.97

Parameter	Value
1 Title	xg-2-222A-h
2 Solvent	CDCl3
3 Relaxation Delay	4.8000
4 Spectrometer Frequency	499.86
5 Nucleus	1H

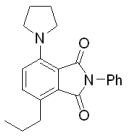

1.4-2a

xg-2-222A-c13-2

168.04 166.93 145.52 137.14 132.49 131.86 129.72 128.97 127.66 127.13 120.91 111.45 77.42 77.16 76.91 51.91 32.75 25.93 24.33 14.14

Parameter	Value
1 Title	xg-2-222A-c13-2
2 Solvent	CDCl3
3 Relaxation Delay	1.0000
4 Spectrometer Frequency	125.70
5 Nucleus	13C

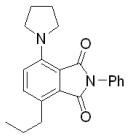

1.4-2a

xg-2-202A-h

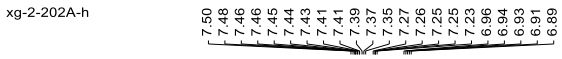

Parameter	Value
1 Title	xg-2-202A-h
2 Solvent	cdcl3
3 Relaxation Delay	4.8000
4 Spectrometer Frequency	399.78
5 Nucleus	1H

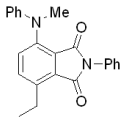

1.4-2f

xg-2-202A-c13

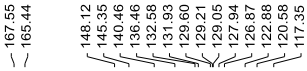

Parameter	Value
1 Title	xg-2-202A-c13
2 Solvent	cdcl3
3 Relaxation Delay	1.0000
4 Spectrometer Frequency	100.53
5 Nucleus	13C

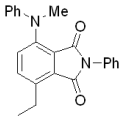

1.4-2f

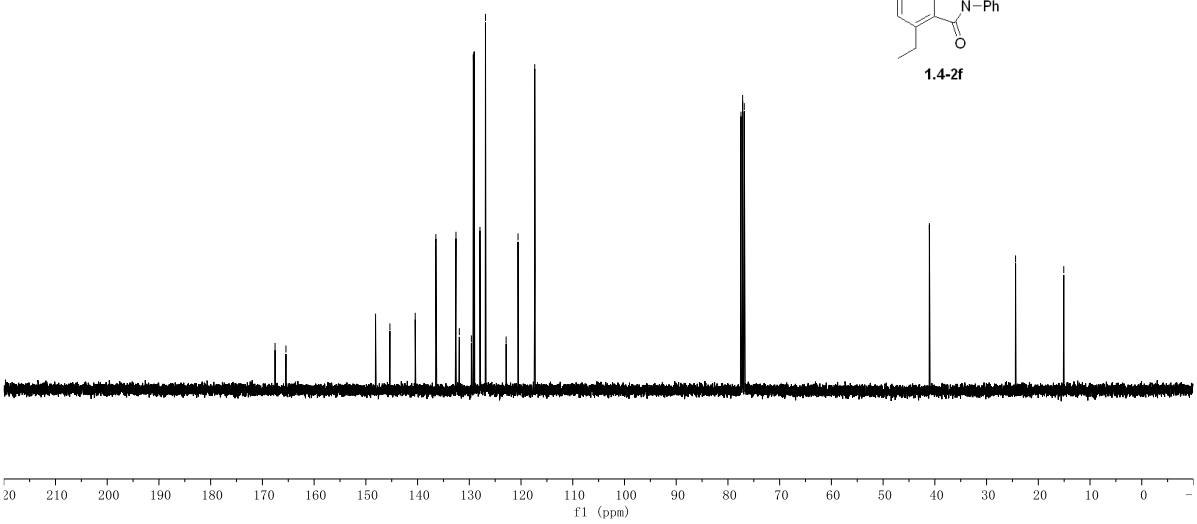

xg-2-202B-h

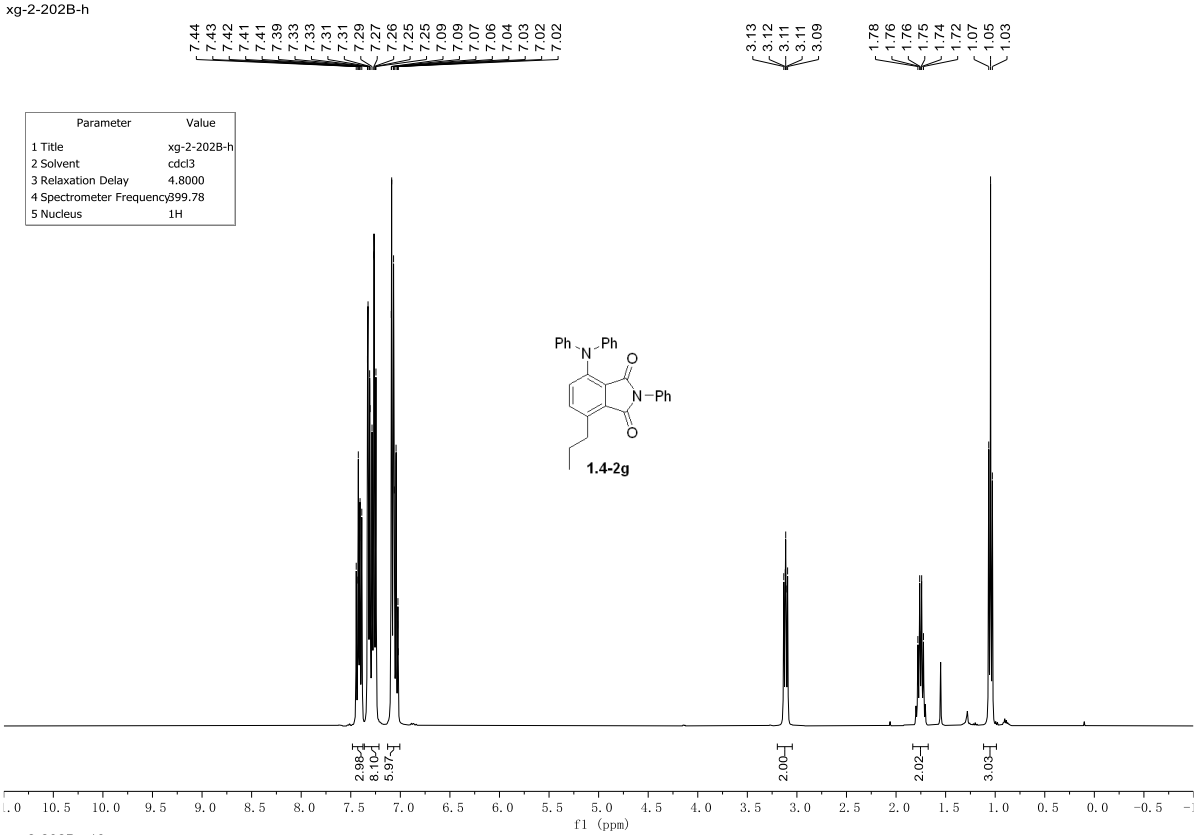

xg-2-202B-c13

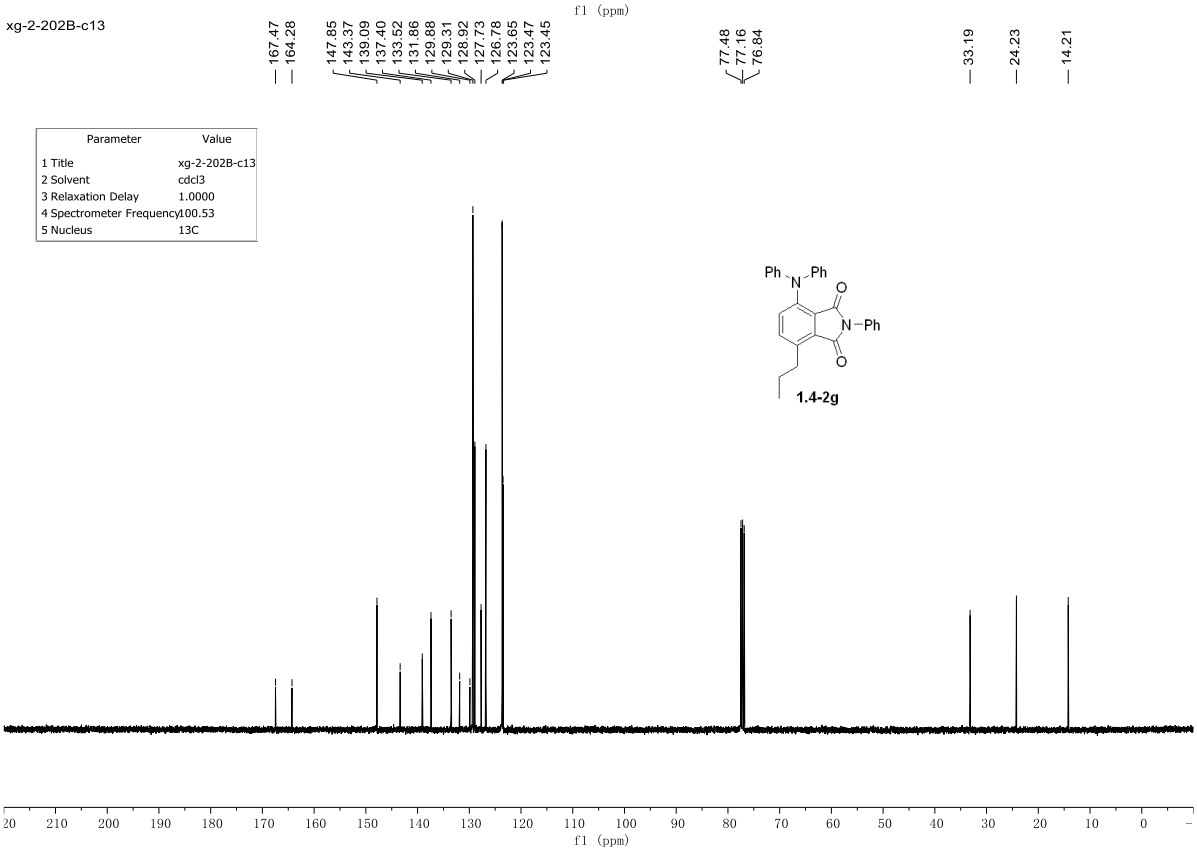

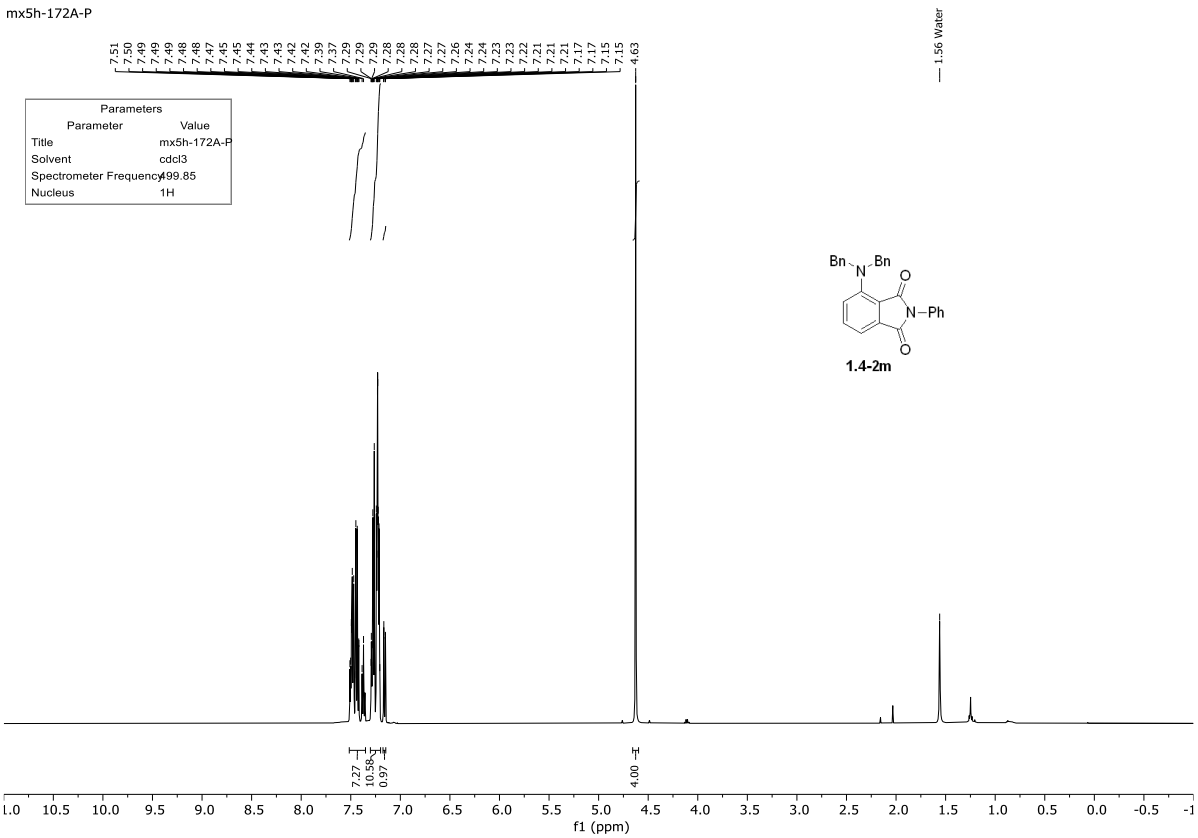
mx5h-172A-P
Parameters
Parameter Value
Title mx5h-172A-P
Solvent cdcl3
Spectrometer Frequency 499.85
Nucleus 1H
1.56 Water
Bn N Bn
N–Ph
1.4-2m
f1 (ppm)

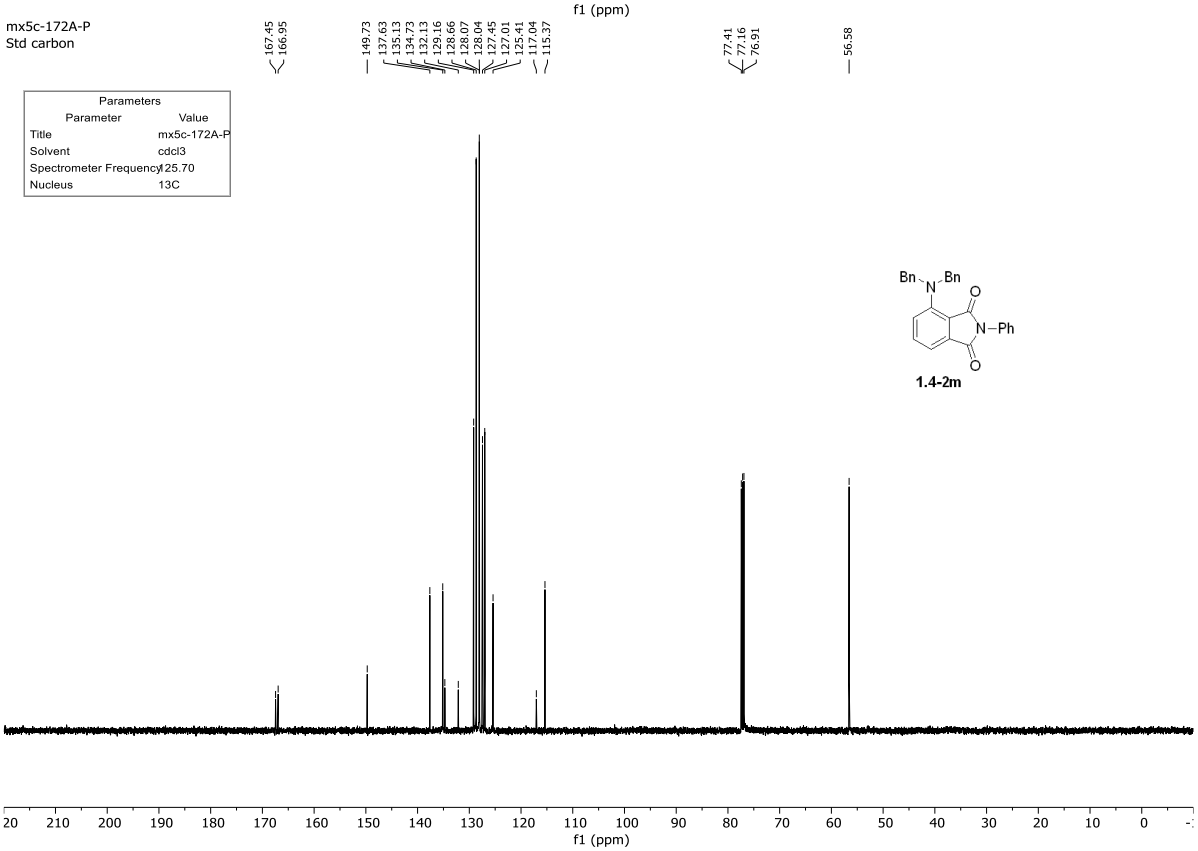
mx5c-172A-P
Std carbon
Parameters
Parameter Value
Title mx5c-172A-P
Solvent cdcl3
Spectrometer Frequency 125.70
Nucleus 13C
Bn N Bn
N–Ph
1.4-2m
f1 (ppm)

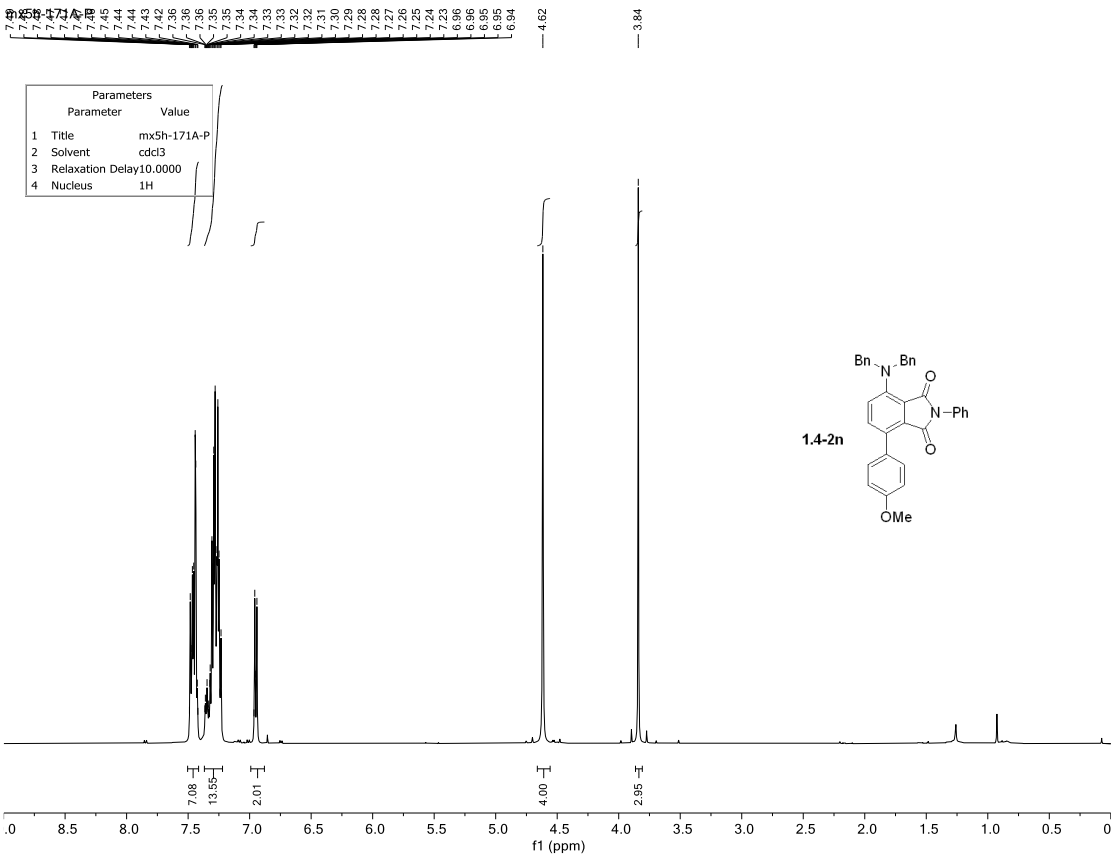
Parameters
Parameter Value
1 Title mx5h-171A-P
2 Solvent cdcl3
3 Relaxation Delay 10.0000
4 Nucleus 1H
4.62
3.84
7.08
13.55
2.01
4.00
2.95
Bn
N
Bn
O
N–Ph
O
1.4-2n
OMe
f1 (ppm)

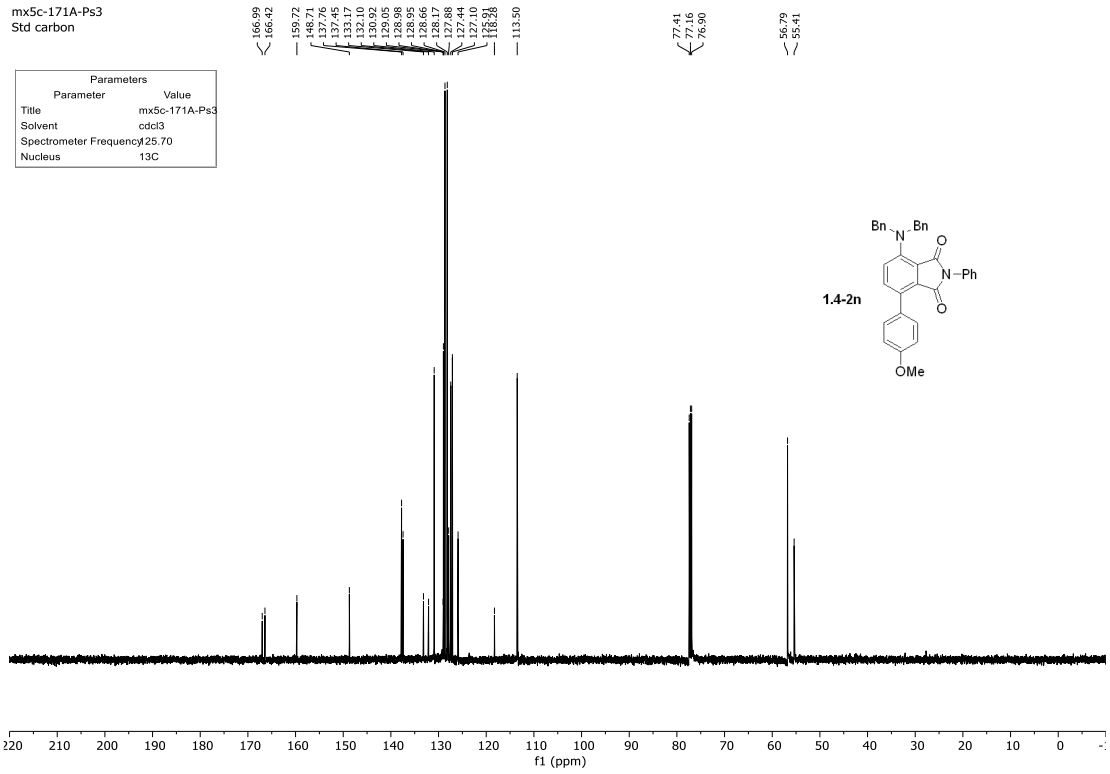
mx5c-171A-Ps3
Std carbon
Parameters
Parameter Value
Title mx5c-171A-Ps3
Solvent cdcl3
Spectrometer Frequency 125.70
Nucleus 13C
166.99
166.42
159.72
148.71
137.76
137.45
133.17
132.10
130.92
129.05
128.88
128.95
128.66
128.17
127.88
127.44
127.10
125.91
118.58
113.50
77.41
77.16
76.90
56.79
55.41
Bn
N
Bn
O
N–Ph
O
1.4-2n
OMe
f1 (ppm)

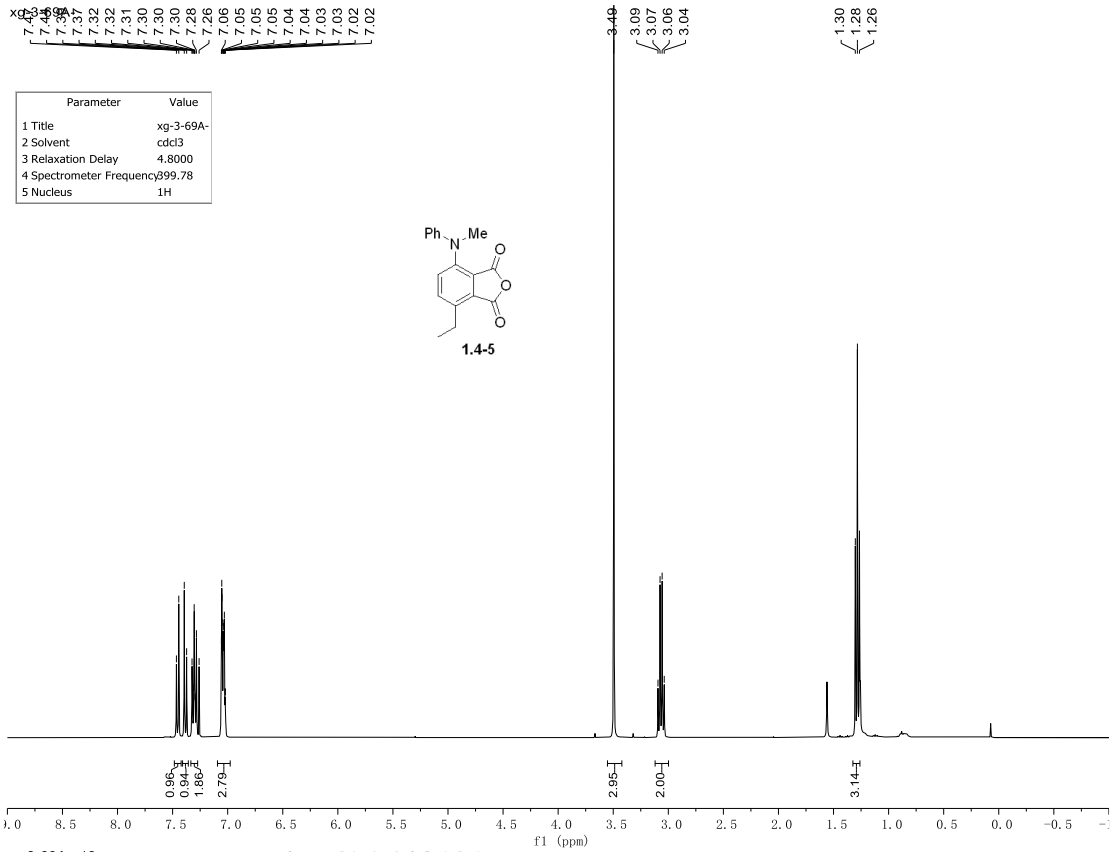
xg-3-69A-
7.44 7.43 7.37 7.32 7.31 7.30 7.30 7.30 7.28 7.26 7.06 7.05 7.05 7.05 7.04 7.04 7.03 7.03 7.02 7.02
3.48 3.09 3.07 3.06 3.04
1.30 1.28 1.26
Parameter Value
1 Title xg-3-69A-
2 Solvent cdcl3
3 Relaxation Delay 4.8000
4 Spectrometer Frequency 399.78
5 Nucleus 1H
Ph N Me
O O O
1.4-5
0.96 0.94 1.86 2.79 2.95 2.00 3.14
f1 (ppm)

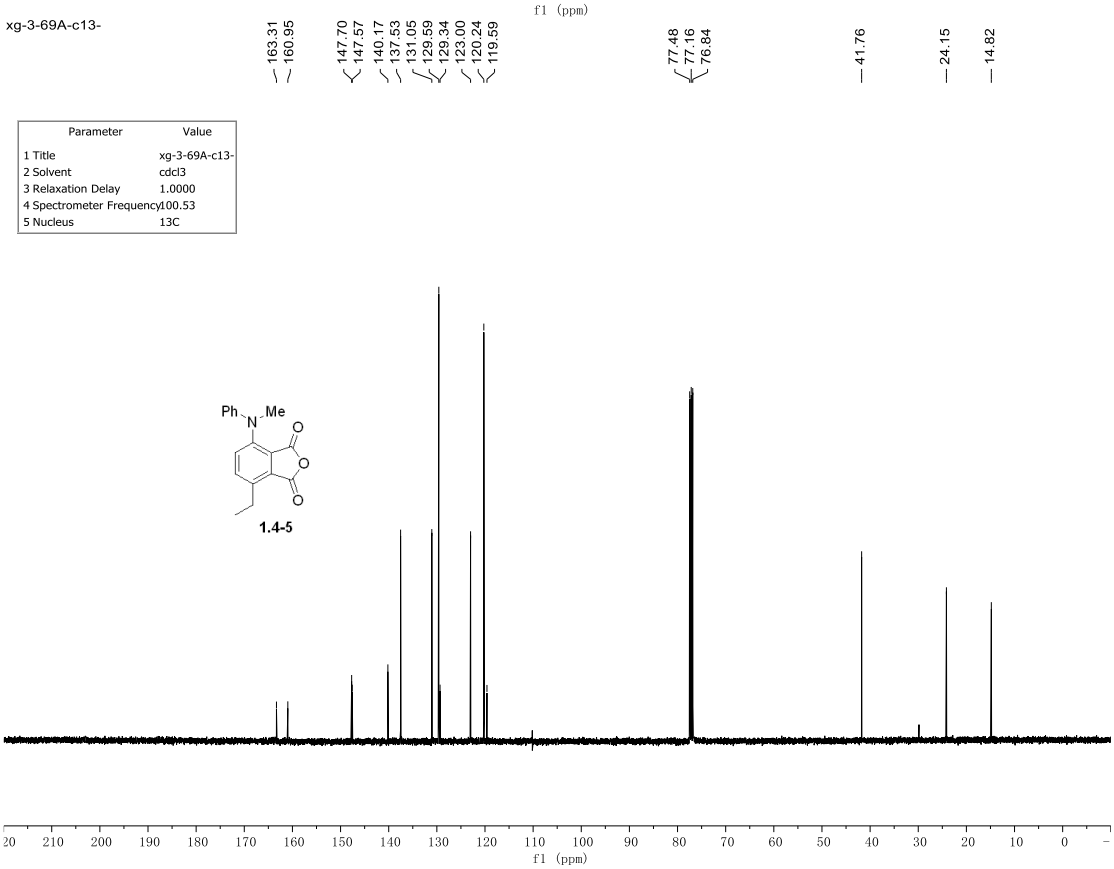
xg-3-69A-c13-
163.31 160.95 147.70 147.57 140.17 137.53 131.05 129.59 129.34 123.00 120.24 119.59
77.48 77.16 76.84
41.76 24.15 14.82
Parameter Value
1 Title xg-3-69A-c13-
2 Solvent cdcl3
3 Relaxation Delay 1.0000
4 Spectrometer Frequency 100.53
5 Nucleus 13C
Ph N Me
O O O
1.4-5
f1 (ppm)

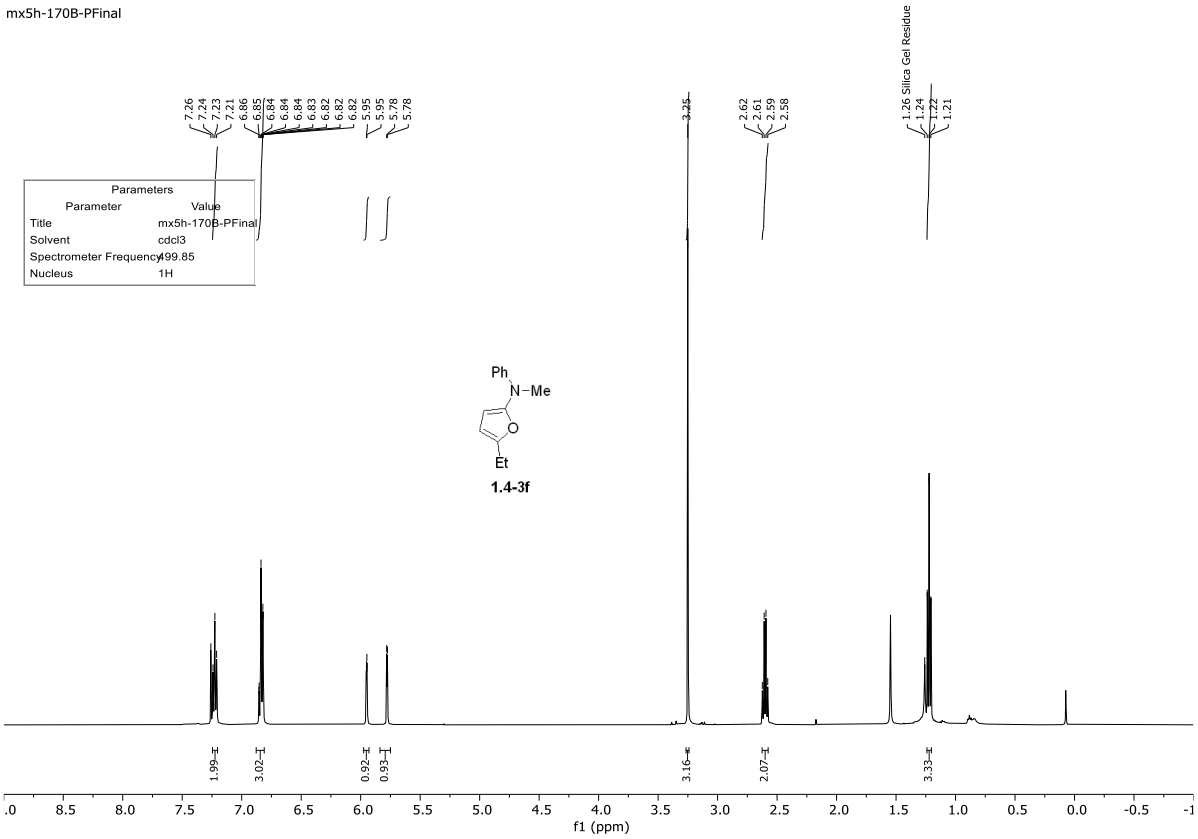
mx5h-170B-PFinal
7.26
7.24
7.23
7.21
6.86
6.85
6.84
6.84
6.84
6.84
6.83
6.82
6.82
6.82
5.95
5.95
5.78
5.78
3.25
2.62
2.61
2.59
2.58
1.26 Silica Gel Residue
1.24
1.22
1.21
Parameters
Parameter Value
Title mx5h-170B-PFinal
Solvent cdcl3
Spectrometer Frequency 499.85
Nucleus 1H
Ph
N–Me
O
Et
1.4-3f
1.99
3.02
0.92
0.93
3.16
2.07
3.33
f1 (ppm)

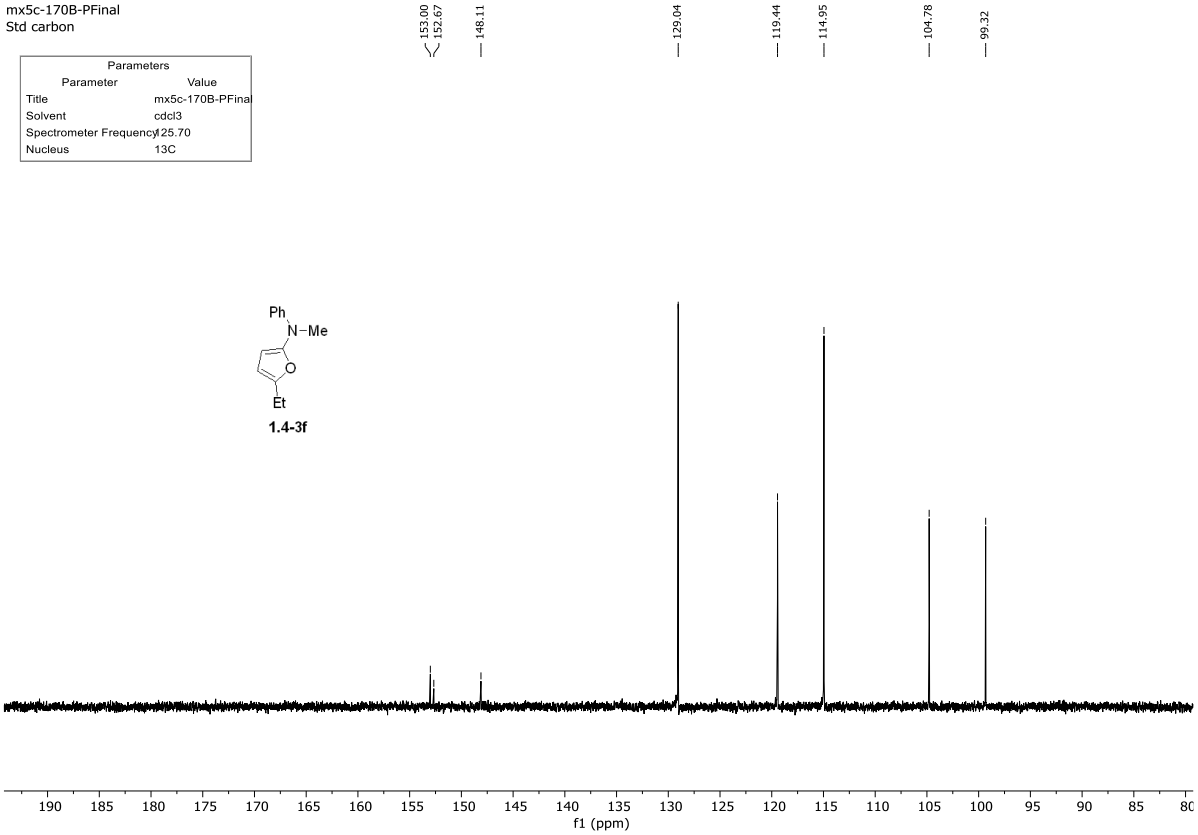
mx5c-170B-PFinal
Std carbon
153.00
152.67
148.11
129.04
119.44
114.95
104.78
99.32
Parameters
Parameter Value
Title mx5c-170B-PFinal
Solvent cdcl3
Spectrometer Frequency 125.70
Nucleus 13C
Ph
N–Me
O
Et
1.4-3f
f1 (ppm)

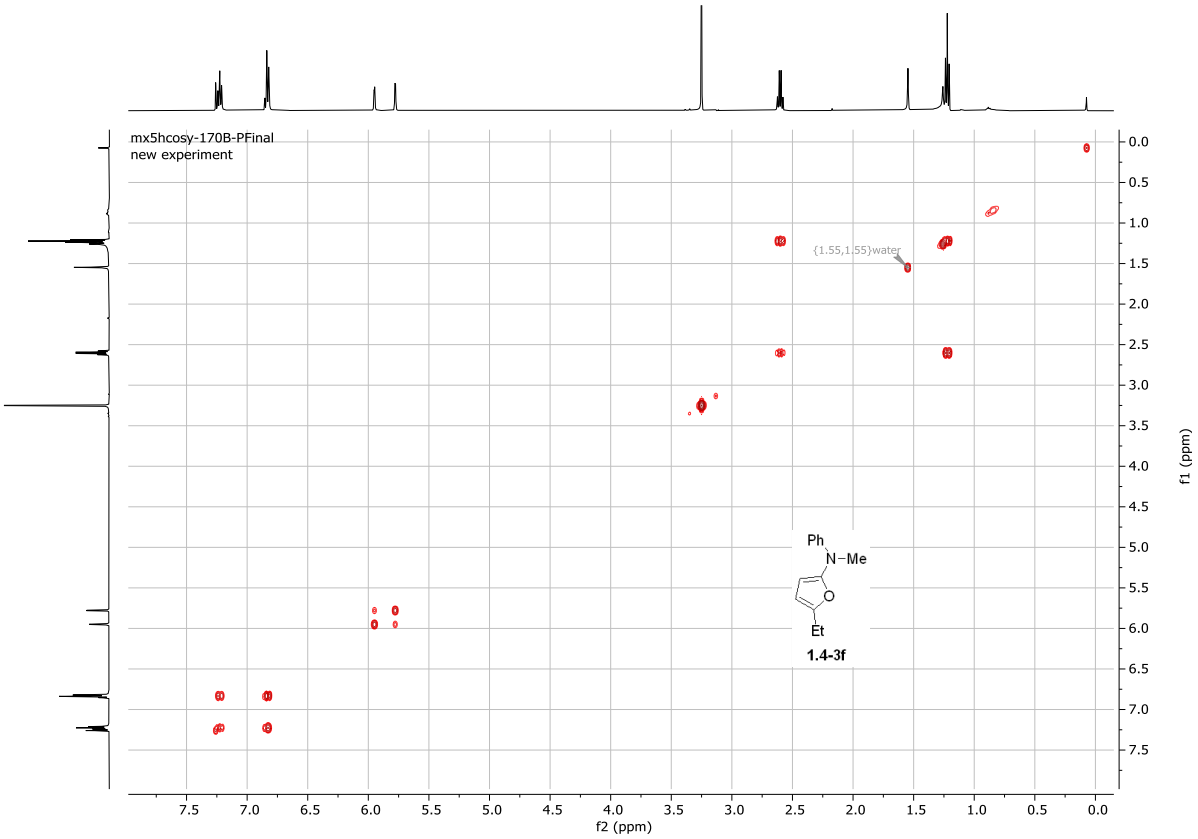
mx5hcosy-170B-PFinal
new experiment
{1.55,1.55}water
Ph
N–Me
Et
1.4-3f
f2 (ppm)
f1 (ppm)

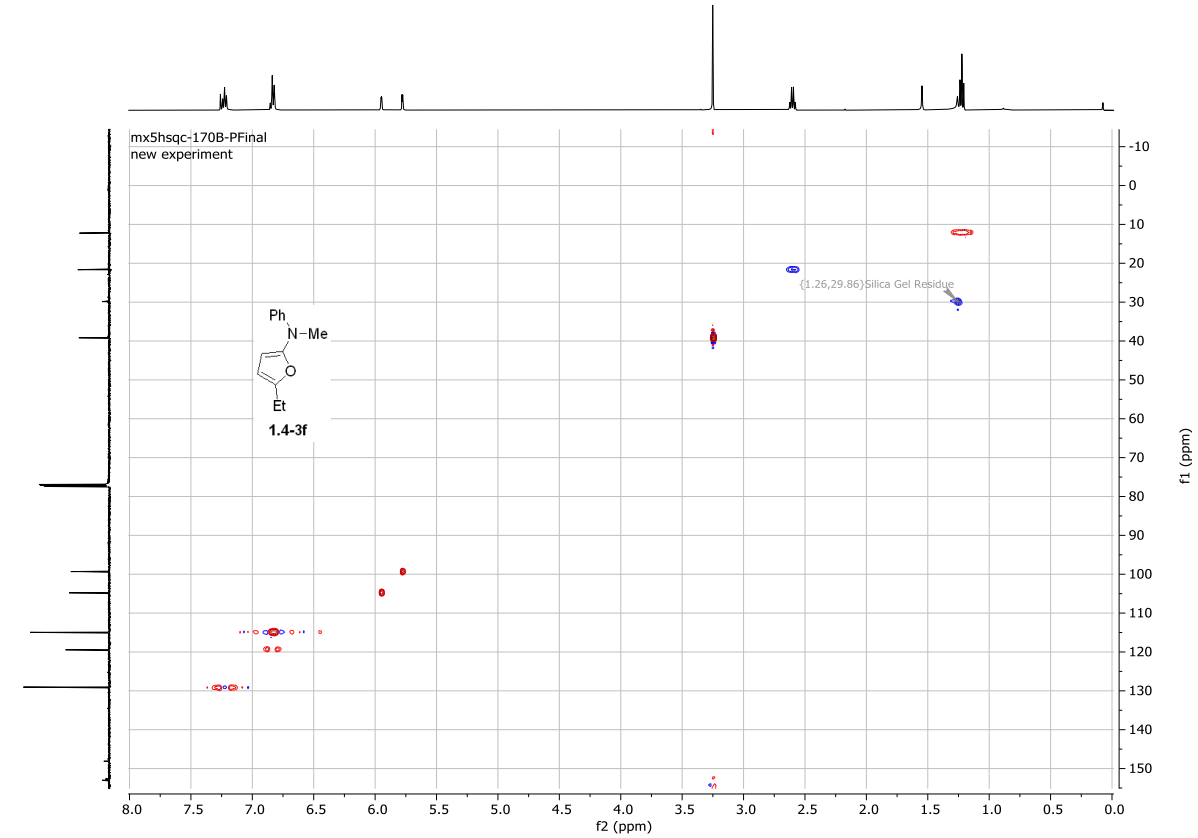
mx5hsqc-170B-PFinal
new experiment
{1.26,29.86}Silica Gel Residue
Ph
N–Me
Et
1.4-3f
f2 (ppm)
f1 (ppm)

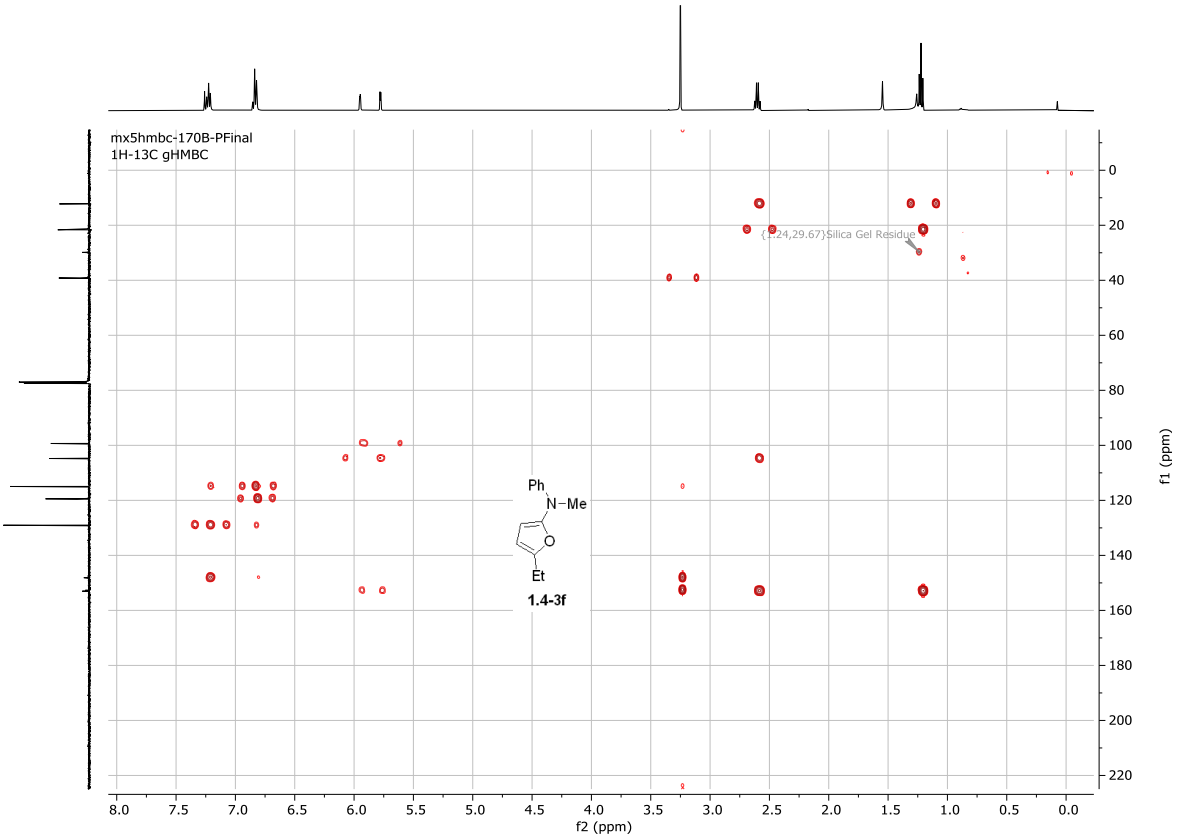
mx5hmbc-170B-PFinal
1H-13C gHMBC
{14.24,29.67}Silica Gel Residue
Ph
N–Me
O
Et
1.4-3f
f2 (ppm)
f1 (ppm)

mx4h-195A-P

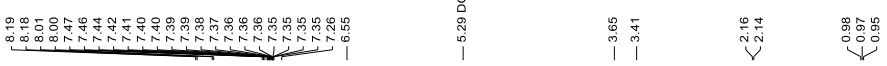

Parameters	
Parameter	Value
Title	mx4h-195A-P
Author	vnmr1
Solvent	cdcl3
Spectrometer Frequency	499.85
Nucleus	1H

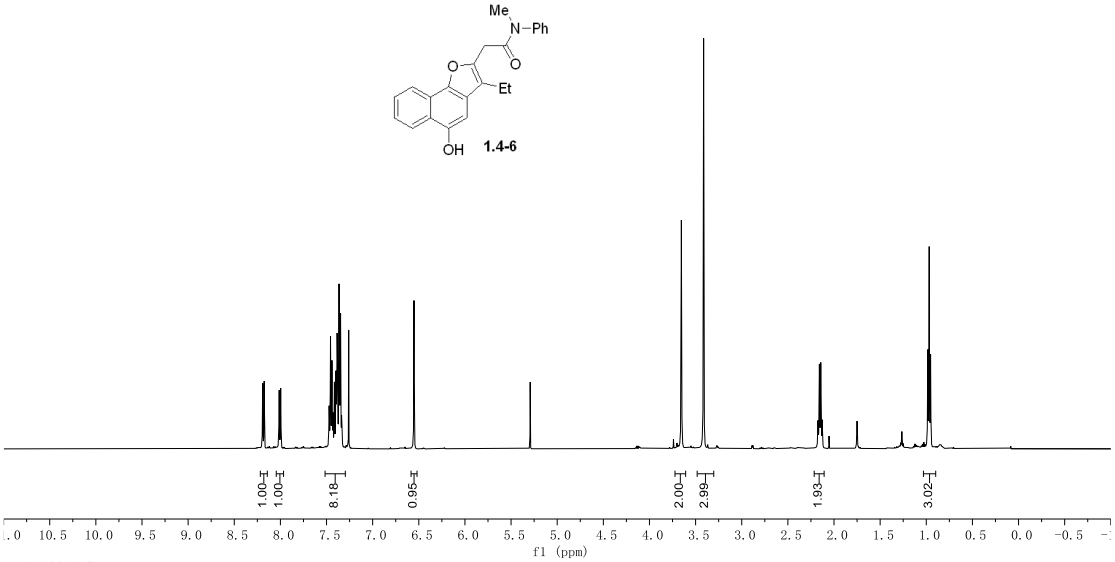

mx4c-195A-Ps5

Parameters		
	Parameter	Value
1	Title	mx4c-195A-Ps5
2	Author	
3	Solvent	cdcl3
4	Spectrometer Frequency	125.70
5	Nucleus	13C

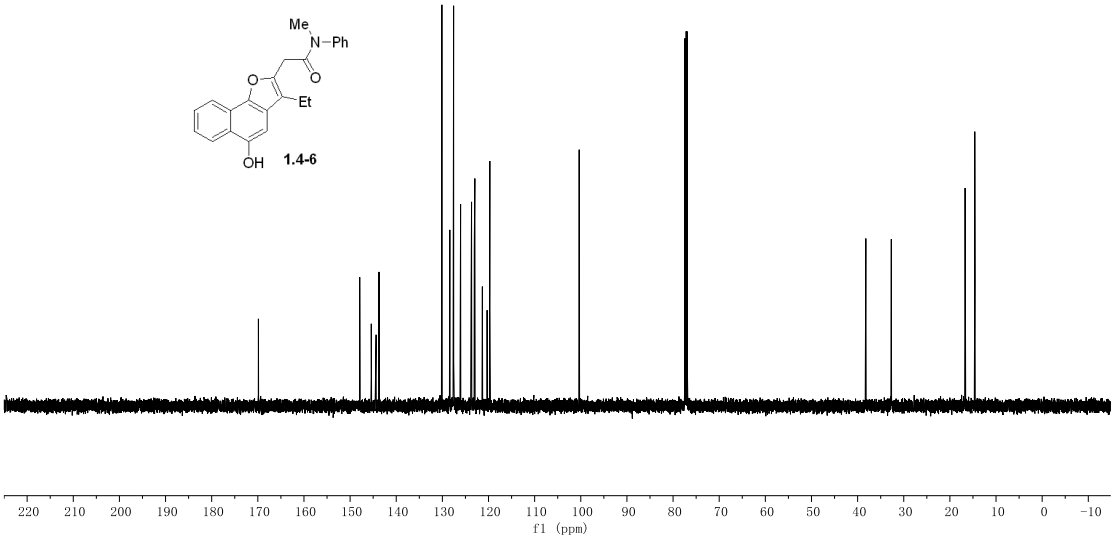

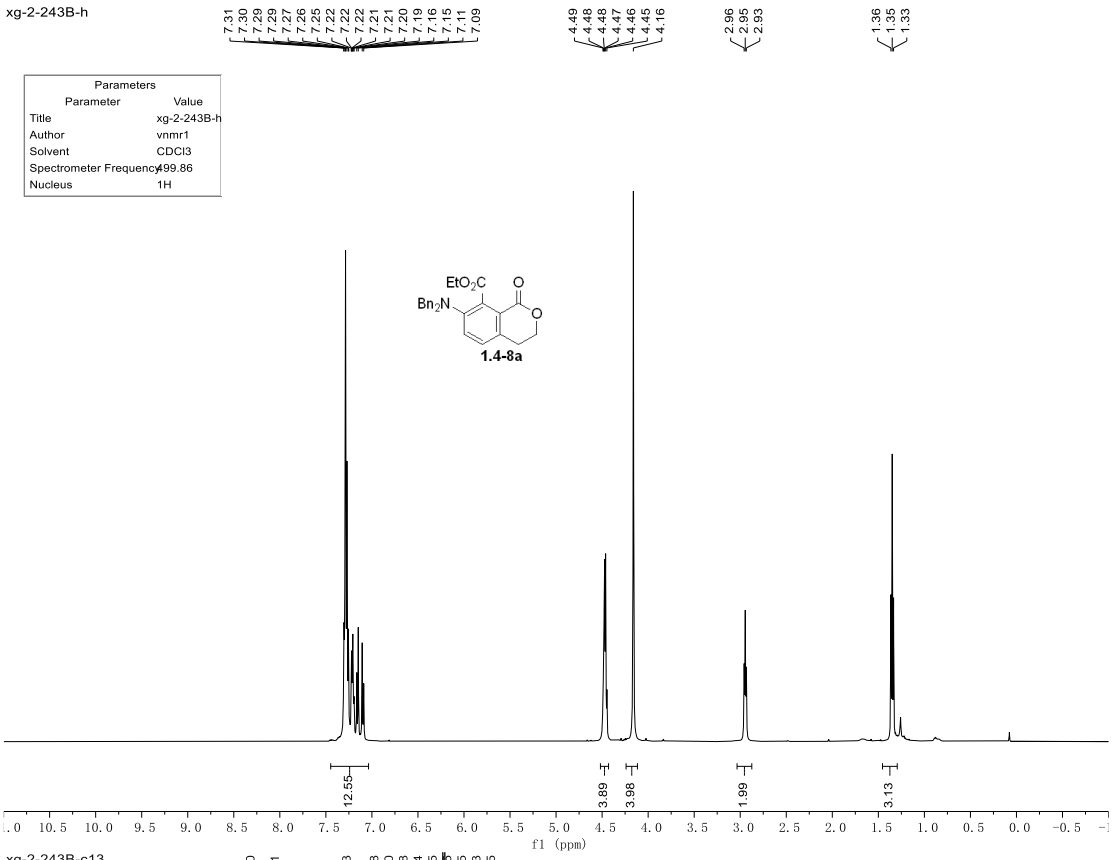
xg-2-243B-h
7.31
7.30
7.29
7.29
7.27
7.26
7.25
7.22
7.22
7.22
7.21
7.21
7.20
7.19
7.16
7.15
7.11
7.09
4.49
4.48
4.48
4.47
4.46
4.45
4.16
2.96
2.95
2.93
1.36
1.35
1.33
Parameters
Parameter Value
Title xg-2-243B-h
Author vnmr1
Solvent CDCl3
Spectrometer Frequency 499.86
Nucleus 1H
EtO2C
O
Bn2N
O
1.4-8a
12.55
3.89
3.98
1.99
3.13
f1 (ppm)

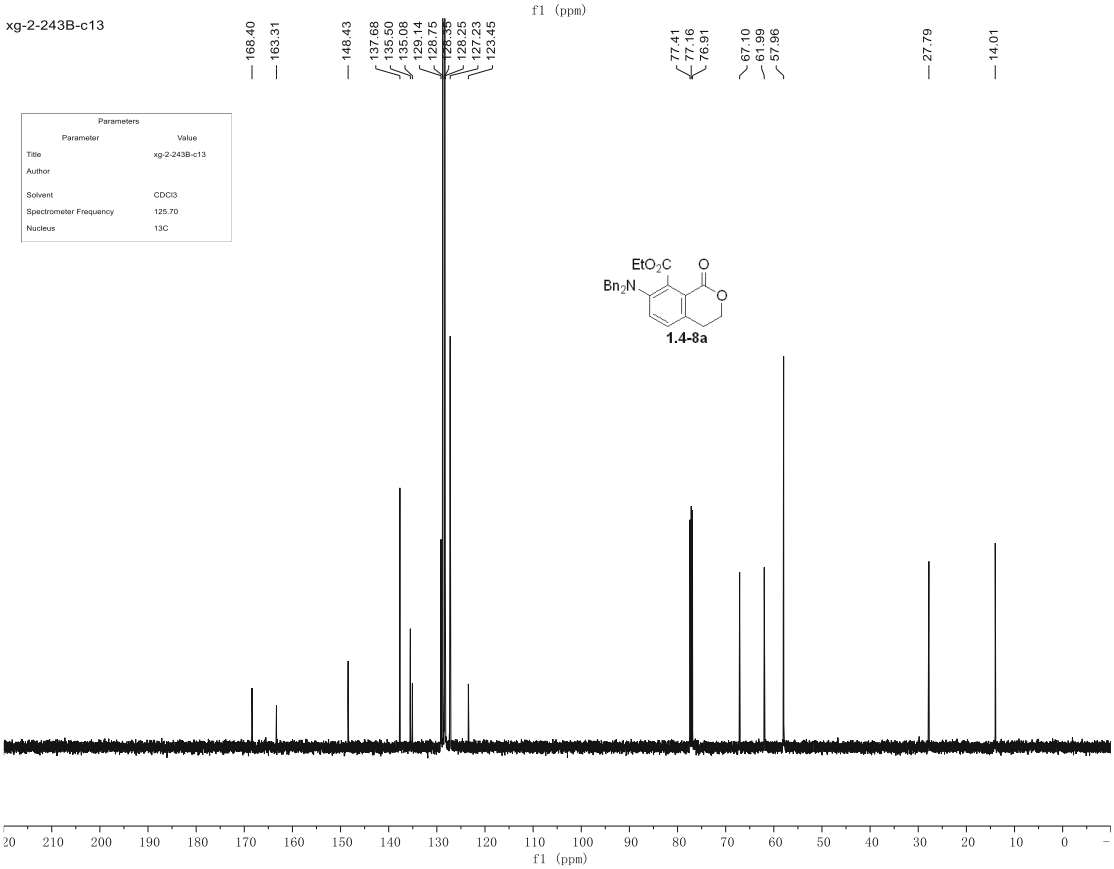
xg-2-243B-c13
168.40
163.31
148.43
137.68
135.50
135.08
129.14
128.75
128.35
128.25
127.23
123.45
77.41
77.16
76.91
67.10
61.99
57.96
27.79
14.01
Parameters
Parameter Value
Title xg-2-243B-c13
Author
Solvent CDCl3
Spectrometer Frequency 125.70
Nucleus 13C
EtO2C
O
Bn2N
O
1.4-8a
f1 (ppm)

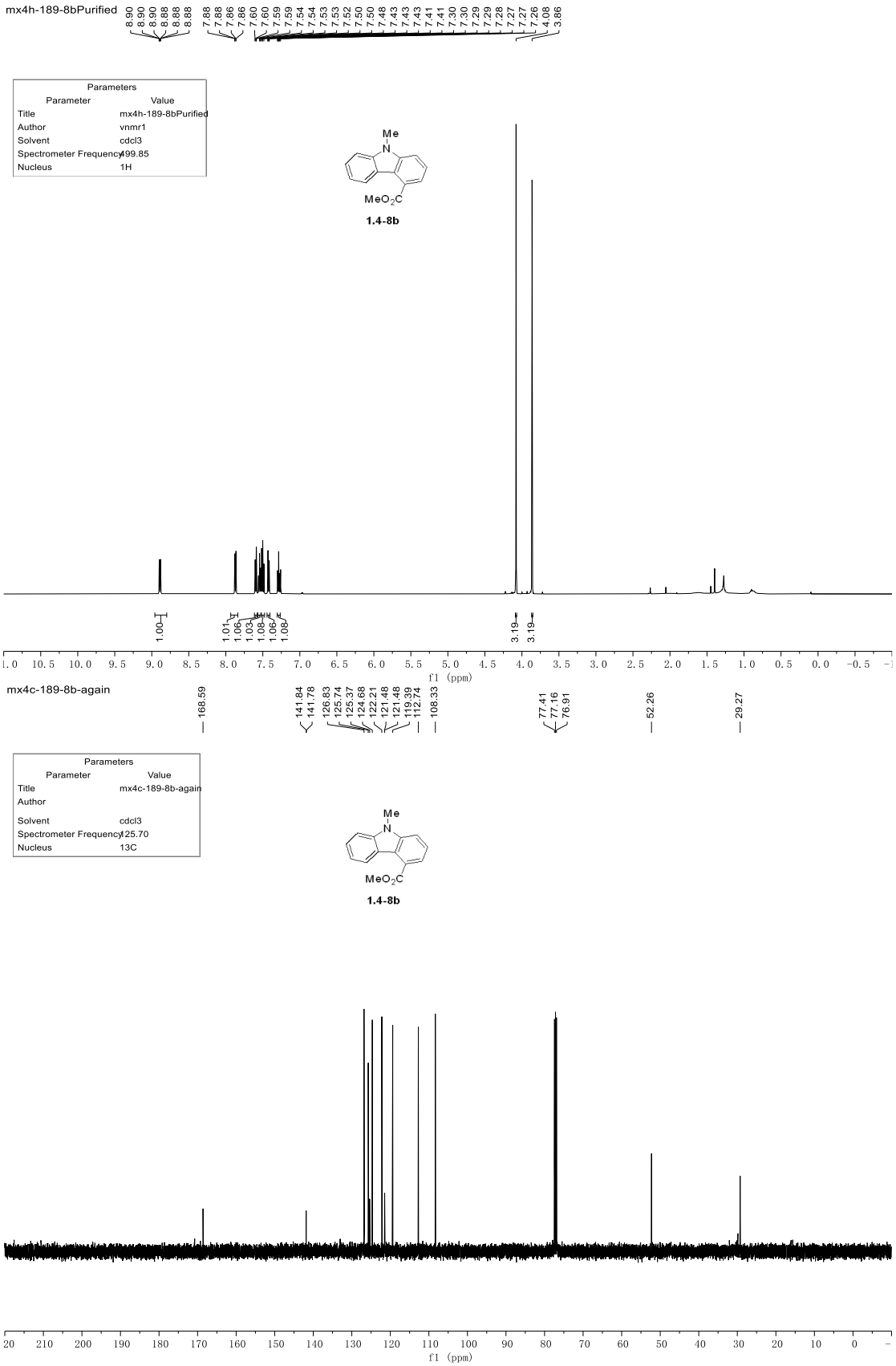
mx4h-189-8bPurified
8.90 8.90 8.90 8.88 8.88 8.88 7.88 7.88 7.86 7.86 7.60 7.60 7.59 7.59 7.54 7.54 7.53 7.53 7.52 7.50 7.50 7.48 7.43 7.43 7.41 7.41 7.30 7.29 7.29 7.28 7.27 7.27 7.26 4.08 3.86
Parameters
Parameter Value
Title mx4h-189-8bPurified
Author vnmr1
Solvent cdcl3
Spectrometer Frequency 499.85
Nucleus 1H
Me
N
MeO2C
1.4-8b
1.00 1.01 1.06 1.03 1.08 1.06 1.08 3.19 3.19
f1 (ppm)
mx4c-189-8b-again
168.59 141.84 141.78 126.83 125.74 125.37 124.68 122.21 121.48 121.48 119.39 112.74 108.33 77.41 77.16 76.91 52.26 29.27
Parameters
Parameter Value
Title mx4c-189-8b-again
Author
Solvent cdcl3
Spectrometer Frequency 125.70
Nucleus 13C
Me
N
MeO2C
1.4-8b
f1 (ppm)

mx4h-189-8c

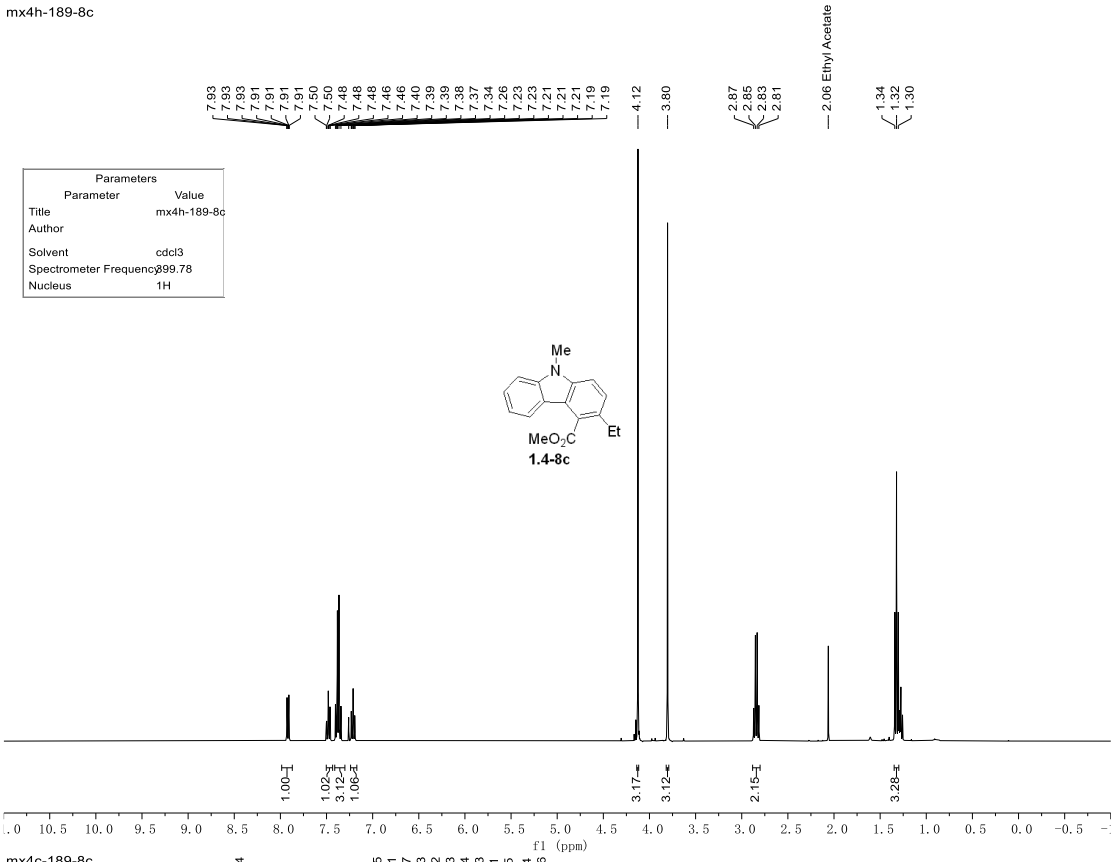

mx4c-189-8c

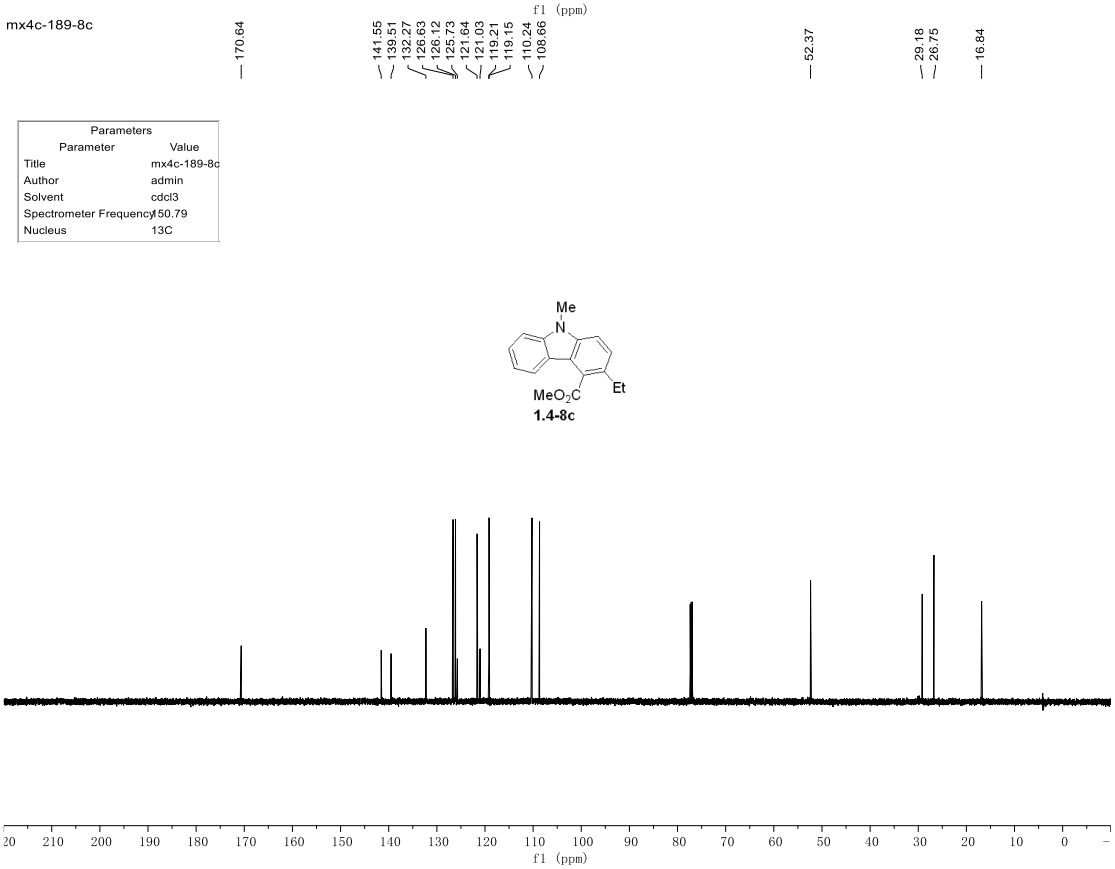

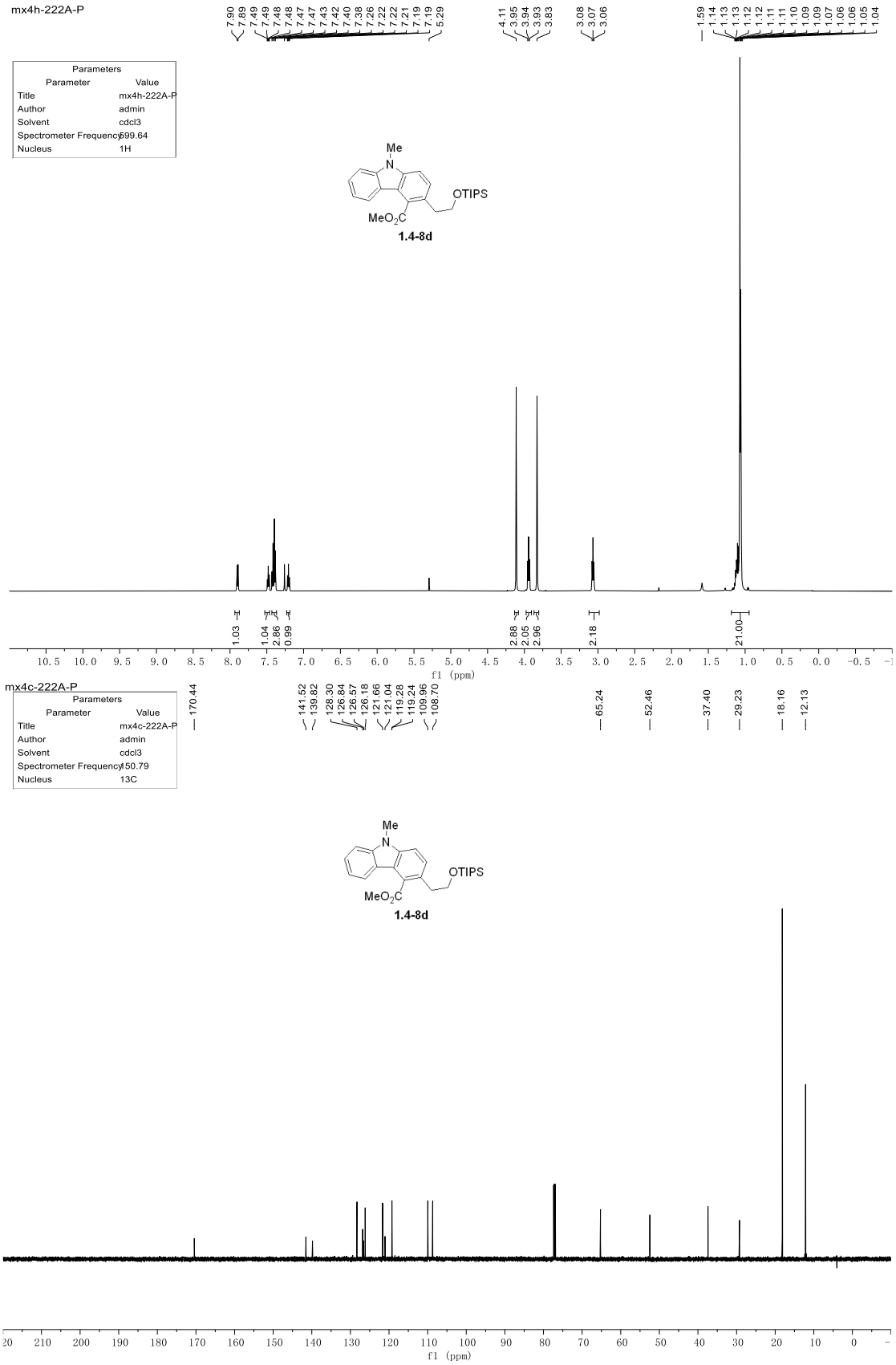
mx4h-222A-P
Parameters
Parameter Value
Title mx4h-222A-P
Author admin
Solvent cdcl3
Spectrometer Frequency 599.64
Nucleus 1H
Me
N
OTIPS
MeO2C
1.4-8d
f1 (ppm)
mx4c-222A-P
Parameters
Parameter Value
Title mx4c-222A-P
Author admin
Solvent cdcl3
Spectrometer Frequency 150.79
Nucleus 13C
Me
N
OTIPS
MeO2C
1.4-8d
f1 (ppm)

NMR Spectra for Compounds in Chapter 2

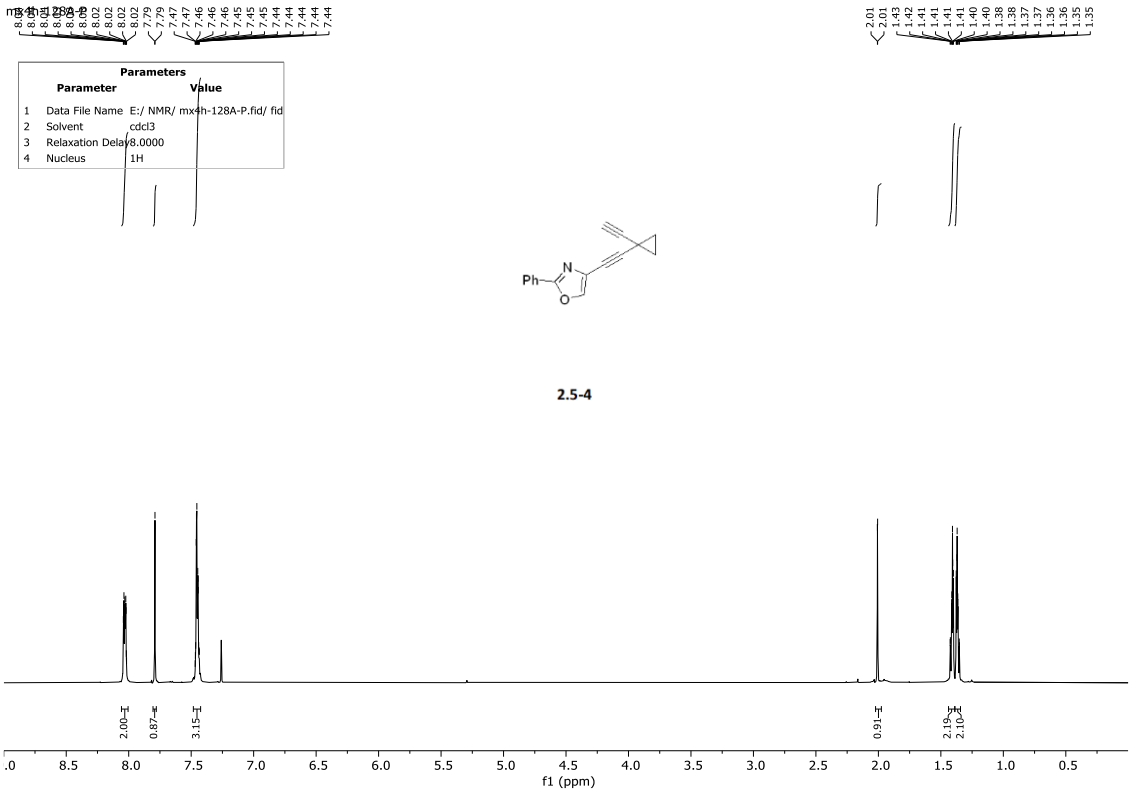

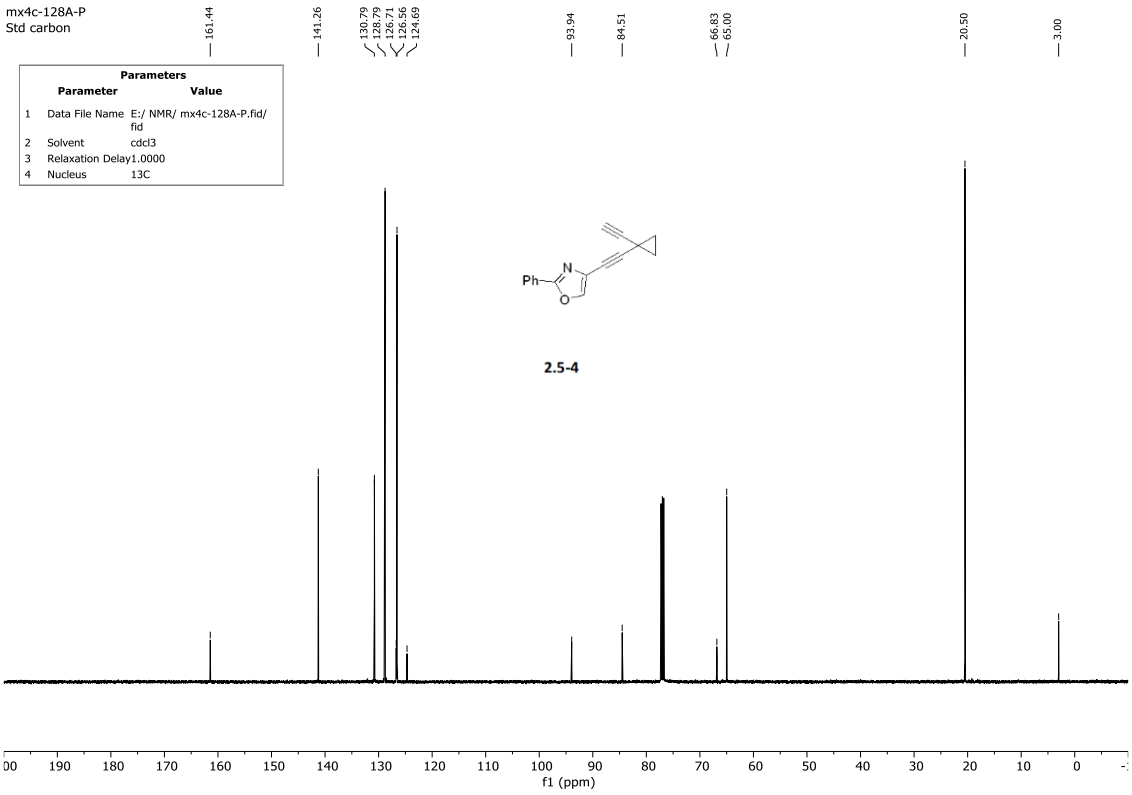

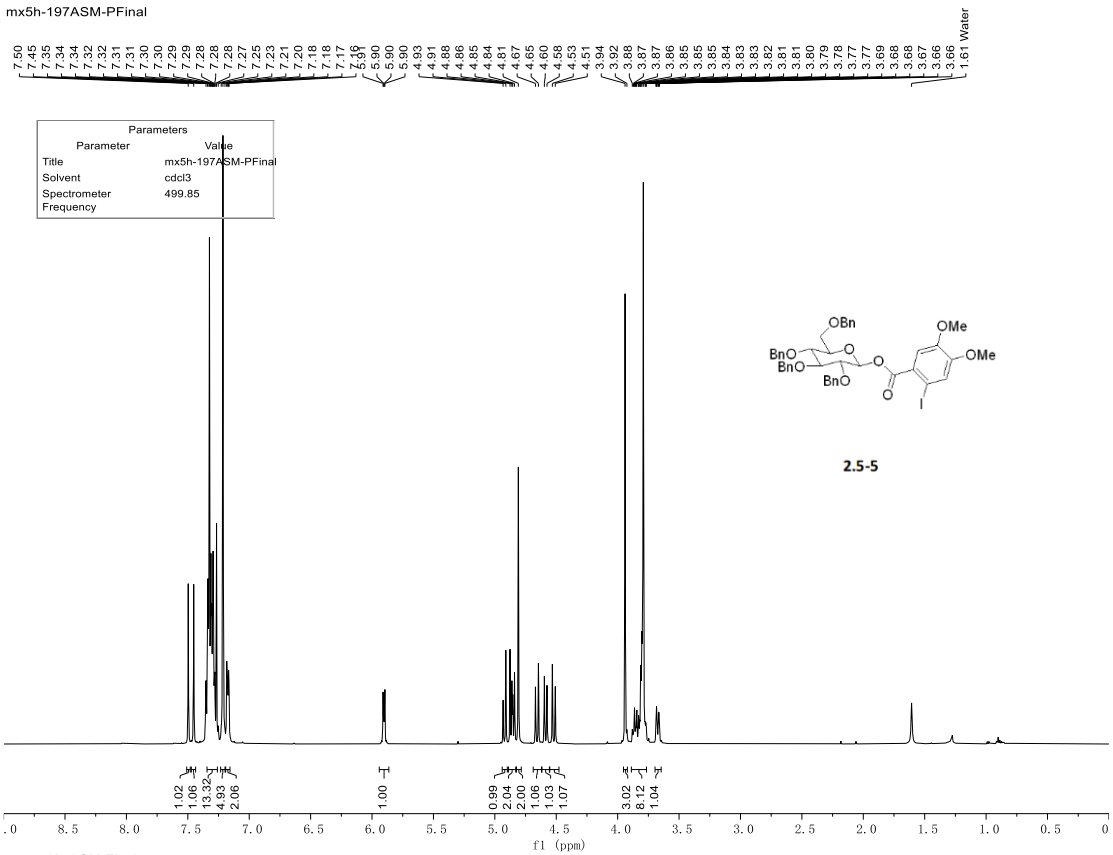
mx5h-197ASM-PFinal
Parameters
Parameter Value
Title mx5h-197ASM-PFinal
Solvent cdcl3
Spectrometer Frequency 499.85
OBn
OMe
OMe
BnO
BnO
BnO
O
O
I
2.5-5
f1 (ppm)

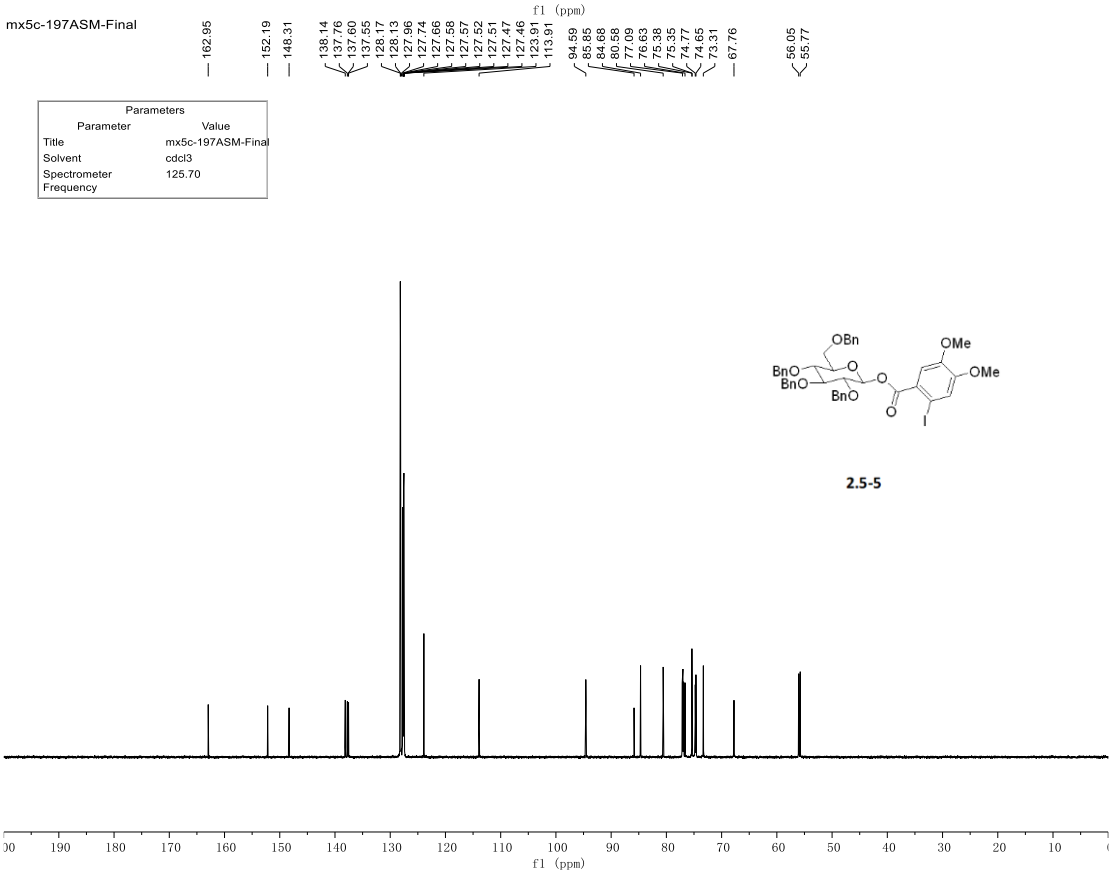
mx5c-197ASM-Final
Parameters
Parameter Value
Title mx5c-197ASM-Final
Solvent cdcl3
Spectrometer Frequency 125.70
OBn
OMe
OMe
BnO
BnO
BnO
O
O
I
2.5-5
f1 (ppm)

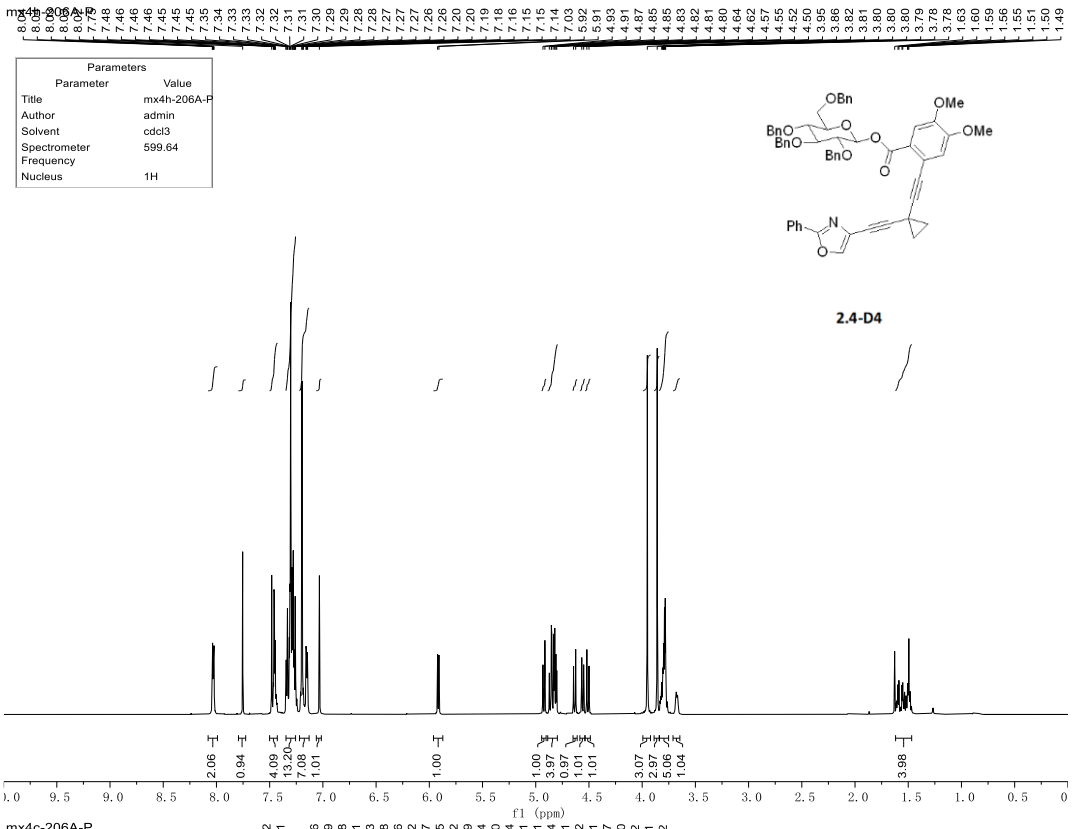
mx4h-206A-P
Parameters
Parameter Value
Title mx4h-206A-P
Author admin
Solvent cdcl3
Spectrometer Frequency 599.64
Nucleus 1H
OBn
BnO
BnO
BnO
O
O
OMe
OMe
Ph
N
O
2.4-D4
2.06
0.94
4.09
13.20
7.08
1.01
1.00
1.00
3.97
0.97
1.01
1.01
3.07
2.97
5.06
1.04
3.98
f1 (ppm)

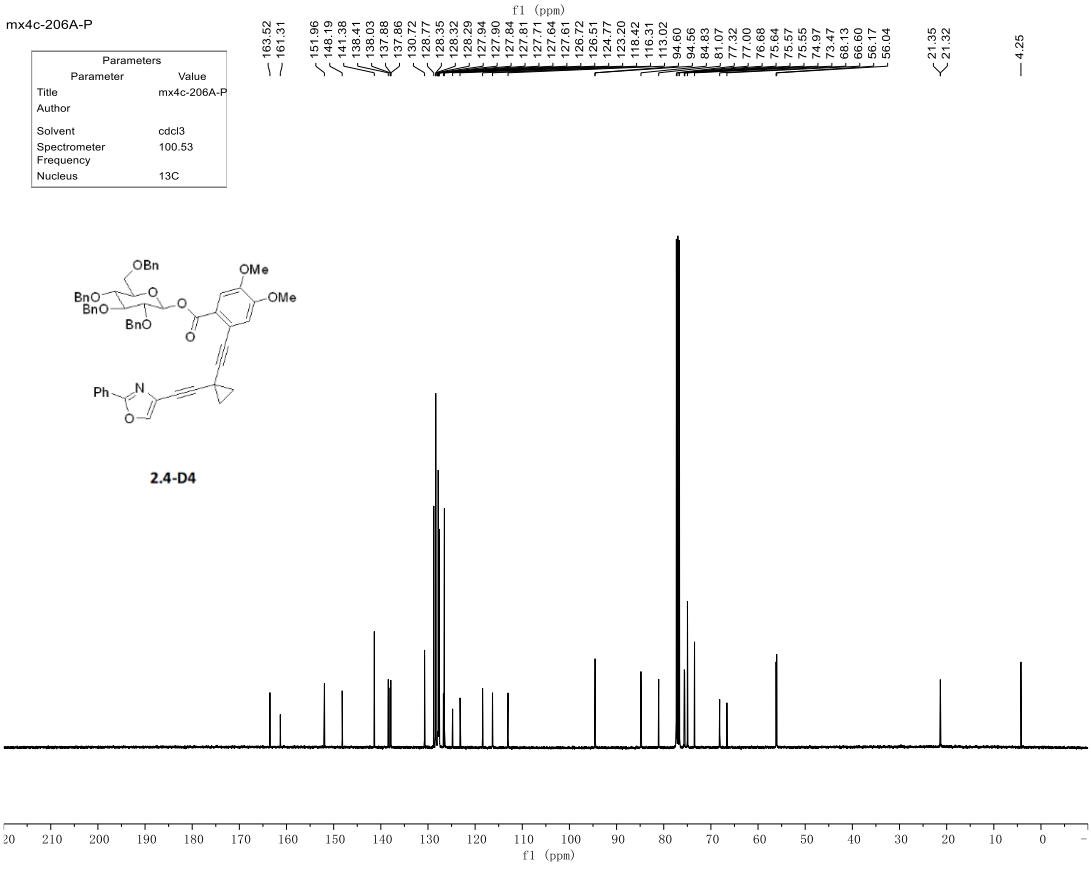
mx4c-206A-P
Parameters
Parameter Value
Title mx4c-206A-P
Author
Solvent cdcl3
Spectrometer Frequency 100.53
Nucleus 13C
163.52
161.31
151.96
148.19
141.38
138.41
138.03
137.88
137.66
130.72
128.77
128.35
128.32
128.29
127.94
127.90
127.81
127.71
127.64
127.61
126.72
126.51
124.77
123.20
118.42
116.31
113.02
94.60
94.56
84.83
81.07
77.32
77.00
76.68
75.64
75.57
75.55
74.97
73.47
68.13
66.60
56.17
56.04
21.35
21.32
4.25
OBn
BnO
BnO
BnO
O
O
OMe
OMe
Ph
N
O
2.4-D4
f1 (ppm)

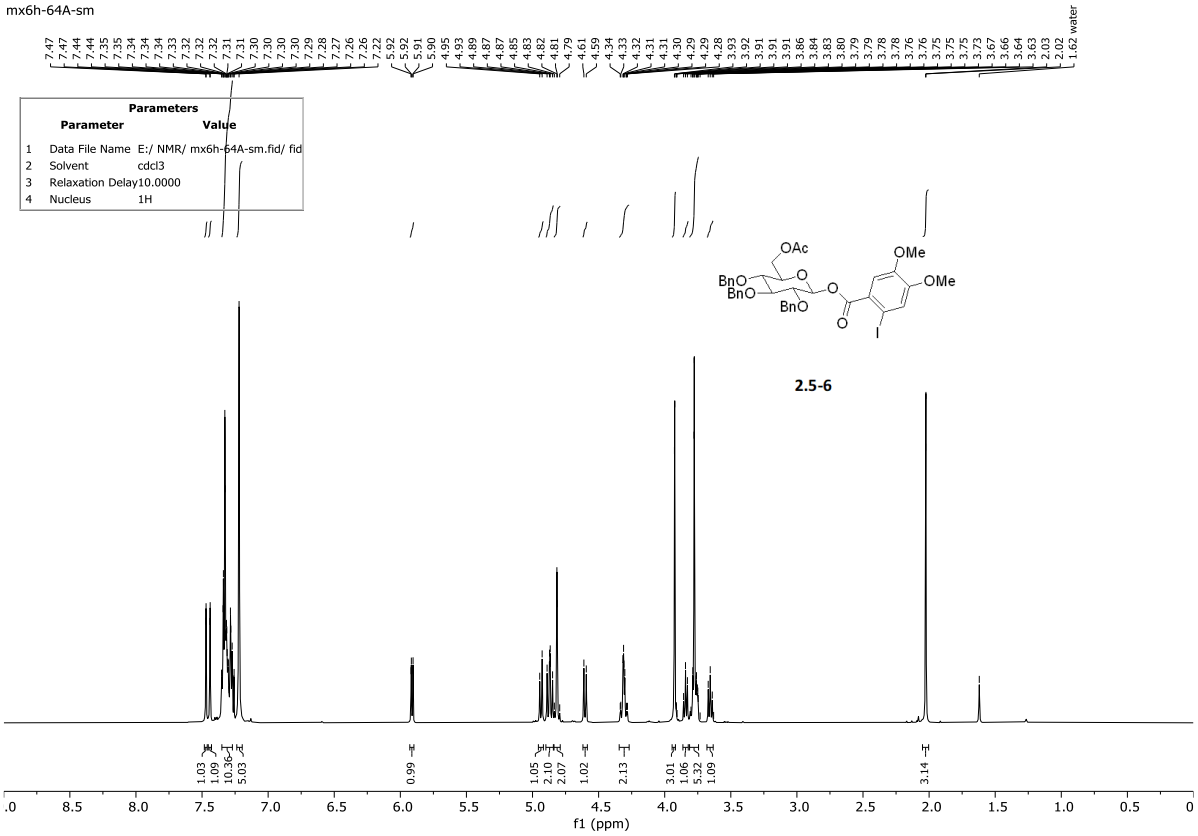
mx6h-64A-sm
Parameters
Parameter Value
1 Data File Name E:/ NMR/ mx6h-64A-sm.fid/ fid
2 Solvent cdcl3
3 Relaxation Delay 10.0000
4 Nucleus 1H
OAc
OMe
OMe
BnO
BnO
BnO
O
I
2.5-6
f1 (ppm)

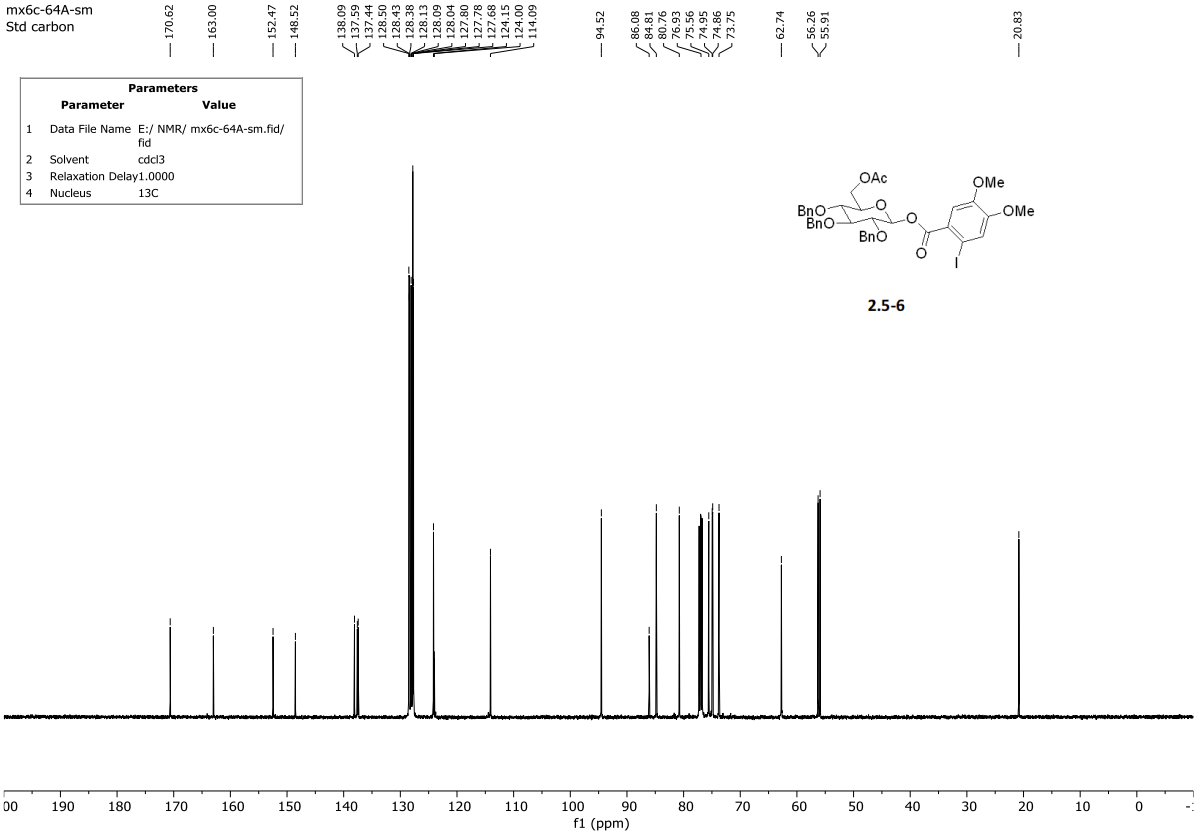
mx6c-64A-sm
Std carbon
Parameters
Parameter Value
1 Data File Name E:/ NMR/ mx6c-64A-sm.fid/ fid
2 Solvent cdcl3
3 Relaxation Delay 1.0000
4 Nucleus 13C
OAc
OMe
OMe
BnO
BnO
BnO
O
I
2.5-6
f1 (ppm)

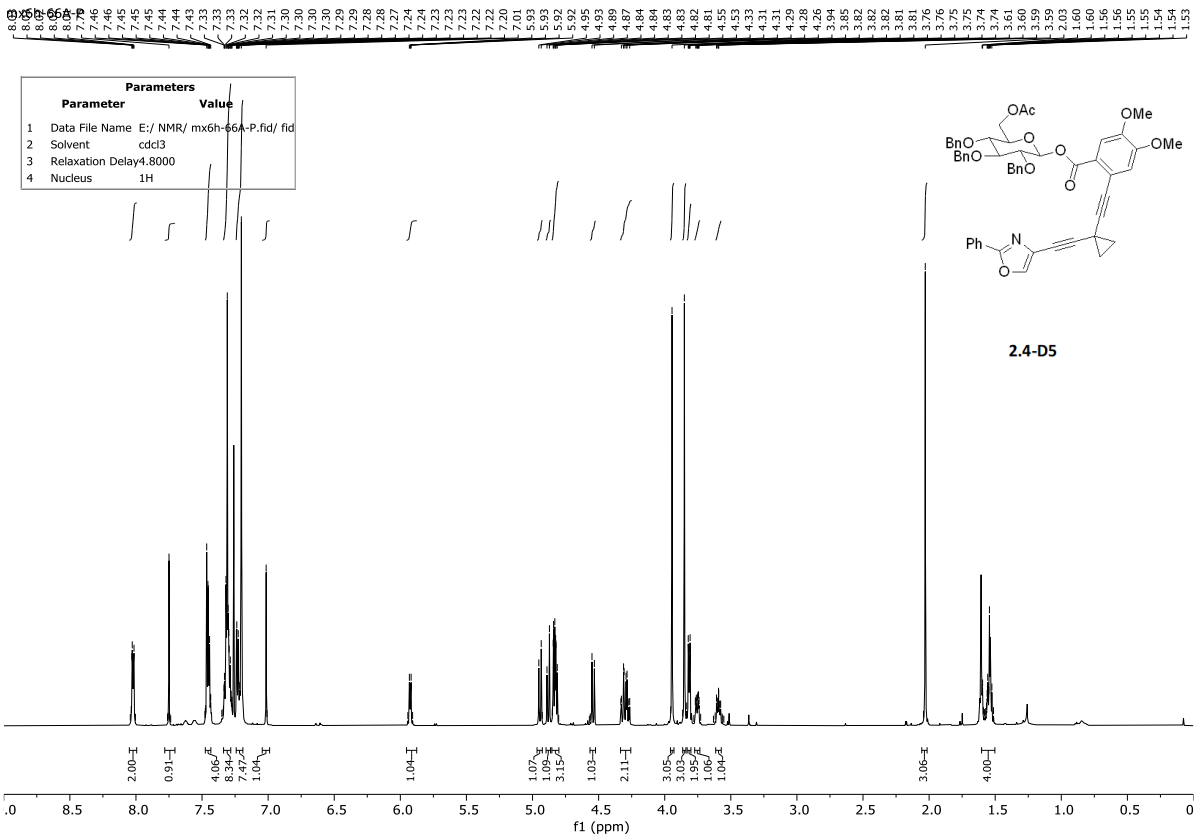
mx6h-66A-P
Parameters
Parameter Value
1 Data File Name E:/ NMR/ mx6h-66A-P.fid/ fid
2 Solvent cdcl3
3 Relaxation Delay 4.8000
4 Nucleus 1H
2.4-D5
f1 (ppm)

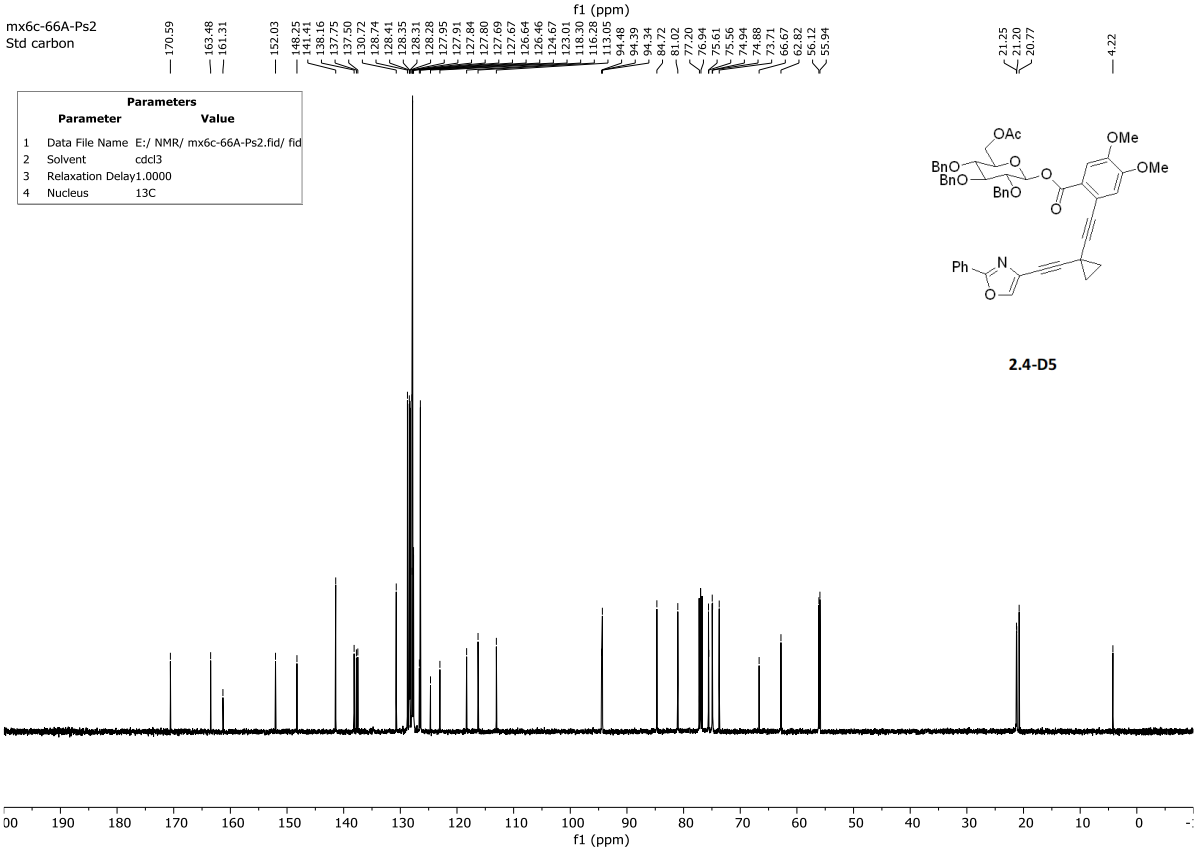
mx6c-66A-Ps2
Std carbon
Parameters
Parameter Value
1 Data File Name E:/ NMR/ mx6c-66A-Ps2.fid/ fid
2 Solvent cdcl3
3 Relaxation Delay 1.0000
4 Nucleus 13C
2.4-D5
f1 (ppm)

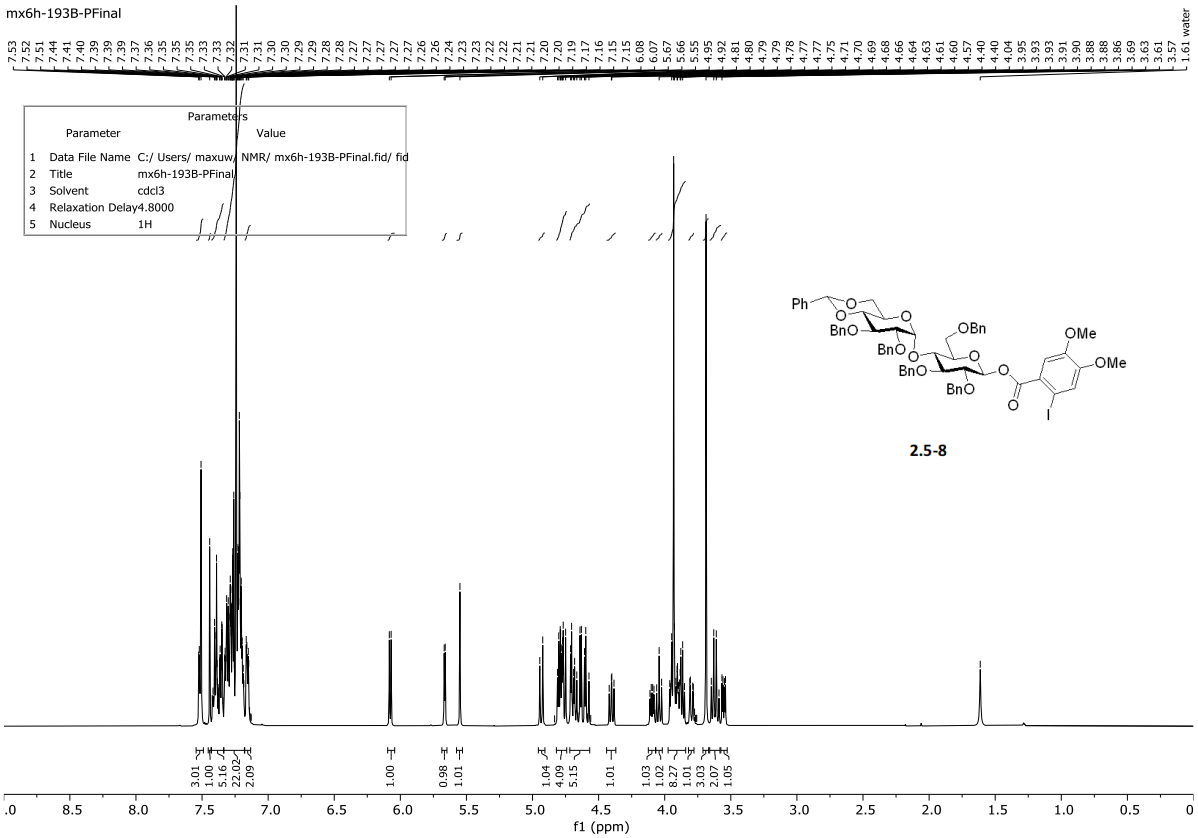
mx6h-193B-PFinal
Parameters
Parameter Value
1 Data File Name C:/ Users/ maxuw/ NMR/ mx6h-193B-PFinal.fid/ fid
2 Title mx6h-193B-PFinal
3 Solvent cdcl3
4 Relaxation Delay 4.8000
5 Nucleus 1H
Ph
BnO
OBn
OMe
OMe
I
2.5-8
f1 (ppm)

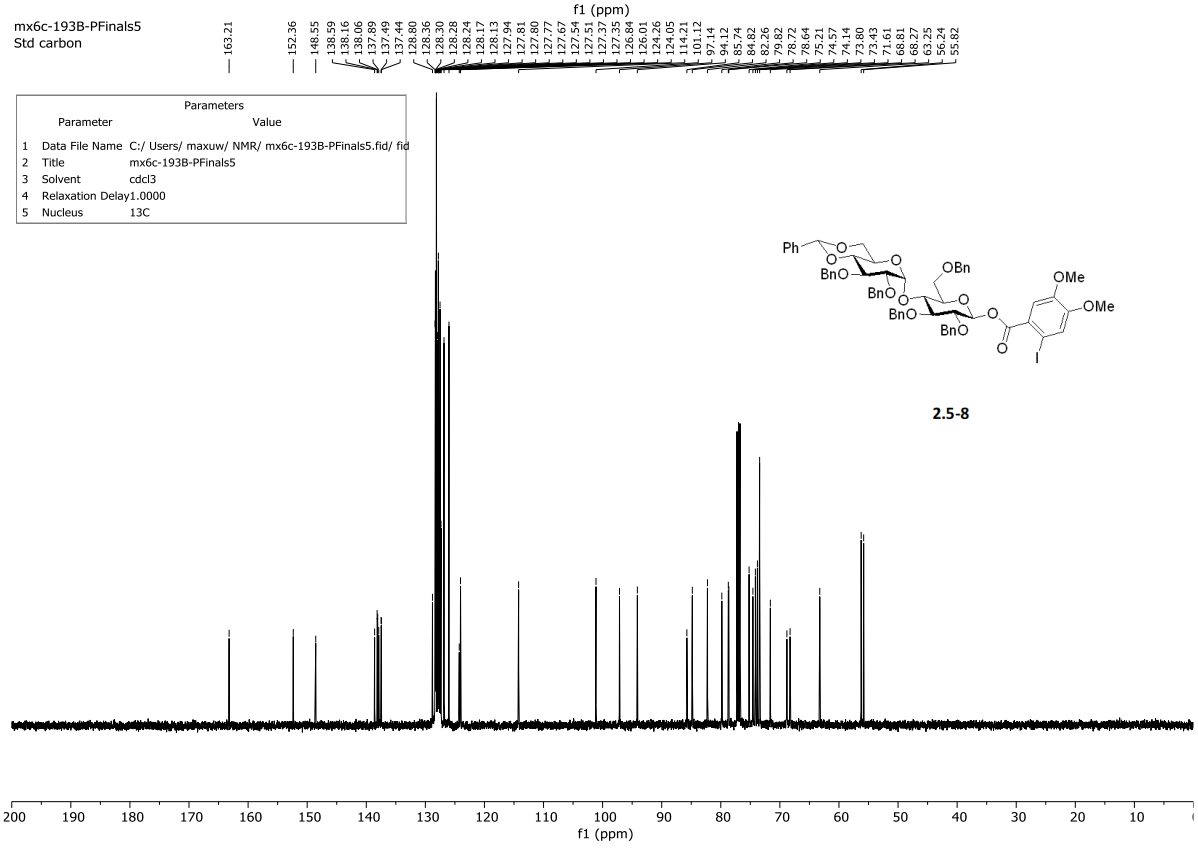
mx6c-193B-PFinals5
Std carbon
Parameters
Parameter Value
1 Data File Name C:/ Users/ maxuw/ NMR/ mx6c-193B-PFinals5.fid/ fid
2 Title mx6c-193B-PFinals5
3 Solvent cdcl3
4 Relaxation Delay 1.0000
5 Nucleus 13C
Ph
BnO
OBn
OMe
OMe
I
2.5-8
f1 (ppm)

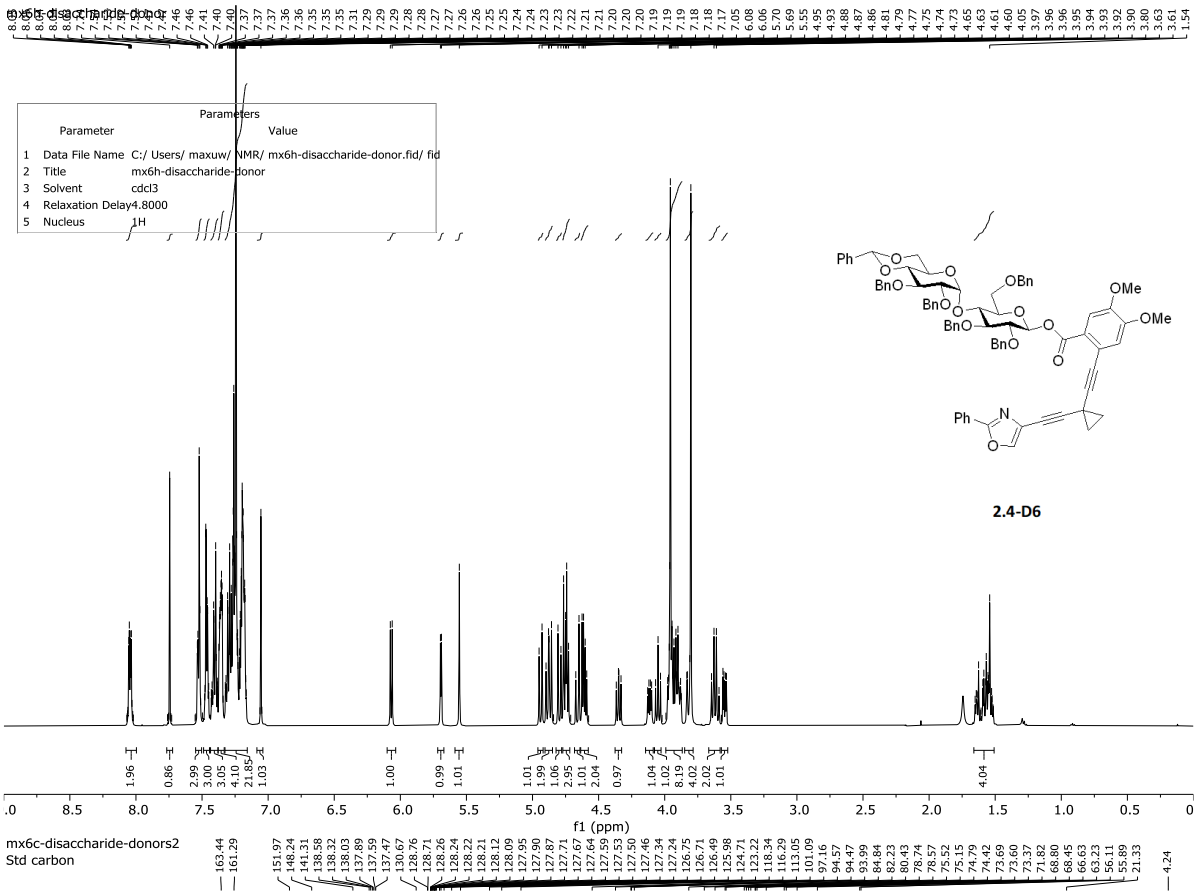
Parameters
Parameter Value
1 Data File Name C:/ Users/ maxuw/ NMR/ mx6h-disaccharide-donor.fid/ fid
2 Title mx6h-disaccharide-donor
3 Solvent cdcl3
4 Relaxation Delay 4.8000
5 Nucleus 1H
2.4-D6
f1 (ppm)

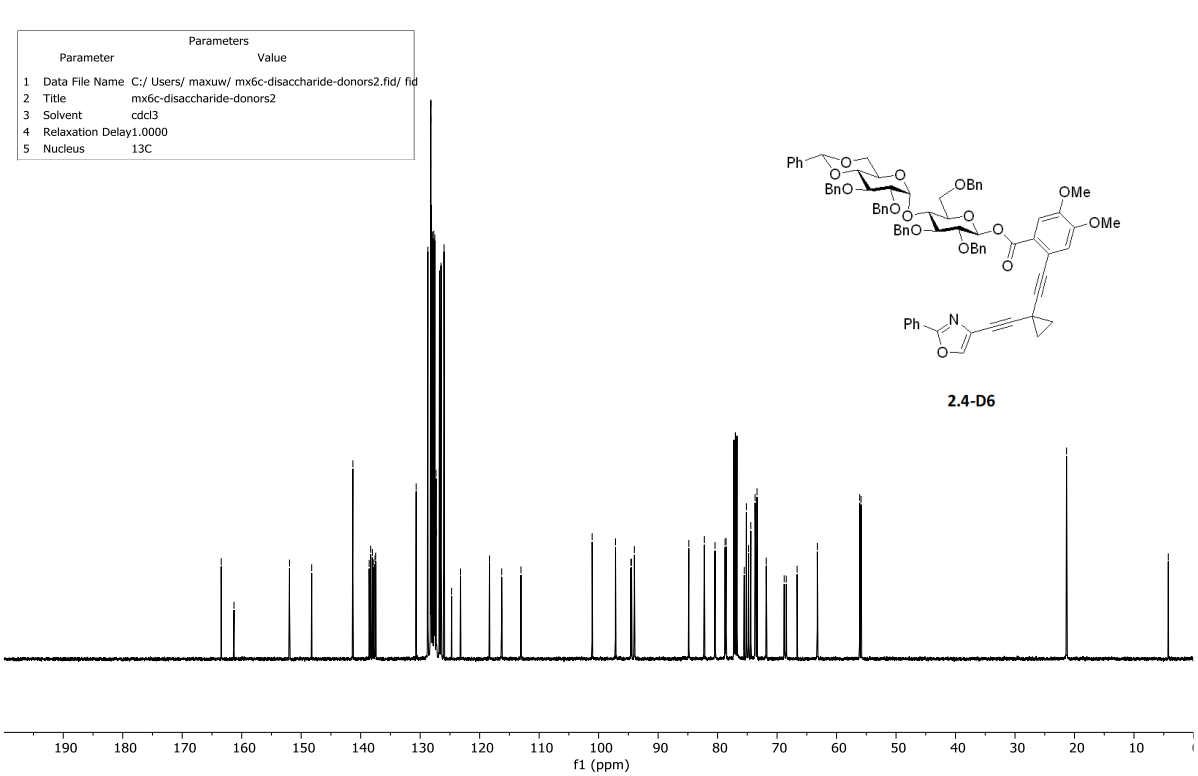
mx6c-disaccharide-donors2
Std carbon
Parameters
Parameter Value
1 Data File Name C:/ Users/ maxuw/ mx6c-disaccharide-donors2.fid/ fid
2 Title mx6c-disaccharide-donors2
3 Solvent cdcl3
4 Relaxation Delay 1.0000
5 Nucleus 13C
2.4-D6
f1 (ppm)

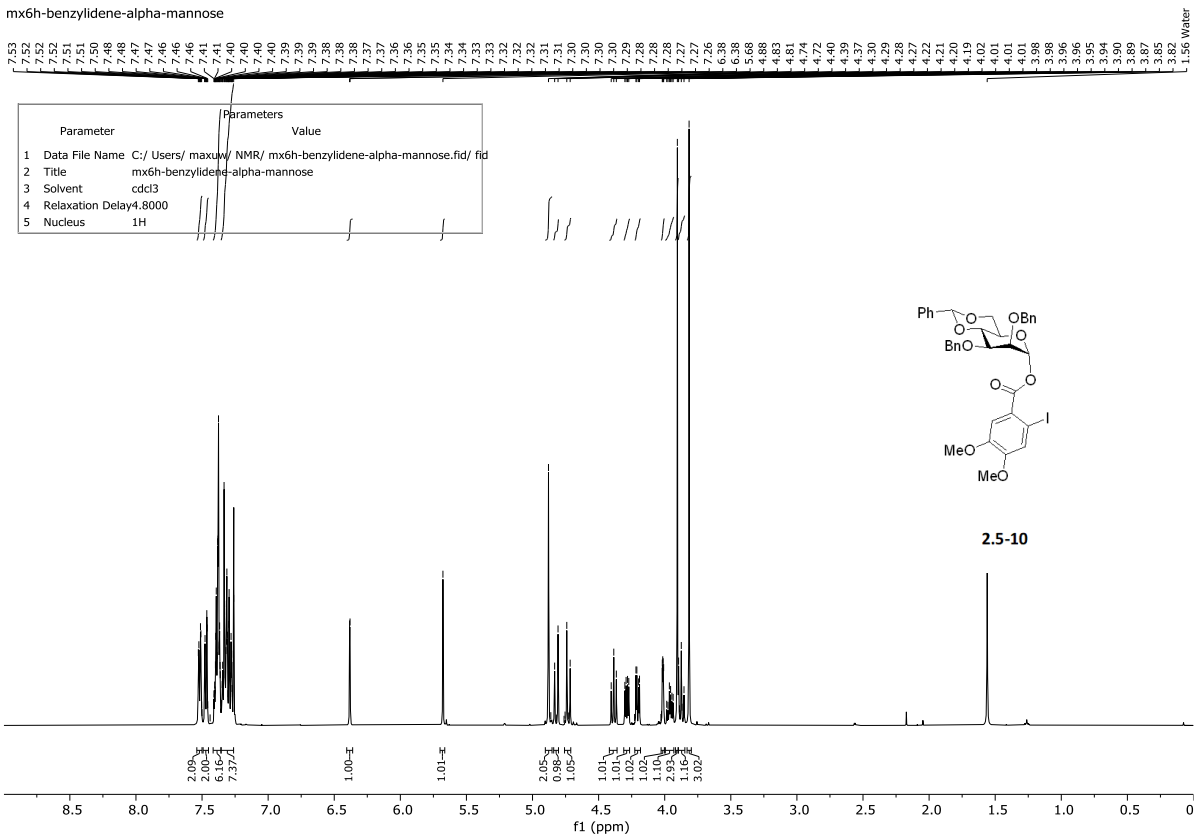
mx6h-benzylidene-alpha-mannose
Parameters
Parameter Value
1 Data File Name C:/ Users/ maxuw/ NMR/ mx6h-benzylidene-alpha-mannose.fid/ fid
2 Title mx6h-benzylidene-alpha-mannose
3 Solvent cdcl3
4 Relaxation Delay 4.8000
5 Nucleus 1H
Ph
OBn
BnO
O
I
MeO
MeO
2.5-10
f1 (ppm)

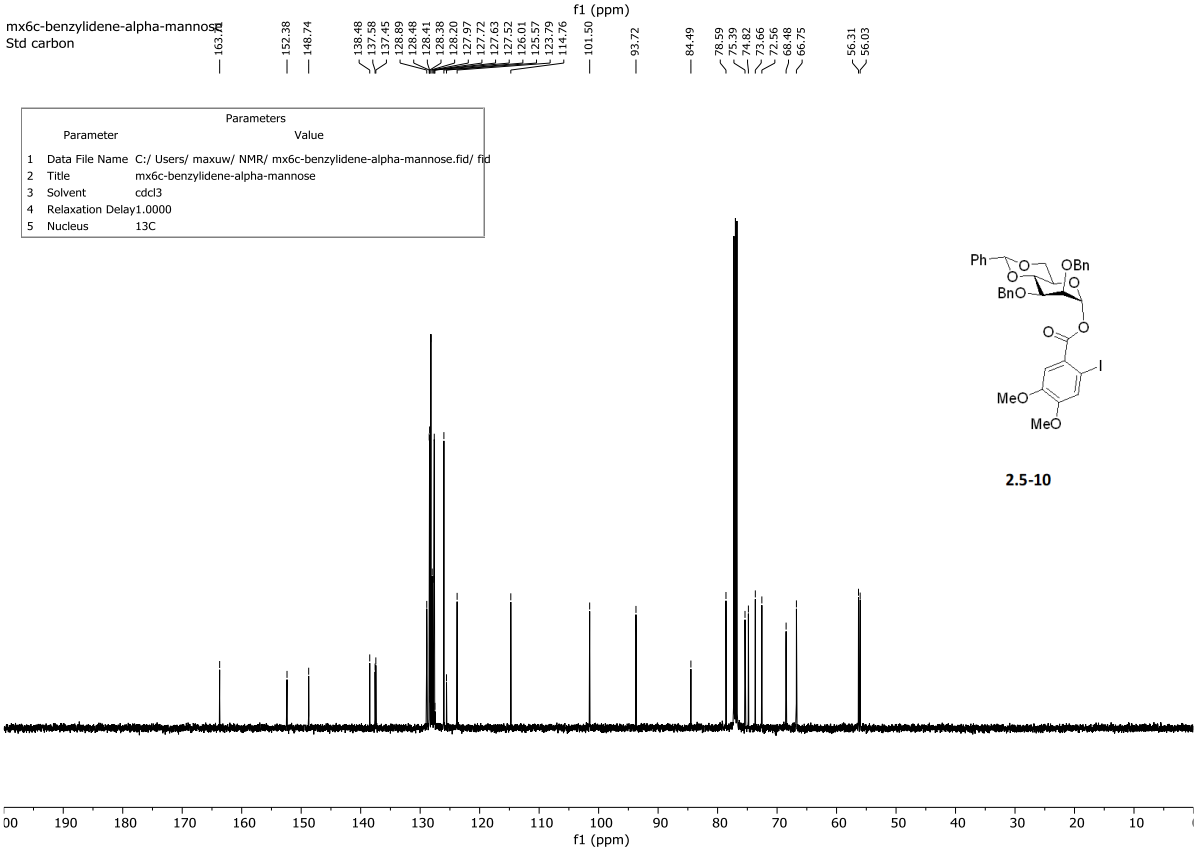
mx6c-benzylidene-alpha-mannose
Std carbon
Parameters
Parameter Value
1 Data File Name C:/ Users/ maxuw/ NMR/ mx6c-benzylidene-alpha-mannose.fid/ fid
2 Title mx6c-benzylidene-alpha-mannose
3 Solvent cdcl3
4 Relaxation Delay 1.0000
5 Nucleus 13C
Ph
OBn
BnO
O
I
MeO
MeO
2.5-10
f1 (ppm)

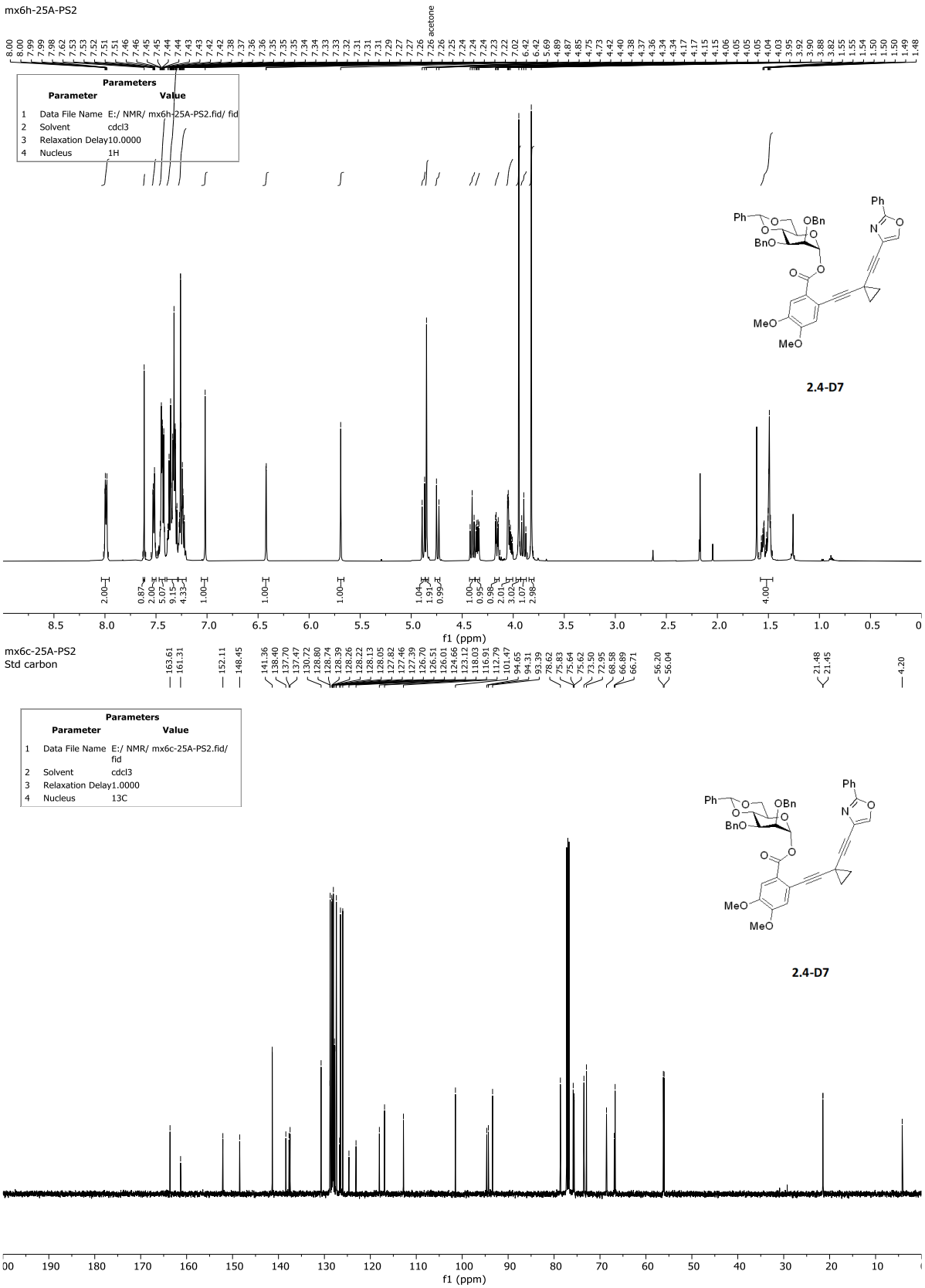
mx6h-25A-PS2
Parameters
Parameter Value
1 Data File Name E:/ NMR/ mx6h-25A-PS2.fid/ fid
2 Solvent cdcl3
3 Relaxation Delay 10.0000
4 Nucleus 1H
acetone
2.4-D7
f1 (ppm)
mx6c-25A-PS2
Std carbon
Parameters
Parameter Value
1 Data File Name E:/ NMR/ mx6c-25A-PS2.fid/ fid
2 Solvent cdcl3
3 Relaxation Delay 1.0000
4 Nucleus 13C
2.4-D7
f1 (ppm)

mx6h-55A-crystal

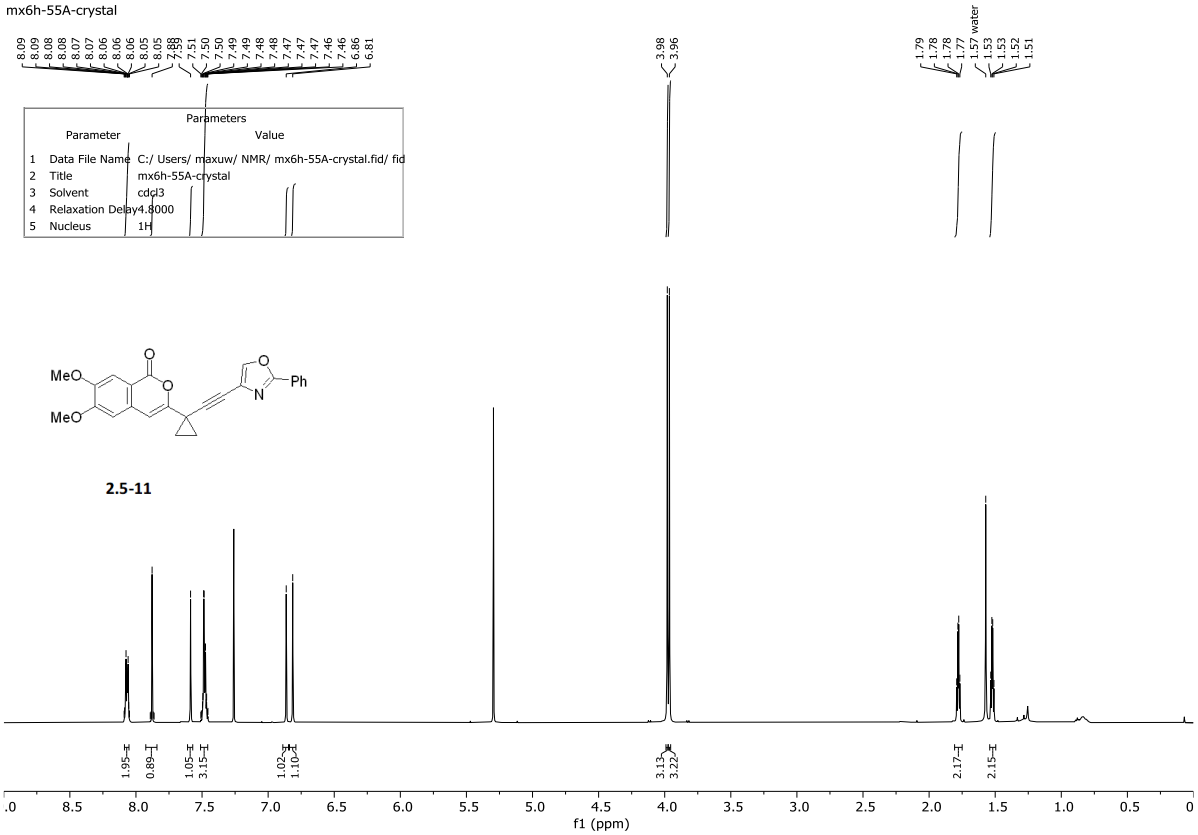

2.5-11

mx6c-55A-crystal-again
Std carbon

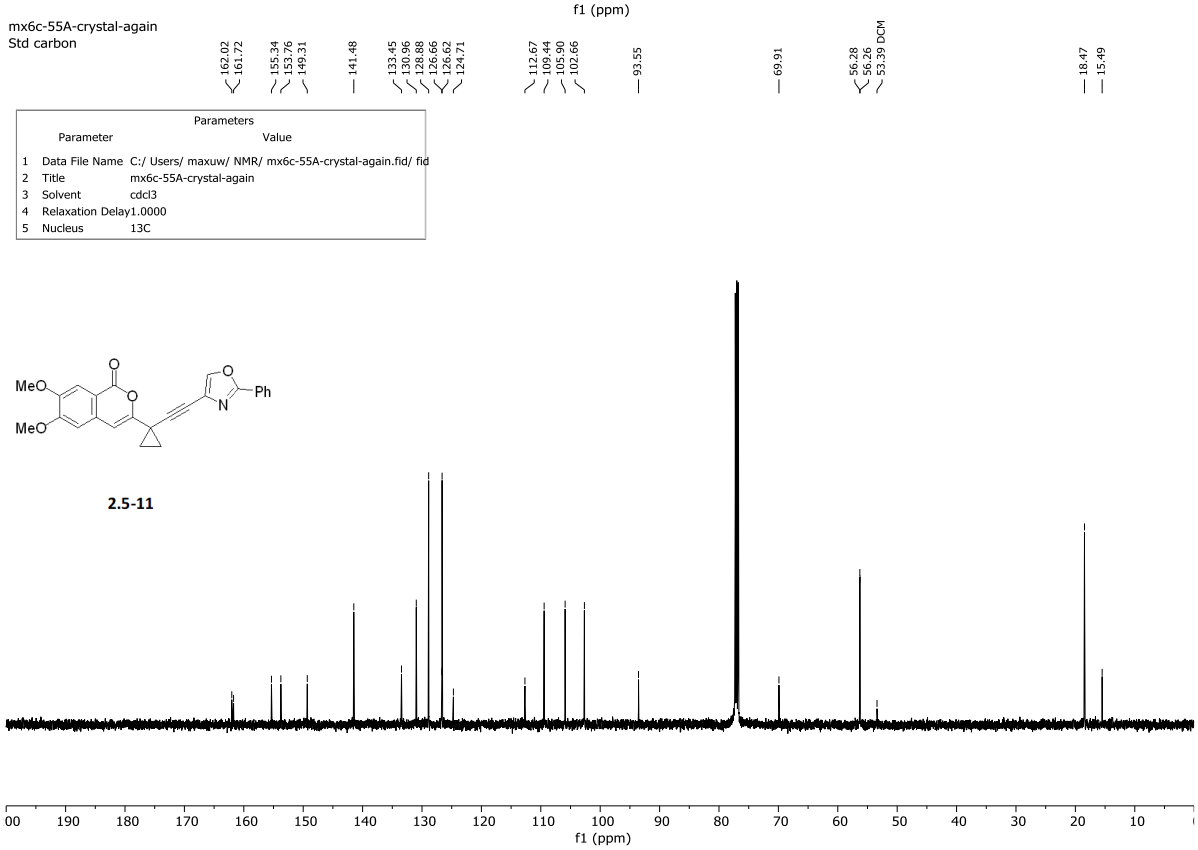

2.5-11

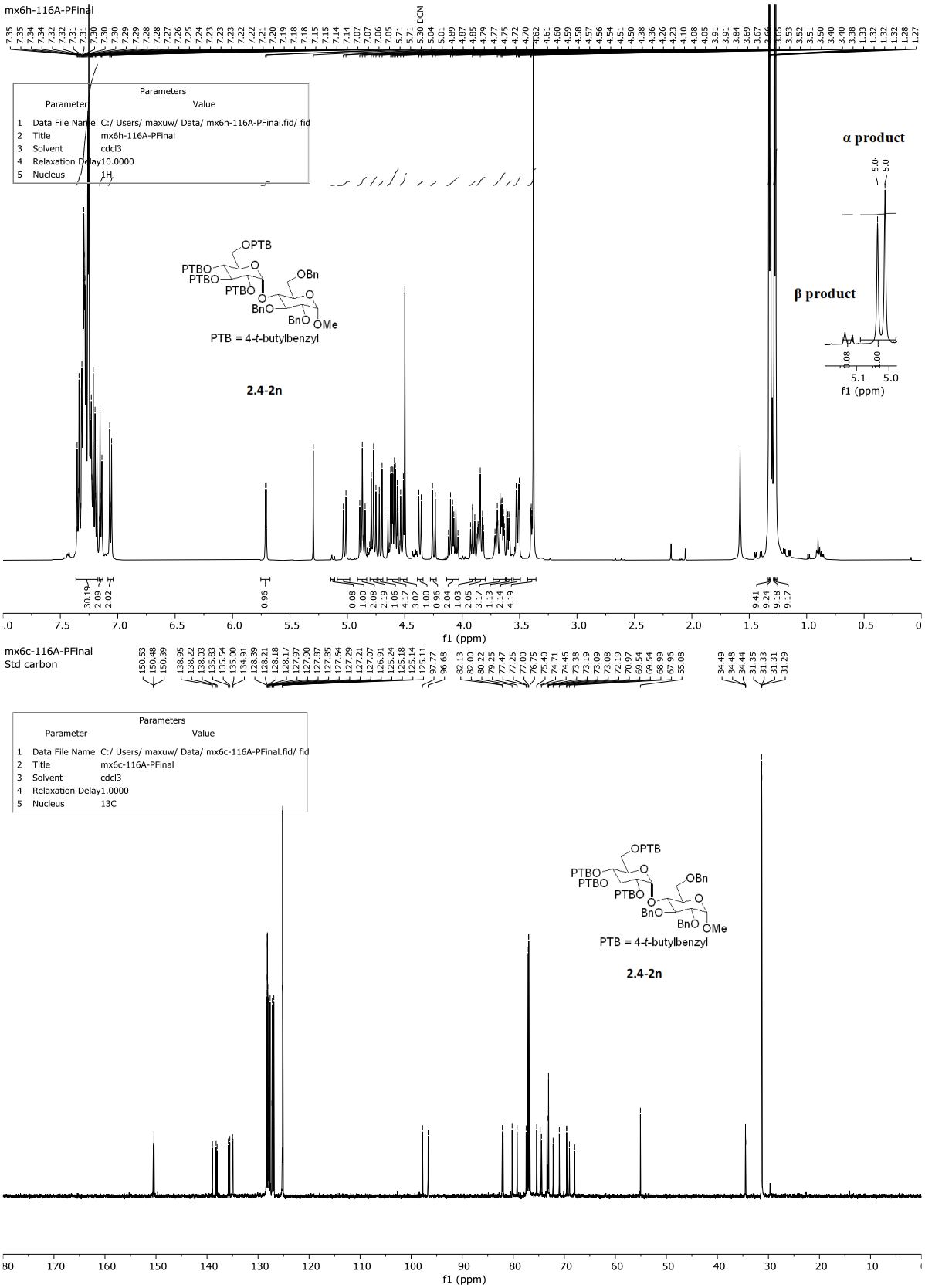
mx6h-116A-PFinal
Parameters
Parameter Value
1 Data File Name C:/ Users/ maxuw/ Data/ mx6h-116A-PFinal.fid/ fid
2 Title mx6h-116A-PFinal
3 Solvent cdcl3
4 Relaxation Delay 10.0000
5 Nucleus 1H
α product
β product
OPTB
PTBO
OBn
BnO
OMe
PTB = 4-t-butylbenzyl
2.4-2n
f1 (ppm)
mx6c-116A-PFinal
Std carbon
Parameters
Parameter Value
1 Data File Name C:/ Users/ maxuw/ Data/ mx6c-116A-PFinal.fid/ fid
2 Title mx6c-116A-PFinal
3 Solvent cdcl3
4 Relaxation Delay 1.0000
5 Nucleus 13C
PTB = 4-t-butylbenzyl
2.4-2n
f1 (ppm)

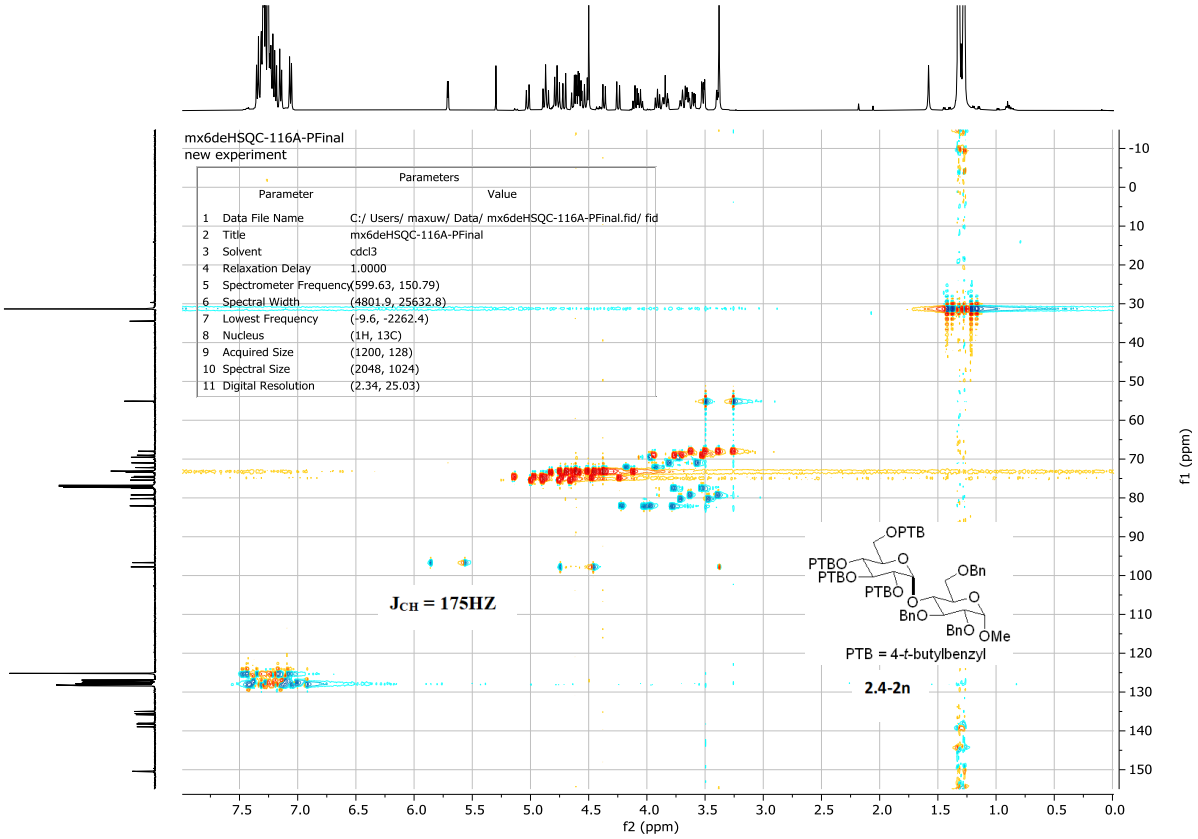
mx6deHSQC-116A-PFinal
new experiment
Parameters
Parameter Value
1 Data File Name C:/ Users/ maxuw/ Data/ mx6deHSQC-116A-PFinal.fid/ fid
2 Title mx6deHSQC-116A-PFinal
3 Solvent cdcl3
4 Relaxation Delay 1.0000
5 Spectrometer Frequency (599.63, 150.79)
6 Spectral Width (4801.9, 25632.8)
7 Lowest Frequency (-9.6, -2262.4)
8 Nucleus (1H, 13C)
9 Acquired Size (1200, 128)
10 Spectral Size (2048, 1024)
11 Digital Resolution (2.34, 25.03)
JCH = 175HZ
OPTB
PTBO
PTBO
PTBO
O
OBn
O
BnO
BnO
OMe
PTB = 4-t-butylbenzyl
2.4-2n
f2 (ppm)
f1 (ppm)

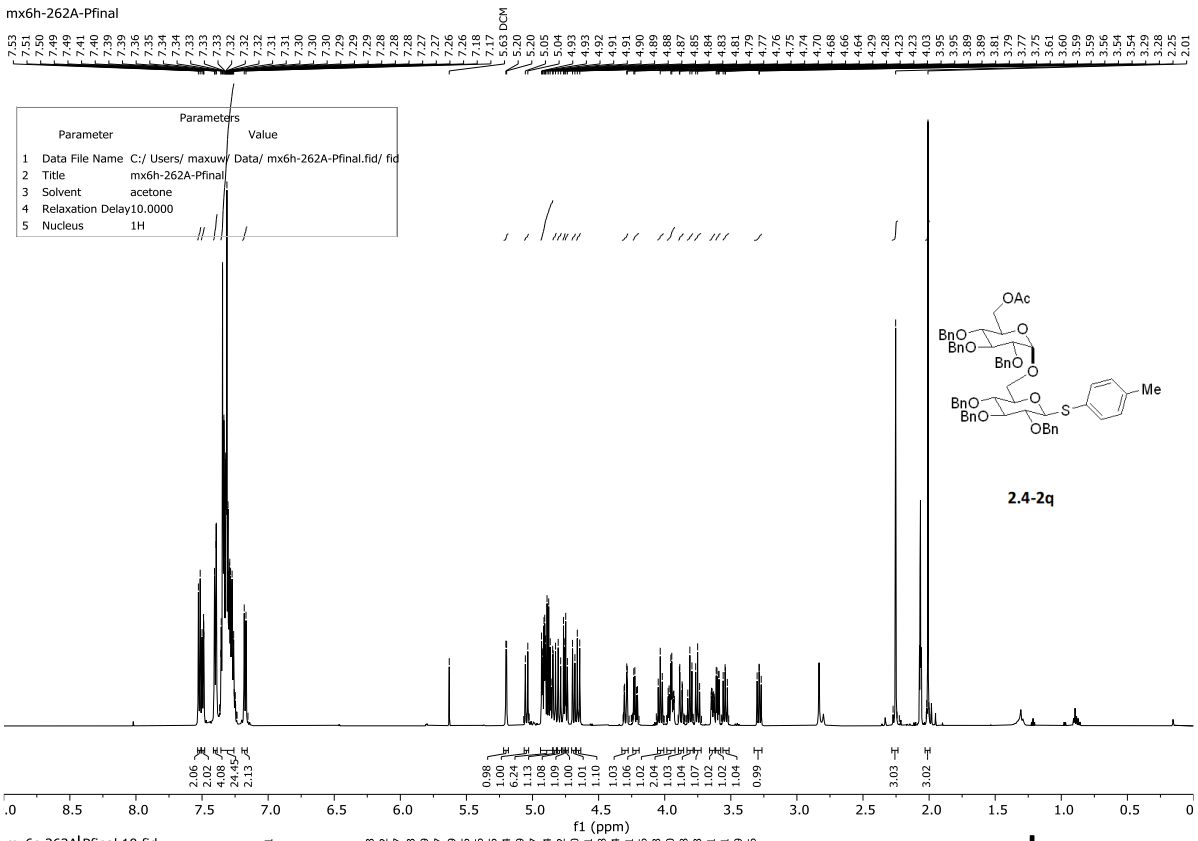
mx6h-262A-Pfinal
Parameters
Parameter Value
1 Data File Name C:/ Users/ maxuw/ Data/ mx6h-262A-Pfinal.fid/ fid
2 Title mx6h-262A-Pfinal
3 Solvent acetone
4 Relaxation Delay 10.0000
5 Nucleus 1H
OAc
BnO
BnO
BnO
O
O
BnO
BnO
O
S
Me
OBn
2.4-2q
f1 (ppm)

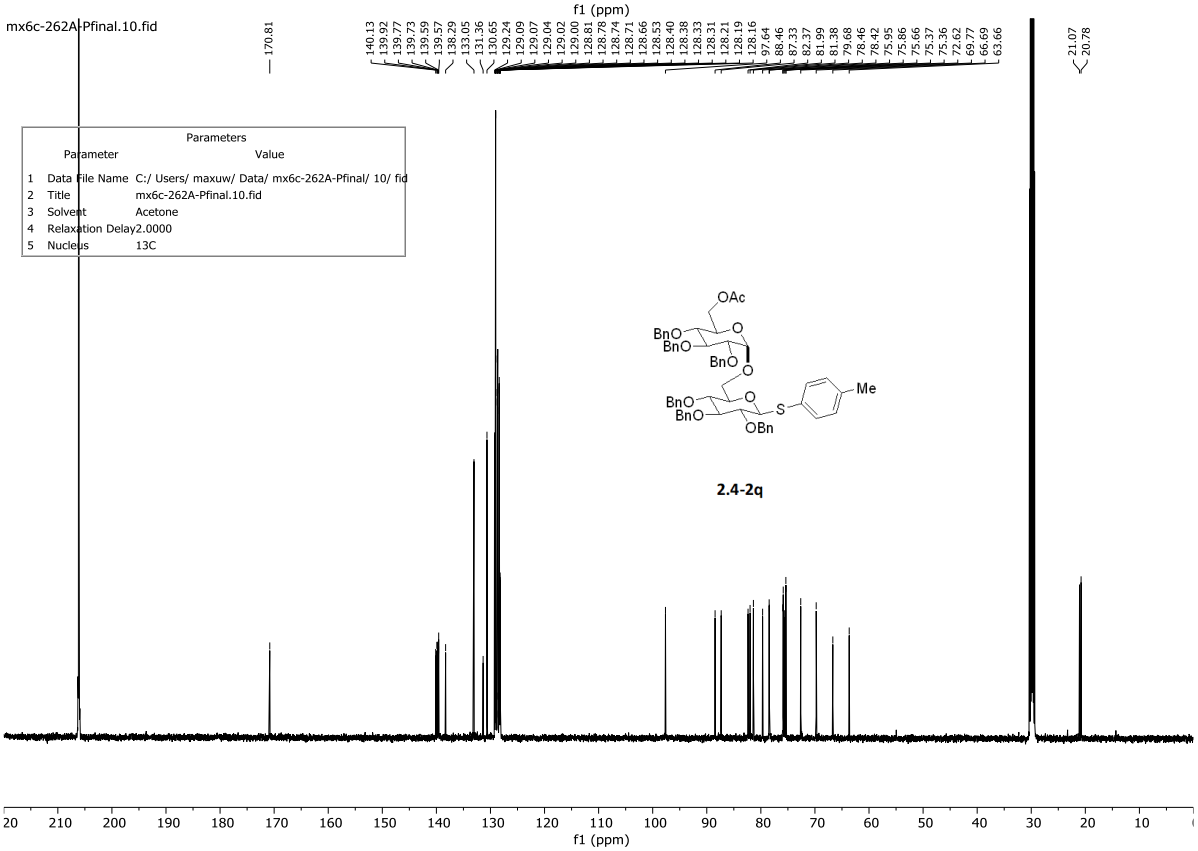
mx6c-262A-Pfinal.10.fid
Parameters
Parameter Value
1 Data File Name C:/ Users/ maxuw/ Data/ mx6c-262A-Pfinal/ 10/ fid
2 Title mx6c-262A-Pfinal.10.fid
3 Solvent Acetone
4 Relaxation Delay 2.0000
5 Nucleus 13C
OAc
BnO
BnO
BnO
O
O
BnO
BnO
O
S
Me
OBn
2.4-2q
f1 (ppm)

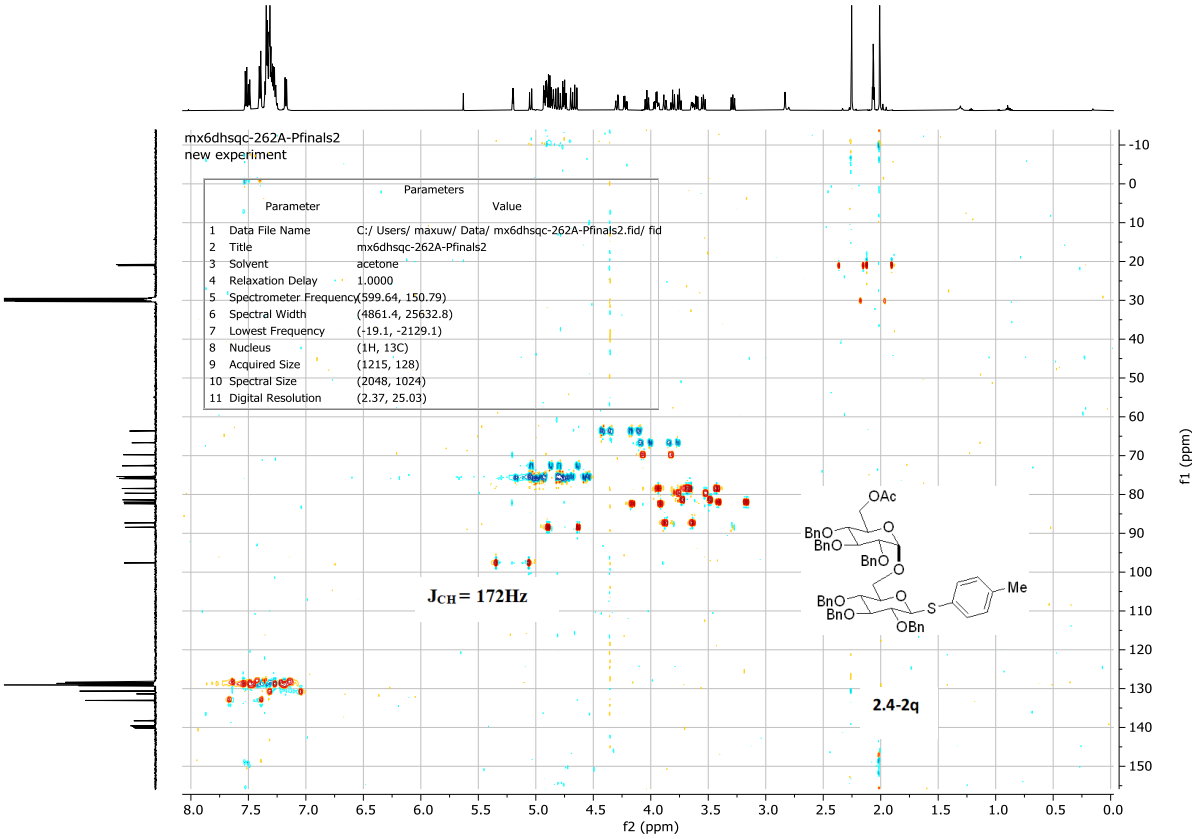
mx6dhsqc-262A-Pfinals2
new experiment
Parameters
Parameter Value
1 Data File Name C:/ Users/ maxuw/ Data/ mx6dhsqc-262A-Pfinals2.fid/ fid
2 Title mx6dhsqc-262A-Pfinals2
3 Solvent acetone
4 Relaxation Delay 1.0000
5 Spectrometer Frequency (599.64, 150.79)
6 Spectral Width (4861.4, 25632.8)
7 Lowest Frequency (+19.1, -2129.1)
8 Nucleus (1H, 13C)
9 Acquired Size (1215, 128)
10 Spectral Size (2048, 1024)
11 Digital Resolution (2.37, 25.03)
JCH = 172Hz
OAc
BnO
BnO
BnO
O
BnO
BnO
O
S
Me
OBn
2.4-2q
f2 (ppm)
f1 (ppm)

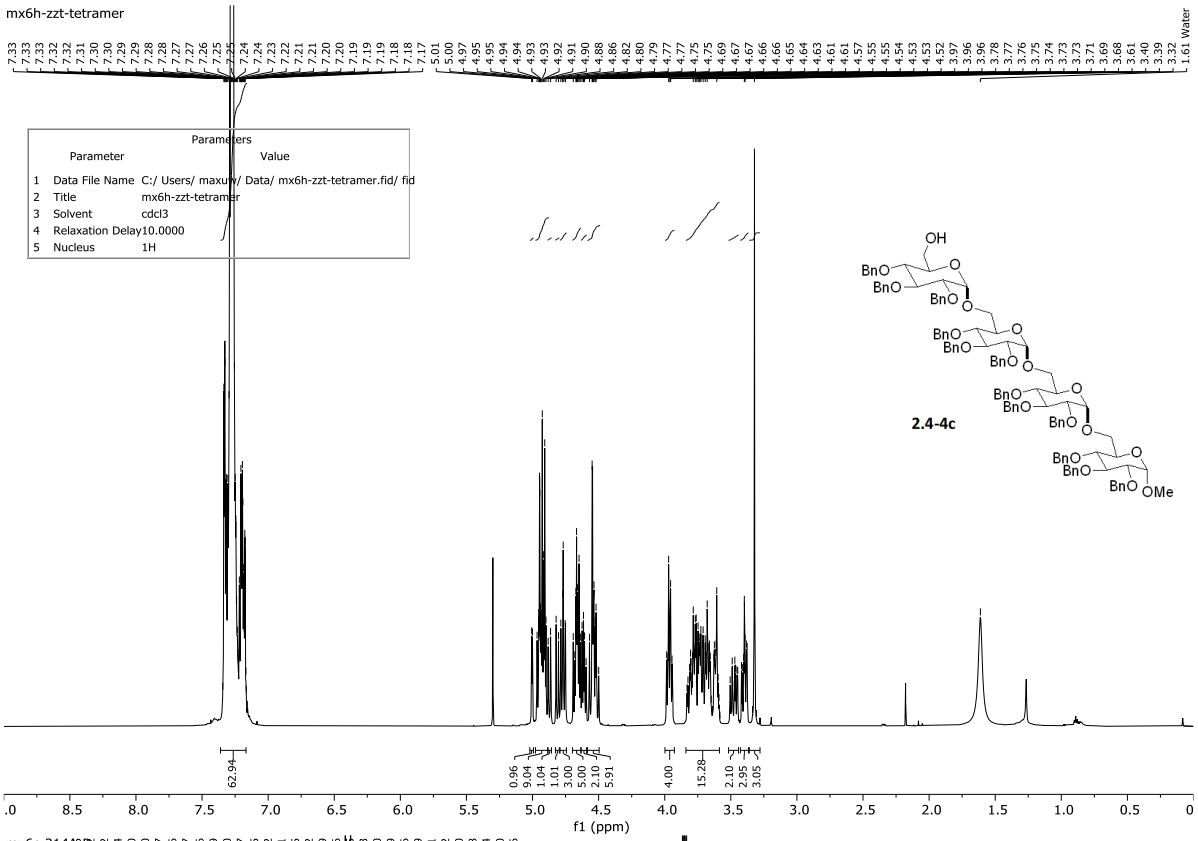
mx6h-zzt-tetramer
Parameters
Parameter Value
1 Data File Name C:/ Users/ maxuw/ Data/ mx6h-zzt-tetramer.fid/ fid
2 Title mx6h-zzt-tetramer
3 Solvent cdcl3
4 Relaxation Delay 10.0000
5 Nucleus 1H
2.4-4c
f1 (ppm)

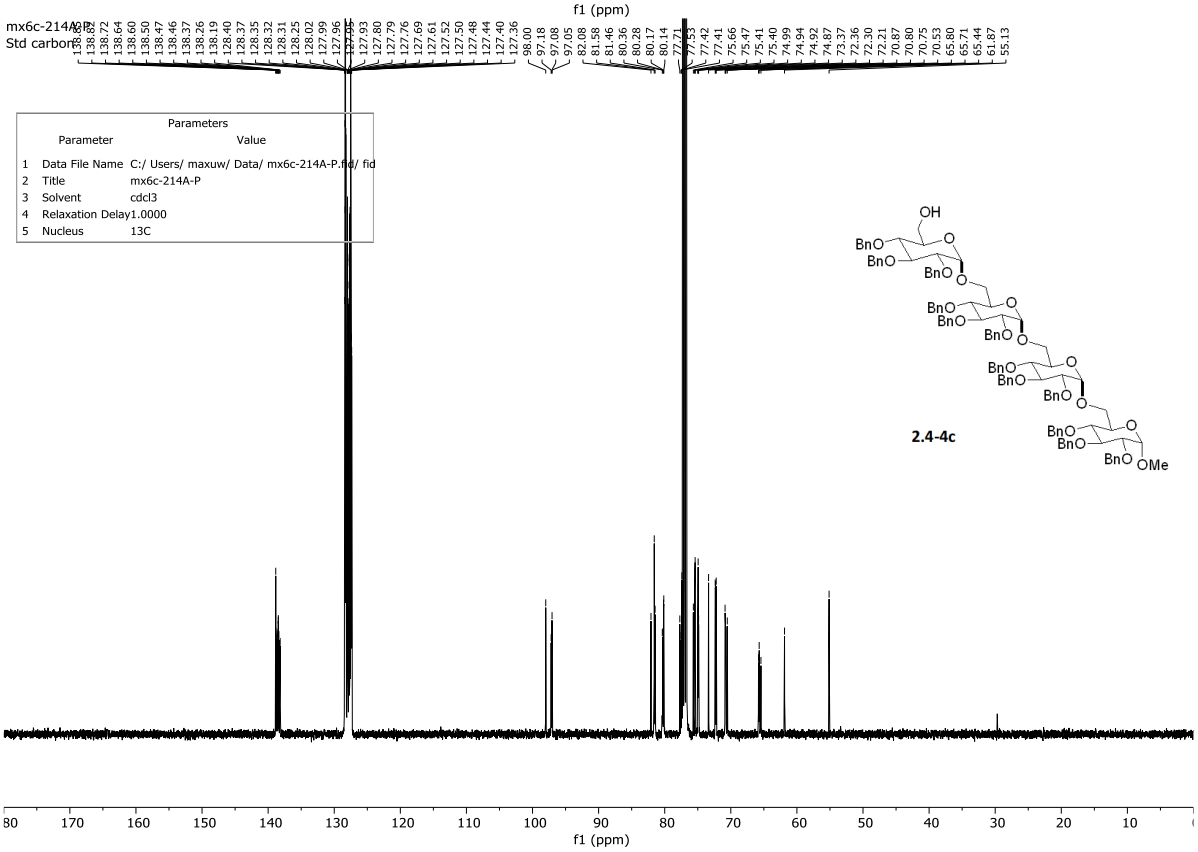
mx6c-214A-P
Std carbon
Parameters
Parameter Value
1 Data File Name C:/ Users/ maxuw/ Data/ mx6c-214A-P.fid/ fid
2 Title mx6c-214A-P
3 Solvent cdcl3
4 Relaxation Delay 1.0000
5 Nucleus 13C
2.4-4c
f1 (ppm)

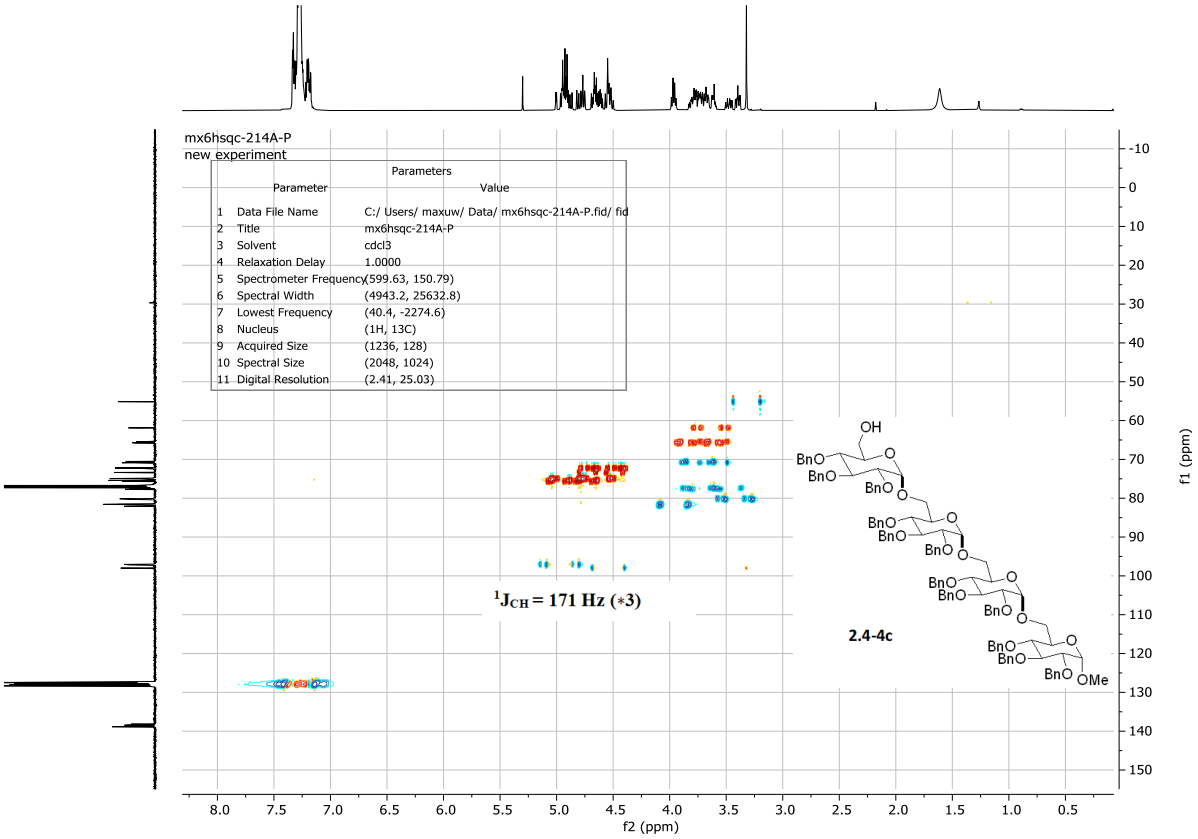
mx6hsqc-214A-P
new experiment
Parameters
Parameter Value
1 Data File Name C:/ Users/ maxuw/ Data/ mx6hsqc-214A-P.fid/ fid
2 Title mx6hsqc-214A-P
3 Solvent cdcl3
4 Relaxation Delay 1.0000
5 Spectrometer Frequency (599.63, 150.79)
6 Spectral Width (4943.2, 25632.8)
7 Lowest Frequency (40.4, -2274.6)
8 Nucleus (1H, 13C)
9 Acquired Size (1236, 128)
10 Spectral Size (2048, 1024)
11 Digital Resolution (2.41, 25.03)
$^1J_{CH}$ = 171 Hz (*3)
2.4-4c
f2 (ppm)
f1 (ppm)

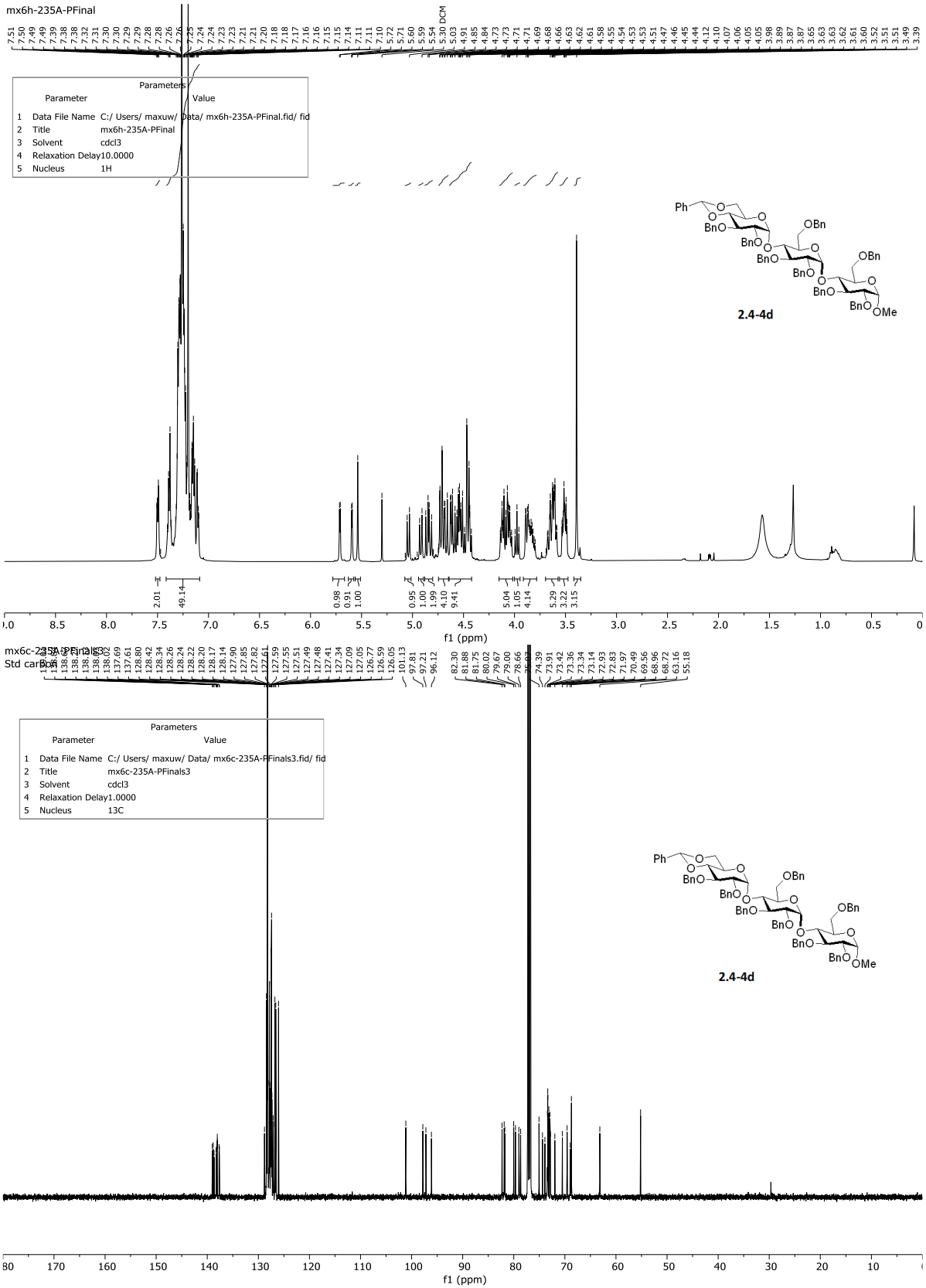
mx6h-235A-PFinal
Parameters
Parameter Value
1 Data File Name C:/ Users/ maxuw/ Data/ mx6h-235A-PFinal.fid/ fid
2 Title mx6h-235A-PFinal
3 Solvent cdcl3
4 Relaxation Delay 10.0000
5 Nucleus 1H
2.4-4d
f1 (ppm)
mx6c-235A-PFinals3
Std carbon
Parameters
Parameter Value
1 Data File Name C:/ Users/ maxuw/ Data/ mx6c-235A-PFinals3.fid/ fid
2 Title mx6c-235A-PFinals3
3 Solvent cdcl3
4 Relaxation Delay 1.0000
5 Nucleus 13C
2.4-4d
f1 (ppm)

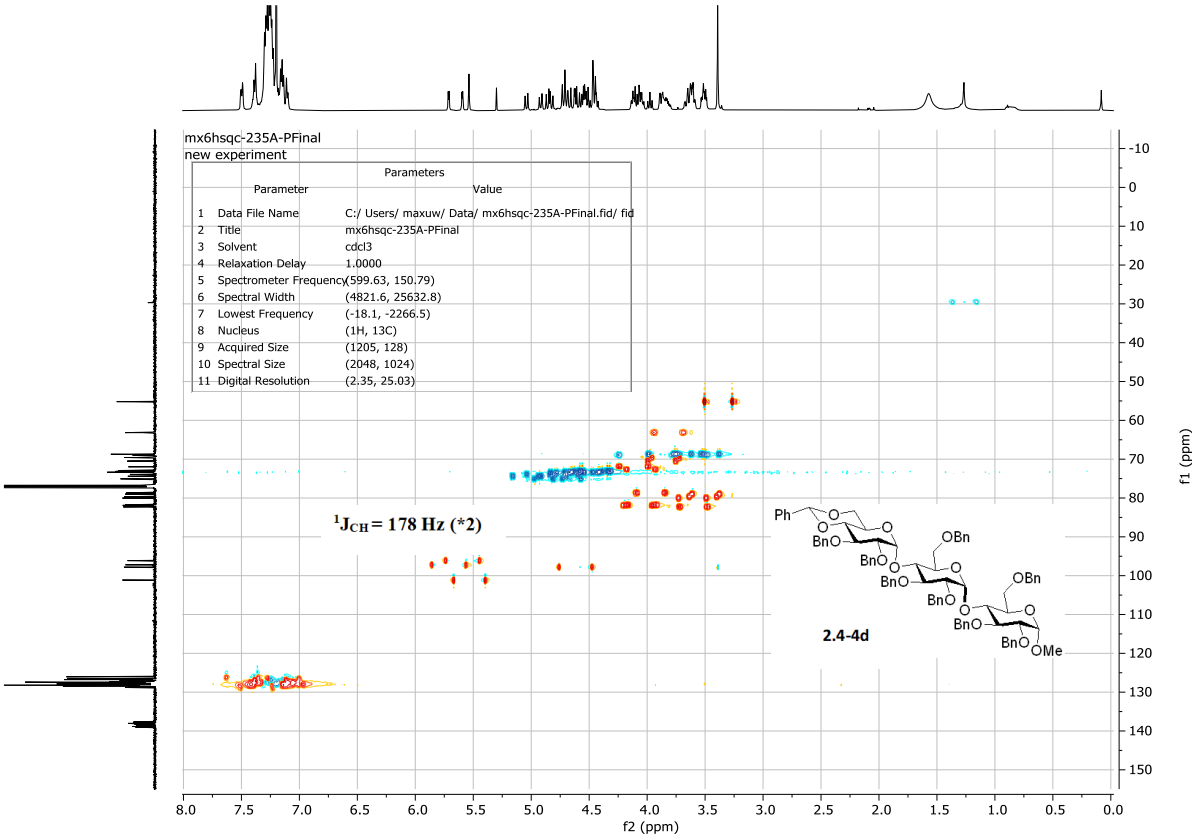
mx6hsqc-235A-PFinal
new experiment
Parameters
Parameter Value
1 Data File Name C:/ Users/ maxuw/ Data/ mx6hsqc-235A-PFinal.fid/ fid
2 Title mx6hsqc-235A-PFinal
3 Solvent cdcl3
4 Relaxation Delay 1.0000
5 Spectrometer Frequency (599.63, 150.79)
6 Spectral Width (4821.6, 25632.8)
7 Lowest Frequency (-18.1, -2266.5)
8 Nucleus (1H, 13C)
9 Acquired Size (1205, 128)
10 Spectral Size (2048, 1024)
11 Digital Resolution (2.35, 25.03)
$^{1}J_{CH}$ = 178 Hz (*2)
Ph
BnO
OBn
OMe
2.4-4d
f2 (ppm)
f1 (ppm)

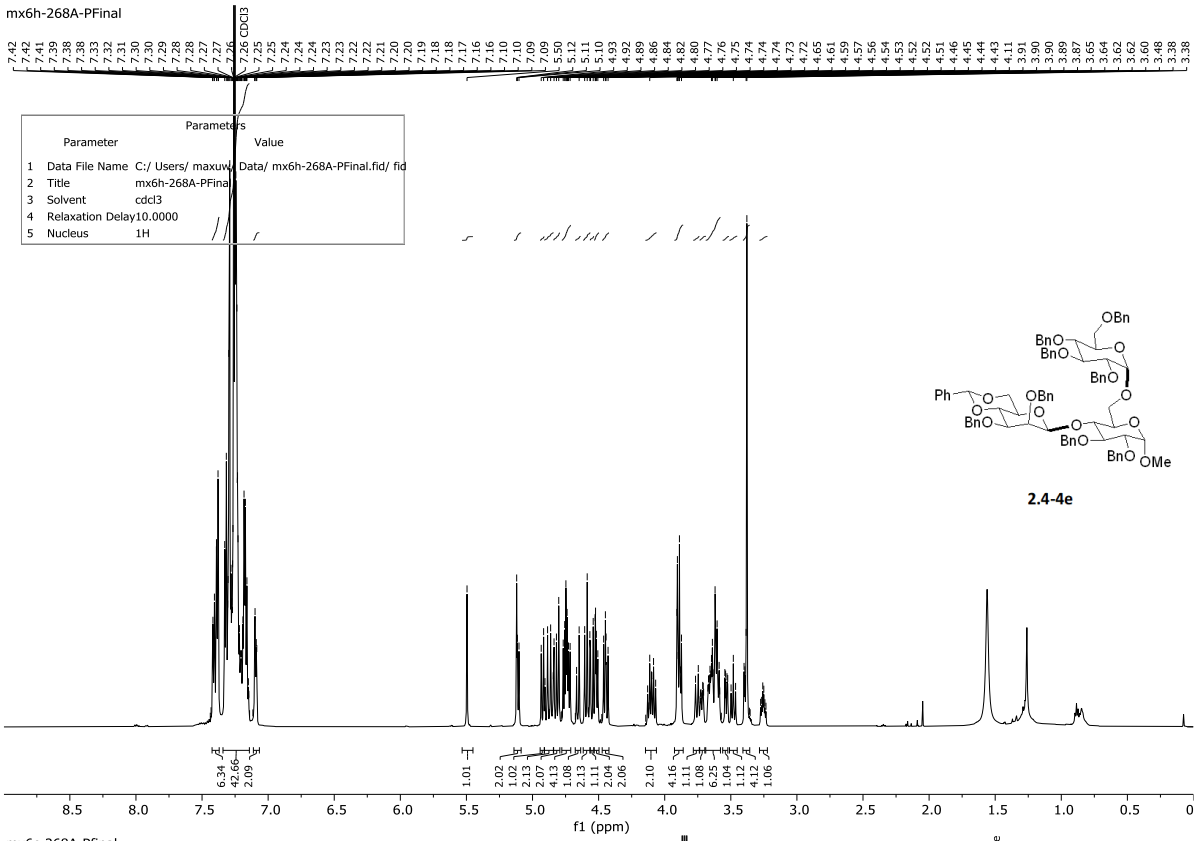
mx6h-268A-PFinal
CDCl3
Parameters
Parameter Value
1 Data File Name C:/ Users/ maxuw/ Data/ mx6h-268A-PFinal.fid/ fid
2 Title mx6h-268A-PFinal
3 Solvent cdcl3
4 Relaxation Delay 10.0000
5 Nucleus 1H
f1 (ppm)

2.4-4e

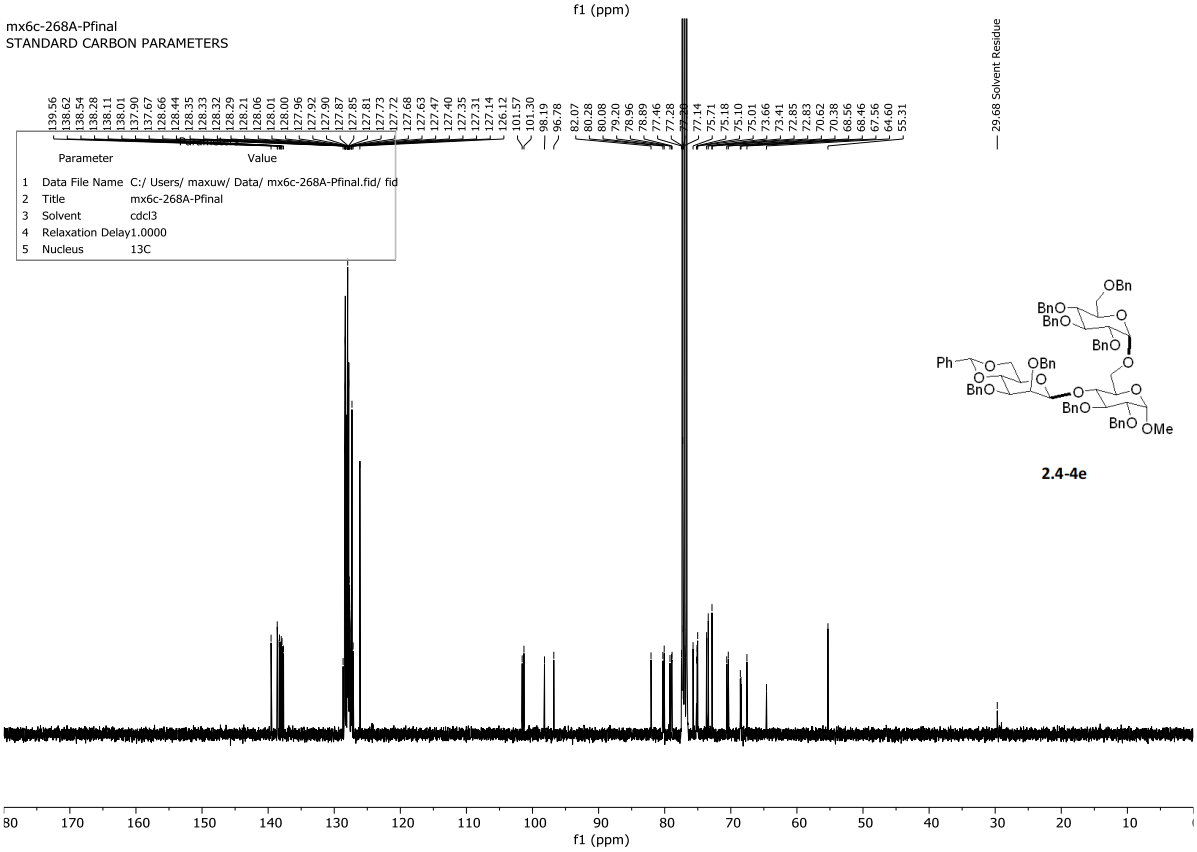
mx6c-268A-Pfinal
STANDARD CARBON PARAMETERS
29.68 Solvent Residue
Parameter Value
1 Data File Name C:/ Users/ maxuw/ Data/ mx6c-268A-Pfinal.fid/ fid
2 Title mx6c-268A-Pfinal
3 Solvent cdcl3
4 Relaxation Delay 1.0000
5 Nucleus 13C
f1 (ppm)

2.4-4e

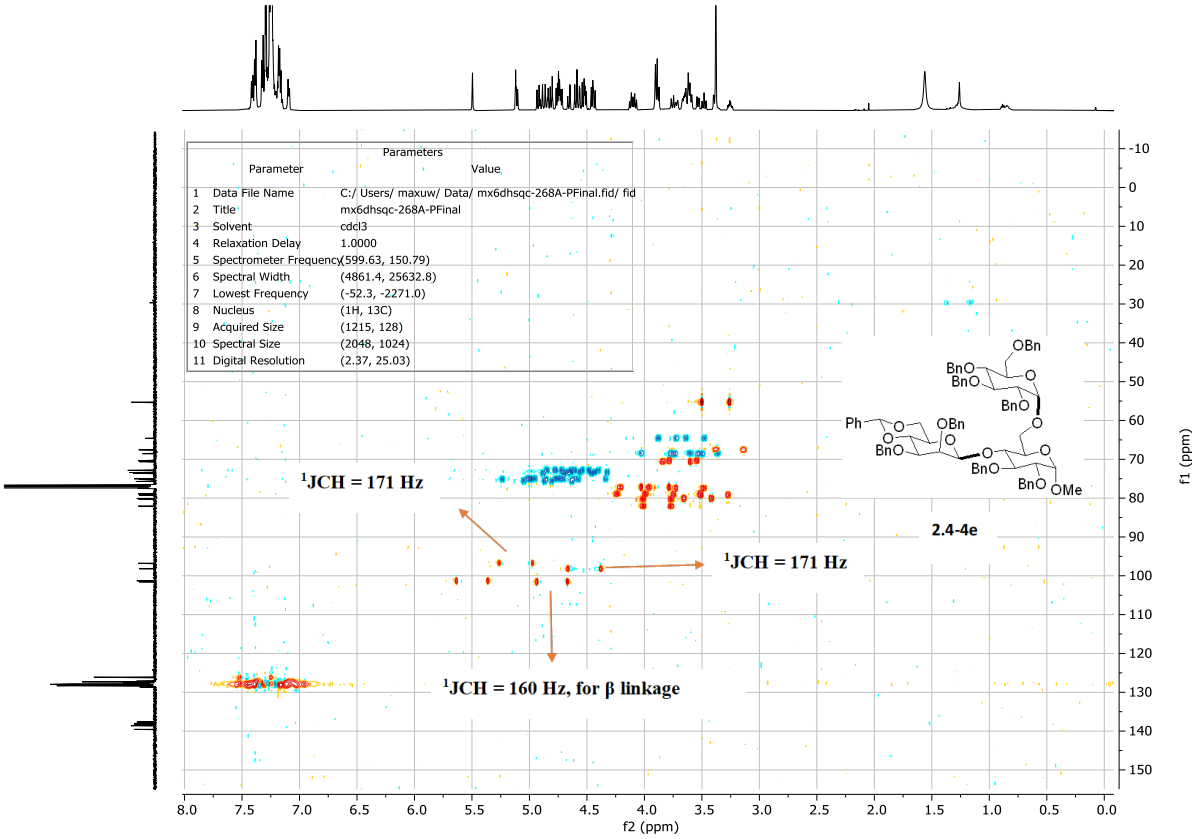
Parameters
Parameter Value
1 Data File Name C:/ Users/ maxuw/ Data/ mx6dhsqc-268A-PFinal.fid/ fid
2 Title mx6dhsqc-268A-PFinal
3 Solvent cdcl3
4 Relaxation Delay 1.0000
5 Spectrometer Frequency (599.63, 150.79)
6 Spectral Width (4861.4, 25632.8)
7 Lowest Frequency (-52.3, -2271.0)
8 Nucleus (1H, 13C)
9 Acquired Size (1215, 128)
10 Spectral Size (2048, 1024)
11 Digital Resolution (2.37, 25.03)
^{1}JCH = 171 Hz
^{1}JCH = 171 Hz
^{1}JCH = 160 Hz, for β linkage
2.4-4e
f2 (ppm)
f1 (ppm)

NMR Spectra for Compounds in Chapter 3

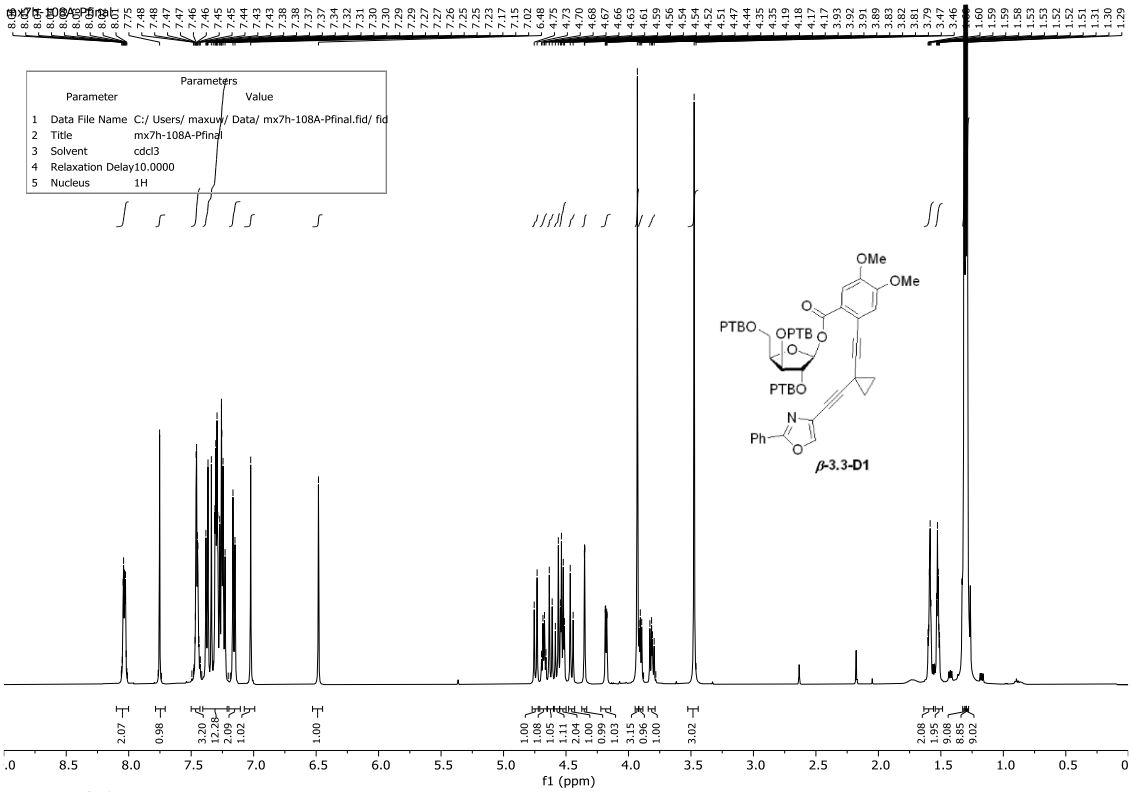

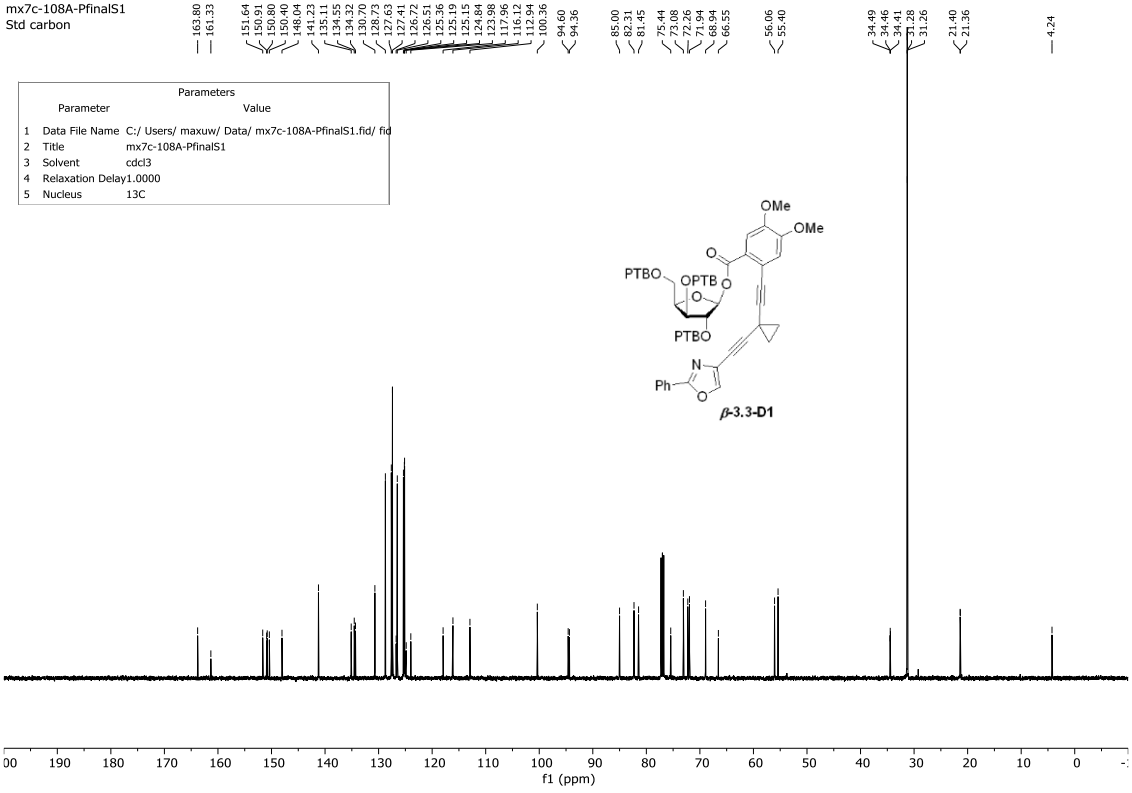

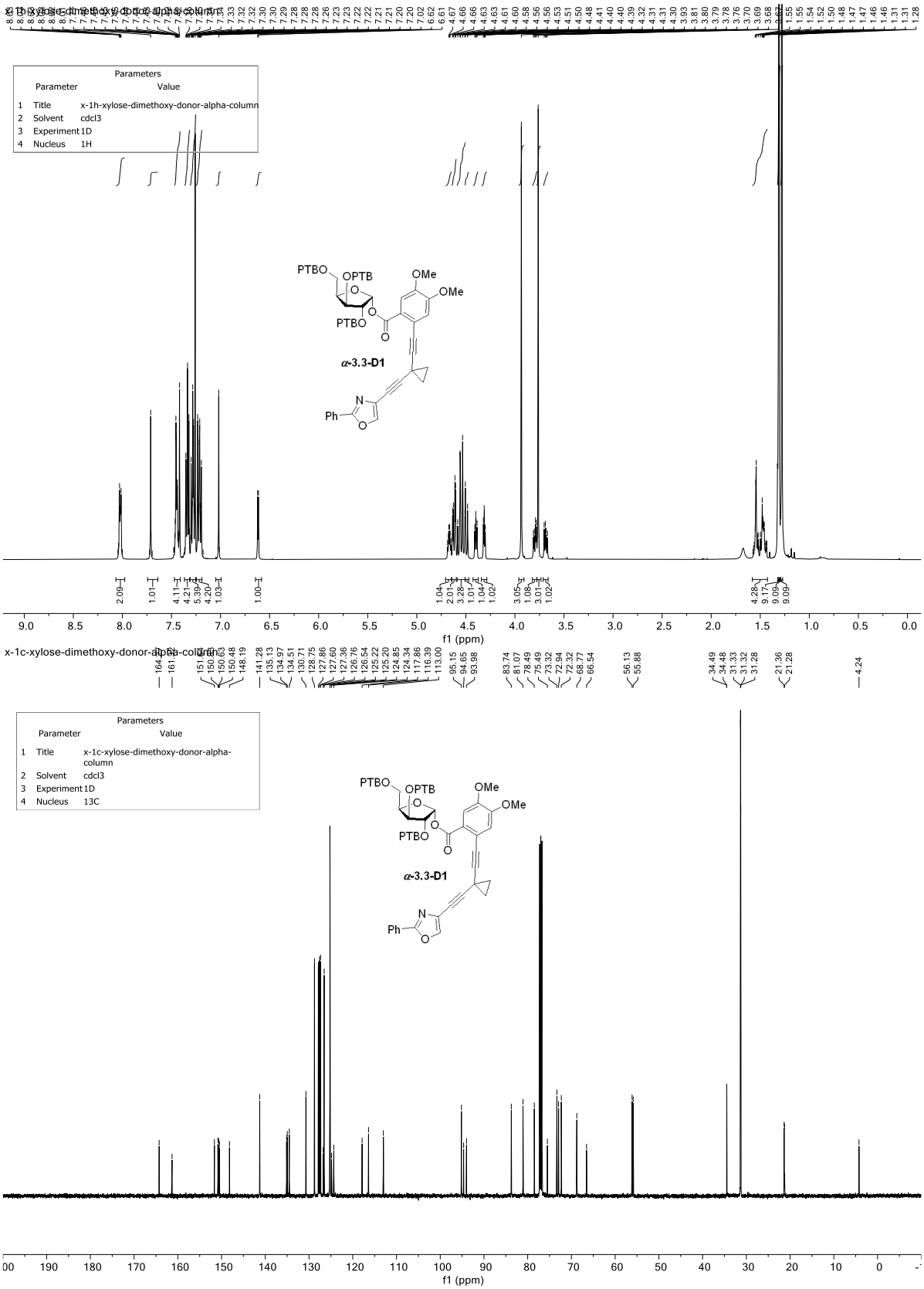
Parameters
Parameter Value
1 Title x-1h-xylose-dimethoxy-donor-alpha-column
2 Solvent cdcl3
3 Experiment 1D
4 Nucleus 1H
PTBO
OPTB
OMe
OMe
PTBO
α-3.3-D1
N
Ph
f1 (ppm)
x-1c-xylose-dimethoxy-donor-alpha-column
Parameters
Parameter Value
1 Title x-1c-xylose-dimethoxy-donor-alpha-column
2 Solvent cdcl3
3 Experiment 1D
4 Nucleus 13C
PTBO
OPTB
OMe
OMe
PTBO
α-3.3-D1
N
Ph
f1 (ppm)

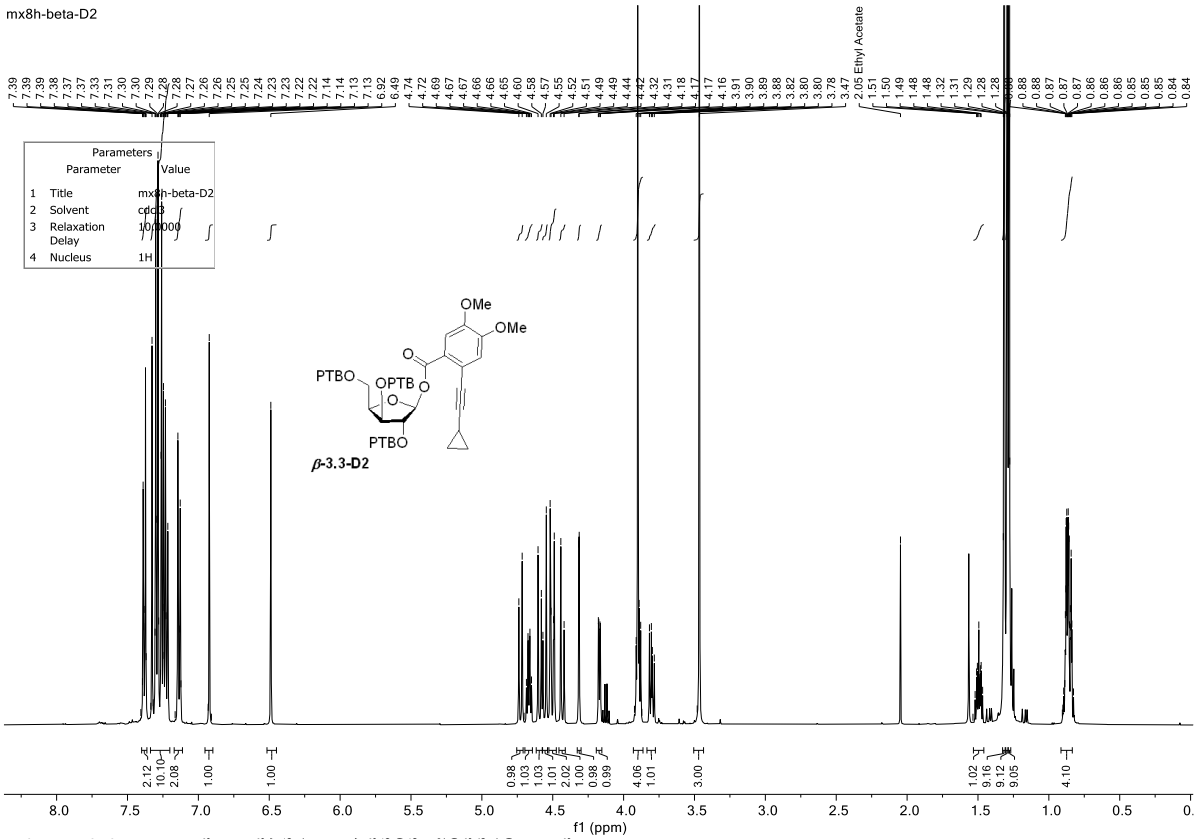
mx8h-beta-D2
Ethyl Acetate
Parameters
Parameter Value
1 Title mx8h-beta-D2
2 Solvent cdcl3
3 Relaxation Delay 1.0000
4 Nucleus 1H
OMe
OMe
PTBO
OPTB
PTBO
β-3.3-D2
f1 (ppm)

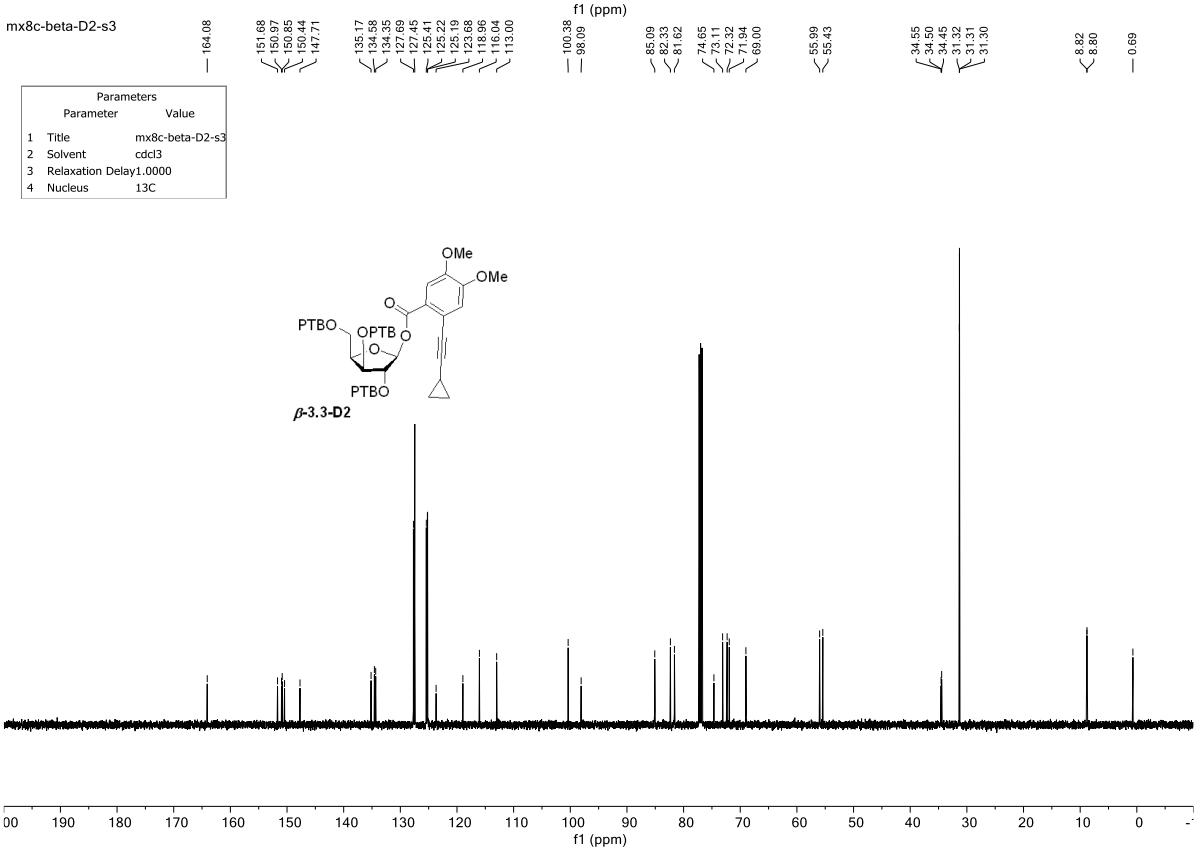
mx8c-beta-D2-s3
Parameters
Parameter Value
1 Title mx8c-beta-D2-s3
2 Solvent cdcl3
3 Relaxation Delay 1.0000
4 Nucleus 13C
OMe
OMe
PTBO
OPTB
PTBO
β-3.3-D2
f1 (ppm)

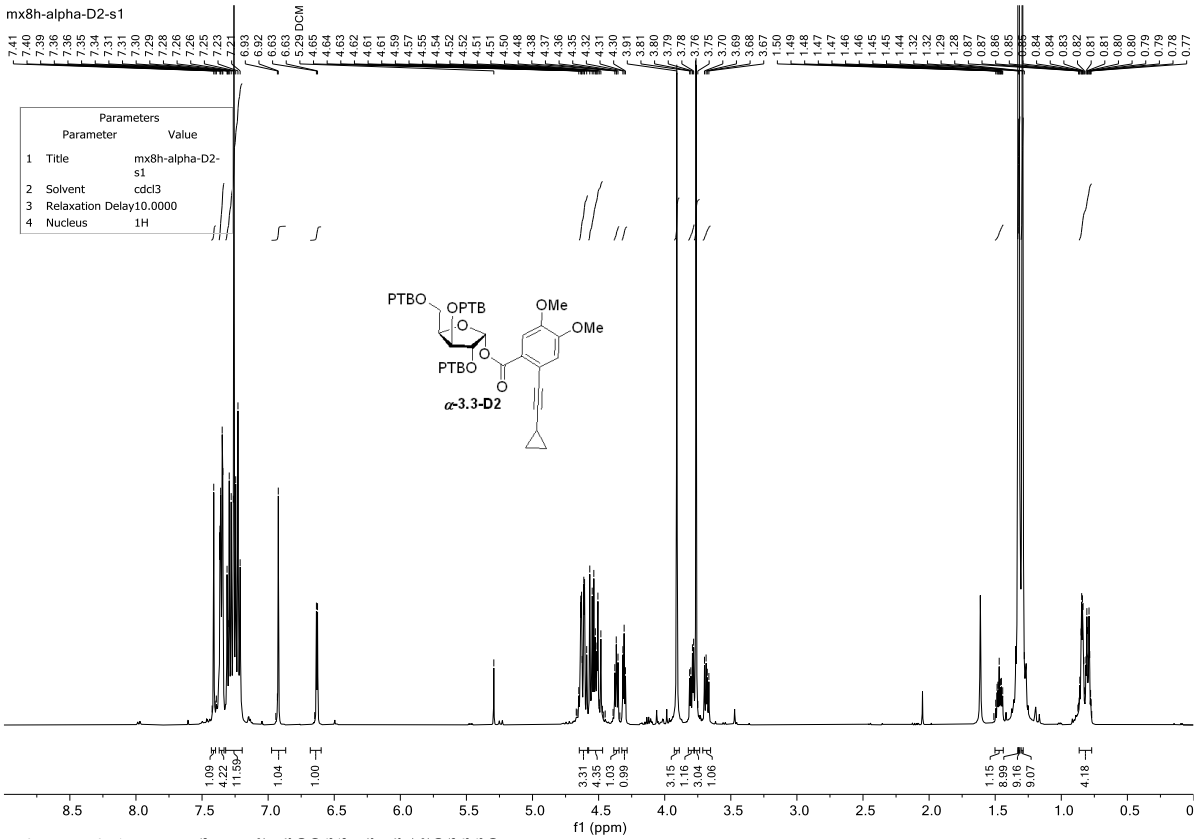
mx8h-alpha-D2-s1
Parameters
Parameter Value
1 Title mx8h-alpha-D2-s1
2 Solvent cdcl3
3 Relaxation Delay 10.0000
4 Nucleus 1H
PTBO
OPTB
OMe
OMe
PTBO
O
α-3.3-D2
f1 (ppm)

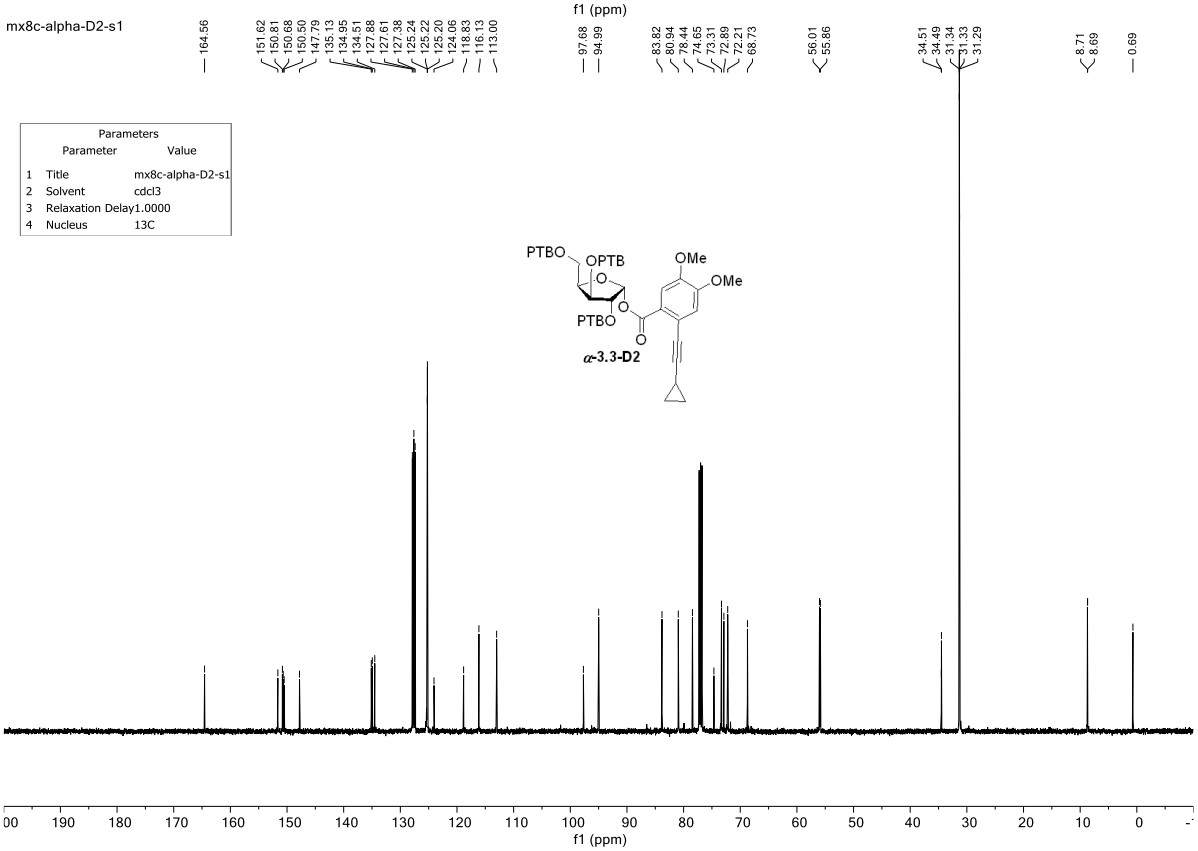
mx8c-alpha-D2-s1
Parameters
Parameter Value
1 Title mx8c-alpha-D2-s1
2 Solvent cdcl3
3 Relaxation Delay 1.0000
4 Nucleus 13C
PTBO
OPTB
OMe
OMe
PTBO
O
α-3.3-D2
f1 (ppm)

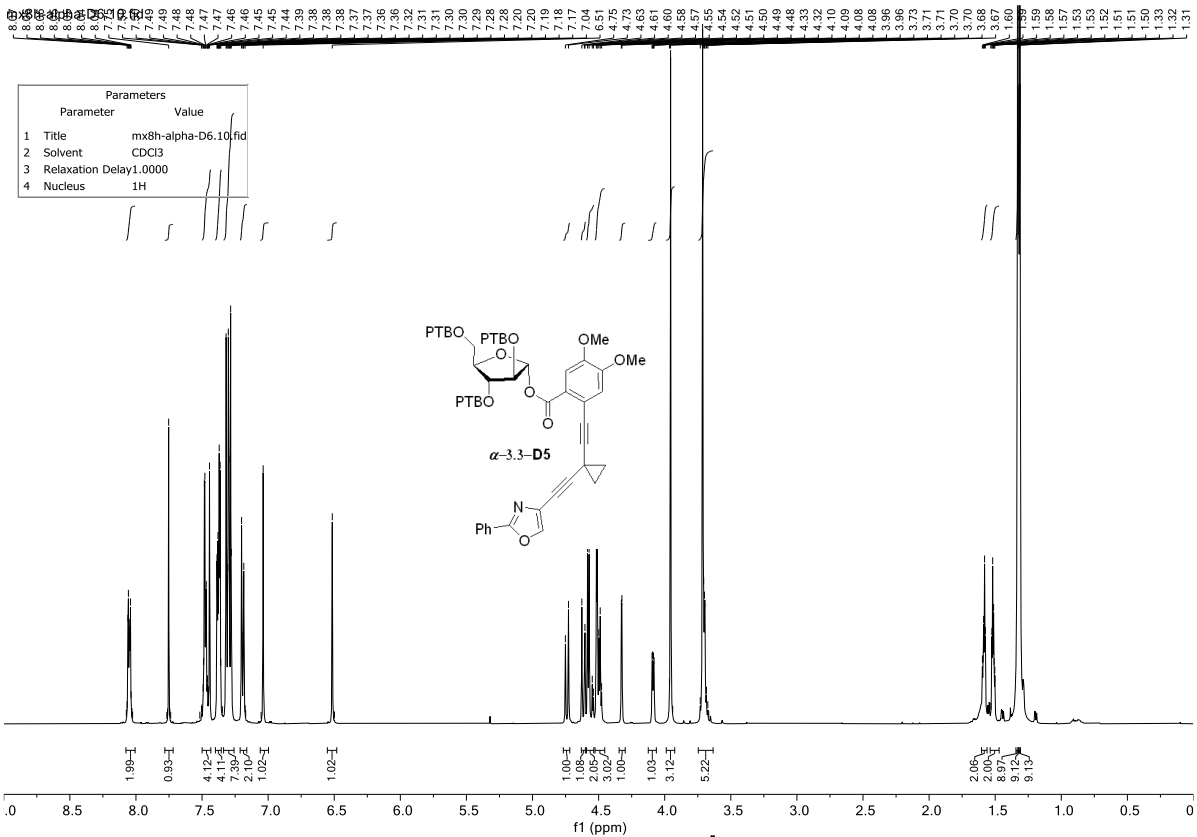
Parameters
Parameter Value
1 Title mx8h-alpha-D6.10.fid
2 Solvent CDCl3
3 Relaxation Delay 1.0000
4 Nucleus 1H
PTBO
PTBO
PTBO
OMe
OMe
O
α–3.3–D5
N
Ph
O
1.99 0.93 4.12 4.11 7.39 2.10 1.02 1.02 1.00 1.08 2.05 3.02 1.00 1.03 3.12 5.22 2.06 2.00 8.97 9.12 9.13
f1 (ppm)

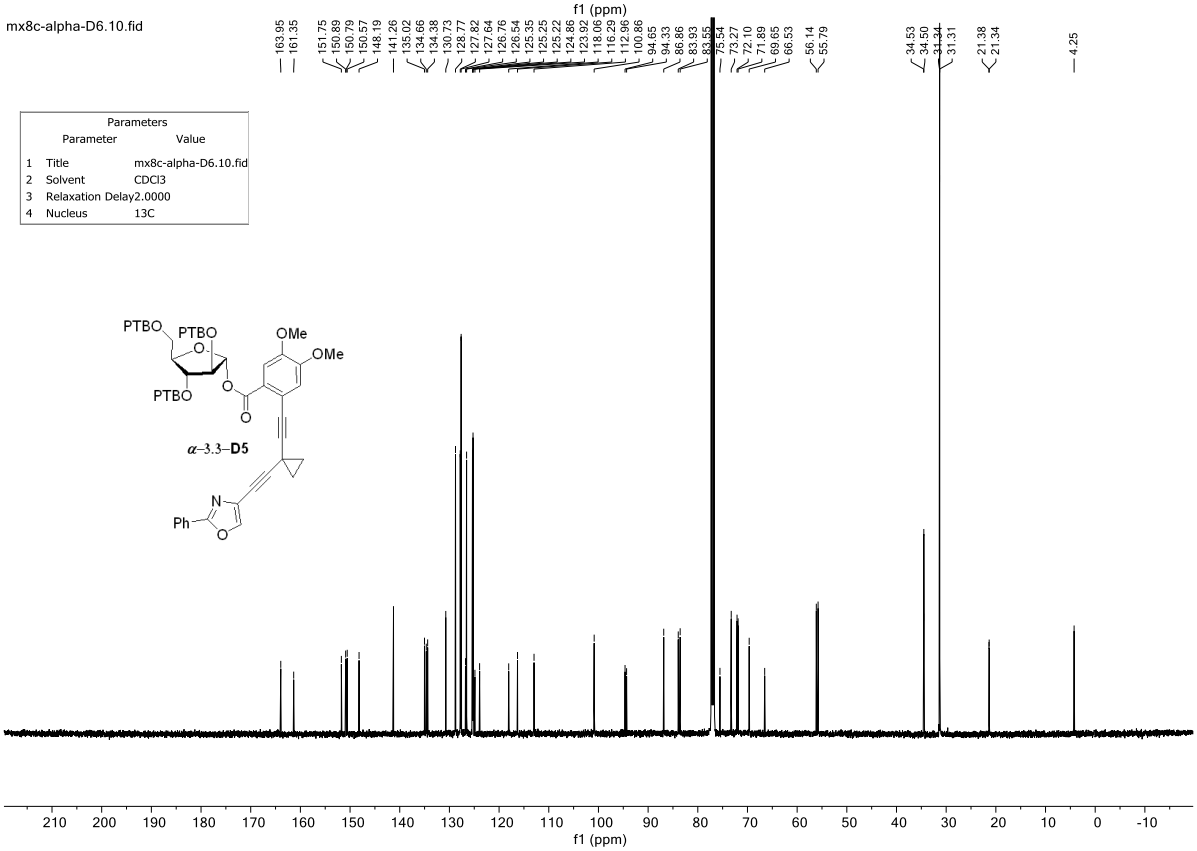
mx8c-alpha-D6.10.fid
163.95 161.35 151.75 150.89 150.79 150.57 148.19 141.26 135.02 134.66 134.38 130.73 128.77 127.82 127.64 126.76 126.54 125.35 125.25 125.22 124.86 123.92 118.06 116.29 112.96 100.86 94.65 94.33 86.86 83.93 83.55 73.54 73.27 72.10 71.88 69.65 66.53 56.14 55.79 34.53 34.50 31.34 31.31 21.38 21.34 4.25
Parameters
Parameter Value
1 Title mx8c-alpha-D6.10.fid
2 Solvent CDCl3
3 Relaxation Delay 2.0000
4 Nucleus 13C
PTBO
PTBO
PTBO
OMe
OMe
O
α–3.3–D5
N
Ph
O
f1 (ppm)

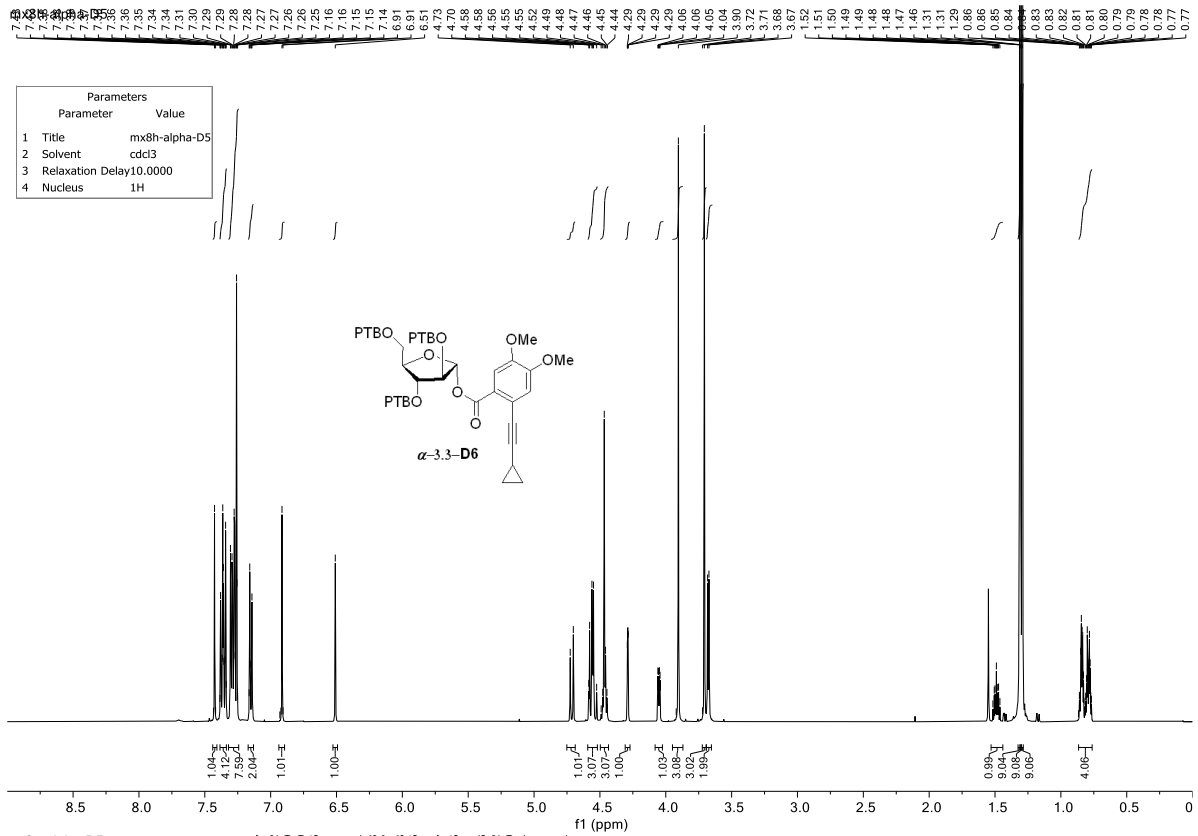
Parameters
Parameter Value
1 Title mx8h-alpha-D5
2 Solvent cdcl3
3 Relaxation Delay 10.0000
4 Nucleus 1H
PTBO
PTBO
PTBO
OMe
OMe
O
O
O
α–3.3–D6
f1 (ppm)

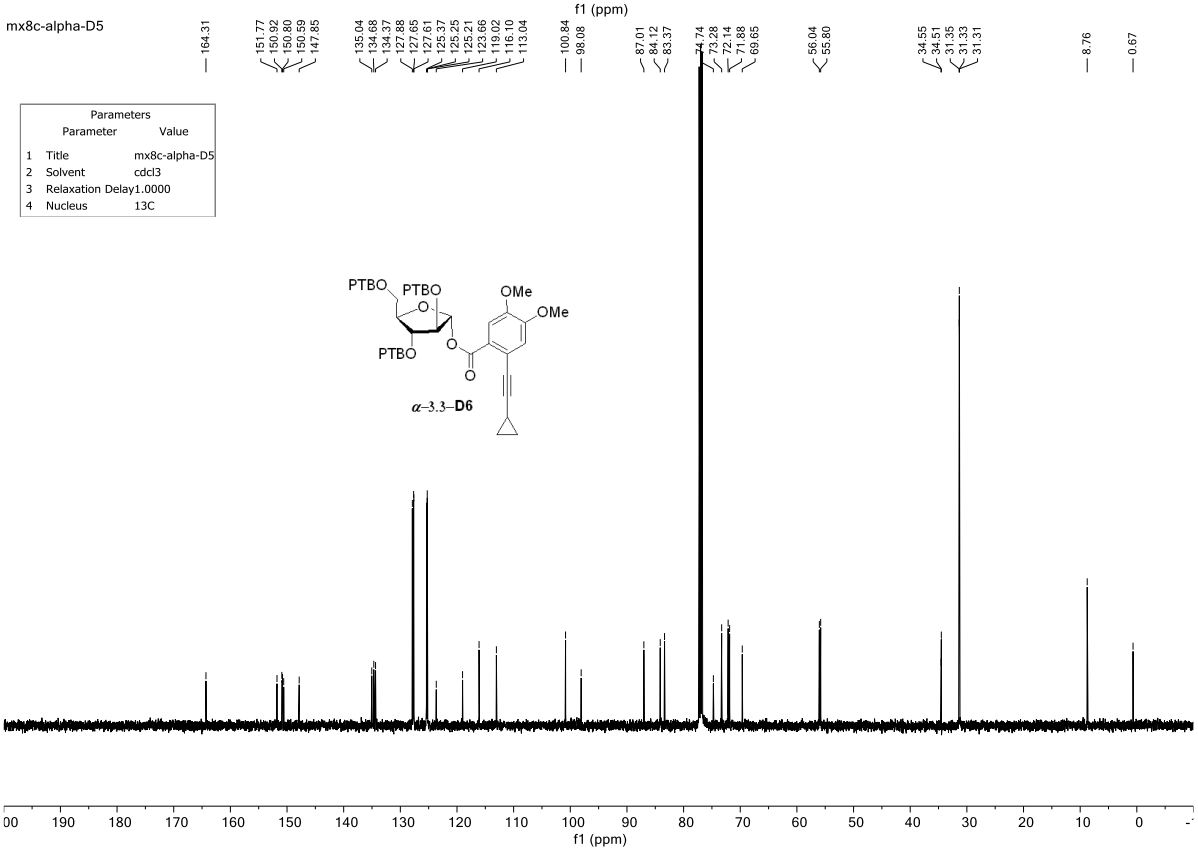
mx8c-alpha-D5
Parameters
Parameter Value
1 Title mx8c-alpha-D5
2 Solvent cdcl3
3 Relaxation Delay 1.0000
4 Nucleus 13C
PTBO
PTBO
PTBO
OMe
OMe
O
O
O
α–3.3–D6
f1 (ppm)

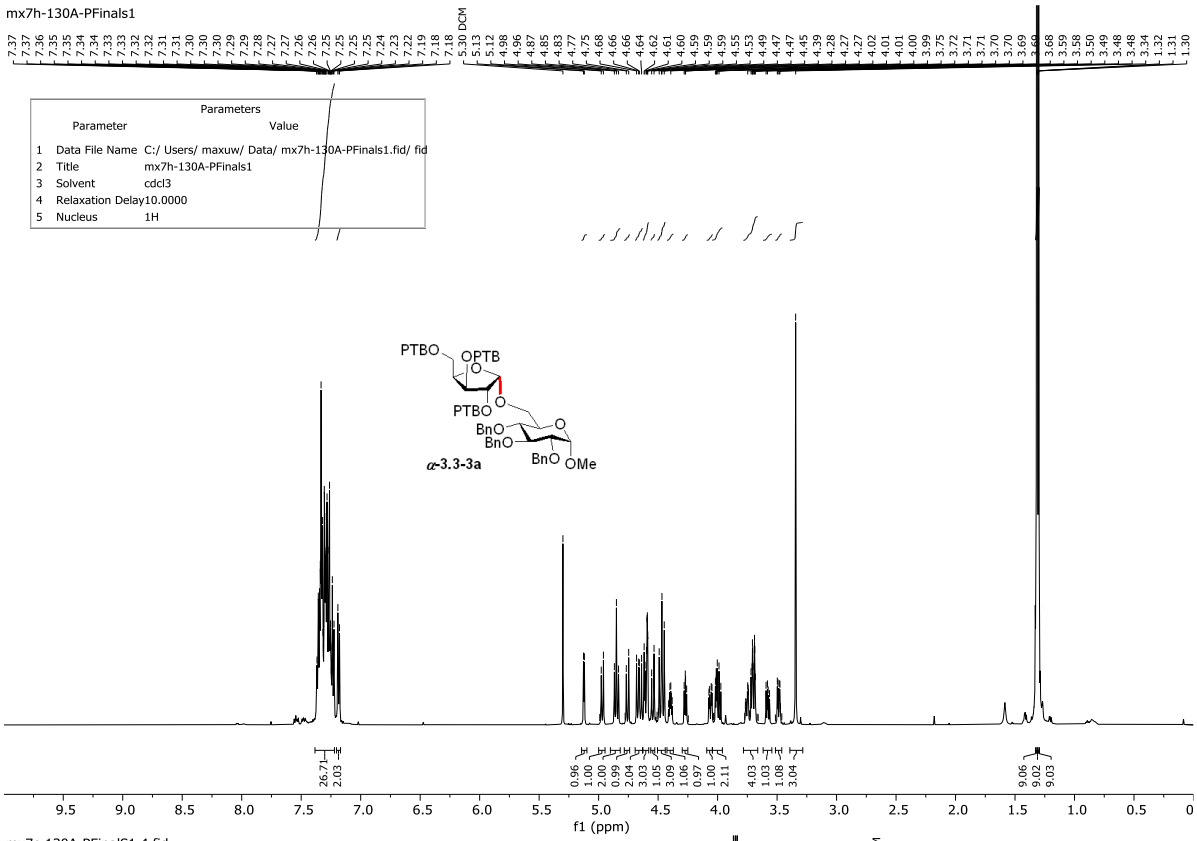
mx7h-130A-PFinals1
Parameters
Parameter Value
1 Data File Name C:/ Users/ maxuw/ Data/ mx7h-130A-PFinals1.fid/ fid
2 Title mx7h-130A-PFinals1
3 Solvent cdcl3
4 Relaxation Delay 10.0000
5 Nucleus 1H
PTBO
OPTB
PTBO
BnO
BnO
BnO
OMe
α-3.3-3a
f1 (ppm)

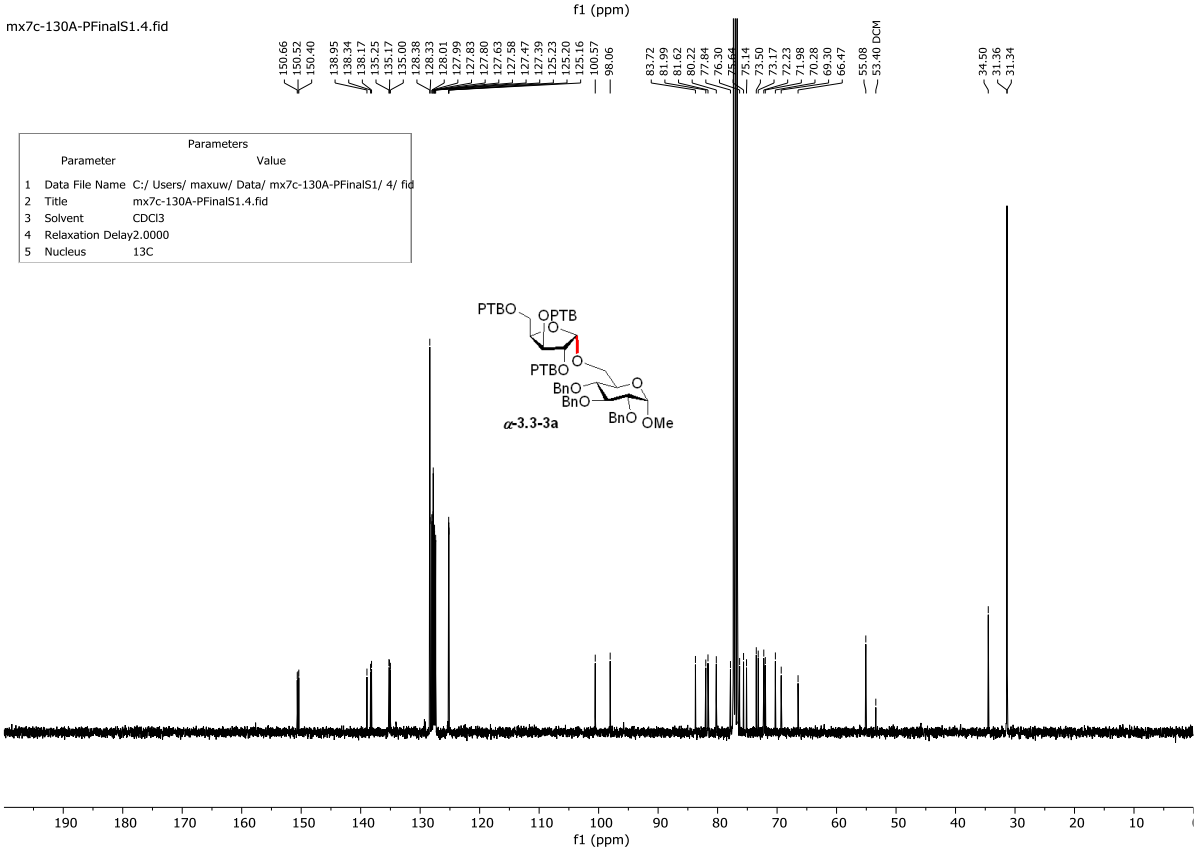
mx7c-130A-PFinalS1.4.fid
Parameters
Parameter Value
1 Data File Name C:/ Users/ maxuw/ Data/ mx7c-130A-PFinalS1/ 4/ fid
2 Title mx7c-130A-PFinalS1.4.fid
3 Solvent CDCl3
4 Relaxation Delay 2.0000
5 Nucleus 13C
PTBO
OPTB
PTBO
BnO
BnO
BnO
OMe
α-3.3-3a
f1 (ppm)

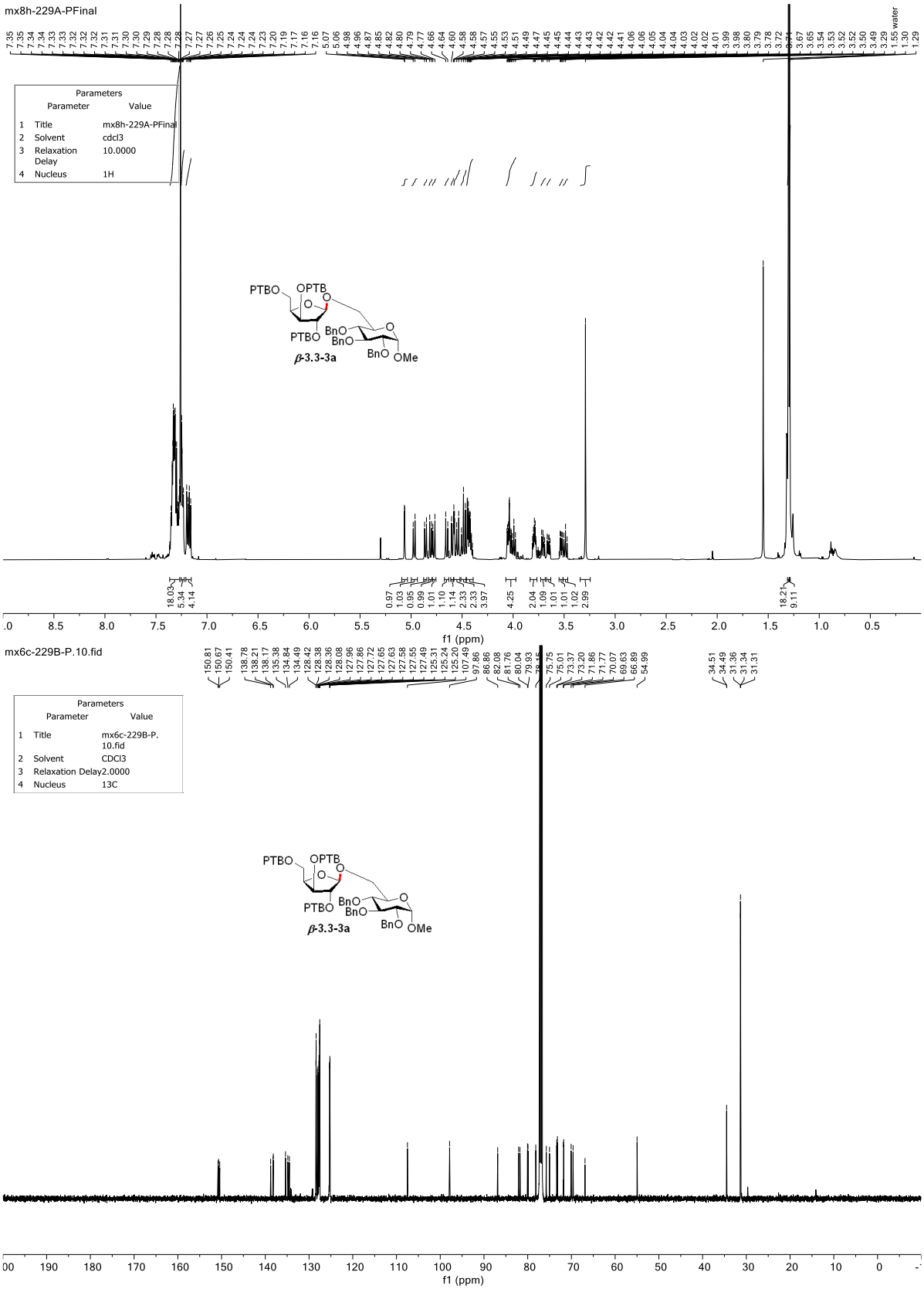
mx8h-229A-PFinal
Parameters
Parameter Value
1 Title mx8h-229A-PFinal
2 Solvent cdcl3
3 Relaxation Delay 10.0000
4 Nucleus 1H
PTBO
OPTB
PTBO
BnO
BnO
BnO
OMe
β-3.3-3a
f1 (ppm)
mx6c-229B-P.10.fid
Parameters
Parameter Value
1 Title mx6c-229B-P.10.fid
2 Solvent CDCl3
3 Relaxation Delay 2.0000
4 Nucleus 13C
PTBO
OPTB
PTBO
BnO
BnO
BnO
OMe
β-3.3-3a
f1 (ppm)

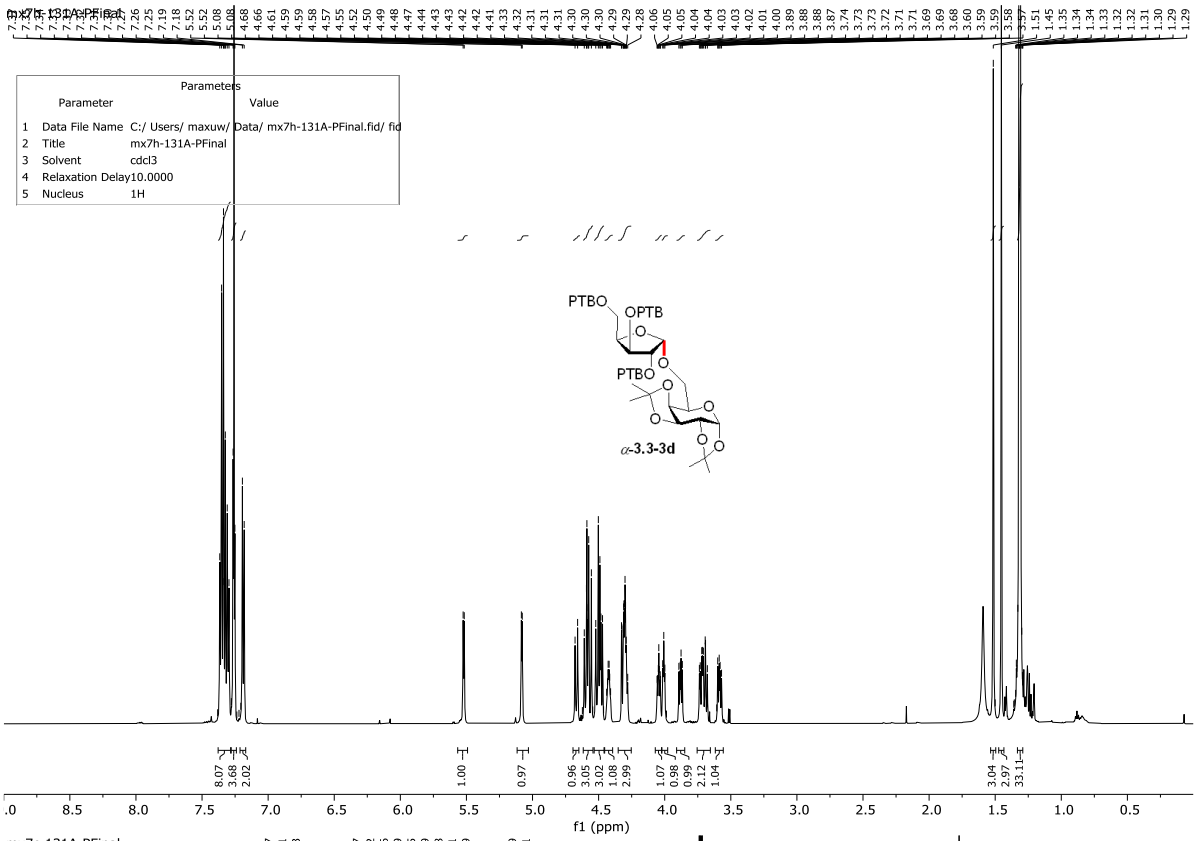
Parameters
Parameter Value
1 Data File Name C:/ Users/ maxuw/ Data/ mx7h-131A-PFinal.fid/ fid
2 Title mx7h-131A-PFinal
3 Solvent cdcl3
4 Relaxation Delay 10.0000
5 Nucleus 1H
PTBO
OPTB
PTBO
α-3.3-3d
f1 (ppm)

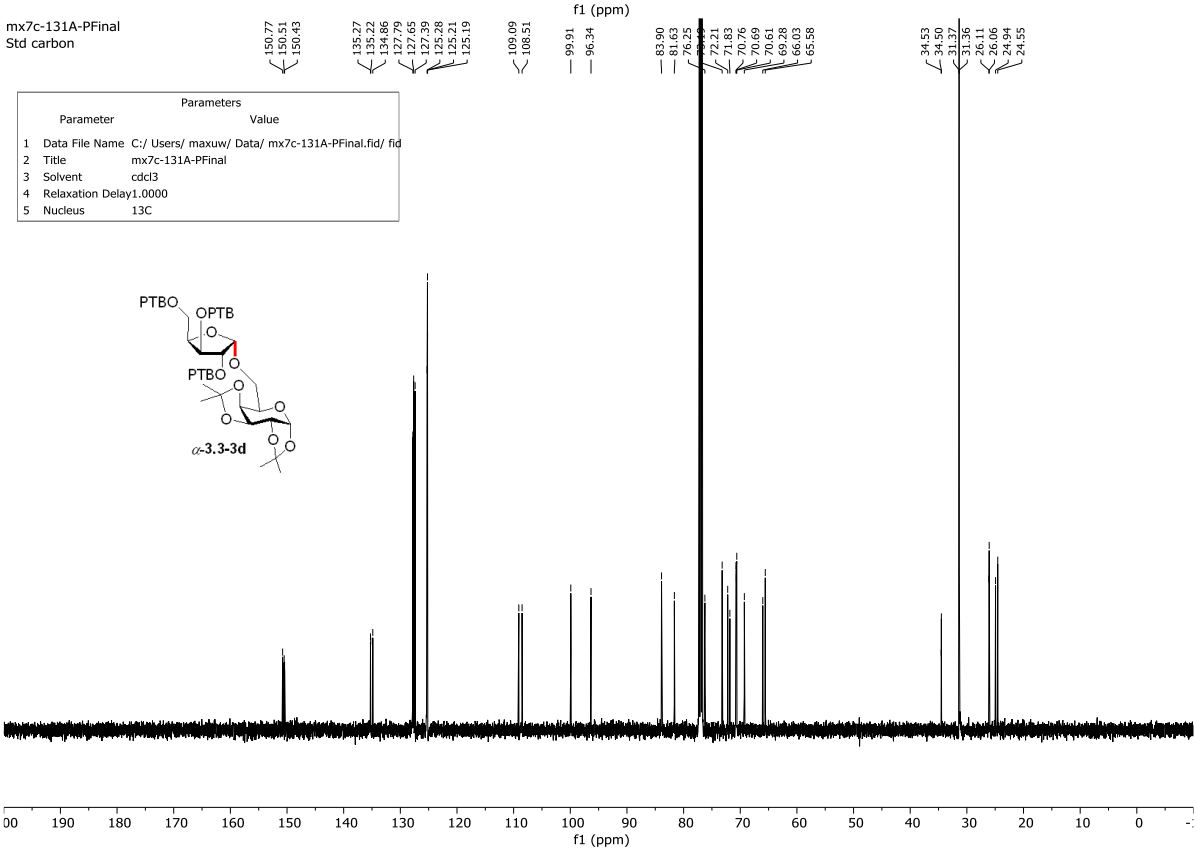
mx7c-131A-PFinal
Std carbon
Parameters
Parameter Value
1 Data File Name C:/ Users/ maxuw/ Data/ mx7c-131A-PFinal.fid/ fid
2 Title mx7c-131A-PFinal
3 Solvent cdcl3
4 Relaxation Delay 1.0000
5 Nucleus 13C
PTBO
OPTB
PTBO
α-3.3-3d
f1 (ppm)

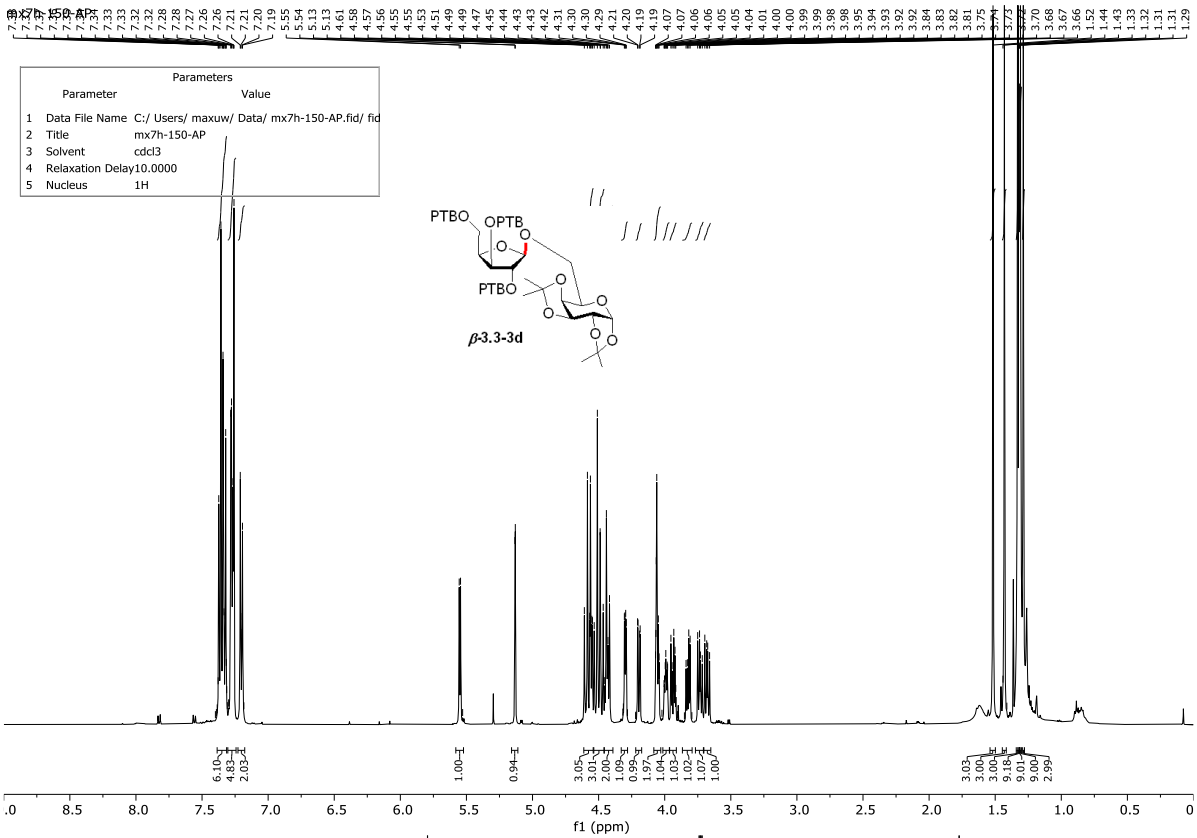
mx7h-150-AP
Parameters
Parameter Value
1 Data File Name C:/ Users/ maxuw/ Data/ mx7h-150-AP.fid/ fid
2 Title mx7h-150-AP
3 Solvent cdcl3
4 Relaxation Delay 10.0000
5 Nucleus 1H
PTBO
OPTB
PTBO
β-3.3-3d
f1 (ppm)

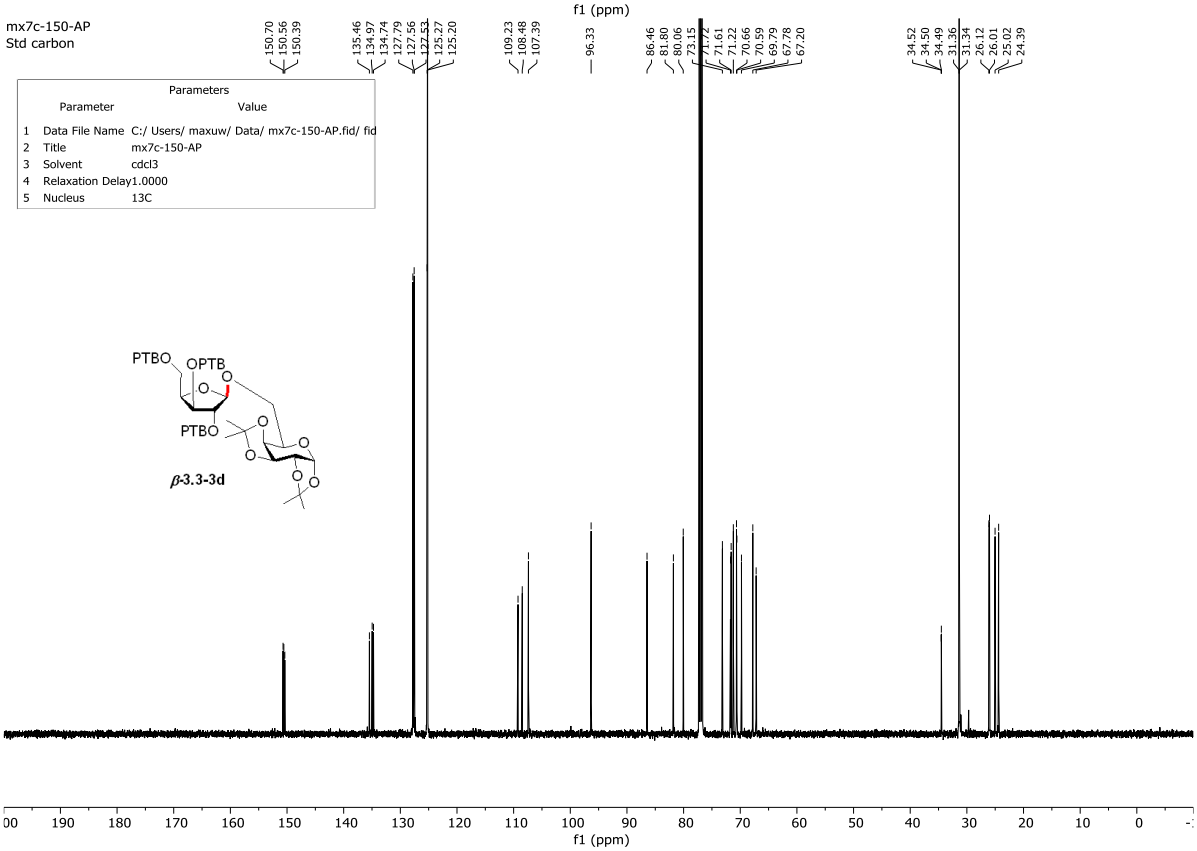
mx7c-150-AP
Std carbon
Parameters
Parameter Value
1 Data File Name C:/ Users/ maxuw/ Data/ mx7c-150-AP.fid/ fid
2 Title mx7c-150-AP
3 Solvent cdcl3
4 Relaxation Delay 1.0000
5 Nucleus 13C
PTBO
OPTB
PTBO
β-3.3-3d
f1 (ppm)

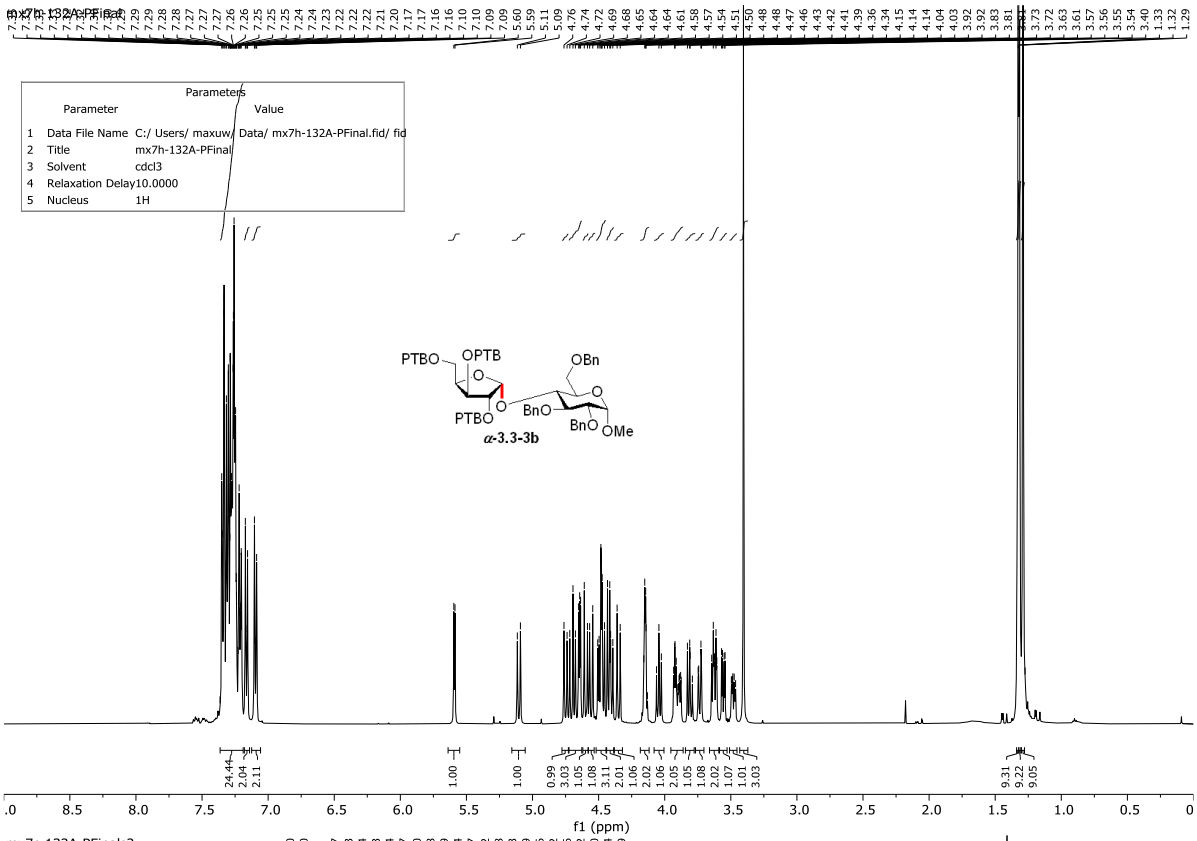
Parameters
Parameter Value
1 Data File Name C:/ Users/ maxuw/ Data/ mx7h-132A-PFinal.fid/ fid
2 Title mx7h-132A-PFinal
3 Solvent cdcl3
4 Relaxation Delay 10.0000
5 Nucleus 1H
PTBO
OPTB
OBn
BnO
BnO
OMe
α-3.3-3b
f1 (ppm)

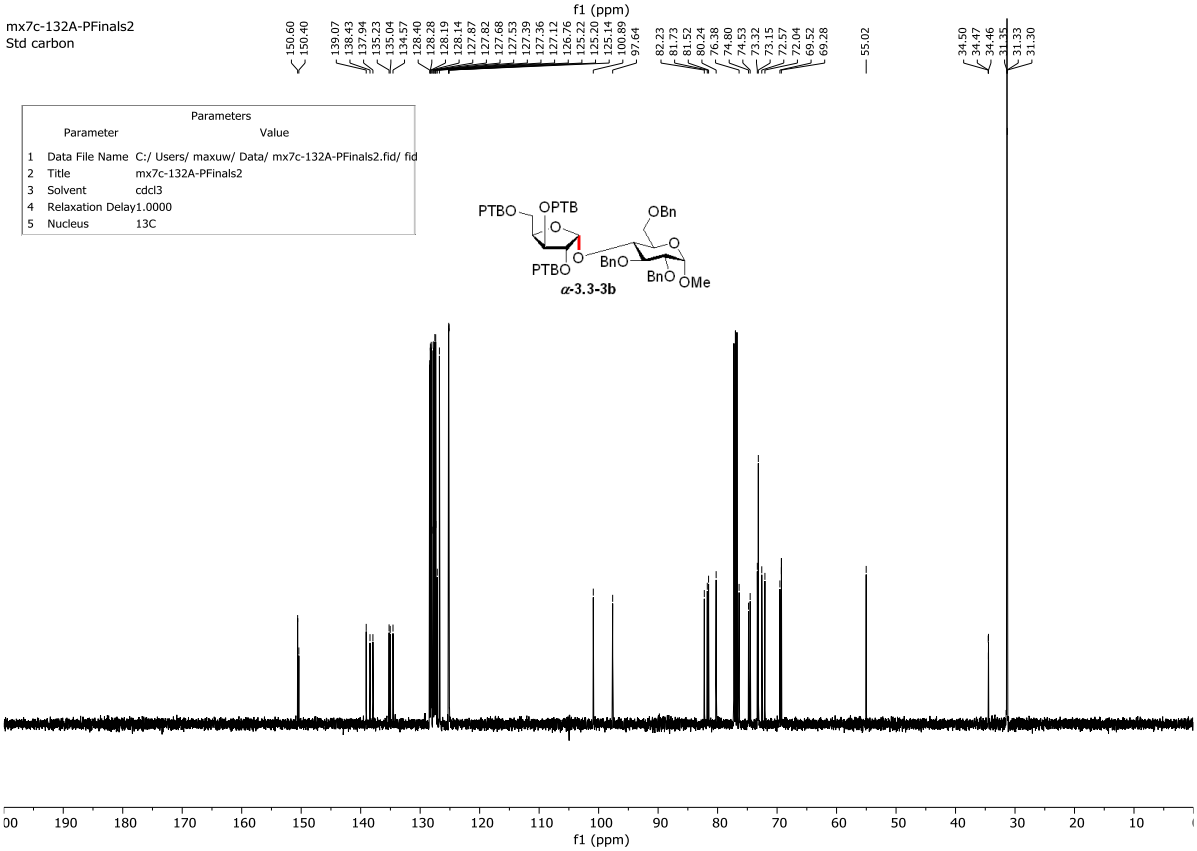
mx7c-132A-PFinals2
Std carbon
Parameters
Parameter Value
1 Data File Name C:/ Users/ maxuw/ Data/ mx7c-132A-PFinals2.fid/ fid
2 Title mx7c-132A-PFinals2
3 Solvent cdcl3
4 Relaxation Delay 1.0000
5 Nucleus 13C
PTBO
OPTB
OBn
BnO
BnO
OMe
α-3.3-3b
f1 (ppm)

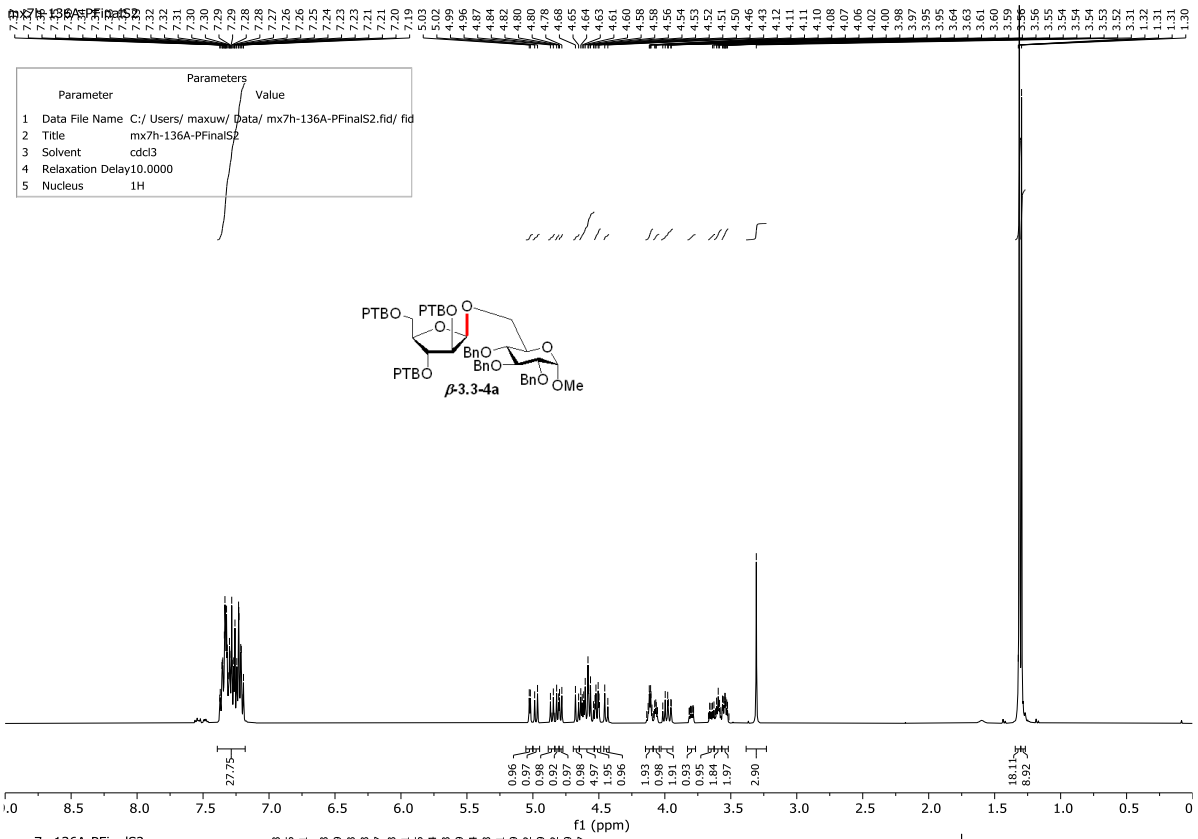
Parameters
Parameter Value
1 Data File Name C:/ Users/ maxuw/ Data/ mx7h-136A-PFinalS2.fid/ fid
2 Title mx7h-136A-PFinalS2
3 Solvent cdcl3
4 Relaxation Delay 10.0000
5 Nucleus 1H
PTBO
PTBO
BnO
BnO
BnO
OMe
PTBO
β-3.3-4a
f1 (ppm)

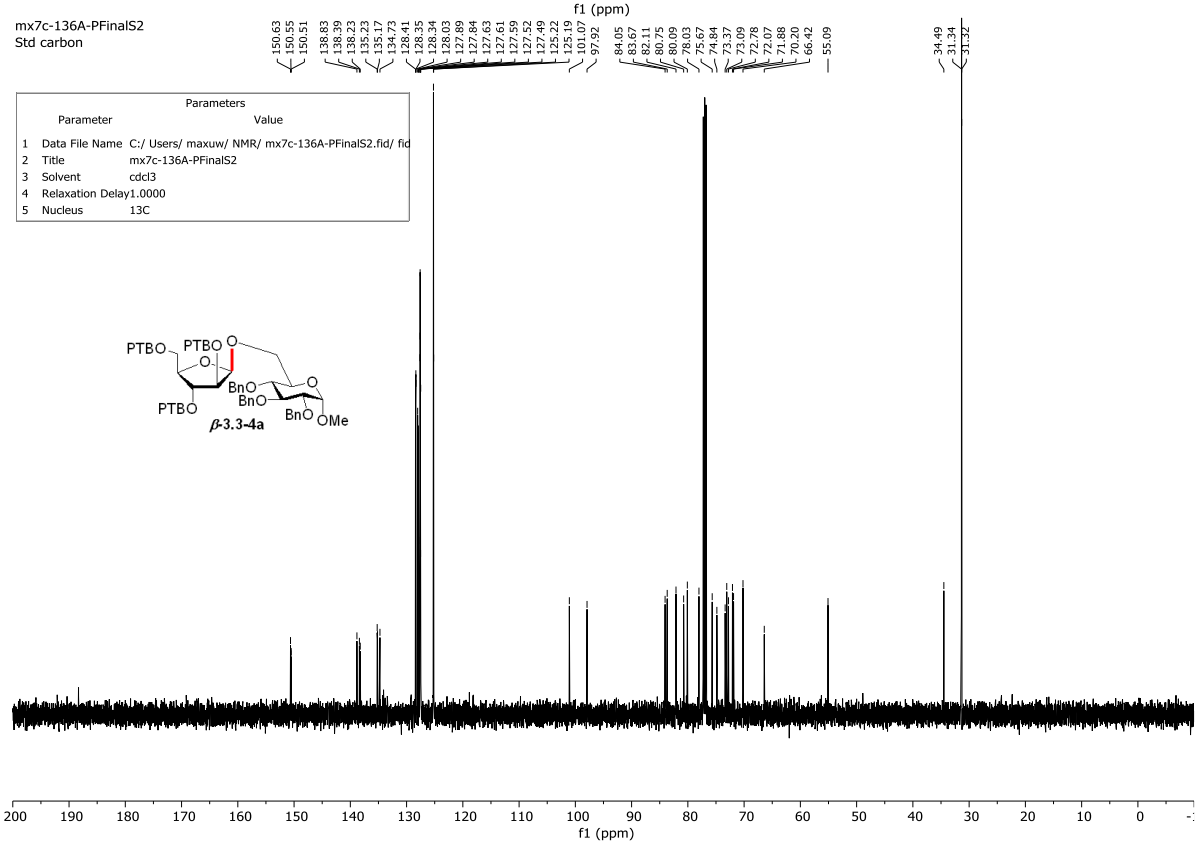
mx7c-136A-PFinalS2
Std carbon
Parameters
Parameter Value
1 Data File Name C:/ Users/ maxuw/ NMR/ mx7c-136A-PFinalS2.fid/ fid
2 Title mx7c-136A-PFinalS2
3 Solvent cdcl3
4 Relaxation Delay 1.0000
5 Nucleus 13C
PTBO
PTBO
BnO
BnO
BnO
OMe
PTBO
β-3.3-4a
f1 (ppm)

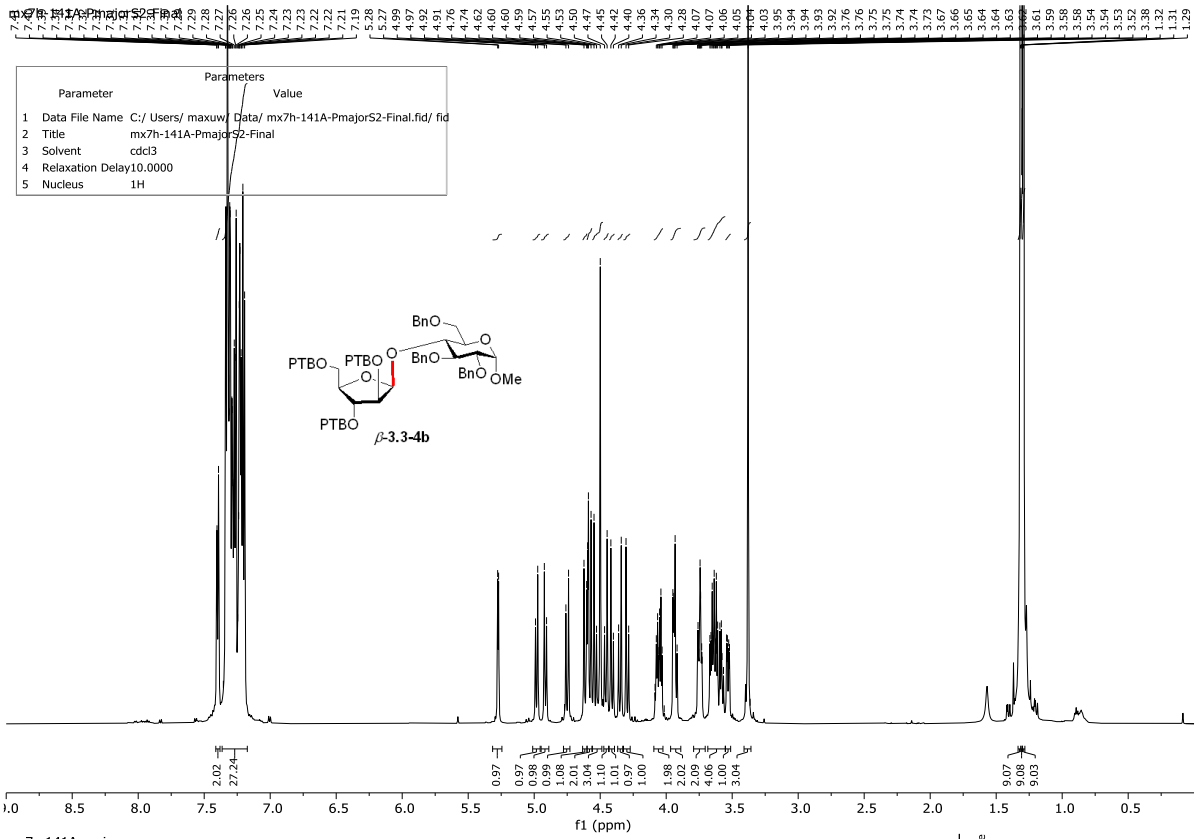
Parameters
Parameter Value
1 Data File Name C:/ Users/ maxuw/ Data/ mx7h-141A-PmajorS2-Final.fid/ fid
2 Title mx7h-141A-PmajorS2-Final
3 Solvent cdcl3
4 Relaxation Delay 10.0000
5 Nucleus 1H
BnO
PTBO
OMe
β-3.3-4b
f1 (ppm)

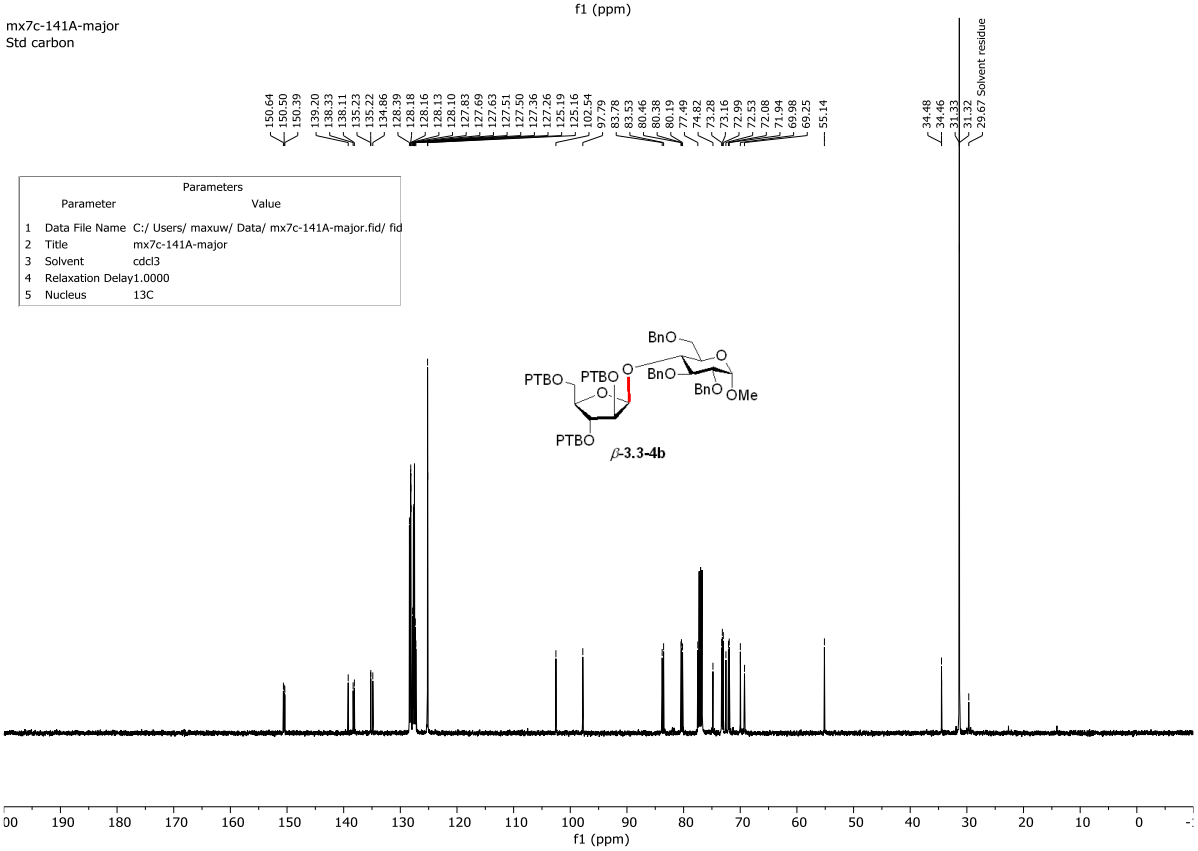
mx7c-141A-major
Std carbon
Parameters
Parameter Value
1 Data File Name C:/ Users/ maxuw/ Data/ mx7c-141A-major.fid/ fid
2 Title mx7c-141A-major
3 Solvent cdcl3
4 Relaxation Delay 1.0000
5 Nucleus 13C
Solvent residue
BnO
PTBO
OMe
β-3.3-4b
f1 (ppm)

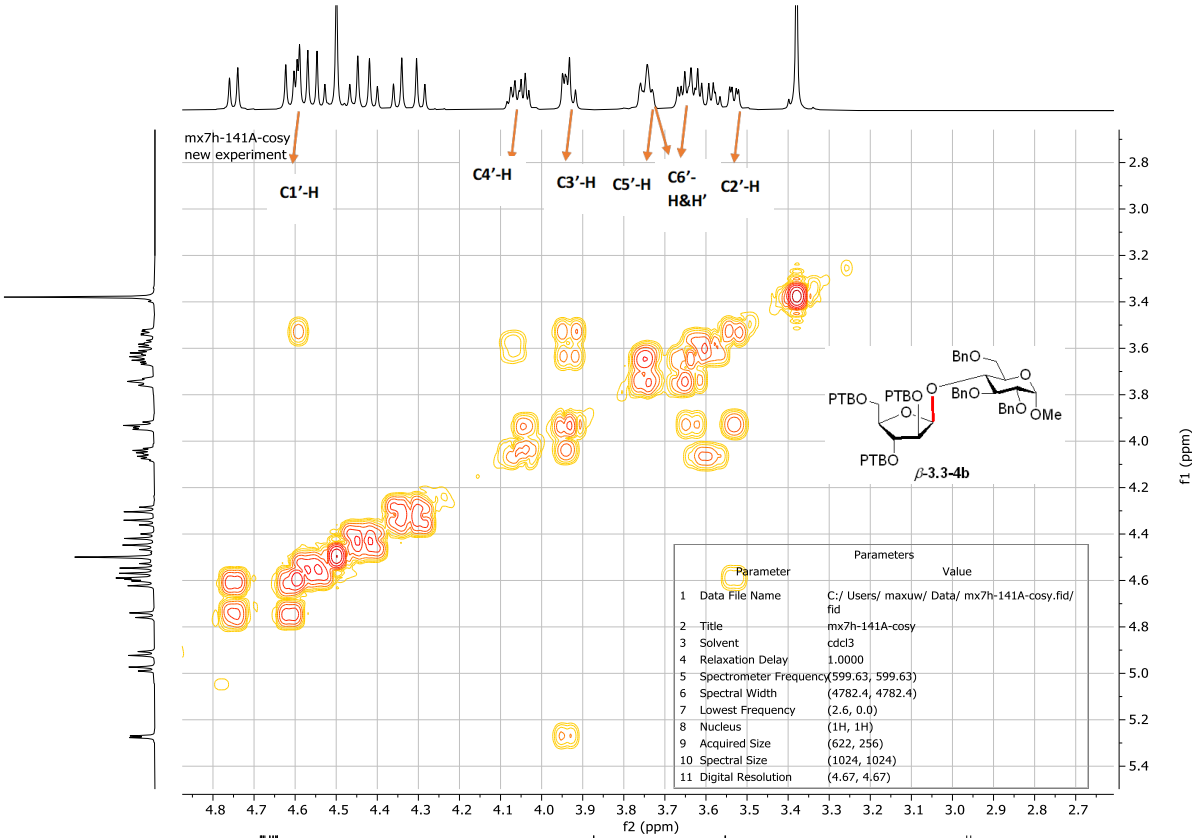
mx7h-141A-cosy
new experiment
C1'-H
C4'-H
C3'-H
C5'-H
C6'-
H&H'
C2'-H
PTBO
BnO
OMe
β-3.3-4b
Parameters
Parameter
Value
1 Data File Name C:/ Users/ maxuw/ Data/ mx7h-141A-cosy.fid/ fid
2 Title mx7h-141A-cosy
3 Solvent cdcl3
4 Relaxation Delay 1.0000
5 Spectrometer Frequency (599.63, 599.63)
6 Spectral Width (4782.4, 4782.4)
7 Lowest Frequency (2.6, 0.0)
8 Nucleus (1H, 1H)
9 Acquired Size (622, 256)
10 Spectral Size (1024, 1024)
11 Digital Resolution (4.67, 4.67)
f2 (ppm)
f1 (ppm)

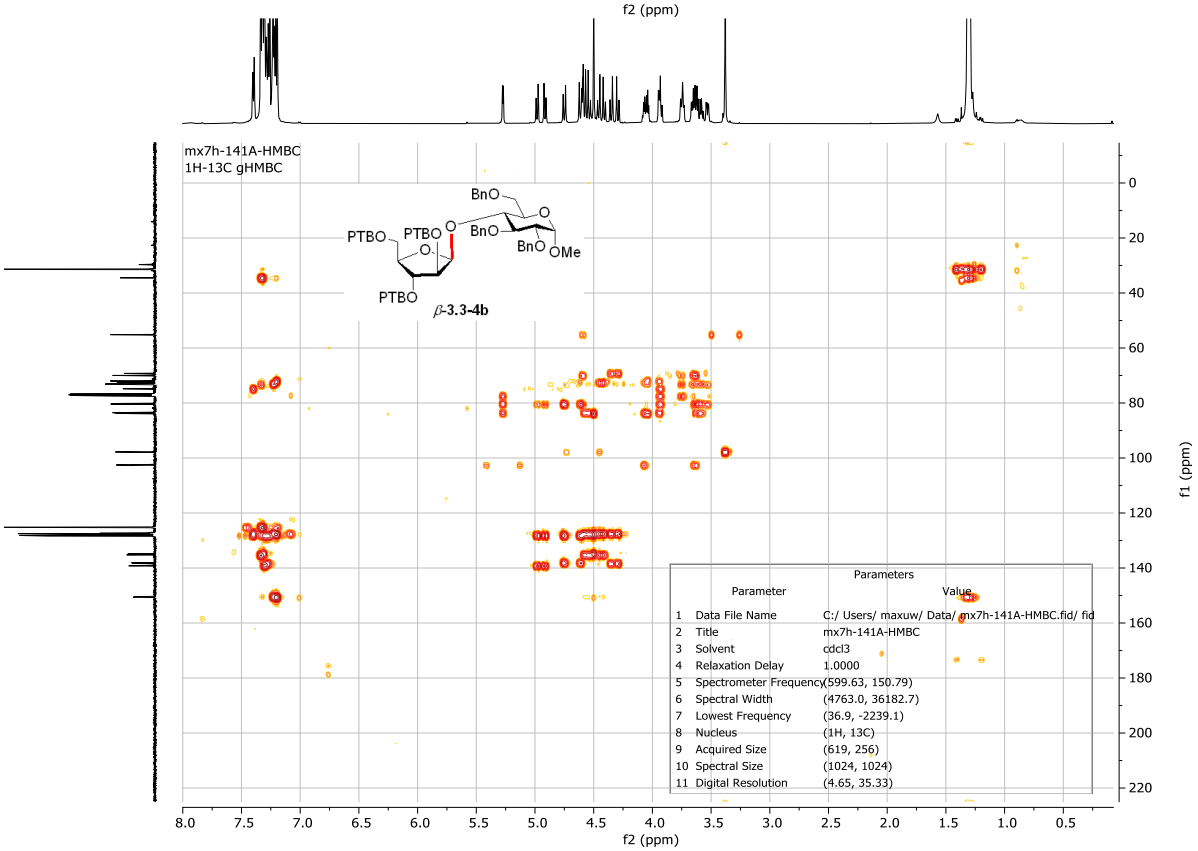
mx7h-141A-HMBC
1H-13C gHMBC
PTBO
BnO
OMe
β-3.3-4b
Parameters
Parameter
Value
1 Data File Name C:/ Users/ maxuw/ Data/ mx7h-141A-HMBC.fid/ fid
2 Title mx7h-141A-HMBC
3 Solvent cdcl3
4 Relaxation Delay 1.0000
5 Spectrometer Frequency (599.63, 150.79)
6 Spectral Width (4763.0, 36182.7)
7 Lowest Frequency (36.9, -2239.1)
8 Nucleus (1H, 13C)
9 Acquired Size (619, 256)
10 Spectral Size (1024, 1024)
11 Digital Resolution (4.65, 35.33)
f2 (ppm)
f1 (ppm)

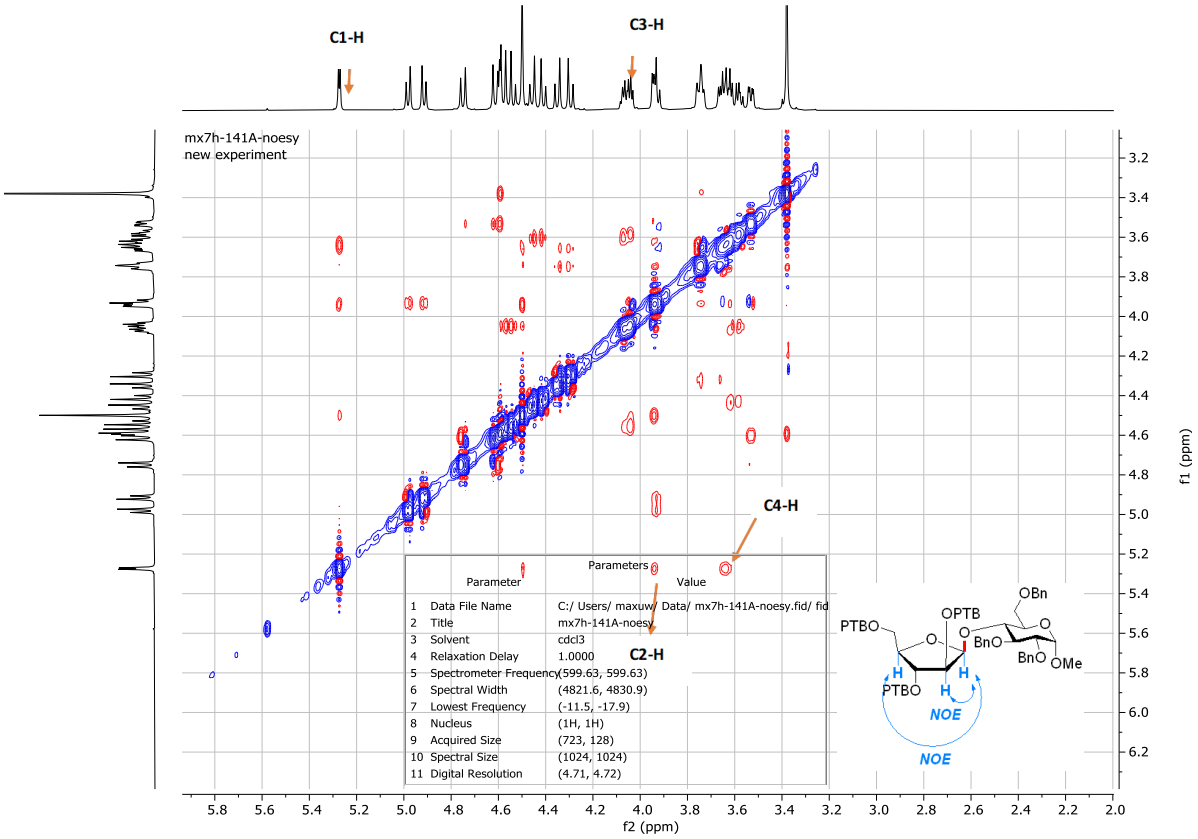
C1-H
C3-H
mx7h-141A-noesy
new experiment
C4-H
C2-H
Parameters
Parameter
Value
1 Data File Name C:/ Users/ maxuw/ Data/ mx7h-141A-noesy.fid/ fid
2 Title mx7h-141A-noesy
3 Solvent cdcl3
4 Relaxation Delay 1.0000
5 Spectrometer Frequency (599.63, 599.63)
6 Spectral Width (4821.6, 4830.9)
7 Lowest Frequency (-11.5, -17.9)
8 Nucleus (1H, 1H)
9 Acquired Size (723, 128)
10 Spectral Size (1024, 1024)
11 Digital Resolution (4.71, 4.72)
OBn
OPTB
PTBO
BnO
BnO
OMe
PTBO
H
H
H
NOE
NOE
f2 (ppm)
f1 (ppm)